

New Salt-Like Dodecahydro-*closo*-Dodecaborates and Efforts for the Partial Hydroxylation of [B₁₂H₁₂]²⁻ Anions

Von der Fakultät Chemie der Universität Stuttgart
zur Erlangung der Würde eines Doktors der
Naturwissenschaften (Dr. rer. nat.) genehmigte Abhandlung

vorgelegt von

Nguyen-Duc Van

aus Hatinh (Vietnam)

Vorsitzender:	Prof. Dr. Emil Roduner
Hauptberichter:	Prof. Dr. Thomas Schleid
Mitberichter:	Prof. Dr. Wolfgang Kaim
Weiterer Prüfer:	Prof. Dr. Klaus Müller

Tag der mündlichen Prüfung: 24. Februar 2009

Institut für Anorganische Chemie der Universität Stuttgart

Acknowledgements

Firstly, I would like to greatly thank Prof. Dr. Thomas Schleid for giving me the opportunity to do this work in his laboratory and for the valuable advice.

I would like to thank:

Prof. Dr. Emil Roduner for agreeing to chair the examination as well as for continuous encouraging me.

Prof. Dr. Wolfgang Kaim and Prof. Dr. Klaus Müller as co-referee and examiner respectively.

I would like to thank Dr. Ioannis Tiritiris for introducing me to the field of research and Mrs. Sumati Panicker-Otto for the helpful discussions during my thesis work.

My gratitude also goes to Dr. Falk Lissner, Dr. Ingo Hartenbach and Dr. Sabine Strobel for the single crystal measurements.

I would also like to thank Christof Schneck for thermal analysis measurements, Mrs. K. Török for NMR measurements.

I appreciate and also thank all members of the research group of Prof. Dr. Schleid for their friendliness and whose comments were very helpful.

I would also like to thank the Graduate College “Modern Methods of Magnetic Resonance in Materials Science” for giving me a scholarship and financial support.

Finally I would like to thank my parents, my wife Hong Diep and all members of my family for their warm encouragement.

Table of Contents

1	Introduction	1
2	Preparation and Characterization Methods	6
2.1	Used Chemicals	6
2.2	Preparation Methods	7
2.3	Characterization Methods	7
2.3.1	Crystal Structure Determination and Crystalline Phase Identification by X-Ray Diffraction Methods	7
2.3.1.1	Basic Principles of X-Ray Diffraction	8
2.3.1.2	Polycrystalline X-Ray Diffraction	9
2.3.1.3	Single Crystal X-Ray Diffraction	10
2.3.1.3.1	Image Plate Diffraction System (IPDS) Single Crystal Diffractometer	11
2.3.1.3.2	κ -CCD Single Crystal Diffractometer	12
2.3.1.4	Crystal Structure Solution and Refinement	14
2.3.1.5	Devices and Computer Programs	17
2.3.2	Thermal Analysis	19
2.3.3	Nuclear Magnetic Resonance Spectroscopy	21
3	Dodecahydro-<i>closo</i>-Dodecaborate Salts	24
3.1	Dithallium(I) Dodecahydro- <i>closo</i> -Dodecaborate	24
3.1.1	Synthesis of $\text{Tl}_2[\text{B}_{12}\text{H}_{12}]$	24
3.1.2	Structure Description of $\text{Tl}_2[\text{B}_{12}\text{H}_{12}]$	24
3.2	Dodecahydro- <i>closo</i> -Dodecaborates with Divalent Cations	30
3.2.1	Mercury(II) Dodecahydro- <i>closo</i> -Dodecaborate	30
3.2.1.1	Synthesis of $\text{Hg}[\text{B}_{12}\text{H}_{12}]$	30
3.2.1.2	Structure Description of $\text{Hg}[\text{B}_{12}\text{H}_{12}]$	30
3.2.2	Hexaaqua-Nickel(II) Dodecahydro- <i>closo</i> -Dodecaborate Hexahydrate	46
3.2.2.1	Synthesis of $\text{Ni}(\text{H}_2\text{O})_6[\text{B}_{12}\text{H}_{12}] \cdot 6 \text{H}_2\text{O}$	46

3.2.2.2	Structure Description of $\text{Ni}(\text{H}_2\text{O})_6[\text{B}_{12}\text{H}_{12}] \cdot 6 \text{H}_2\text{O}$	46
3.2.2.3	Thermal Analysis of $\text{Ni}(\text{H}_2\text{O})_6[\text{B}_{12}\text{H}_{12}] \cdot 6 \text{H}_2\text{O}$	53
3.2.3	Dioxonium Dodecahydro- <i>closo</i> -Dodecaborates with Divalent Transition Metal Cations	54
3.2.3.1	Synthesis of the Compounds $[\text{M}(\text{H}_2\text{O})_6](\text{H}_3\text{O})_2[\text{B}_{12}\text{H}_{12}]_2 \cdot 6 \text{H}_2\text{O}$ (M = Mn, Fe, Co, Ni, Cu, Zn and Cd)	54
3.2.3.2	Structure Description of the Compounds $[\text{M}(\text{H}_2\text{O})_6](\text{H}_3\text{O})_2[\text{B}_{12}\text{H}_{12}]_2 \cdot 6 \text{H}_2\text{O}$ (M = Mn, Fe, Co, Ni, Cu, Zn and Cd)	54
3.2.3.3	Thermal Analysis of $[\text{Ni}(\text{H}_2\text{O})_6](\text{H}_3\text{O})_2[\text{B}_{12}\text{H}_{12}]_2 \cdot 6 \text{H}_2\text{O}$	82
3.2.4	Hexaaqua-Iron(II) Dodecahydro- <i>closo</i> -Dodecaborate	83
3.2.4.1	Synthesis of $\text{Fe}(\text{H}_2\text{O})_6[\text{B}_{12}\text{H}_{12}]$	83
3.2.4.2	Structure Description of $\text{Fe}(\text{H}_2\text{O})_6[\text{B}_{12}\text{H}_{12}]$	83
3.2.5	Triqua-Lead(II) Dodecahydro- <i>closo</i> -Dodecaborate Trihydrate $\text{Pb}(\text{H}_2\text{O})_3[\text{B}_{12}\text{H}_{12}] \cdot 3 \text{H}_2\text{O}$	91
3.2.5.1	Synthesis of $\text{Pb}(\text{H}_2\text{O})_3[\text{B}_{12}\text{H}_{12}] \cdot 3 \text{H}_2\text{O}$	91
3.2.5.2	Structure Description of $\text{Pb}(\text{H}_2\text{O})_3[\text{B}_{12}\text{H}_{12}] \cdot 3 \text{H}_2\text{O}$	91
3.3	Dodecahydro- <i>closo</i> -Dodecaborate Salts with Trivalent Cations	99
3.3.1	Crystal Structure of Diaqua-Monohydroxo-Bismuth(III) Dodecahydro- <i>closo</i> -Dodecaborate	99
3.3.1.1	Synthesis of $\text{Bi}(\text{H}_2\text{O})_2(\text{OH})[\text{B}_{12}\text{H}_{12}]$	99
3.3.1.2	Structure Description of $\text{Bi}(\text{H}_2\text{O})_2(\text{OH})[\text{B}_{12}\text{H}_{12}]$	99
3.3.2	Bis-Hexaaqua-Chromium(III) and Bis-Hexaaqua-Indium(III) Tris-Dodecahydro- <i>closo</i> -Dodecaborate Pentadecahydrate	107
3.3.2.1	Synthesis of $[\text{M}(\text{H}_2\text{O})_6]_2[\text{B}_{12}\text{H}_{12}]_3 \cdot 15 \text{H}_2\text{O}$ (M = Cr and In)	107
3.3.2.2	Structure Description of $[\text{M}(\text{H}_2\text{O})_6]_2[\text{B}_{12}\text{H}_{12}]_3 \cdot 15 \text{H}_2\text{O}$ (M = Cr and In)	108
3.3.3	Hexaaqua-Chromium(III) Aqua-Oxonium Bis-Dodecahydro- <i>closo</i> -Dodecaborate Hexahydrate	120
3.3.3.1	Synthesis of $[\text{Cr}(\text{H}_2\text{O})_6](\text{H}_5\text{O}_2)[\text{B}_{12}\text{H}_{12}]_2 \cdot 6 \text{H}_2\text{O}$	120
3.3.3.2	Structure Description of $[\text{Cr}(\text{H}_2\text{O})_6](\text{H}_5\text{O}_2)[\text{B}_{12}\text{H}_{12}]_2 \cdot 6 \text{H}_2\text{O}$	120
3.3.4	Bis-Hexaaqua-Aluminium(III) Oxosulfate Bis-Dodecahydro- <i>closo</i> -Dodecaborate Pentadecahydrate	130

3.3.4.1	Synthesis of $[\text{Al}(\text{H}_2\text{O})_6]_2(\text{SO}_4)[\text{B}_{12}\text{H}_{12}]_2 \cdot 15 \text{H}_2\text{O}$	130
3.3.4.2	Structure Description of $[\text{Al}(\text{H}_2\text{O})_6]_2(\text{SO}_4)[\text{B}_{12}\text{H}_{12}]_2 \cdot 15 \text{H}_2\text{O}$	130
3.3.5	Bis-Enneaqua-Lanthanum(III) Tris-Dodecahydro- <i>closo</i> -Dodecaborate Heptahydrate $[\text{La}(\text{H}_2\text{O})_9]_2[\text{B}_{12}\text{H}_{12}]_3 \cdot 7 \text{H}_2\text{O}$	138
3.3.5.1	Synthesis of $[\text{La}(\text{H}_2\text{O})_9]_2[\text{B}_{12}\text{H}_{12}]_3 \cdot 7 \text{H}_2\text{O}$	138
3.3.5.2	Structure Description of $[\text{La}(\text{H}_2\text{O})_9]_2[\text{B}_{12}\text{H}_{12}]_3 \cdot 7 \text{H}_2\text{O}$	138
3.3.6	Bis-Enneaqua-Praseodymium(III) and Bis-Enneaqua-Holmium(III) Tris-Dodecahydro- <i>closo</i> -Dodecaborate Pentadecahydrate	154
3.3.6.1	Synthesis of $[\text{M}(\text{H}_2\text{O})_9]_2[\text{B}_{12}\text{H}_{12}]_3 \cdot 15 \text{H}_2\text{O}$ (M = Pr and Ho)	154
3.3.6.2	Structure Description of $[\text{M}(\text{H}_2\text{O})_9]_2[\text{B}_{12}\text{H}_{12}]_3 \cdot 15 \text{H}_2\text{O}$ (M = Pr and Ho)	154
3.3.7	Enneaqua-Holmium(III) Tris-Oxonium Tris-Dodecahydro- <i>closo</i> -Dodecaborate Enneahydrate $[\text{Ho}(\text{H}_2\text{O})_9](\text{H}_3\text{O})_3[\text{B}_{12}\text{H}_{12}]_3 \cdot 9 \text{H}_2\text{O}$	165
3.3.7.1	Synthesis of $[\text{Ho}(\text{H}_2\text{O})_9](\text{H}_3\text{O})_3[\text{B}_{12}\text{H}_{12}]_3 \cdot 9 \text{H}_2\text{O}$	165
3.3.7.2	Structure Description of $[\text{Ho}(\text{H}_2\text{O})_9](\text{H}_3\text{O})_3[\text{B}_{12}\text{H}_{12}]_3 \cdot 9 \text{H}_2\text{O}$	165
4	Partially Hydroxylated Dodecahydro-<i>closo</i>-Dodecaborate Derivatives	174
4.1	Bis-Oxonium Undecahydro-Monohydroxo- <i>closo</i> -Dodecaborate Monohydrate	174
4.1.1	Synthesis of $(\text{H}_3\text{O})_2[\text{B}_{12}\text{H}_{11}(\text{OH})] \cdot \text{H}_2\text{O}$	174
4.1.2	Structure Description of $(\text{H}_3\text{O})_2[\text{B}_{12}\text{H}_{11}(\text{OH})] \cdot \text{H}_2\text{O}$	174
4.2	Dicesium Undecahydro-Monohydroxo- <i>closo</i> -Dodecaborate Monohydrate	181
4.2.1	Synthesis of $\text{Cs}_2[\text{B}_{12}\text{H}_{11}(\text{OH})] \cdot \text{H}_2\text{O}$	181
4.2.2	$^{11}\text{B}\{^1\text{H}\}$ -NMR Measurement of $\text{Cs}_2[\text{B}_{12}\text{H}_{11}(\text{OH})] \cdot \text{H}_2\text{O}$	181
4.2.3	Structure Description of $\text{Cs}_2[\text{B}_{12}\text{H}_{11}(\text{OH})] \cdot \text{H}_2\text{O}$	182
4.2.4	Thermal Analysis of $\text{Cs}_2[\text{B}_{12}\text{H}_{11}(\text{OH})] \cdot \text{H}_2\text{O}$	190
4.3	Dicesium 1,7-Dihydroxo-Decahydro- <i>closo</i> -Dodecaborate	191
4.3.1	Synthesis of $\text{Cs}_2[1,7\text{-B}_{12}\text{H}_{10}(\text{OH})_2]$	191
4.3.2	Structure Description of $\text{Cs}_2[1,7\text{-B}_{12}\text{H}_{10}(\text{OH})_2]$	191
4.3.3	Thermal Analysis of $\text{Cs}_2[1,7\text{-B}_{12}\text{H}_{10}(\text{OH})_2]$	200
4.4	Dicesium 1,2,3-Trihydroxo-Enneahydro- <i>closo</i> -Dodecaborate Monohydrate	202

4.4.1	Synthesis of $\text{Cs}_2[1,2,3\text{-B}_{12}\text{H}_9(\text{OH})_3] \cdot \text{H}_2\text{O}$	202
4.4.2	Structure Description of $\text{Cs}_2[1,2,3\text{-B}_{12}\text{H}_9(\text{OH})_3] \cdot \text{H}_2\text{O}$	202
4.5	Dicesium 1,2,3,5-Tetrahydroxo-Octahydro- <i>closo</i> -Dodecaborate Dihydrate	209
4.5.1	Synthesis of $\text{Cs}_2[1,2,3,5\text{-B}_{12}\text{H}_8(\text{OH})_4] \cdot 2 \text{H}_2\text{O}$	209
4.5.2	Structure Description of $\text{Cs}_2[1,2,3,5\text{-B}_{12}\text{H}_8(\text{OH})_4] \cdot 2 \text{H}_2\text{O}$	209
5	Dodecahydroxo-<i>closo</i>-Dodecaborates	217
5.1	Dirubidium Dodecahydroxo- <i>closo</i> -Dodecaborate Dihydrates	217
5.1.1	Synthesis and Crystal of P-orthorhombic $\text{Rb}_2[\text{B}_{12}(\text{OH})_{12}] \cdot 2 \text{H}_2\text{O}$	217
5.1.1.1	Synthesis of P-orthorhombic $\text{Rb}_2[\text{B}_{12}(\text{OH})_{12}] \cdot 2 \text{H}_2\text{O}$	217
5.1.1.2	Structure Description of P-orthorhombic $\text{Rb}_2[\text{B}_{12}(\text{OH})_{12}] \cdot 2 \text{H}_2\text{O}$	219
5.1.2	Synthesis and Crystal Structure of C-orthorhombic $\text{Rb}_2[\text{B}_{12}(\text{OH})_{12}] \cdot 2 \text{H}_2\text{O}$	226
5.1.2.1	Synthesis of C-orthorhombic $\text{Rb}_2[\text{B}_{12}(\text{OH})_{12}] \cdot 2 \text{H}_2\text{O}$	226
5.1.2.2	Structure Description of C-orthorhombic $\text{Rb}_2[\text{B}_{12}(\text{OH})_{12}] \cdot 2 \text{H}_2\text{O}$	226
5.1.3	Synthesis and Crystal Structure of P-monoclinic $\text{Rb}_2[\text{B}_{12}(\text{OH})_{12}] \cdot 2 \text{H}_2\text{O}$	232
5.1.3.1	Synthesis of P-monoclinic $\text{Rb}_2[\text{B}_{12}(\text{OH})_{12}] \cdot 2 \text{H}_2\text{O}$	232
5.1.3.2	Structure Description of P-monoclinic $\text{Rb}_2[\text{B}_{12}(\text{OH})_{12}] \cdot 2 \text{H}_2\text{O}$	232
5.2	Synthesis, Characterization and Crystal Structure of $\text{Cs}[\text{B}_{12}(\text{OH})_{12}]$	240
5.2.1	Synthesis of $\text{Cs}[\text{B}_{12}(\text{OH})_{12}]$	241
5.2.2	Electron Paramagnetic Resonance (EPR) and UV-VIS Investigations	242
5.2.3	Results of Cyclic Voltammetry Measurements	244
5.2.4	Structure Description of $\text{Cs}[\text{B}_{12}(\text{OH})_{12}]$	244
6	Summary and Outlook	251
6.1	Results	251
6.1.1	Dodecahydro- <i>closo</i> -Dodecaborates	251
6.1.1.1	Dithallium(I) Dodecahydro- <i>closo</i> -Dodecaborate	251
6.1.1.2	Mercury(II) Dodecahydro- <i>closo</i> -Dodecaborate	251
6.1.1.3	Dodecahydro- <i>closo</i> -Dodecaborates with Divalent Transition Metals	251

6.1.1.4	Dioxonium Dodecahydro- <i>closo</i> -Dodecaborates with Divalent Transition Metals	252
6.1.1.5	Triaqua-Lead(II) Dodecahydro- <i>closo</i> -Dodecaborate Trihydrate	252
6.1.1.6	Diaqua-Monohydroxo-Bismuth(III) Dodecahydro- <i>closo</i> -Dodecaborate	253
6.1.1.7	Bis-Hexaaqua Chromium(III) and Bis-Hexaaqua Indium(III) Tris-Dodecahydro- <i>closo</i> -Dodecaborate Pentadecahydrate	253
6.1.1.8	Hexaaqua-Chromium(III) Aqua-Oxonium Dodecahydro- <i>closo</i> -Dodecaborate Hexahydrate	253
6.1.1.9	Bis-Hexaaqua-Aluminium(III) Oxosulfate Bis-Dodecahydro- <i>closo</i> -Dodecaborate Pentadecahydrate	254
6.1.1.10	Dodecahydro- <i>closo</i> -Dodecaborate Hydrates of Trivalent Rare-Earth Metals	254
6.1.1.11	A Mixed Cationic Holmium(III) Oxonium Dodecahydro- <i>closo</i> -Dodecaborate Hydrate	255
6.1.2	Partially Hydroxylated Dodecahydro- <i>closo</i> -Dodecaborates	255
6.1.2.1	Undeca-hydro-Monohydroxo- <i>closo</i> -Dodecaborate Monohydrates	255
6.1.2.2	Dicesium 1,7-Dihydroxo-Decahydro- <i>closo</i> -Dodecaborate	256
6.1.2.3	Dicesium 1,2,3-Trihydroxo-Ennea-hydro- <i>closo</i> -Dodecaborate Monohydrate	256
6.1.2.4	Dicesium 1,2,3,5-Tetrahydroxo-Octahydro- <i>closo</i> -Dodecaborate Dihydrate	256
6.1.3	Dodecahydroxo- <i>closo</i> -Dodecaborates	257
6.1.3.1	Dirubidium Dodecahydroxo- <i>closo</i> -Dodecaborate Dihydrates	257
6.1.3.2	Cesium Dodecahydroxo- <i>hypocloso</i> -Dodecaborate	258
6.2	Outlook	258
7	Zusammenfassung und Ausblick	260
7.1	Ergebnisse	260
7.1.1	Dodecahydro- <i>closo</i> -Dodecaborate	260
7.1.1.1	Dithallium(I)-Dodecahydro- <i>closo</i> -Dodecaborat	260
7.1.1.2	Quecksilber(II)-Dodecahydro- <i>closo</i> -Dodecaborat	260
7.1.1.3	Dodecahydro- <i>closo</i> -Dodecaborate mit zweiwertigen Übergangsmetallen	261
7.1.1.4	Dioxonium-Dodecahydro- <i>closo</i> -Dodecaborate mit zweiwertigen Übergangsmetallkationen	261

7.1.1.5	Triaqua-Blei(II)-Dodekahydro- <i>closo</i> -Dodekaborat-Trihydrat	262
7.1.1.6	Diaqua-Monohydroxo-Bismut(III)-Dodekahydro- <i>closo</i> -Dodekaborat	262
7.1.1.7	Bis-Hexaaqua-Chrom(III)- und Bis-Hexaaqua-Indium(III)-Tris- Dodekahydro- <i>closo</i> -Dodekaborat-Pentadekahydrat	262
7.1.1.8	Hexaaqua-Chrom(III)-Oxonium Dodekahydro- <i>closo</i> -Dodekaborat- Hexahydrat	263
7.1.1.9	Bis-Hexaaqua-Aluminium(III) Oxosulfat Bis-Dodekahydro- <i>closo</i> - Dodekaborat-Pentadekahydrat	263
7.1.1.10	Dodekahydro- <i>closo</i> -Dodekaborate mit dreiwertigen Selten-Erd-Metallen	263
7.1.1.11	Gemischt-kationisches Holmium(III) Oxonium Dodekahydro- <i>closo</i> - Dodekaborat-Hydrat	264
7.1.2	Teilhydroxylierte Dodekahydro- <i>closo</i> -Dodekaborate	264
7.1.2.1	Undekahydro-Monohydroxo- <i>closo</i> -Dodekaborat-Monohydrate	264
7.1.2.2	Dicäsium-1,7-Dihydroxo-Dekahydro- <i>closo</i> -Dodekaborat	265
7.1.2.3	Dicäsium-1,2,3-Trihydroxo-Enneahydro- <i>closo</i> -Dodekaborat-Monohydrat	266
7.1.2.4	Dicäsium-1,2,3,5-Tetrahydroxo-Octahydro- <i>closo</i> -Dodekaborat-Dihydrat	266
7.1.3	Dodekahydroxo- <i>closo</i> -Dodekaborate	266
7.1.3.1	Dirubidium-Dodekahydroxo- <i>closo</i> -Dodekaborat-Dihydrate	266
7.1.3.2	Cäsium-Dodekahydroxo- <i>hypocloso</i> -Dodekaborat	267
7.2	Ausblick	268
8	References	270

1 Introduction

There is a large number of chemical compounds of boron with itself and with other elements and boron has a richness of chemistry second only to carbon. Boron hydrides, especially, can be considered as hydrocarbon analogues, which are an attractive research subject in inorganic chemistry. However, using structural and bonding models in the chemistry of hydrocarbons it is not possible to explain the structural and bonding feature of the neutral boron-hydrogen compounds (boranes). This fact was revealed even in the simplest borane: the diborane B_2H_6 . The stoichiometry of this compound and other boranes e. g. B_2H_6 , B_4H_{10} , B_5H_9 , B_5H_{11} , B_6H_{10} , and $B_{10}H_{14}$ were determined by A. Stock and coworkers, who carried out pioneering work in the field of neutral boron-hydrogen compounds between the years 1912 and 1936 [1]. Diborane possesses the stoichiometry of the hydrocarbon ethane (C_2H_6), even with two electrons less. It was also not clear for a long time that the boron trihalides, BX_3 ($X = F - I$), are stable as monomers, but BH_3 only exists as a dimer. In the middle of the 20th century W. N. Lipscomb, based on results of X-ray crystal structure analysis and the prediction of Longuet-Higgins and Roberts, suggested a bonding model for boron hydrides, for which he was awarded the Nobel Prize in 1976. By applying the concept of three center two electron bonding, the bonding feature in the boranes now is successfully explained [2–5]. With the electronic configuration of the boron atoms being $1s^2 2s^2 2p^1$, diborane (B_2H_6) is an electron deficient compound with twelve electrons for eight bonds. Four terminal hydrogen atoms form two center electron pair bonds with the boron atoms and there are only four remaining electrons for four bonds. The electron deficiency will be solved only when two boron atoms are linked by three center two electron B–H–B bonds (Fig. 1). Chemical bonding in a diborane molecule can be described by Molecular Orbital theory in terms of hybridization concepts. If each boron atom in this molecule is considered to be sp^3 hybridized, two terminal

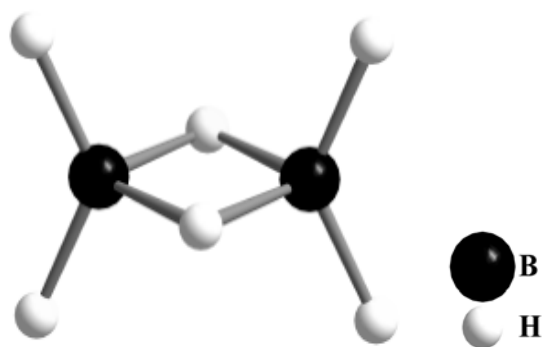


Fig. 1: Molecular structure of diborane (B_2H_6)

B–H bonds on each boron atom presumably are simple σ bonds involving a pair of electrons each. Each of the bridging B–H–B linkages then involves a delocalized or three center two electron bond. In the boranes with a higher number of boron atoms, not only B–H–B bonds are three center two electron bonds, but also the open and closed B–B–B bonds [6, 7]. Lipscomb and coworkers showed that among these three types of three center two electron bonding the energy level of the molecular orbital that two electrons occupy is lowest for the closed B–B–B bond. The boranes are therefore stable, even though they are electron deficient compounds and their structures tend to give closed shell systems. This tendency was not characteristic for hydrocarbons, in which chemical bonds are “normal” covalent (two center two electron) ones [8]. Lipscomb formalized the numerical generalization of a process to establish the bonding scheme in the *styx* rule, which includes parameters that specify the numbers of two (x B–H and y B–B) and three center bonds (s B–H–B and t B–B–B) necessary to describe a borane with specific stoichiometry. Lipscomb also suggested that the structures of some unknown boranes can be derived from the B_{12} icosahedron (Fig. 2), when the free

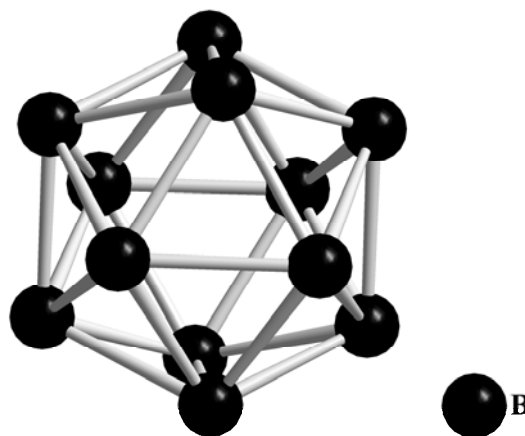


Fig. 2: Structure of the B_{12} icosahedron

valences at the edges saturated by additional hydrogen atoms [3]. Detailed investigation on the B_{12} icosahedron, a dominant structural element in the chemistry of boron, was carried out by Longuet-Higgins and Roberts [4]. They focussed on criteria for the B_{12} icosahedron to occur in a real compound. This occurrence is favoured, when twelve covalent bonds are formed between the icosahedron and its neighbouring *exo*-atoms and there are twenty-six valence electrons to fill the molecular orbitals inside the icosahedral cage. It was experimentally pointed out by Hawthorne and Pitochelli in 1960 that the real borane with

icosahedral shape can only be the $[\text{B}_{12}\text{H}_{12}]^{2-}$ anion. Thus the salt-like $((\text{C}_2\text{H}_5)_3\text{NH})_2[\text{B}_{12}\text{H}_{12}]$ was obtained as a by-product for the first time by the reaction between monoiodo decaborane ($\text{B}_{10}\text{H}_{10}\text{I}$) and triethylamine $((\text{C}_2\text{H}_5)_3\text{N})$ in benzene [9]. Further investigation showed that B_{12} icosahedron is only to recruit the upper limit of a series of deltahedral $[\text{B}_n\text{H}_n]^{2-}$ dianions ($n = 6 - 12$). These anionic boron-hydrogen compounds are called *closo*-hydroborates, which are derived from boranes by withdrawing the acidic protons. They are closed boron cages (or clusters) with triangular faces (hence deltahedra) and their geometric shapes are just slightly distorted in the solid state. The construction of molecular orbitals for boranes, particularly large and open cages, is not a trivial matter without the aid of computers. However, it is easier using an empirical set of rules proposed by K. Wade [10]. Wade set up the relationship between the structure of boranes and the number of scaffolding electrons for the deltahedra. This set is used for predicting or, conversely, for rationalizing the structure of cluster molecules. The theories are best suited for clusters of the main group elements and are, therefore, ideal for the boranes. The basis of Wade's rules is that a closed deltahedral cluster with n vertices requires a number of scaffolding electrons that equal $(2n + 2)$ to completely occupy the bonding molecular orbitals. By removing one vertex from a closed deltahedral cluster, a *nido* structure is formed with $(2n + 4)$ scaffold electrons. Hydrogen atoms bridge the edges around the open face, which remains after the removal of one vertex. Removes one more corners of a deltahedral cluster, an *arachno* structure is obtained. As two more hydrogen atoms are added, this structure possesses $(2n + 6)$ scaffolding electrons. The synthesis and characterization of salts containing the *closo*-anions $[\text{B}_{11}\text{H}_{11}]^{2-}$ [11], $[\text{B}_{10}\text{H}_{10}]^{2-}$ [12–16], $[\text{B}_9\text{H}_9]^{2-}$ [17, 18], $[\text{B}_8\text{H}_8]^{2-}$ [19], $[\text{B}_7\text{H}_7]^{2-}$ [20, 21] and $[\text{B}_6\text{H}_6]^{2-}$ [22, 23] shows that a closed boron polyhedron, which consists of triangular surfaces, is encountered for all these cages. Similar deltahedral structures are also found in the ternary compounds containing carbon, boron and hydrogen. The neutral carboranes ($\text{C}_2\text{B}_{n-2}\text{H}_n$) with two B–H bonds substituted by isoelectronic C–H⁺ fragments and are isosteric to the corresponding *closo*-dodecaborate anions $[\text{B}_n\text{H}_n]^{2-}$ [24]. Compounds containing closed boron polyhedra show an astonishingly high stability, whereas neutral boron-hydrogen compounds with open structures are rather unstable. Especially, compounds containing B_{12} icosahedra appear to be very stable and have low chemical reactivity, such as the $[\text{B}_{12}\text{H}_{12}]^{2-}$ anion, (*ortho*-, *meta*- and *para*-) carborane $\text{C}_2\text{B}_{10}\text{H}_{12}$ and even elemental boron with its allotropic modifications [16, 24, 25, 26]. The concept of cage aromaticity, which is originally used for two-dimensional polygonal molecules and ions in organic chemistry, can be applied to three-dimensional polyhedral

molecules to explain their extraordinary stability. This concept of three-dimensional aromaticity for the deltahedral boranes was first applied in 1978 by Aihara [27]. The resonance energy, a factor for estimating the stability of an aromatic compound, was calculated for all boranes. The resonance energy of the highly symmetric $[\text{B}_{12}\text{H}_{12}]^{2-}$ anion was theoretically calculated to be the highest one as compared to that of all other *closo*-hydroborate anions. This enormous stability of the $[\text{B}_{12}\text{H}_{12}]^{2-}$ anion is also revealed by its weak chemical reactivity [15, 28]. Among all *closo*-hydroborate anions, the $[\text{B}_{12}\text{H}_{12}]^{2-}$ anion has received an intense interest since 1960. The $[\text{B}_{12}\text{H}_{12}]^{2-}$ anion normally lacks two well established kinds of features, which characterize the chemistry of organic aromatic compounds: it is less easily functionalized, and it usually does not undergo facile reversible electron transfer. However, it is possible for the hydrogen atoms to be partially or fully substituted by various functional groups via direct or multi-step reactions. The direct substitution of the $[\text{B}_{12}\text{H}_{12}]^{2-}$ -cluster anion by substituents is usually difficult and, with exceptions of halogenation and deuteration, only mono- or disubstituted derivatives were obtained [29–32]. The direct reaction between $[\text{B}_{12}\text{H}_{12}]^{2-}$ anions and elemental halogen provides a variety of halogenated derivatives [33–37]. Among known halogenated and deuterated derivatives of the $[\text{B}_{12}\text{H}_{12}]^{2-}$ anion, only $[\text{B}_{12}\text{H}_{11}\text{I}]^{2-}$ was used as an intermediate species for further functionalization such as alkylation or arylation [38]. The functionalization of $[\text{B}_{12}\text{H}_{12}]^{2-}$ anions singly, in groups or totally is often carried out by multi-step reactions via intermediate compounds containing boron-carbon, boron-nitrogen, boron-sulfur, boron-phosphorus, boron-arsenic and boron-oxygen bonds [39–47]. Among these intermediate compounds, hydroxylated dodecahydro-*closo*-dodecaborates are prospective ones with the discovery of $[\text{B}_{12}\text{H}_{12-n}(\text{OH})_n]^{2-}$ anions ($n = 1 - 4, 12$) [48, 49]. The functionalization of $[\text{B}_{12}\text{H}_{12-n}(\text{OH})_n]^{2-}$ anions by organic and inorganic substituents is much easier than that of the parent $[\text{B}_{12}\text{H}_{12}]^{2-}$ anion and has provided a variety of closomers [50–52]. The study of dodecahydro-*closo*-dodecaborates and their derivatives has drawn the attention of researchers not only in sense of basic research but also for application. Dodecahydro-*closo*-dodecaborates and their derivatives are used in boron neutron capture therapy (BNCT) for treating cancer, because of possessing high chemical and hydrolytic stability, high solubility in water in the form of their sodium salts, and low toxicity, which are ideal properties necessary for the design of pharmaceuticals [53–56]. In addition to this traditional application, there are many other applications of dodecahydro-*closo*-dodecaborates and their derivatives owing to their properties. A large number of properties depending on the size of the boron cluster, which lies

between in the range of size from molecule to nanosolid, has been intensively exploited [57]. Dodecahydro-*closo*-dodecaborates and their derivatives can be used as multifunctional nanomolecular drug delivery systems and as hydrogen storage materials for reasons of their non-toxicity [58, 59]. They can be used also as contrast agents for Magnetic Resonance Imaging (MRI) with expected maximal water exchange, while creating a higher relaxivity than commercialized contrast agents, largely based upon gadolinium (III) chelate complexes [60]. Dodecahydro-*closo*-dodecaborates and their derivatives also have been intensively studied for molecular motors and actuators capable of delivering useful work to nano-devices for electrochemical or photochemical power sources [61, 62].

Possessing many special chemical properties and a potential for application, dodecahydro-*closo*-dodecaborates and their derivatives are still a current research subject in chemistry. From the crystallographic point of view, only few crystal structures of dodecahydro-*closo*-dodecaborates and their derivatives with purely inorganic cations had been elucidated in literature so far. The scope of this thesis therefore is the synthesis, characterization and crystal structure determination of ionic salts with dodecahydro-*closo*-dodecaborate and hydroxylated *closo*-dodecaborate anions.

2 Preparation and Characterization Methods

2.1 Used Chemicals

Almost all chemicals used in this work were commercial products, which are listed in Table 1. The only exception was $\text{Cr}(\text{OH})_3$, which is obtained by the reaction between chromium(III) chloride CrCl_3 (Strem: 99 %) and sodium hydroxide NaOH (Merck: 99 %) from aqueous solution.

Table 1: List of used chemicals

Chemical	Purity	Supplier
Dicesium dodecahydro- <i>closo</i> -dodecaborate ($\text{Cs}_2[\text{B}_{12}\text{H}_{12}]$)	98 %	Strem
Strong acidic cation exchanger (DOWEX-50 WX8)		Merck
Dithallium(I) carbonate (Tl_2CO_3)	99.9 %	Merck
Mercury(II) nitrate ($\text{Hg}(\text{NO}_3)_2$)	99.9 %	Merck
Nickel(II) carbonate (NiCO_3)	99.9 %	Merck
Zinc hydroxide carbonate ($3 \text{Zn}(\text{OH})_2 \cdot 2 \text{ZnCO}_3$)	96 %	Acros Organic
Cobalt carbonate (CoCO_3)	99.9 %	Alfa Aesar
Cadmium carbonate (CdCO_3)	98.5 %	Merck
Copper(II) hydroxide carbonate ($\text{Cu}(\text{OH})_2 \cdot \text{CuCO}_3$)	95 %	Merck
Aluminium sulfate octadecahydrate ($\text{Al}_3(\text{SO}_4)_3 \cdot 18 \text{H}_2\text{O}$)	98 %	Strem
Iron powder (Fe)	99.9 %	Strem
Lanthanum nitrate hexahydrate ($\text{La}(\text{NO}_3)_3 \cdot 6 \text{H}_2\text{O}$)	99 %	Merck
Lead(II) carbonate (PbCO_3)	99.9 %	Merck
Bismuth(III) oxide (Bi_2O_3)	99.9 %	Merck
Manganese(II) carbonate hydrate ($\text{MnCO}_3 \cdot n \text{H}_2\text{O}$)	96 %	Merck
Chromium(III) chloride (CrCl_3)	99 %	Strem
Indium(III) oxide (In_2O_3)	99.999 %	Strem
Hydrogen peroxide 30 % (w/w) in H_2O (H_2O_2)		Aldrich
Rubidium hydroxide 30 % (w/w) in H_2O (RbOH)		Aldrich
Praseodymium(III, IV) oxide (Pr_6O_{11})	99.9 %	CHEMPUR
Holmium(III) oxide (Ho_2O_3)	99.9 %	CHEMPUR
Calcium carbonate (CaCO_3)	99 %	Aldrich
Calcium sulfate (CaSO_4)	99.99 %	Aldrich

2.2 Preparation Methods

All single crystals described in this work were grown from aqueous solution. Many synthesized compounds in this work are air sensitive, tend strongly to hydrolysis or are salts of multivalent metals. Therefore, the preparation of most dodecahydro-*closo*-dodecaborates and their derivatives was carried out under inert gas atmosphere. Detailed descriptions of the synthesis methods for each compound are given in the next three chapters (Chapter 3–5).

2.3 Characterization Methods

A number of analysis and characterization methods were used in this work. Only some frequently used methods are briefly described.

2.3.1 Crystal Structure Determination and Crystalline Phase Identification by X-Ray Diffraction Methods

A large range of information for the investigated chemical compound, such as accurate chemical composition or bond lengths and angles in the solid state, interatomic connectivity, conformation, stoichiometry, three-dimensional packing of atoms are obtained by diffraction methods. Furthermore, for crystalline compounds containing weak hydrogen bonds, the crystal structure analysis provides information about these weak hydrogen bonds much easier than most spectroscopic methods. Laboratory X-ray diffraction facilities including both single crystal and polycrystalline (powder) X-ray diffractometers are more accessible compared to those of neutron, electron or synchrotron X-ray diffraction. Single crystal X-ray diffraction is the most conventional direct characterization method to obtain the structure of a pure crystalline compound in the solid phase. However, it is not always possible to obtain all the information of a crystal structure from its single crystal X-ray diffraction structure determination. The accurate position of hydrogen atoms involved in a crystal structure is not always indicated due to the fact that of their weak scattering powers since X-rays are scattered by the electron shells of an atom. In addition, the discrimination between atoms of adjacent atomic numbers, such as Co and Ni or Mn and Fe can not be achieved by X-ray diffraction structure determination. If a studied compound contains only microcrystals that are not sufficiently good for single crystal X-ray diffraction structure determination, its crystal structure can be determined from polycrystalline X-ray diffraction data by Rietveld methods.

As powder data usually lack the three-dimensionality of a diffraction image, the Rietveld method, however, is appropriate for the refining of small structures only providing a sufficiently good starting structural model for a particular crystal structure can be devised. Traditionally, the polycrystalline X-ray diffraction method is used in chemistry as phase analysis to identify the crystalline phases qualitatively and quantitatively.

2.3.1.1 Basic Principles of X-Ray Diffraction

Conventional crystallography was developed using the explicit assumption that crystalline objects maintain an ideal three-dimensional periodicity. Thus any three-dimensional periodic crystal structure, in which a basic pattern of atoms is repeated over the three-dimensional space, can be described by a periodic lattice and one of the 230 possible crystallographic space groups. The 230 crystallographic space groups are obtained by combining the 32 crystallographic point groups (or crystal classes) with the 14 Bravais lattices (or translation lattices) and translational symmetry elements. These crystallographic space groups in turn are categorized into seven crystal systems, which classify space groups and crystallographic point groups, but not lattice types, or into fourteen lattice systems classifying space groups and lattice types, but not crystallographic point groups. The point group of a crystal is the point group of a unit cell, which represents the smallest repeating volume of the lattice. As a consequence, if the content of the unit cell is known, the crystal structure will be described completely. The determination of a crystal structure is then simplified to the determination of the content of the unit cell. When a crystal is irradiated by radiation or a particle beam with a wavelength in the vicinity of interatomic distances (e. g. X-rays, neutrons, electrons), the Bragg diffraction occurs. In this phenomenon the direction of radiation is scattered coherently and elastically by atoms located at lattice points of crystal lattice planes and the interference takes place constructively or destructively between scattered radiation waves. The lattice planes have orientations relative to the lattice, which are defined by Miller indices with the values hkl . The incident angle θ of radiation can be calculated in terms of the path difference between a radiation wave diffracted by one plane and that one diffracted by the next plane following in the lattice from the Bragg equation:

$$2 \cdot d_{hkl} \cdot \sin\theta = n \cdot \lambda \quad (n: \text{positive integer})$$

where: d_{hkl} : interplanar spacing for each set of lattice planes hkl ,

- θ : incident angle,
- λ : wavelength of incident radiation,
- n : order of diffraction.

The relationship between interplanar spacing for each set of lattice planes hkl , incident angle, wavelength of incident radiation and order of the diffraction process is established by the Bragg equation. During a diffraction measurement, for a radiation with defined given wavelength, at each step of the incident angle of radiation, the intensity of the diffracted beam is recorded. The interplanar spacing is calculated from the Bragg equation for each diffraction spot. The task of crystal structure determination is then determining the measured lattice parameters of the unit cell, the space group and the actual atomic arrangement in the asymmetric unit. This task is relatively straight ahead, whenever suitable single crystals are available for single crystal X-ray diffraction measurements.

2.3.1.2 Polycrystalline X-Ray Diffraction

For a polycrystalline sample consisting of a large number of randomly oriented crystallites, polycrystalline diffraction is fundamentally one-dimensional, because the diffracted intensity can not be measured for an individually diffracted spots (reflections), but only as a function of one variable (the Bragg angle θ) instead. It results in six identifiable "powder" Laue groups and the crystallographic point group is difficult to determine, even in a case where the whole powder diffraction pattern is contributed by only one crystal structure. As a result the crystal structure determination from X-ray powder diffraction data is much more difficult than that from single crystal X-ray diffraction data. However, the crystalline phases of a polycrystalline sample can be identified from X-ray powder diffraction data. The position and intensity of diffraction peaks of a measured diffraction pattern is compared with those of known crystalline phases. The reference powder diffraction pattern for this "search-and-match" procedure can be obtained from a commercialized database for published crystalline phases or can be simulated by the user himself from newly determined single crystal data. Information obtained from this phase identification can be used, for example, to optimize the synthesis method of the target compound to be prepared with high yield and purity. Laboratory X-ray powder diffractometers can be classified into two main categories: one employing transmission geometry (Fig. 3) and another employing reflection geometry. An incident beam

is transmitted through the sample, and the X-ray source and the detector are positioned at two sides with respect to the surface of the sample in transmission geometry. The incident beam is then reflected from the surface of the sample when the X-ray source and the detector are positioned at the same side relative to the surface of the sample in reflection geometry. The reflection geometry is suitable for crystalline phases containing light chemical elements, while the transmission one is preferable for air sensitive samples or crystalline phases containing heavy chemical elements.

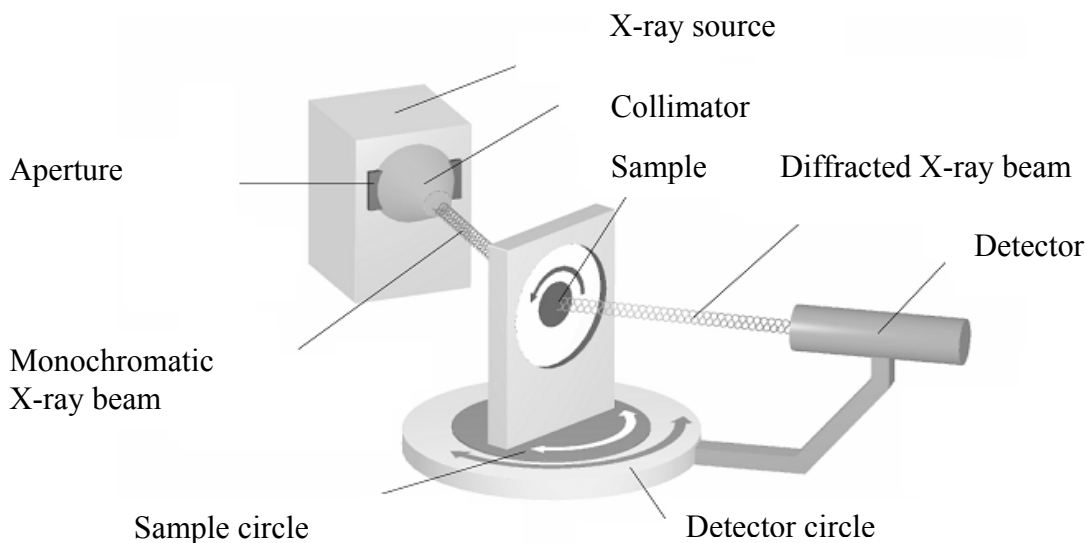


Fig. 3: Schematic view of a Stoe STADI P X-ray powder diffractometer in transmission geometry

2.3.1.3 Single Crystal X-Ray Diffraction

The determination of a crystal structure by single crystal X-ray diffraction methods follows a flowchart including five main steps: single crystal growth, data collection, data reduction, crystal structure solution and crystal structure refinement [63]. In the first step suitable crystals, which were grown as described previously (Section 2.2), are selected to be mounted onto the X-ray diffractometer. The next step is the determination of the unit cell and the data collection following a strategy that gives a complete set of data and a high multiplicity of observations. In the third step the raw intensities from the detector are translated into structure factors (or squared structure factors). In this step, the data reduction programs apply several corrections (e. g. Lorentz, polarization, absorption, etc.) and determine values for the standard uncertainties for each reflection. To complete these two steps a single crystal X-ray diffractometer is used with accessory computer programs. Single crystal X-ray

diffractometers are, based on their detector devices, classified into four types: single photon counter, photographic film, Image Plate (IP), and Charge Coupled Device (CCD) cameras. The first one has been used since the early days of X-ray diffraction and is nowadays usually of the scintillation type. Photographic films also belong to the classical detectors, but they are not used any more, because of the availability of far more sensitive image plates and area detectors. In this thesis, single crystals were measured on two modern diffractometers: STOE IPDS and NONIUS κ -CCD. Both of them are equipped with molybdenum X-ray tubes and graphite monochromators (Mo-K α : $\lambda = 71.07$ pm).

2.3.1.3.1 Image Plate Diffraction System (IPDS) Single Crystal Diffractometer

An Image Plate Diffraction System (IPDS) single crystal diffractometer is shown in Figure 4. Image plates are used in the same manner as X-ray film, but have several advantages. Image plates are made by depositing a thin layer of Eu²⁺-doped BaFCl or BaBrF material. During exposure, and due to the oxidation of Eu²⁺ to Eu³⁺, incident X-ray photons are converted to colour centers and then an appreciable amount of energy is retained in the material. This stored energy can be later released up on illumination with light by a laser scanner. The incident red laser beam causes the free electron to reduce Eu³⁺ to Eu²⁺ again, with the emission of photons in the blue region of the visible spectrum. The red light is filtered away and the blue light can be measured with a photomultiplier. After full exposure in intense white light, to remove any possible remaining colour centers, the plate is ready for reuse again. Each reading and regenerating period requires 2 – 5 minutes only depending on the instrument. For this reason, despite the much larger diameter of the plate, Image Plate systems are usually still somewhat slower than CCD systems. After turning the crystal by a certain amount (0.5 – 1.0 °), a new sequence of scanning and deleting is automatically recorded. About 200 – 400 of such recordings are required to collect enough information for a structural solution. The total time needed to measure a crystal takes around 24 hours and depends on the scattering power of the crystal, but not on the size of its unit cell. Image plates are at least 10 times more sensitive than X-ray films and their dynamic range is much wider. With this technique, intermediate and foreign reflexes are always involved into the estimation of the elementary cell. However, during the subsequent reflex integration with the correct unit cell, these are neglected likewise. The great disadvantage of IPDS diffractometers is the empirical absorption correction that has to be made for solving the crystal structure, because it is not possible to measure the intensities of individual diffracted spots in different orientation. In

using the computer program X-SHAPE [64], however, this disadvantage is overcome by providing enough reflections, which are collected. Based on symmetry equivalent reflections for a given space group, all possible shapes of the very crystal are calculated iteratively. From these possible habits, the intensities of all reflections can be corrected eventually.

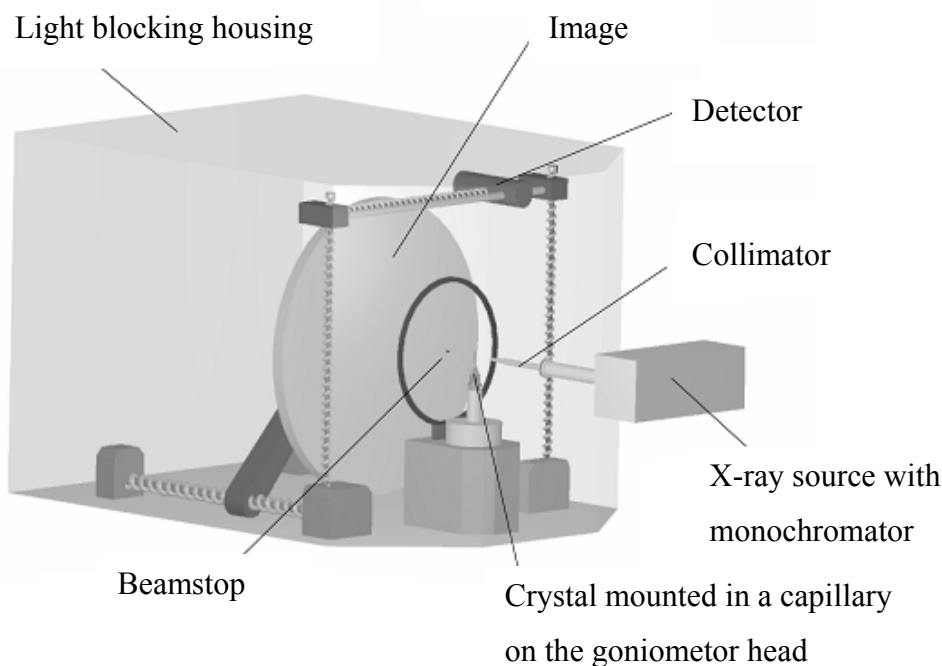


Fig. 4: View of a STOE IPDS single crystal diffractometer

2.3.1.3.2 κ -CCD Single Crystal Diffractometer

Although photographic films and image plates are area detectors, the use of this term is restricted to electronic devices such as CCD detectors that detect X-ray photons on a two-dimensional surface and process the signal immediately after photon detection. A basic difference with image plates is that CCD detectors scan through a diffraction spot every 0.1° or so, giving a three-dimensional picture of this diffraction spot. The detector does not need to move for seeking diffraction spots, and the movement of the crystal is reduced. During the measurement, the crystal must, nevertheless, rotate for allowing a large number of reciprocal lattice nodes to cross the Ewald sphere of course. In practice, only rotations around the ϕ -axis of the four-circle Eulerian geometry or the ω -axis of the κ -geometry are realized. Because of the known crystal dimension and the divergence of the incidental crystal beam, the reciprocal network node has a known volume. Images are collected in two iterations in order to diminish

disturbing effects of cosmic radiation. In this type of diffractometer, the distance between X-ray source beam and crystal remains constant, and the one between the crystal and the detector is adjustable (adjustment of the detector resolution). The diffracted X-ray photons arriving at the detector are directly converted to electronic signals. The thermal electronic noise is reduced by cooling the detector with a Peltier element down to between -40 and -80 °C. With instantaneous observation of a broad reciprocal space, the CCD diffractometer is privileged for structural phase transition studies. Particularly, it allows to easily identify satellite lines, characteristics of super-structures or incommensurate structures. Another advantage of measurements using NONIUS κ -CCD single crystal diffractometers is their κ -geometry (Fig. 5). The χ -circle in Eulerian geometry of a traditional four-circle diffractometer is here replaced by the κ -circle, the axis of which is tilted at 50° to the horizontal. It supports an arm carrying the goniometer head, with the ϕ -axis also tilted by 50° relative to κ . Using a combination of κ and ϕ settings, the crystal can be brought to most positions attainable by a χ rotation in Eulerian geometry. Using the κ geometry, it is easier to find space for a cooling device to be installed than in the case of Eulerian geometry.

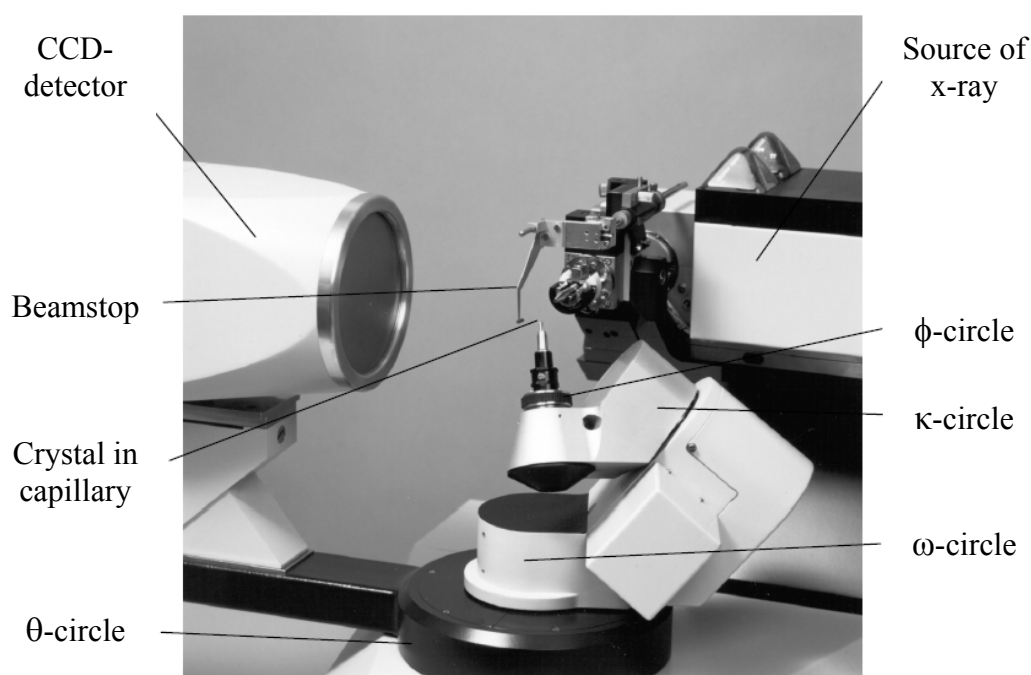


Fig. 5: The NONIUS κ -CCD single crystal diffractometer

2.3.1.4 Crystal Structure Solution and Refinement

When the data reduction is completed, the space group should be determined afterwards. This is achieved by finding out to which crystallographic point group and which Bravais lattice the crystal structure belongs and then combining them usefully. Similar to neutrons and electrons, X-rays interact with a crystal structure in a way that the resulting diffraction pattern is always centrosymmetric, regardless of whether an inversion center is present in the crystal structure or not. Therefore, the absolute structure of non-centrosymmetric space groups can not be determined by any diffraction method using coherent X-ray sources. This property of radiation leads to the fact that only 11 distinct Laue groups out of 32 crystal classes can be identifiable without intensity analysis. The absolute structure of a centrosymmetric space group can be examined by applying the Friedel law, but that one of a non-centrosymmetric space group can not be elucidated. To find out the correct absolute structures in non-centrosymmetric space groups, an anomalous X-ray scattering investigation is the best option to be carried out. If one or more symmetry elements of a space group include translation components, there are systematic absences of definite diffracted spots. As a result, the determination of the Bravais lattice of this kind of space group can not rely on the information of measured diffracted spots only, but also on that of absent spots. Since the systematic absences are determined by crystallographic symmetry rules, Bravais lattice and translational symmetry elements of the investigated crystal can be determined. Based on the dataset of the data collection and data reduction the space group can often be chosen by using the computer program X-RED [65]. The fourth step of the crystal structure determination, also called structure solution, begins after the above-mentioned information about unit cell, crystal system, space group and peak intensities are obtained. The task of this step is solving the phase problem by determining the phase angle for each structure factor, which can not be obtained readily from the experiment [66]. The solution of a crystal structure is almost always a result of successive approximations, making use of the fact that the repeating structure and the diffraction pattern are related to one another by Fourier analysis. In general, at the outset the usual situation is that the structure with known unit-cell contents, but unknown atomic positions and the diffraction pattern with its diffraction spots having known amplitudes, but unknown phases. In the crystal structure solution from X-ray diffraction data, this mutual relationship is actually established between the periodic array of electron density and the individual structure factors. This means that the structure factors as variables of the

phase problem determination are obtained when the elucidation of the electron density map, a more feasible task, is done. A crystal structure can generally be considered to be solved when most of the atoms have been located in the unit cell and therefore a structural model of the investigated crystal structure is built up. Using the computer program SHELXS-86 [67] or its update version SHELXS-97 [68], some atoms can be located in the unit cell either by "Patterson-Syntheses" or "Direct Methods" [69]. The choice of the best of these methods depends on individual problems such as size of the structure, presence of heavy atoms, occurrence of anomalous scattering, maximum resolution, and so forth. These methods are problematic when the crystal structure contains only some few heavy atoms against many light ones. By using Difference Fourier syntheses, the maximal residual electron density is localized, thus allowing to get information about the positions of the remaining atoms in the unit cell. After this step a list of atomic coordinates for some or all non-hydrogen atoms is obtained. However, frequently the atom types assigned to some of these coordinates are incorrect or no atom types have been assigned at all. In addition, the coordinates in this crystal structure solution are usually not very accurate: they might be within $\pm 0.1 \text{ \AA}$ apart from the correct positions. Moreover, many details of the structure are yet to be determined: groups of lighter atoms, disorders, hydrogen positions, etc. All these problems arise from the fact that the atomic positions in the first solution are not the direct result of the diffraction experiment, but an interpretation of the electron density calculated from the measured intensities and the "somehow-determined" initial phase angles. The entire procedure from the initial atomic positions to the complete, accurate and (if achievable) anisotropic model with all hydrogen positions is finally called refinement. When a suitable structure model was found, the computer programs SHELXL-93 [70] or SHELXL-97 [68] based on the "least-squares" method are utilized for optimization, firstly with isotropic temperature factors for all atoms, followed by a refinement with anisotropic temperature factors for all of them if possible. Results of a crystal structure solution and a refinement for some crystal structures having a moderate number of atoms in its unit cell are evaluated via following statistical crystallographic criteria. Firstly, to estimate how good the quality of a set of data appears, an internal residual value (R_{int}) must be calculated with the use of the computer programs SHELXL-93 or SHELXL-97. This value is defined as follows:

$$R_{\text{int}} = \frac{\sum_{i=1}^n |F_o^2 - \overline{F_o^2}|}{\sum_{i=1}^n F_o^2}$$

with n : number of measured reflections,
 F_o^2 : square of the observed structure amplitude,
 $\overline{F_o^2}$: average square of the symmetry equivalent of the observed structure amplitude,

and

$$R_\sigma = \frac{\sum_{i=1}^n \sigma(F_o^2)}{\sum_{i=1}^n F_o^2}$$

with $\sigma(F_o^2)$: standard uncertainty of the observed reflections.

To estimate the agreement of the crystallographic data and the structural model, different factors of qualities are calculated. Due to the fact that the various reflections making up the whole data set have not been measured with the same accuracy, the weight w has to be taken into account in estimating both the structure factors and the intensities. The weighted R-factor is directly related to the quantity that minimized in the least squares refinement and its changes show whether changes in the structure model are meaningful. From SHELXL-93 or SHELXL-97 the directly minimized value is wR_2 , which incorporates the reflection weights, and it is defined as follows:

$$wR_2 = \sqrt{\frac{\sum_{i=1}^n w(F_o^2 - F_c^2)^2}{\sum_{i=1}^n w(F_o^2)^2}}$$

with w : weight factor,
 F_c^2 : square of the calculated structure amplitude.

This weight factor itself is defined by:

$$w = [\sigma^2(F_o^2) + (aP)^2 - bP]^{-1}$$

with $P = \frac{1}{3}(F_o^2 + 2(F_c^2))$ and a and b are parameters to minimize the difference in the variances for reflections in different ranges of intensity and the actual diffraction angle.

Besides the received value of wR_2 there is also the conventional unweighted index R-value (R_1) given in this work, defined as follows:

$$R_1 = \frac{\sum_{i=1}^n ||F_o| - |F_c||}{\sum_{i=1}^n |F_o|}$$

but this one is not obtained from the squares of the observable structure amplitudes, but only from their (non-observable) amounts. The advantages of calculating and quoting this index together with wR_2 are that this provides a comparison with older work in literature, for it is generally considerably smaller than wR_2 for F^2 -refinements, and it is relatively insensitive to changes in the weighting scheme, which dramatically alter for wR_2 . Another quality criterion for a structural model is the “factor of quality” (“Goodness of Fit”, GooF): it is a useful index oftenly output by least squares refinement programs or a measure of the degree, to which the found distribution of differences between $|F_o|$ and $|F_c|$ fits the distribution expected from the weights used in the refinement. It is defined as:

$$\text{GooF} = S = \sqrt{\frac{\sum_{i=1}^n w(F_o^2 - F_c^2)^2}{n - p}}$$

with p as the number of refined parameters and n as the number of reflections. The degree of the structure parameters’ agreement is related to the difference $n - p$. With a suitable weighting scheme, which implies that the errors in the data are strictly random and correctly estimated, and if the model properly represents the structure that gives rise to the data, this value must be close to *one*. To obtain a publishable result of the crystal structure determination, not only the above-mentioned crystallographic criteria, but also other factors such as chemical reasonableness or chemical and physical properties of the crystal are necessary to be taken into account.

2.3.1.5 Devices and Computer Programs

All devices and licensed computer programs used for the analyses and structural investigations of new crystal structures are listed in the Table 2 and 3, respectively. They are available in the research group of Prof. Dr. Thomas Schleid, Institute of Inorganic Chemistry, University of Stuttgart.

Table 2: List of used devices

Apparatus	Model	Manufacturer
Microscope	SZ 40	OLYMPUS, Hamburg
Powder diffractometer	STADI P	STOE & CIE, Darmstadt
Single crystal diffractometer	IPDS	STOE & CIE, Darmstadt
Single crystal diffractometer	κ -CCD	BRUKER-NONIUS, Karlsruhe

Table 3: List of used computer programs

Program	Ref.	Function
STOE WinX ^{POW}	[71]	Program for recording, analysis and simulation of powder diffraction data and for operating the STOE STADI-P powder diffractometer
X-SHAPE	[64]	Program for numerical absorption correction (IPDS and CCD data)
X-RED	[65]	Program for space group regulation and numerical absorption correction (based on X-SHAPE)
SHELXS-86	[67]	Program for crystal structure determination
SHELXL-93	[70]	Program for crystal structure refinement
SHELX-97	[68]	Program packet as update version of SHELXS-86 and SHELXL-93
X-STEP 32	[72]	Working interface, which supports SHELXS-97 and SHELXL-97 to be processed
MAPLE 4.0	[73]	Program for the calculation of interatomic distances and angles, effective coordination numbers, and lattice energies from crystal structure data
DIAMOND 2.0	[74]	Program for the graphical presentation of molecules, coordination polyhedra, unit cells and crystal structures

2.3.2 Thermal Analysis

Temperature and pressure are two important thermodynamic variables of a chemical system. Usually, the physical and chemical properties of solid objects depend on temperature more variable than on pressure. Changing the temperature of a solid object leads to changes in its thermodynamic behaviour such as polymorphic transformations, melting, evaporation, decomposition and reactions to the gas atmosphere. These changes can be characterized by measuring the physical and chemical properties of substances. Thermal analysis means the analysis of the change in a property of an object, which is related to an imposed temperature alteration [75]. The term "thermal analysis" is common for all experimental methods used to measure at least one certain feature of the investigated object during a continuous or stepwise change of temperature [76]. It includes therefore a series of measurements, in which physical and chemical properties of a substance or a mixture of substances (even a reaction mixture) is measured as a function of temperature or time. These are, for example, measurements of changes in dimension (dilatometry), in mechanical properties (thermomechanometry), in mass (thermogravimetry), in temperature (differential thermal analysis), and in specific heat or enthalpy (calorimetry). In order to investigate the nature of thermal effects several thermoanalytical methods are oftenly combined. In a narrower sense, the term "thermal analysis" is only referred to experimental methods involving the changes of temperature, heat or mass. These are the differential thermal analysis (DTA), the dynamic calorimetry (DSC), and the thermogravimetry (TG). By using Difference Thermal Analysis (DTA), the temperature at which a phase transformation takes place, as well as the accompanying thermal effects (exothermic and endothermic reactions) are detected. Investigated sample and a standard reference are heated at a same heating rate in a furnace. The temperature difference ΔT between the sample and the reference as a function of time is measured by a thermocouple (Fig. 6). The sample and the reference have the same temperature as long as no thermal effects or reactions occur in the sample, thus both thermovoltages are the same and cancel each another. When a thermal effect or reaction occurs in the sample the corresponding voltage difference will be amplified and registered. The temperature difference between the furnace and the reference is recorded. Both thermal effect and temperature are shown on the DTA curve. A Differential Scanning Calorimetry (DSC) analyzer measures the energy changes that occur as a sample is heated, cooled or held isothermally, together with the temperature, at which these changes occur, while the change in the heat flux rate of the sample against a reference sample as a function of time is recorded. The temperature

difference between the sample and the reference can be best detected after an appropriate heat calibration. The relationship between the temperature difference and the heat flux difference is given as follows:

$$\Delta T = T_{sm} - T_{rm} = -RT(dT/dt)(C_s - C_r)$$

with T_{sm} : Measured temperature of the sample,
 T_{rm} : Measured temperature of the reference,
 R : Instrumental constant,
 C_s : Heat capacity of the sample,
 C_r : Heat capacity of the reference.

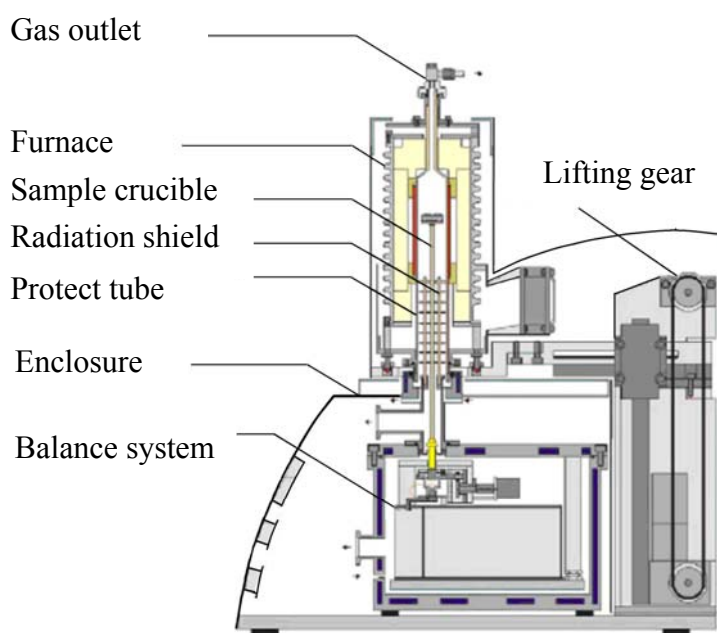


Fig. 6: View of the DTA / TG apparatus STA 449 (Netzsch)

The DSC analyzer Netzsch DSC 404 was used to measure the samples in this work. Its electrically controlled furnace with a resistive Pt/Rh-alloy wire allows working up to 1500 °C (Fig. 7). Another popular thermal analysis technique is by thermogravimetry (TG), in which the mass or the mass change of a substance is measured as a function of temperature, whilst the substance is subjected to a controlled temperature program. The mass change of a sample, which is heated with a constant heating rate in a furnace, is recorded continuously. The results of a thermogravimetric investigation often facilitate the interpretation of the corresponding DTA curve and a combination of DTA and TG measurements is very useful in practice.

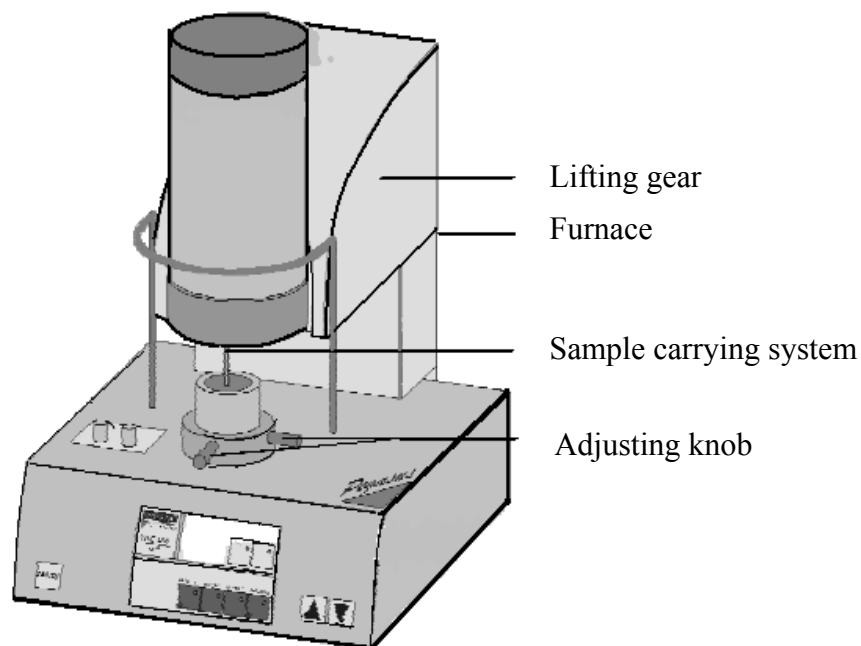


Fig. 7: View of the DSC 204 Phoenix (Netzsch)

2.3.3 Nuclear Magnetic Resonance Spectroscopy

As mentioned previously (Section 2.1), single crystal X-ray diffraction is the most preferable method to obtain the structure of a pure crystalline compound in the solid phase. Suitable crystals for measurements with this method are, however, not always easily accessible. Even if the single crystals can be obtained, they may be not representative for the solution or the solid they came from. Another factor needed to be taken into account is that the whole process of growing crystals, obtaining and determining a crystal structure is a time consuming procedure. Moreover, many problems such as isomer identification, hydrogen atom detection, and mechanism of a chemical reaction can not be solved to obtain a complete structural feature of a compound, if using the single crystal X-ray diffraction method exclusively. There are many spectroscopic methods that have been well developed to date. Among them, Nuclear Magnetic Resonance (NMR) spectroscopy is one of the most widely used and important physical techniques available to the modern practical chemist [77–79]. This method is applied to investigate properties of a molecular arrangement, in which atomic nuclei have a non-zero nuclear spin I . The most widely studied nuclei possess the spin $I = 1/2$ such as ^1H , ^{13}C , ^{19}F , ^{31}P , but there are a number of common nuclei, which have greater magnetic moments such as ^7Li

with $I = 3/2$, ^{10}B with $I = 3$, and ^{11}B with $I = 3/2$, for example. In the absence of a magnetic field all the magnetic states of a nucleus having non-zero nuclear spin are degenerate. However, this is no longer the case, if the nucleus is placed in an external magnetic field when a number of allowed orientations can be adopted:

$$m = I, I - 1, I - 2, \dots, 0, \dots, -I + 2, -I + 1, -I$$

with m : nuclear magnetic quantum number.

This results in a total of $(2 \cdot I + 1)$ possible orientations, from which transitions resulting in a change of $\Delta m = \pm 1$ are allowed. It is this splitting of the otherwise degenerate energy levels in a magnetic field that makes NMR spectroscopy possible. As the simplest case, the transition between energy levels of a nucleus with spin $I = 1/2$ is chosen for discussion (Fig. 8). When this nucleus is placed in a magnetic field two spin states arise ($m = +1/2$, $m = -1/2$) and a transition between two energy levels is possible with the difference between these two states given by:

$$\Delta E = \gamma \cdot \hbar \cdot B_0,$$

where B_0 is the strength of the applied magnetic field, and γ is the gyromagnetic ratio for the nucleus under study. The frequency of radiation that corresponds to this energy is called the resonance frequency ν , which is given as follows:

$$2 \cdot \pi \cdot \nu = \gamma \cdot B_0.$$

For the type of magnetic field strengths usually applied (2 – 14 Tesla) this corresponds to radiation within the radio frequency part of the electromagnetic spectrum. The ratio of the equilibrium nuclear spin populations in the upper and lower states is related to their energy difference and given by the Boltzmann distribution. For example, for a set of protons that resonate at 200 MHz at 298 K, the population ratio $n_{\text{upper}}/n_{\text{lower}}$ is 0.999975. Because of this small difference in nuclear spin populations, the NMR technique, from spectroscopic point of view, has just a relatively weak effect. To obtain the resonance phenomenon, a magnetic field B_1 is applied perpendicular to the magnetic field B_0 to flip over the nuclear moments. Information from a NMR spectrum is given by the positions of the resonance lines and their splitting patterns, both of which reflect the chemical environment of the nucleus. The numbers of line sets represent the numbers of distinct chemical environments, and a good

indication of the structure of a molecule can normally be obtained from its NMR spectrums alone. When the chemically distinct positions of the isotope can be distinguished via spin coupling between non-equivalent magnetically active nuclei, more useful information can be obtained such as the position of atoms in a molecule and its type of isomer. This can be done

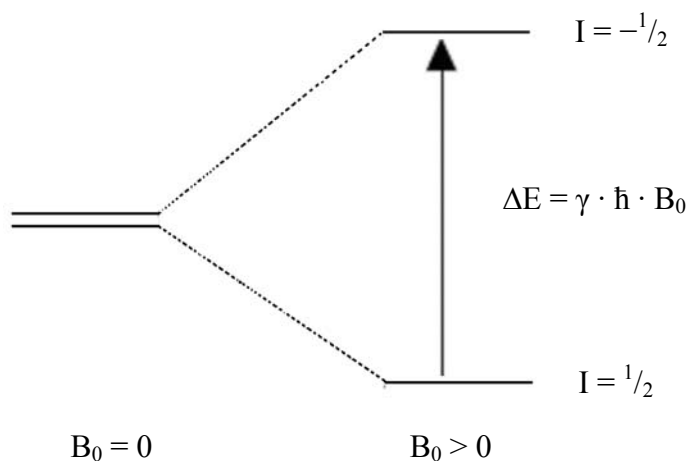


Fig. 8: Energy levels for a nucleus with spin $I = 1/2$ in an externally applied magnetic field

by interpretation of the splitting pattern in a NMR spectrum. The interpretation, however, is often more difficult the larger the number of potential coupling interactions, either due to chemical or magnetic non-equivalence, becomes. This problem is solved by decoupling NMR measurements, in which nuclei belonging to one group of chemical or magnetic equivalent species are irradiated at their specific resonance frequency to induce rapid transitions between the possible spin orientations. Neighbouring nuclei belonging to other groups of chemical or magnetic equivalent atoms then only see a single, averaged field, rather than the distinct field, for the different spin orientations of the nuclear magnetic moments of the irradiated nuclei. If the splitting of lines can not be distinguished by 1D-NMR spectroscopy, multidimensional NMR measurements needed to be carried out to assign the spectral lines [80].

The measurement of the one-dimensional solution ^{11}B -NMR spectra was carried out at 128.38 MHz with a Bruker AM 400 spectrometer equipped with a multinuclear sample head and standard broadband decoupling. D_2O was used as both solvent and internal lock signal. The chemical shift values are evaluated using $\text{BF}_3(\text{O}(\text{C}_2\text{H}_5)_2)$ as a standard. All samples were measured at room temperature only.

3 Dodecahydro-*closo*-Dodecaborate Salts

3.1 Dithallium(I) Dodecahydro-*closo*-Dodecaborate

Studies on the synthesis of dithallium(I) dodecahydro-*closo*-dodecaborate $\text{Tl}_2[\text{B}_{12}\text{H}_{12}]$ have been carried out by Muetterties *et al.* [16] and Kuznetsov *et al.* [81] already. The title compound has been reported to be obtained by a metathesis reaction between thallium(I) hydroxide TlOH and the free acid $(\text{H}_3\text{O})_2[\text{B}_{12}\text{H}_{12}]$. Recently, even the luminescence properties of $\text{Tl}_2[\text{B}_{12}\text{H}_{12}]$ have been studied, but its crystal structure was never determined so far [82].

3.1.1 Synthesis of $\text{Tl}_2[\text{B}_{12}\text{H}_{12}]$

The free acid $(\text{H}_3\text{O})_2[\text{B}_{12}\text{H}_{12}]$, which is required for the preparation of $\text{Tl}_2[\text{B}_{12}\text{H}_{12}]$ as well as many other dodecahydro-*closo*-dodecaborate salts, was prepared by passing an aqueous solution of $\text{Cs}_2[\text{B}_{12}\text{H}_{12}]$ (Strem: 98 %) through a strong acidic cation exchange column (DOWEX-50 WX8). The title compound was prepared by neutralizing the aqueous solution of the free acid $(\text{H}_3\text{O})_2[\text{B}_{12}\text{H}_{12}]$ with dithallium(I) carbonate Tl_2CO_3 (Merck: 99.9 %). Colourless, transparent, octahedral single crystals were obtained by recrystallization of the crude product from hot water. In comparison with reported dodecahydro-*closo*-dodecaborate salts of the heavy alkali metals, the title compound has a significantly lower water solubility. A suitable single crystal was selected for X-ray single crystal measurements at room temperature. The crystal structure determination and structure refinement was then carried out with all atoms (Tl, B and H) involved.

3.1.2 Structure Description of $\text{Tl}_2[\text{B}_{12}\text{H}_{12}]$

The title compound crystallizes in space group $\text{Fm}\bar{3}$ (no. 202) with four formula units per unit cell. This cubic crystal structure of $\text{Tl}_2[\text{B}_{12}\text{H}_{12}]$ (Fig. 9) is isostructural to that one of the dodecahydro-*closo*-dodecaborates with the heavy alkali metal cations (K^+ , Rb^+ and Cs^+) reported previously [83, 84]. It can be described as an *anti*- CaF_2 -type arrangement, in which the Tl^+ cations occupy all tetrahedral interstices within a cubic closest packed host lattice of

the *quasi*-icosahedral $[\text{B}_{12}\text{H}_{12}]^{2-}$ -cluster dianions. The Tl^+ cations thus reside at the special *Wyckoff* position $8c$ ($x/a = y/b = z/c = 1/4$; site symmetry: $23.$) and are tetrahedrally coordinated by four nearest neighbour $[\text{B}_{12}\text{H}_{12}]^{2-}$ units. So twelve hydrogen atoms belonging to four triangular faces of these clusters provide an almost perfect cuboctahedral coordination sphere for each Tl^+ cation ($d(\text{Tl}-\text{H}) = 296$ pm, $12\times$; Fig. 10). The *quasi*-icosahedral cage is formed by twelve boron atoms, each having an *exo*-polyhedral hydrogen bond. Boron and hydrogen atoms of the *quasi*-icosahedral $[\text{B}_{12}\text{H}_{12}]^{2-}$ -cluster anions are both located at the *Wyckoff* position $48h$ ($x/a = 1/2, y/b, z/c$; site symmetry: $m.$). The icosahedral anion exhibits its center of gravity at the special *Wyckoff* position $4a$ ($x/a = y/b = z/c = 0$; site symmetry: $m\bar{3}$) with 171 pm distance to each of the twelve cage boron atoms (Fig. 11). The intracluster bond distances are 179 pm ($1\times$) and 181 pm ($4\times$) for the B–B bonds and 112 pm for the B–H bonds, a quite typical range for dodecahydro-*closo*-dodecaborate anions [83, 84]. Within the series of $\text{A}_2[\text{B}_{12}\text{H}_{12}]$ -type compounds, the lattice constant of $\text{Tl}_2[\text{B}_{12}\text{H}_{12}]$ ($a \approx 1076$ pm) ranges

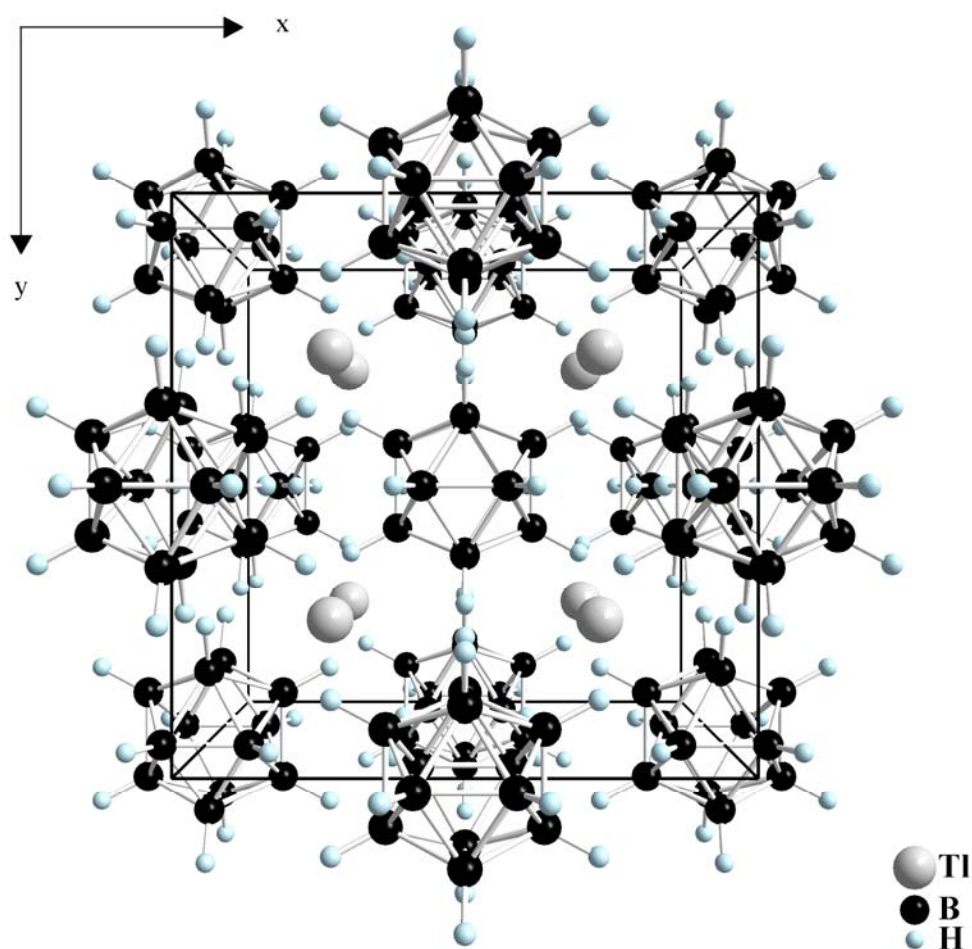


Fig. 9: Central projection of a unit cell of the crystal structure of $\text{Tl}_2[\text{B}_{12}\text{H}_{12}]$

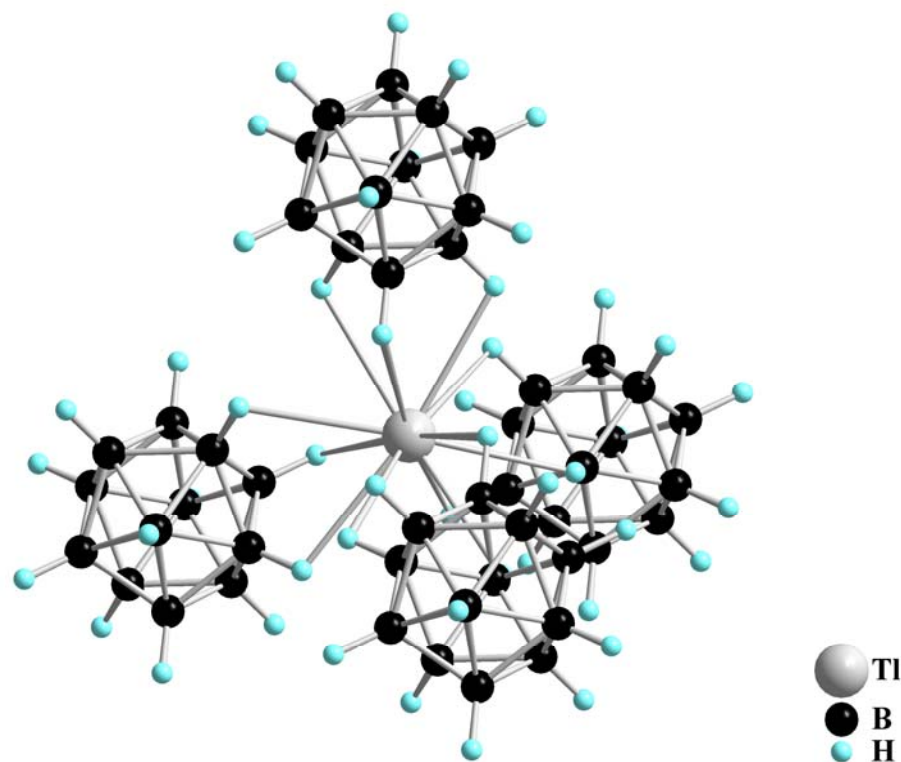


Fig. 10: View of the tetrahedral coordination sphere made of four $[\text{B}_{12}\text{H}_{12}]^{2-}$ -cluster anions around each Tl^+ cation in the crystal structure of $\text{Tl}_2[\text{B}_{12}\text{H}_{12}]$

between that one of $\text{K}_2[\text{B}_{12}\text{H}_{12}]$ ($a \approx 1063$ pm) and $\text{Rb}_2[\text{B}_{12}\text{H}_{12}]$ ($a \approx 1087$ pm), but far below that of $\text{Cs}_2[\text{B}_{12}\text{H}_{12}]$ ($a \approx 1128$ pm) [84]. The same trend can be observed for the binary chlorides ACl (KCl : $a \approx 628$ pm, H.T.- TlCl : $a \approx 632$ pm, RbCl : $a \approx 654$ pm, and H.T.- CsCl : $a \approx 692$ pm) with NaCl-type crystal structure. Among the dodecahydro-*closo*-dodecaborate salts with alkali metal cations ($\text{A} = \text{Li} - \text{Cs}$) only those with the heavier ones (K^+ , Rb^+ and Cs^+) and also the ammonium compound (with the NH_4^+ cation, $a \approx 1088$ pm [85]) crystallize solvent-free from aqueous solution in a cubic *anti*-fluorite type structure according to $\text{A}_2[\text{B}_{12}\text{H}_{12}]$. On the other hand with Li^+ and Na^+ , just hydrated salts like $\text{Na}_2(\text{H}_2\text{O})_4[\text{B}_{12}\text{H}_{12}]$ [81] and $\text{Li}_2(\text{H}_2\text{O})_7[\text{B}_{12}\text{H}_{12}]$ [87] were obtained by reactions between the aqueous free acid $(\text{H}_3\text{O})_2[\text{B}_{12}\text{H}_{12}]$ and the corresponding hydroxides or carbonates at room temperature. In all compounds, isolated cage-like $[\text{B}_{12}\text{H}_{12}]^{2-}$ anions are found, however, in which twelve boron atoms form a nearly perfect icosahedron. While in aqueous solution free $[\text{B}_{12}\text{H}_{12}]^{2-}$ anions with the highest possible symmetry (I_h) are present, an icosahedron can not realize a fivefold axis of rotation in a crystalline solid. Thus a decrease of the anion symmetry by distortion is

necessary, in the case of $\text{Tl}_2[\text{B}_{12}\text{H}_{12}]$ from $\bar{5}\bar{3}2/m$ to $\bar{3}2/m$ together with the occurrence of two different values for the B–B bond lengths such as 179 pm (1 \times) and 181 pm (4 \times). The lone-pair electrons at the Tl^+ cations have obviously real $6s^2$ character and are therefore stereochemically inactive, in contrast to those of Bi^{3+} in $\text{Bi}(\text{H}_2\text{O})_2(\text{OH})[\text{B}_{12}\text{H}_{12}]$ and Pb^{2+} in $\text{Pb}(\text{H}_2\text{O})_3[\text{B}_{12}\text{H}_{12}] \cdot 3 \text{H}_2\text{O}$.

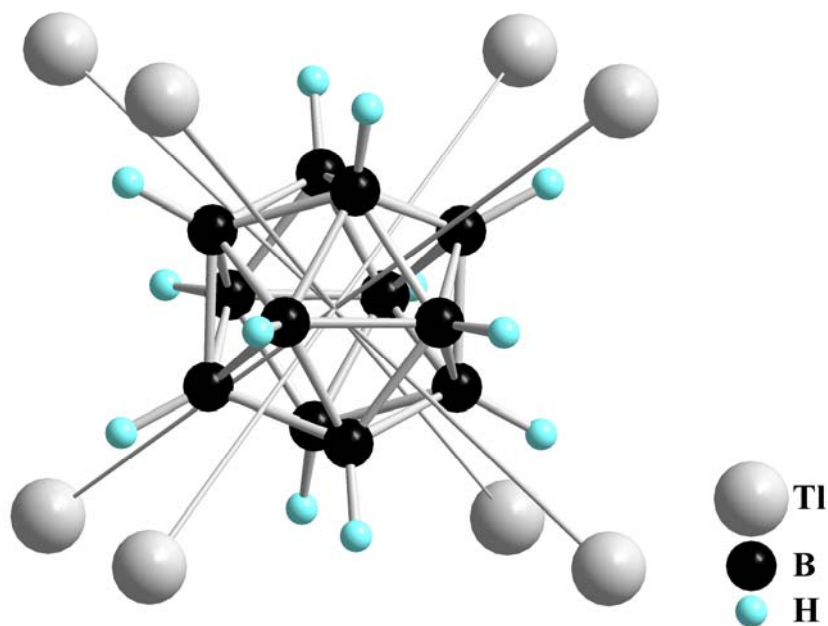


Fig. 11: View of the *quasi*-icosahedral $[\text{B}_{12}\text{H}_{12}]^{2-}$ -cluster dianion and its cube-shaped coordination sphere of eight Tl^+ cations in the crystal structure of $\text{Tl}_2[\text{B}_{12}\text{H}_{12}]$

Table 4: Crystallographic data for $Tl_2[B_{12}H_{12}]$ and their determination

Crystallographic data	
Crystal system	cubic
Space group	$Fm\bar{3}$ (no. 202)
Unit cell parameters: a (pm)	1075.51(6)
Number of formula units per unit cell	$Z = 4$
Calculated density ($D_x/g\text{ cm}^{-3}$)	2.939
Molar volume ($V_m/cm^3\text{ mol}^{-1}$)	183.7
Diffractometer	κ -CCD (Bruker-Nonius)
Radiation	Mo-K α : $\lambda = 71.07\text{ pm}$, graphite monochromator
Index range	$\pm h_{\max} = 23, \pm k_{\max} = 15, \pm l_{\max} = 9$
θ_{\max} (deg)	27.4
F(000)	936
Absorption coefficient (μ/mm^{-1})	10.97
Absorption correction	numerical, Program X-SHAPE [64]
Other data corrections	background, polarization and <i>Lorentz</i> factors
Collected reflections	25544
Unique reflections	3489
$R_{\text{int}}, R_{\sigma}$	0.056, 0.037
Structure solution and refinement	Program SHELXS-97 and SHELXL-97 [68]
Scattering factors	International Tables for Crystallography, Vol. C [87]
R_1, R_1 with $ F_o \geq 4\sigma(F_o)$	0.039, 0.030
Reflections with $ F_o \geq 4\sigma(F_o)$	3015
wR_2 , Goodness of fit (GooF)	0.072, 1.039
Extinction (g)	0.0081(4)
Residual electron density (<i>max.</i> , <i>min.</i> in $\rho/e^{-1}\text{ 10}^6\text{ pm}$)	1.47, -1.31

Table 5: Atomic coordinates for $\text{Tl}_2[\text{B}_{12}\text{H}_{12}]$

Atom	Wyckoff position	x/a	y/b	z/c
Tl	8c	$1/4$	$1/4$	$1/4$
B	48h	0	0.0830(5)	0.1360(5)
H	48h	0	0.139(3)	0.224(3)

Table 6: Anisotropic thermal displacement coefficients^{a)} (U_{ij}/pm^2) for $\text{Tl}_2[\text{B}_{12}\text{H}_{12}]$

Atom	U_{11}	U_{22}	U_{33}	U_{23}	U_{13}	U_{12}
Tl	415(2)	U_{11}	U_{11}	0	0	0
B	309(23)	315(25)	315(24)	26(20)	0	0
H	501(77)					

^{a)} For Tl and B defined as anisotropic temperature factor according to: $\exp[-2\pi^2 (U_{11}h^2a^{*2} + U_{22}k^2b^{*2} + U_{33}l^2c^{*2} + 2U_{23}klb^*c^* + 2U_{13}hla^*c^* + 2U_{13}hka^*b^*)]$; for H isotropically defined as temperature factor in: $\exp[-8\pi^2(U_{\text{iso}}\sin^2\theta/\lambda^2)]$.

Table 7: Selected interatomic distances (d/pm) for $\text{Tl}_2[\text{B}_{12}\text{H}_{12}]$

$[\text{B}_{12}\text{H}_{12}]^{2-}$ anion:		Tl^+ coordination:	
B1 – B	178.5 (1×)	Tl – H	295.5 (12×)
– B'	180.6 (4×)	– B	345.4 (12×)
– H	112.2 (1×)	– Tl	537.5 (6×)

3.2 Dodecahydro-*closo*-Dodecaborates with Divalent Cations

3.2.1 Mercury(II) Dodecahydro-*closo*-Dodecaborate

Apart from $A_2[B_{12}H_{12}]$ ($A = K, Rb, Cs; NH_4, Tl$), non-solvent containing dodecahydro-*closo*-dodecaborate salts can be expected only with those cations having strong polarizing properties such as Au^+ , Ag^+ , Cu^+ or Hg^{2+} . Dodecahydro-*closo*-dodecaborates of these cations are water insoluble and a strong interaction between cation and $[B_{12}H_{12}]^{2-}$ anion is expected in these salts. The synthesis and some physical and chemical properties of the above solvent-free salts have been reported already, but their crystallographic data are still not available in literature. Crystal growing of these dodecahydro-*closo*-dodecaborates from aqueous solution is not straightforward due to their low solubility. Recently, the crystal structures of $AmAg[B_{12}H_{12}]$, $Am(AgL)_2Ag[B_{12}H_{12}]_2$, $(AgL)_2[B_{12}H_{12}]$ (Am : benzyltriethylammonium, L : acetonitrile) were published. In these compounds the observed $Ag-H$ distances cover a broad range from 193 to 264 pm [88]. In this work, the synthesis and crystal structure determination of non-solvent containing mercury(II) dodecahydro-*closo*-dodecaborate was studied, after all attempts to produce $Ag_2[B_{12}H_{12}]$ had failed.

3.2.1.1 Synthesis of $Hg[B_{12}H_{12}]$

Mercury(II) dodecahydro-*closo*-dodecaborate was prepared by the reaction between $Hg(NO_3)_2$ (Merck: 99.9 %) and an aqueous solution of the free acid $(H_3O)_2[B_{12}H_{12}]$. The mixture was then left for 60 days. Colourless, polyhedral single crystals were obtained by recrystallization of the filtered precipitate from water and subsequent isothermal evaporation of the resulting solution at room temperature. Suitable single crystals were selected for X-ray diffraction measurements and the crystal structure of $Hg[B_{12}H_{12}]$ was elucidated as the first non-solvent containing dodecahydro-*closo*-dodecaborate with a divalent metal cation.

3.2.1.2 Structure Description of $Hg[B_{12}H_{12}]$

The title compound crystallizes triclinically in space group $P\bar{1}$ (no. 2) with seven formula units per unit cell (Fig. 12). The Hg^{2+} cations ($Hg1 - Hg4$) are located at four crystallographically distinct *Wyckoff* positions. In this crystal structure, $Hg1$ resides at the

special *Wyckoff* site $1h$ ($x/a = y/b = z/c = 1/2$; site symmetry: $\bar{1}$), while Hg2, Hg3 and Hg4 are occupying the general *Wyckoff* sites $2i$ ($x/a, y/b, z/c$; site symmetry: 1). All four different *quasi*-icosahedral $[\text{B}_{12}\text{H}_{12}]^{2-}$ -cluster anions are coordinated by eight nearest Hg^{2+} cations arranged as an almost perfect cube (Fig. 13). The $\text{Hg}\cdots\text{Hg}$ distances range at about 565 pm. The coordination environment of the mercury cations is similar to that one of Hg^{2+} in HgF_2 and the A^+ cations in non-solvent containing $\text{A}_2[\text{B}_{12}\text{H}_{12}]$ -type compounds ($\text{A} = \text{K} - \text{Cs}; \text{NH}_4, \text{Tl}$). However, each Hg^{2+} cation is cubically surrounded by eight *quasi*-icosahedral $[\text{B}_{12}\text{H}_{12}]^{2-}$ -cluster anions, which have their centers of gravity at distances from 487 to 489 pm apart from

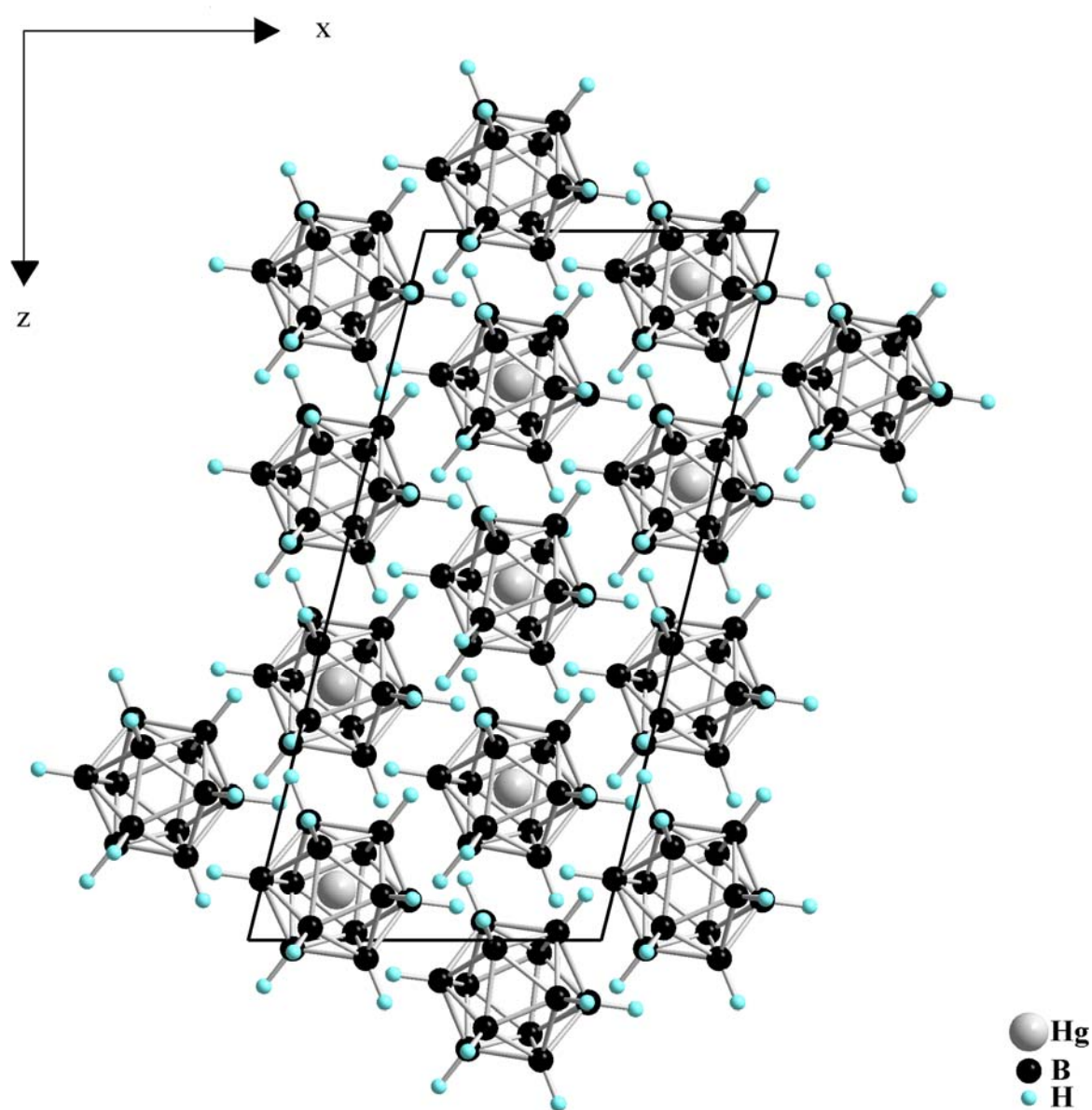


Fig. 12: View of a unit cell of the crystal structure of $\text{Hg}[\text{B}_{12}\text{H}_{12}]$ along $[010]$

the Hg^{2+} cations (Fig. 14). Thus the crystal structure of $\text{Hg}[\text{B}_{12}\text{H}_{12}]$ can be described as a CsCl-type structure. The shortest distances from Hg^{2+} to the hydrogen atoms of the nearest $[\text{B}_{12}\text{H}_{12}]^{2-}$ -cluster anions range from 304 to 328 pm. Unlike the unusual short Cu–B bonds ($d(\text{Cu}-\text{B}) = 214 - 233$ pm) in $\text{Cu}_2[\text{B}_{10}\text{H}_{10}]$ [12] and Ag–H bonds in $\text{AmAg}[\text{B}_{12}\text{H}_{12}]$, $\text{Am}(\text{AgL})_2\text{Ag}[\text{B}_{12}\text{H}_{12}]_2$, and $(\text{AgL})_2[\text{B}_{12}\text{H}_{12}]$ (*Am*: benzyltriethylammonium, *L*: acetonitrile) ($d(\text{Ag}-\text{H}) = 193 - 264$ pm), the observed $\text{Hg}\cdots\text{H}$ distances in $\text{Hg}[\text{B}_{12}\text{H}_{12}]$ are far too long to be covalent bonds [88]. All boron and hydrogen atoms of the *quasi*-icosahedral $[\text{B}_{12}\text{H}_{12}]^{2-}$ anions are located at the *Wyckoff* positions $2i$. The centers of gravity cluster anions for the boron cages reside at three crystallographically different *Wyckoff* positions $2i$ and one *Wyckoff* site $1f$ ($x/a = z/c = 1/2$, $y/b = 0$; symmetry: $\bar{1}$; Fig. 15). The B–B bond lengths of *quasi*-icosahedral $[\text{B}_{12}\text{H}_{12}]^{2-}$ -cluster anions cover a wide range from 169 to 189 pm, reflecting their strong distortion from ideal icosahedra.

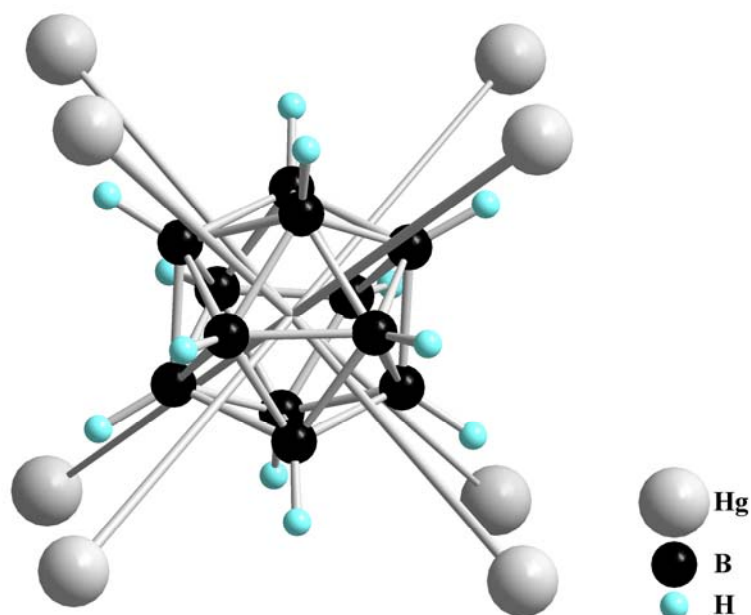


Fig. 13: View of a *quasi*-icosahedral $[\text{B}_{12}\text{H}_{12}]^{2-}$ -cluster dianion and its cube-shaped coordination sphere of eight Hg^{2+} cations in the crystal structure of $\text{Hg}[\text{B}_{12}\text{H}_{12}]$

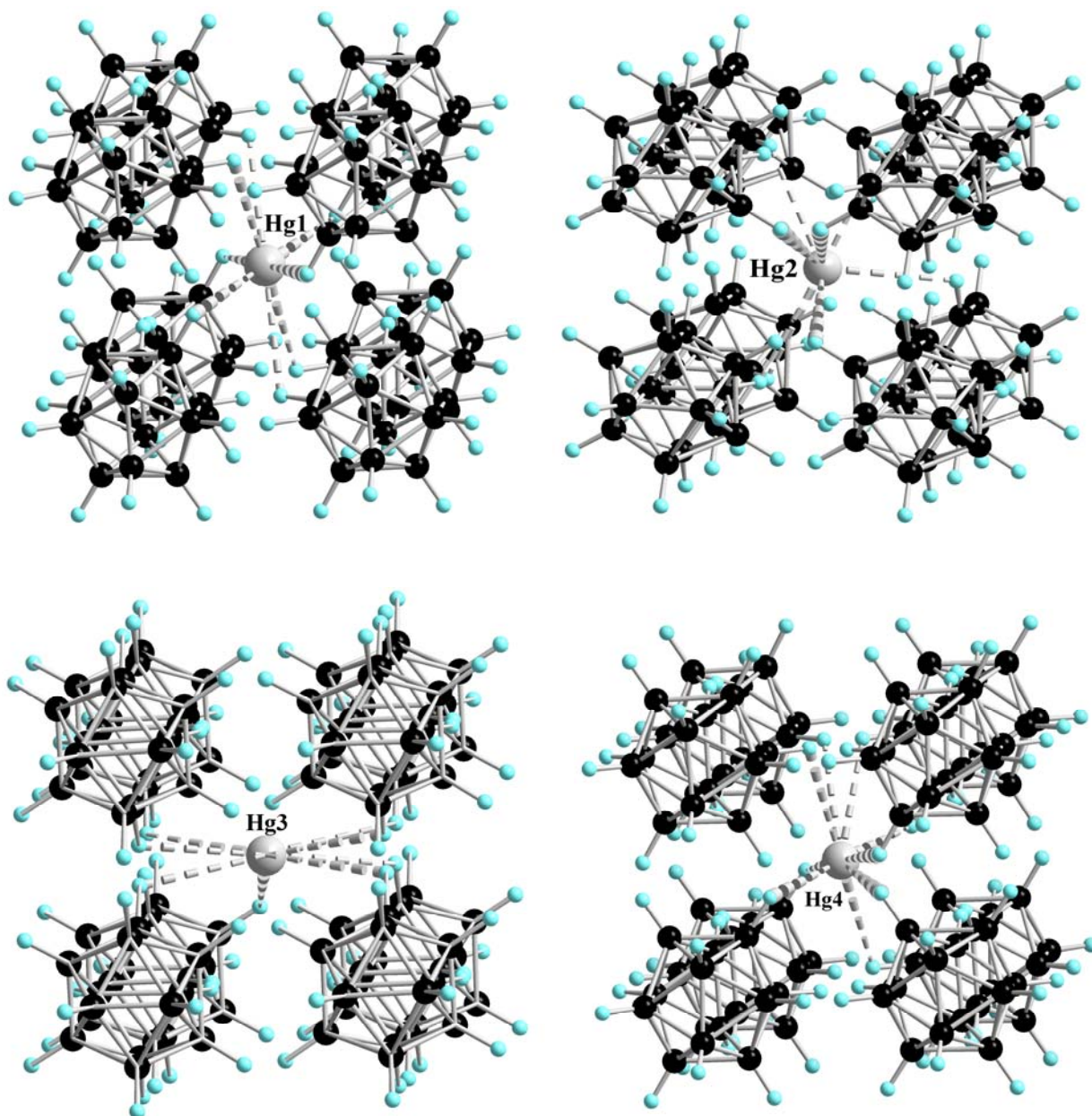


Fig. 14: Cubical arrangement of the *quasi*-icosahedral $[B_{12}H_{12}]^{2-}$ -clusters around four crystallographically different Hg^{2+} cations (*top left*: Hg1 at $x/a = y/b = z/c = 1/2$; *top right*: Hg2 at $x/a \approx 0.768$, $y/b \approx 0.3754$, $z/c \approx 0.071$; *bottom left*: Hg3 at $x/a \approx 0.368$, $y/b \approx 0.072$, $z/c \approx 0.214$; *bottom right*: Hg4 at $x/a \approx 0.929$, $y/b \approx 0.786$, $z/c \approx 0.357$)

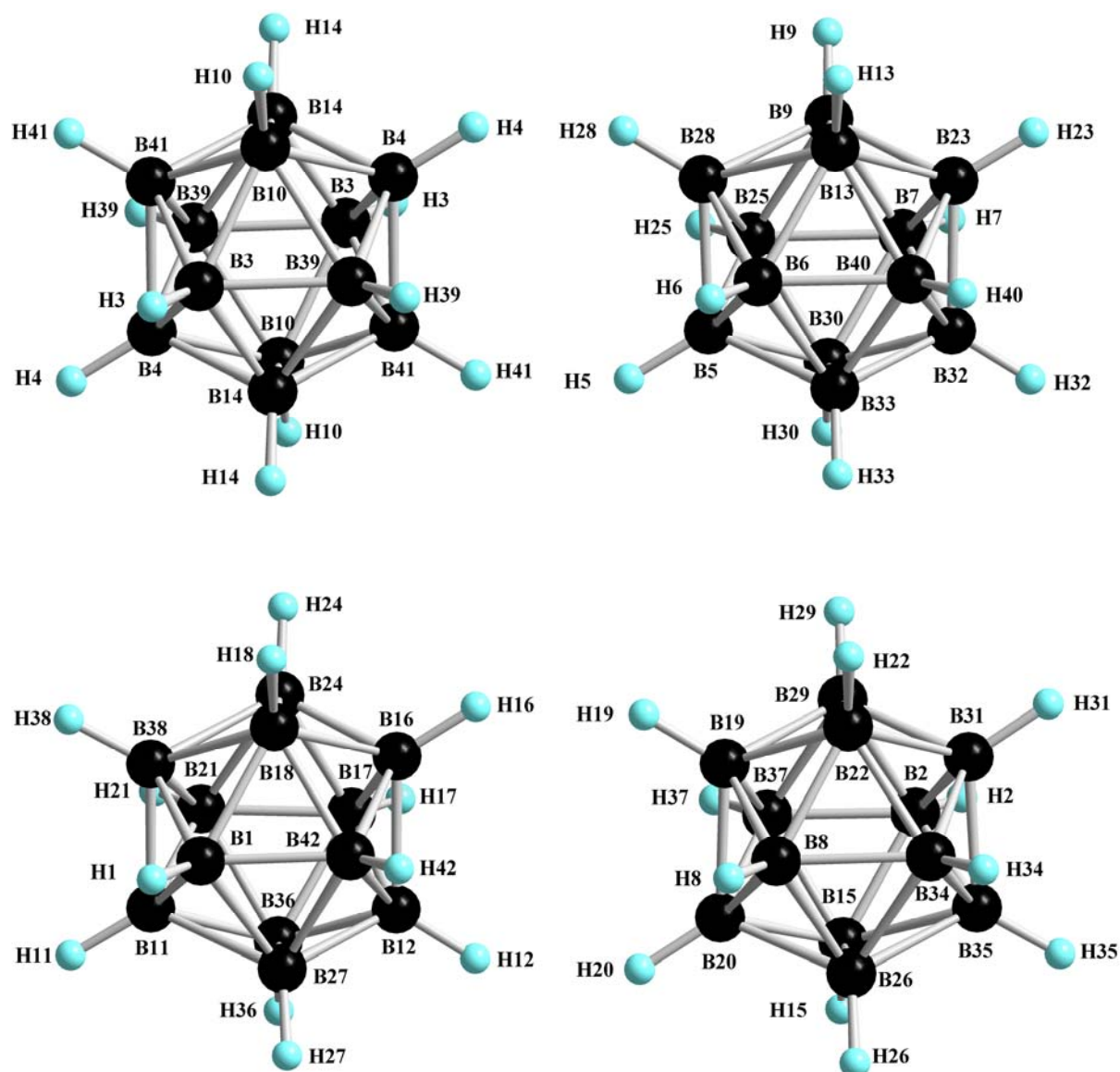


Fig. 15: View of the four crystallographically independent *quasi*-icosahedral $[B_{12}H_{12}]^{2-}$ cluster anions in the crystal structure of $Hg[B_{12}H_{12}]$ (*top left*: center of gravity at $x/a = z/c = 1/2, y/b = 0$; *top right*: center of gravity at $x/a \approx 0.216, y/b \approx 0.114, z/c \approx 0.071$; *bottom left*: center of gravity at $x/a \approx 0.928, y/b \approx 0.287, z/c \approx 0.358$; *bottom right*: center of gravity at $x/a \approx 0.357, y/b \approx 0.571, z/c \approx 0.214$)

Table 8: Crystallographic data for Hg[B₁₂H₁₂] and their determination

Crystal system	triclinic
Space group	P $\bar{1}$ (no. 2)
Unit cell parameters:	
a (pm)	798.69(4)
b (pm)	978.21(5)
c (pm)	1694.12(9)
α (deg)	101.105(3)
β (deg)	103.630(3)
γ (deg)	90.027(3)
Number of formula units per unit cell	Z = 7
Calculated density (D _x /g cm ⁻³)	3.157
Molar volume (V _m /cm ³ mol ⁻¹)	108.5
Diffractometer	κ -CCD (Bruker-Nonius)
Radiation	Mo-K α : λ = 71.07 pm, graphite monochromator
Index range	$\pm h_{\max} = 10, \pm k_{\max} = 13, \pm l_{\max} = 22$
θ_{\max} (deg)	28.3
F(000)	1064
Absorption coefficient (μ /mm ⁻¹)	21.26
Absorption correction	numerical, Program X-SHAPE [64]
Other data corrections	background, polarization and <i>Lorentz</i> factors
Collected reflections	27927
Unique reflections	6183
R _{int} , R _{σ}	0.130, 0.092
Reflections with $ F_o \geq 4\sigma(F_o)$	1434
Structure solution and refinement	Program SHELXS-97 and SHELXL-97 [68]
Scattering factors	International Tables for Crystallography, Vol. C [87]
R ₁ , R ₁ with $ F_o \geq 4\sigma(F_o)$	0.121, 0.114
wR ₂ , Goodness of fit (GooF)	0.187, 1.117
Extinction (g)	0.0011(1)
Residual electron density	
(<i>max.</i> , <i>min.</i> in ρ/e^{-1} 10 ⁶ pm)	1.42, -0.96

Table 9: Atomic coordinates for Hg[B₁₂H₁₂]

Atom	Wyckoff position	x/a	y/b	z/c
Hg1	1 <i>h</i>	$\frac{1}{2}$	$\frac{1}{2}$	$\frac{1}{2}$
Hg2	2 <i>i</i>	0.78574(1)	0.37515(1)	0.07138(1)
Hg3	2 <i>i</i>	0.35699(1)	0.07156(1)	0.21431(1)
Hg4	2 <i>i</i>	0.92876(1)	0.78567(1)	0.35719(1)
B1	2 <i>i</i>	0.1585(4)	0.7178(4)	0.5609(2)
B2	2 <i>i</i>	0.4400(4)	0.5764(4)	0.1362(3)
B3	2 <i>i</i>	0.5790(8)	0.0073(4)	0.4166(3)
B4	2 <i>i</i>	0.3724(5)	0.8613(3)	0.4923(3)
B5	2 <i>i</i>	0.9172(5)	0.9967(4)	0.0816(3)
B6	2 <i>i</i>	0.1323(5)	0.1352(5)	0.0120(2)
B7	2 <i>i</i>	0.6990(6)	0.8507(4)	0.1525(2)
B8	2 <i>i</i>	0.2694(6)	0.5633(5)	0.2928(3)
B9	2 <i>i</i>	0.8633(5)	0.7352(4)	0.1315(2)
B10	2 <i>i</i>	0.5621(6)	0.8473(4)	0.4525(3)
B11	2 <i>i</i>	0.7894(5)	0.1459(4)	0.3473(2)
B12	2 <i>i</i>	0.1378(5)	0.2551(3)	0.3727(2)
B13	2 <i>i</i>	0.8328(6)	0.6972(5)	0.0177(2)
B14	2 <i>i</i>	0.4250(6)	0.1162(5)	0.4397(3)
B15	2 <i>i</i>	0.4093(6)	0.4159(3)	0.1597(2)
B16	2 <i>i</i>	0.0580(6)	0.4296(5)	0.3660(3)
B17	2 <i>i</i>	0.0171(5)	0.2871(4)	0.2772(2)
B18	2 <i>i</i>	0.8727(6)	0.4450(5)	0.4077(3)
B19	2 <i>i</i>	0.1479(5)	0.5992(5)	0.2026(3)
B20	2 <i>i</i>	0.2239(6)	0.4260(5)	0.2081(2)
B21	2 <i>i</i>	0.8023(5)	0.2224(4)	0.2607(3)
B22	2 <i>i</i>	0.2978(6)	0.7268(4)	0.2656(3)
B23	2 <i>i</i>	0.3499(5)	0.2839(5)	0.9369(2)
B24	2 <i>i</i>	0.8567(5)	0.4115(4)	0.2999(2)
B25	2 <i>i</i>	0.9124(6)	0.9236(5)	0.9236(5)
B26	2 <i>i</i>	0.4342(5)	0.4526(4)	0.2722(3)
B27	2 <i>i</i>	0.9885(6)	0.8261(6)	0.5817(3)
B28	2 <i>i</i>	0.0065(6)	0.8274(5)	0.0872(2)

Table 9: (continued)

Atom	Wyckoff position	x/a	y/b	z/c
B29	2i	0.2789(4)	0.6867(4)	0.1549(3)
B30	2i	0.7334(5)	0.0115(5)	0.1228(3)
B31	2i	0.4824(6)	0.7115(3)	0.2213(3)
B32	2i	0.5726(6)	0.8861(5)	0.0567(3)
B33	2i	0.2964(6)	0.0284(4)	0.9889(2)
B34	2i	0.4809(6)	0.6386(5)	0.3112(3)
B35	2i	0.5748(6)	0.5488(4)	0.2300(3)
B36	2i	0.9839(4)	0.1310(4)	0.3101(2)
B37	2i	0.7640(6)	0.4932(4)	0.8810(3)
B38	2i	0.7133(5)	0.3113(4)	0.3429(3)
B39	2i	0.3702(5)	0.9375(4)	0.4054(2)
B40	2i	0.3468(6)	0.2068(5)	0.0256(3)
B41	2i	0.2931(6)	0.0289(5)	0.4864(3)
B42	2i	0.9492(6)	0.6456(4)	0.5473(3)
H1 ^{a)}	2i	0.214	0.722	0.508
H2 ^{a)}	2i	0.498	0.580	0.084
H3 ^{a)}	2i	0.629	0.012	0.362
H4 ^{a)}	2i	0.287	0.770	0.486
H5 ^{a)}	2i	0.004	0.088	0.088
H6 ^{a)}	2i	0.077	0.128	0.065
H7 ^{a)}	2i	0.643	0.846	0.205
H8 ^{a)}	2i	0.211	0.557	0.345
H9 ^{a)}	2i	0.914	0.658	0.170
H10 ^{a)}	2i	0.606	0.749	0.422
H11 ^{a)}	2i	0.700	0.056	0.340
H12 ^{a)}	2i	0.276	0.234	0.382
H13 ^{a)}	2i	0.863	0.597	-0.017
H14 ^{a)}	2i	0.379	0.193	0.400
H15 ^{a)}	2i	0.442	0.318	0.124
H16 ^{a)}	2i	0.144	0.521	0.371
H17 ^{a)}	2i	0.075	0.285	0.224
H18 ^{a)}	2i	0.835	0.545	0.440

Table 9: (continued)

Atom	Wyckoff position	x/a	y/b	z/c
H19 ^{a)}	2i	0.010	0.618	0.194
H20 ^{a)}	2i	0.140	0.335	0.205
H21 ^{a)}	2i	0.722	0.183	0.198
H22 ^{a)}	2i	0.261	0.826	0.298
H23 ^{a)}	2i	0.437	0.374	0.941
H24 ^{a)}	2i	0.812	0.492	0.263
H25 ^{a)}	2i	0.993	0.968	0.230
H26 ^{a)}	2i	0.486	0.375	0.310
H27 ^{a)}	2i	0.933	0.899	0.542
H28 ^{a)}	2i	0.145	0.809	0.097
H29 ^{a)}	2i	0.228	0.761	0.115
H30 ^{a)}	2i	0.700	0.112	0.156
H31 ^{a)}	2i	0.565	0.804	0.225
H32 ^{a)}	2i	0.435	0.907	0.048
H33 ^{a)}	2i	0.349	-0.047	0.028
H34 ^{a)}	2i	0.560	0.682	0.374
H35 ^{a)}	2i	0.715	0.535	0.241
H36 ^{a)}	2i	0.019	0.029	0.280
H37 ^{a)}	2i	0.844	0.535	0.944
H38 ^{a)}	2i	0.574	0.326	0.333
H39 ^{a)}	2i	0.284	0.895	0.345
H40 ^{a)}	2i	0.430	0.248	0.087
H41 ^{a)}	2i	0.155	0.048	0.478
H42 ^{a)}	2i	0.869	0.601	0.485

^{a)} refinement with DFIX constraint ($d(\text{B-H}) = 110 \text{ pm}$); $U_{\text{iso}}(\text{H}) = 1.2 \cdot U_{\text{iso}}(\text{B})$.

Table 10: Anisotropic thermal displacement coefficients^{a)} (U_{ij}/pm^2) for $\text{Hg}[\text{B}_{12}\text{H}_{12}]$

Atom	U_{11}	U_{22}	U_{33}	U_{23}	U_{13}	U_{12}
Hg1	281(8)	285(7)	285(7)	59(6)	62(6)	-1(6)
Hg2	266(6)	266(5)	263(5)	51(4)	61(4)	-1(4)
Hg3	363(7)	371(6)	361(6)	71(5)	91(5)	21(5)
Hg4	527(9)	554(8)	513(8)	96(6)	123(7)	46(6)
B1	178(149)	429(180)	372(172)	36(142)	100(130)	-1(129)
B2	66(130)	402(179)	735(257)	221(177)	26(144)	-15(120)
B3	913(368)	426(207)	390(204)	269(174)	128(213)	-104(213)
B4	435(200)	112(119)	398(174)	18(115)	59(149)	30(119)
B5	226(161)	357(168)	619(226)	106(157)	287(162)	2(130)
B6	367(207)	690(261)	222(154)	-105(160)	34(142)	-95(185)
B7	653(283)	397(191)	245(164)	-51(142)	33(167)	-26(183)
B8	431(226)	515(222)	483(216)	-1(177)	210(180)	-197(182)
B9	293(182)	471(198)	426(194)	118(161)	64(150)	7(150)
B10	613(273)	361(185)	366(191)	-21(152)	25(179)	-137(178)
B11	475(199)	453(199)	432(197)	-115(159)	308(180)	-242(176)
B12	413(200)	263(149)	372(175)	29(130)	111(150)	86(136)
B13	748(271)	481(155)	207(124)	92(118)	-1(143)	234(209)
B14	560(270)	588(250)	334(191)	-42(176)	-4(179)	-247(212)
B15	719(286)	190(141)	305(168)	-34(124)	82(171)	-135(156)
B16	426(228)	558(242)	380(198)	-8(177)	-59(168)	129(186)
B17	401(203)	501(202)	213(147)	-125(138)	106(139)	178(163)
B18	631(284)	650(250)	576(248)	401(221)	408(228)	221(217)
B19	299(196)	500(222)	581(242)	82(188)	57(175)	1(164)
B20	573(268)	695(276)	216(162)	-142(169)	113(166)	-13(215)
B21	225(164)	446(190)	396(184)	61(153)	-111(139)	73(141)
B22	440(225)	447(204)	473(214)	196(174)	34(175)	101(169)
B23	359(201)	727(267)	422(199)	456(204)	3(158)	-61(181)
B24	460(220)	430(191)	335(175)	23(146)	209(160)	169(163)
B25	414(219)	648(250)	267(166)	-47(162)	116(155)	200(187)
B26	303(185)	492(207)	641(241)	261(185)	344(182)	167(156)
B27	506(266)	957(32)	481(234)	353(49)	221(206)	-48(246)
B28	705(305)	706(272)	286(176)	-121(178)	362(199)	-231(233)

Table 10: (continued)

Atom	U ₁₁	U ₂₂	U ₃₃	U ₂₃	U ₁₃	U ₁₂
B29	191(153)	307(159)	560(215)	162(150)	-104(144)	-121(125)
B30	348(204)	554(229)	435(203)	125(176)	45(164)	208(173)
B31	423(231)	269(170)	873(327)	234(192)	-39(216)	110(154)
B32	374(211)	619(250)	467(215)	208(193)	45(171)	-139(184)
B33	577(254)	304(165)	335(177)	-15(136)	158(168)	30(159)
B34	750(324)	729(287)	404(211)	303(209)	345(218)	191(131)
B35	445(225)	350(179)	539(224)	115(163)	230(185)	30(157)
B36	204(152)	322(157)	383(172)	65(131)	-8(128)	-193(127)
B37	547(252)	491(194)	423(198)	239(164)	159(180)	126(172)
B38	154(158)	505(217)	839(304)	275(212)	15(173)	-159(149)
B39	368(198)	361(175)	349(177)	-38(141)	-30(148)	42(147)
B40	356(211)	526(226)	517(229)	137(185)	43(174)	-103(174)
B41	719(329)	563(251)	461(229)	176(196)	198(219)	302(229)
B42	750(328)	318(188)	533(243)	134(174)	-62(218)	-156(194)
H1	392					
H2	477					
H3	666					
H4	392					
H5	442					
H6	551					
H7	552					
H8	568					
H9	476					
H10	570					
H11	537					
H12	421					
H13	793					
H14	638					
H15	508					
H16	598					
H17	472					
H18	643					

Table 10: (continued)

Atom	U ₁₁	U ₂₂	U ₃₃	U ₂₃	U ₁₃	U ₁₂
H19	566					
H20	628					
H21	468					
H22	542					
H23	565					
H24	476					
H25	547					
H26	503					
H27	722					
H28	666					
H29	450					
H30	540					
H31	645					
H32	579					
H33	490					
H34	672					
H35	507					
H36	399					
H37	521					
H38	597					
H39	472					
H40	567					
H41	673					
H42	676					

^{a)} For Hg and B defined as anisotropic temperature factor according to: $\exp[-2\pi^2 (U_{11}h^2a^{*2} + U_{22}k^2b^{*2} + U_{33}l^2c^{*2} + 2U_{23}klb^*c^* + 2U_{13}hla^*c^* + 2U_{13}hka^*b^*)]$; for H defined as isotropic temperature factor in: $\exp[-8\pi^2(U_{\text{iso}}\sin^2\theta/\lambda^2)]$.

Table 11: Selected interatomic distances (d/pm) for Hg[B₁₂H₁₂]

[HgH ₈] polyhedra:					
Hg1 – H18	314.4 (2×)			Hg2 – H29	312.9
– H34	315.1 (2×)			– H23	314.6
– H4	315.8 (2×)			– H28	316.6
– H16	318.9 (2×)			– H30	317.2
				– H2	317.8
				– H23	318.8
				– H19	320.3
				– H24	321.9
Hg3 – H3	305.7			Hg4 – H24	303.7
– H11	307.8			– H35	305.8
– H17	308.6			– H10	308.1
– H6	309.9			– H22	309.2
– H20	311.6			– H36	309.3
– H31	311.6			– H39	309.8
– H5	314.2			– H27	310.1
– H32	316.2			– H9	315.8
[B ₁₂ H ₁₂] ²⁻ anions:					
B1 – B42	176.0	B2 – B37	170.3	B3 – B14	169.4
– B27	178.1	– B15	172.3	– B39	175.6
– B38	178.3	– B31	172.4	– B4	177.2
– B11	180.8	– B29	172.7	– B10	180.2
– B18	180.7	– B35	176.5	– B41	181.7
– H1	110.0	– H2	110.0	– H3	110.0
B4 – B14	173.7	B5 – B25	175.5	B6 – B33	174.6
– B39	177.0	– B30	176.3	– B40	179.7
– B41	177.1	– B6	180.3	– B5	180.3
– B3	177.2	– B28	181.4	– B13	184.4
– B10	179.1	– B33	182.3	– B28	188.2
– H4	110.0	– H5	110.0	– H6	110.0

Table 11: (*continued*)

B7	– B23	170.0	B8	– B19	170.6	B9	– B7	178.7
	– B30	178.1		– B20	173.4		– B23	180.6
	– B25	178.3		– B26	176.0		– B28	183.0
	– B9	178.7		– B22	177.6		– B25	183.8
	– B32	179.3		– B34	177.6		– B13	184.8
	– H7	110.0		– H8	110.0		– H9	110.0
B10	– B41	168.2	B11	– B38	173.8	B12	– B27	168.8
	– B14	177.0		– B21	179.3		– B36	173.2
	– B4	179.1		– B36	180.4		– B17	176.3
	– B3	180.2		– B1	180.8		– B42	178.9
	– B39	186.1		– B27	188.1		– B16	183.8
	– H10	110.0		– H11	110.0		– H12	110.0
B13	– B23	179.6	B14	– B3	169.4	B15	– B37	172.3
	– B40	180.2		– B4	173.7		– B2	172.3
	– B6	184.4		– B39	175.3		– B26	183.4
	– B9	184.8		– B41	176.6		– B20	184.9
	– B28	189.3		– B10	177.0		– B35	187.5
	– H13	110.0		– H14	110.0		– H15	110.0
B16	– B24	171.6	B17	– B12	176.3	B18	– B24	176.6
	– B18	178.0		– B36	176.3		– B42	177.2
	– B42	177.9		– B21	176.8		– B16	178.0
	– B17	180.9		– B16	180.9		– B1	180.8
	– B12	183.8		– B24	182.3		– B38	182.3
	– H16	110.0		– H17	110.0		– H18	110.0
B19	– B8	170.6	B20	– B12	173.4	B21	– B17	176.8
	– B22	173.6		– B36	176.1		– B38	178.9
	– B29	177.3		– B21	181.3		– B11	179.3
	– B20	181.3		– B16	184.9		– B36	182.2
	– B37	181.5		– B24	185.4		– B24	185.5
	– H19	110.0		– H20	110.0		– H21	110.0

Table 11: (continued)

B22 – B19	173.6	B23 – B7	177.0	B24 – B16	171.6
– B8	177.6	– B32	178.9	– B18	176.6
– B34	179.1	– B13	179.6	– B17	182.3
– B31	180.0	– B9	180.6	– B21	185.5
– B29	181.0	– B40	181.2	– B38	186.3
– H22	110.0	– H23	110.0	– H24	110.0
B25 – B5	175.5	B26 – B8	176.0	B27 – B12	168.8
– B30	176.2	– B20	176.1	– B42	175.3
– B7	178.8	– B34	181.5	– B36	176.1
– B28	181.9	– B35	181.8	– B1	178.1
– B9	183.8	– B15	183.4	– B11	188.1
– H25	110.0	– H26	110.0	– H27	110.0
B28 – B5	181.4	B29 – B2	172.7	B30 – B5	176.3
– B25	181.9	– B31	173.1	– B25	176.2
– B9	183.0	– B37	175.4	– B7	178.1
– B6	188.2	– B19	177.3	– B32	178.9
– B13	189.3	– B22	181.0	– B33	181.5
– H28	110.0	– H29	110.0	– H30	110.0
B31 – B2	172.4	B32 – B33	173.8	B33 – B32	173.8
– B29	173.1	– B40	176.7	– B6	174.6
– B35	177.2	– B23	178.9	– B40	174.8
– B22	180.0	– B30	178.9	– B30	181.5
– B34	180.6	– B7	179.3	– B5	182.3
– H31	110.0	– H32	110.0	– H33	110.0
B34 – B8	177.6	B35 – B2	176.5	B36 – B12	173.2
– B22	179.1	– B31	177.2	– B27	176.1
– B35	180.2	– B34	180.2	– B17	176.3
– B31	180.6	– B26	181.5	– B11	180.4
– B26	181.8	– B15	187.5	– B21	182.2
– H34	110.0	– H35	110.0	– H36	110.0

Table 11: (*continued*)

B37	– B2	170.4	B38	– B11	173.8	B39	– B41	172.9
	– B15	172.3		– B1	178.3		– B14	175.4
	– B29	175.4		– B21	178.9		– B3	175.6
	– B19	181.5		– B18	182.3		– B4	177.0
	– B20	185.4		– B24	186.3		– B10	186.1
	– H37	110.0		– H38	110.0		– H39	110.0
<hr/>								
B40	– B33	174.8	B41	– B10	168.2	B42	– B27	175.3
	– B32	176.7		– B39	172.9		– B1	176.0
	– B6	179.7		– B14	176.6		– B18	177.2
	– B13	180.3		– B4	177.1		– B16	177.9
	– B23	181.2		– B3	181.7		– B12	178.9
	– H40	110.0		– H41	110.0		– H42	110.0

3.2.2 Hexaaqua-Nickel(II) Dodecahydro-*closo*-Dodecaborate Hexahydrate

Since 1960, we know that the hydrated dodecahydro-*closo*-dodecaborate salt with Ni²⁺ cations can be synthesized [16]. By metathesis reactions between nickel(II) carbonate NiCO₃ and the free acid (H₃O)₂[B₁₂H₁₂] followed by drying the aqueous solution under vacuum at 100 °C (P₄O₁₀ was used as drying agent) and 25 °C, Ni[B₁₂H₁₂] · 5 H₂O and Ni(H₂O)₆[B₁₂H₁₂] · 0.25 H₂O were reported to be obtained, respectively. In addition, the synthesis of Ni(NH₃)₆[B₁₂H₁₂] · 0.5 H₂O, which is expected to be even more stable than the hydrated dodecahydro-*closo*-dodecaborate of nickel(II), has also been studied. However, the exact compositions and the crystal structures of all dodecahydro-*closo*-dodecaborate salts with Ni²⁺ cations either as aqua or as ammine complex have never been determined.

3.2.2.1 Synthesis of Ni(H₂O)₆[B₁₂H₁₂] · 6 H₂O

Greenish, bead-shaped single crystals of the title compound Ni(H₂O)₆[B₁₂H₁₂] · 6 H₂O were obtained by neutralizing an aqueous solution of the free acid (H₃O)₂[B₁₂H₁₂] with NiCO₃ (Merck: 99.9 %) and subsequent isothermal evaporation of the resulting solution at room temperature.

3.2.2.2 Structure Description of Ni(H₂O)₆[B₁₂H₁₂] · 6 H₂O

The hexaaqua-nickel(II) dodecahydro-*closo*-dodecaborate hexahydrate crystallizes cubically in space group F4₃2 (no. 210) with eight formula units per unit cell. In this crystal structure, the Ni²⁺ cations reside at the special crystallographic *Wyckoff* position 8*a* ($x/a = y/b = z/c = 0$; site symmetry: 23.). The oxygen atoms are located at two crystallographically different *Wyckoff* positions: 48*f* ($x/a, y/b = z/c = 0$; site symmetry: 2..) and 48*g* ($x/a = 1/8, y/b, z/c$; site symmetry: ..2) (Table 13). All boron and hydrogen atoms occupy the general *Wyckoff* position 96*h* ($x/a, y/b, z/c$; site symmetry: 1). The center of gravity of the *quasi*-icosahedral [B₁₂H₁₂]²⁻-cluster anions lies at the *Wyckoff* position 8*b* ($x/a = y/b = z/c = 1/2$; site symmetry: 23.). The cubic crystal structure of Ni(H₂O)₆[B₁₂H₁₂] · 6 H₂O ($a = 1633.47(8)$ pm) (Fig. 16) is isostructural to that one of Mg(H₂O)₆[B₁₂H₁₂] · 6 H₂O ($a = 1643.21(9)$ pm) [89] and Co(H₂O)₆[B₁₂H₁₂] · 6 H₂O ($a = 1636.80(9)$ pm) [85]. Neglecting all water molecules, the crystal structure of the title compound can be best described as a NaTl-type arrangement (Fig.

17), in which the centers of gravity of the *quasi*-icosahedral $[\text{B}_{12}\text{H}_{12}]^{2-}$ -cluster anions occupy the positions of Ti^- , whereas the Ni^{2+} cations occupy the Na^+ positions. With the shortest $\text{Ni}\cdots\text{H}_{\text{Cluster}}$ distance of 499 pm, there is no direct contact between the counter-cation and exopolyhedral hydrogen atoms of the $[\text{B}_{12}\text{H}_{12}]^{2-}$ anions. Instead, the Ni^{2+} cations are octahedrally coordinated by six water molecules forming isolated hexaqua-complex cations $[\text{Ni}(\text{H}_2\text{O})_6]^{2+}$ ($d(\text{Ni}-\text{O}) = 203$ pm (6 \times) and $\angle(\text{O}-\text{Ni}-\text{O}) = 90^\circ$). Moreover, six “zeolitic” water molecules are located in the crystal structure for the formation of a strong classical $\text{O}-\text{H}^{\delta+}\cdots\delta^-\text{O}$ hydrogen bonding system ($d(\text{O1}-\text{H1w}) = 106$ pm, $d(\text{O2}-\text{H2w}) = 69$ pm, $d(\text{O1}\cdots\text{H2w}) = 233$ pm, 2 \times each; Fig. 18). The strong donor-acceptor interactions between oxygen atoms of “zeolitic” water molecules (O2w and H2w) and those of the $[\text{Ni}(\text{H}_2\text{O})_6]^{2+}$ coordination spheres (O1 and H1) are indicated by relative short $\text{O}_{\text{Donor}}\cdots\text{O}_{\text{Acceptor}}$ distances (274 pm for $\text{O1}\cdots\text{O2w}$, as compared with 287 pm for the $\text{O1}\cdots\text{O1}'$ intra-complex contacts). It

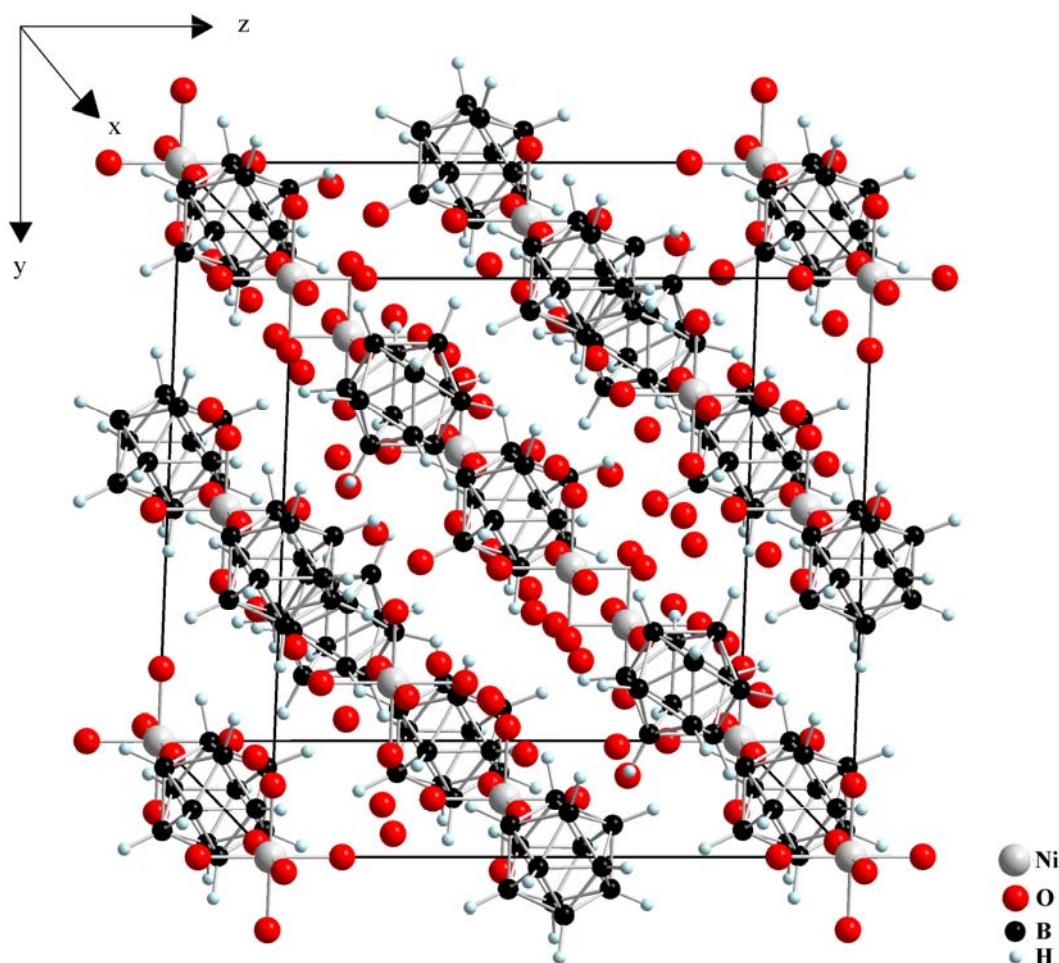


Fig. 16: View at a unit cell of the crystal structure of $\text{Ni}(\text{H}_2\text{O})_6[\text{B}_{12}\text{H}_{12}] \cdot 6 \text{H}_2\text{O}$ along $[100]$

can be concluded that $[\text{Ni}(\text{H}_2\text{O})_6]^{2+}$ itself is icosahedrally surrounded by twelve “zeolitic” water molecules (Fig. 19). Moreover, it becomes obvious that the existence of non-classical $\text{B}-\text{H}^{\delta-} \cdots \delta^+\text{H}-\text{O}$ hydrogen bridging bonds between the hydrogen atoms of water molecules and the hydrogen atoms of $[\text{B}_{12}\text{H}_{12}]^{2-}$ clusters ($d(\text{H}\cdots\text{H1w}) = 290$ and 294 pm, $d(\text{H}\cdots\text{H2w}) = 246$ pm; $1\times$ each) has also to be considered. In contrast, the cubic crystal structures of $\text{Mn}(\text{H}_2\text{O})_6[\text{B}_{12}\text{H}_{12}] \cdot 6 \text{H}_2\text{O}$ ($a = 1648.62(9)$ pm) [85] and $\text{Zn}(\text{H}_2\text{O})_6[\text{B}_{12}\text{H}_{12}] \cdot 6 \text{H}_2\text{O}$ ($a = 1637.43(9)$ pm) [90] can not be described isostructurally, but rather in the space group $F23$ (no. 196) with two crystallographically independent octahedral hexaqua-dications and some disorder at room temperature for one of them. The B–B and B–H bond lengths within the $[\text{B}_{12}\text{H}_{12}]^{2-}$ cage again range in rather typical intervals ($d(\text{B}-\text{B}) = 176 - 179$ pm, $d(\text{B}-\text{H}) = 117$ pm; Fig. 20).

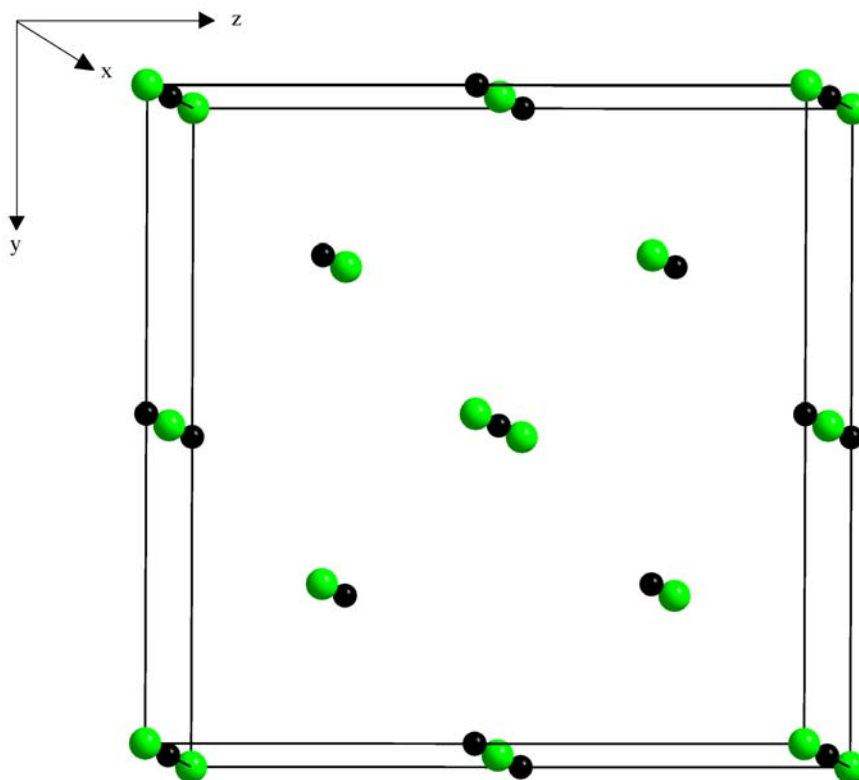


Fig. 17: View at the NaTl-type structure motif in $\text{Ni}(\text{H}_2\text{O})_6[\text{B}_{12}\text{H}_{12}] \cdot 6 \text{H}_2\text{O}$ (centers of gravity of the $[\text{B}_{12}\text{H}_{12}]^{2-}$ anions: small black circles; centers of gravity of the $[\text{Ni}(\text{H}_2\text{O})_6]^{2+}$ cations: large grey circles)

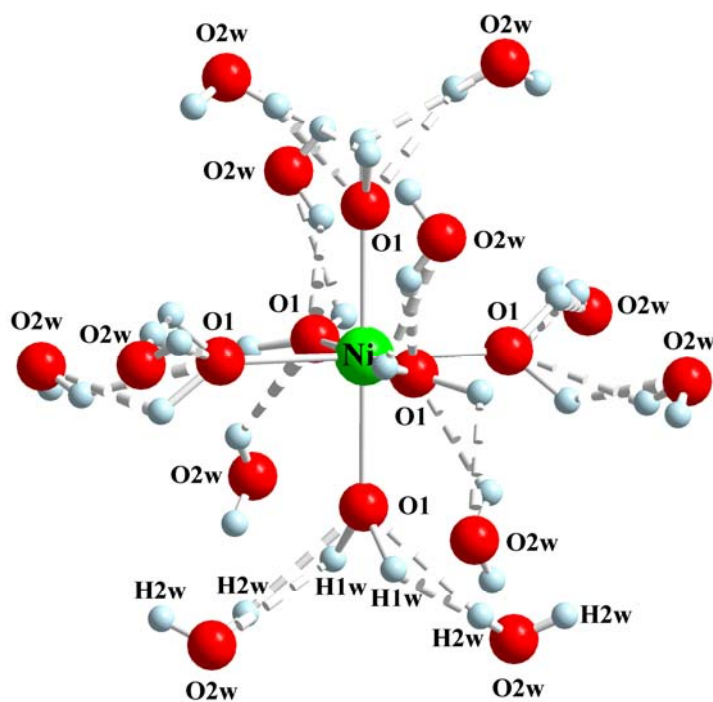


Fig. 18: The $\text{O}-\text{H}^{\delta+}\cdots\delta-\text{O}$ hydrogen bonding system of water molecules within the $[\text{Ni}(\text{H}_2\text{O})_6]^{2+}$ octahedra

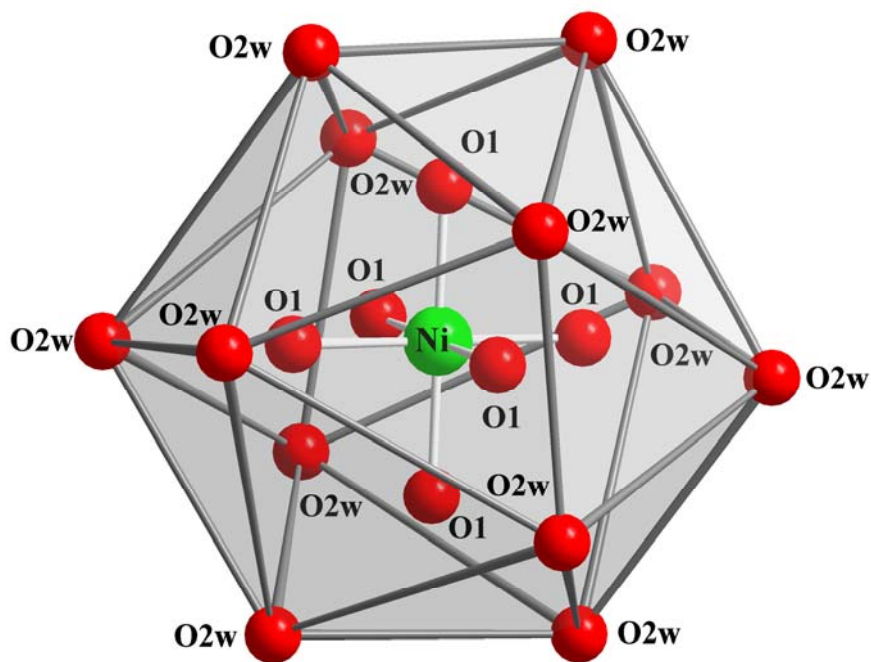


Fig. 19: Icosahedral arrangement of twelve “zeolitic” crystal water molecules (O2w) around each $[\text{Ni}(\text{H}_2\text{O})_6]^{2+}$ octahedron in the crystal structure of $\text{Ni}(\text{H}_2\text{O})_6[\text{B}_{12}\text{H}_{12}] \cdot 6 \text{H}_2\text{O}$

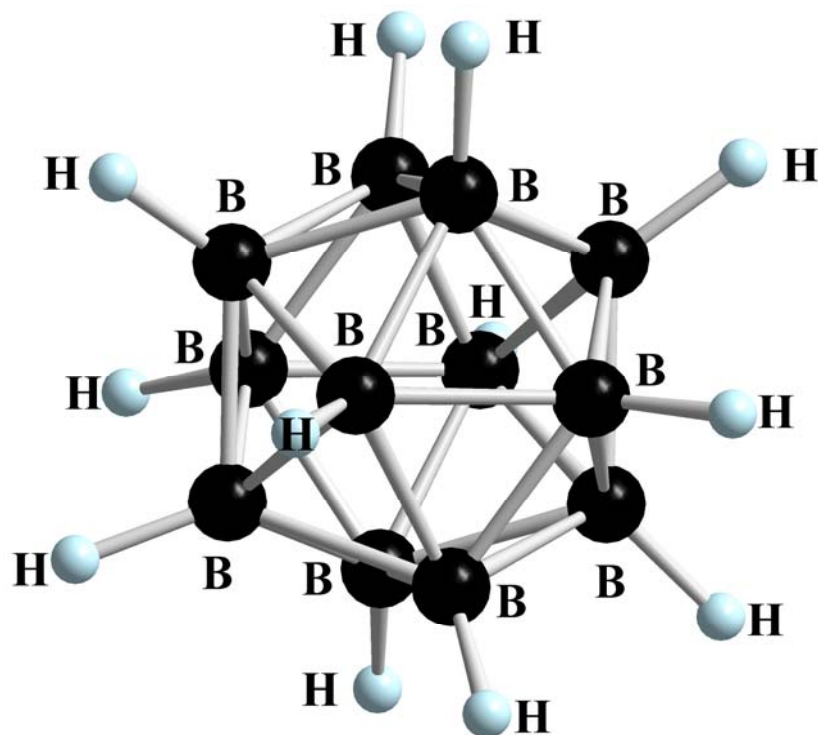


Fig. 20: The *quasi*-icosahedral $[B_{12}H_{12}]^{2-}$ -cluster anion in the crystal structure of $Ni(H_2O)_6[B_{12}H_{12}] \cdot 6 H_2O$

Table 12: Crystallographic data for Ni(H₂O)₆[B₁₂H₁₂] · 6 H₂O and their determination

Crystallographic data	
Crystal system	cubic
Space group	F4 ₃ 2 (no. 210)
Unit cell parameters: a (pm)	1633.47(8)
Number of formula units per unit cell	Z = 8
Calculated density (D _x /g cm ⁻³)	1.270
Molar volume (V _m /cm ³ mol ⁻¹)	328.9
Diffractometer	κ-CCD (Bruker-Nonius)
Radiation	Mo-Kα: λ = 71.07 pm, graphite monochromator
Index range	±h _{max} = 21, ±k _{max} = 21, ±l _{max} = 21
θ _{max} (deg)	27.3
F(000)	1760
Absorption coefficient (μ/mm ⁻¹)	0.93
Absorption correction	numerical, Program X-SHAPE [64]
Other data corrections	background, polarization and <i>Lorentz</i> factors
Collected reflections	5504
Unique reflections	421
R _{int} , R _σ	0.045, 0.018
Structure solution and refinement	Program SHELXS-97 and SHELXL-97 [68]
Scattering factors	International Tables for Crystallography, Vol. C [87]
R ₁ , R _w with F _o ≥ 4σ(F _o)	0.039, 0.032
Reflections with F _o ≥ 4σ(F _o)	404
wR ₂ , Goodness of fit (GooF)	0.098, 1.192
Extinction (g)	0.0073(3)
<i>Flack</i> -x-parameter	0.02(1)
Residual electron density (<i>max.</i> , <i>min.</i> in ρ/e ⁻¹ 10 ⁶ pm)	0.40, -0.41

Table 13: Atomic coordinates for Ni(H₂O)₆[B₁₂H₁₂] · 6 H₂O

Atom	Wyckoff position	x/a	y/b	z/c
Ni	8a	0	0	0
O1	48f	0.1254(5)	0	0
O2w	48g	1/8	0.0151(2)	0.2349(2)
B	96h	0.4119(2)	0.4997(3)	0.4456(2)
H	96h	0.353(3)	0.501(1)	0.519(1)
H1w	96h	0.172(2)	0.014(2)	0.041(2)
H2w	96h	0.089(3)	0.034(3)	0.230(3)

Table 14: Anisotropic thermal displacement coefficients^{a)} (U_{ij}/pm²) for Ni(H₂O)₆[B₁₂H₁₂] · 6 H₂O

Atom	U ₁₁	U ₂₂	U ₃₃	U ₂₃	U ₁₃	U ₁₂
Ni	472(7)	= U ₁₁	= U ₁₁	0	0	0
O1	891(41)	1147(54)	2103(100)	-3(37)	0	0
O2w	929(29)	615(16)	= U ₂₂	41(16)	-37(14)	= U ₁₃
B	498(19)	554(19)	478(16)	-13(3)	-8(4)	25(15)
H	555(98)					
H1w	1069(92)					
H2w	1198(114)					

^{a)} For Ni, O and B defined as anisotropic temperature factor according to: $\exp[-2\pi^2 (U_{11}h^2a^{*2} + U_{22}k^2b^{*2} + U_{33}l^2c^{*2} + 2U_{23}klb^*c^* + 2U_{13}hla^*c^* + 2U_{13}hka^*b^*)]$; for H isotropically defined as temperature factor in: $\exp[-8\pi^2(U_{\text{iso}}\sin^2\theta/\lambda^2)]$.

Table 15: Selected interatomic distances (d/pm) and angles (∠/deg) for Ni(H₂O)₆[B₁₂H₁₂] · 6 H₂O

[B ₁₂ H ₁₂] ²⁻ anion:		[NiO ₆] polyhedron:	
B – B	176.3 (2×)	Ni – O1	202.2 (6×)
– B'	179.0 (1×)	O1 – Ni – O1	180.0 (3×)
– B''	179.3 (2×)	O1 – Ni – O1'	90.0 (12×)
– H	117.0 (1×)		

3.2.2.3 Thermal Analysis of $\text{Ni}(\text{H}_2\text{O})_6[\text{B}_{12}\text{H}_{12}] \cdot 6 \text{H}_2\text{O}$

The thermal stability of $\text{Ni}(\text{H}_2\text{O})_6[\text{B}_{12}\text{H}_{12}] \cdot 6 \text{H}_2\text{O}$ was investigated by DTA/TG methods in argon atmosphere (Fig. 21). The compound loses four free water molecules at 183 °C corresponding to the first endothermic signal in the DTA curve. After losing three more water molecules at 215 °C, the compound containing only five water molecules is left behind and this composition apparently becomes thermally stable. Thus no further changes in the TG curve are observed up to 500 °C. The crystal structure of the remaining green compound $\text{Ni}[\text{B}_{12}\text{H}_{12}] \cdot n \text{H}_2\text{O}$ ($5 < n < 6$), which has been even mentioned since 1964 by Muetterties *et al.* in literature [16], would be interesting to know, but X-ray powder diffraction experiments revealed it to be amorphous.

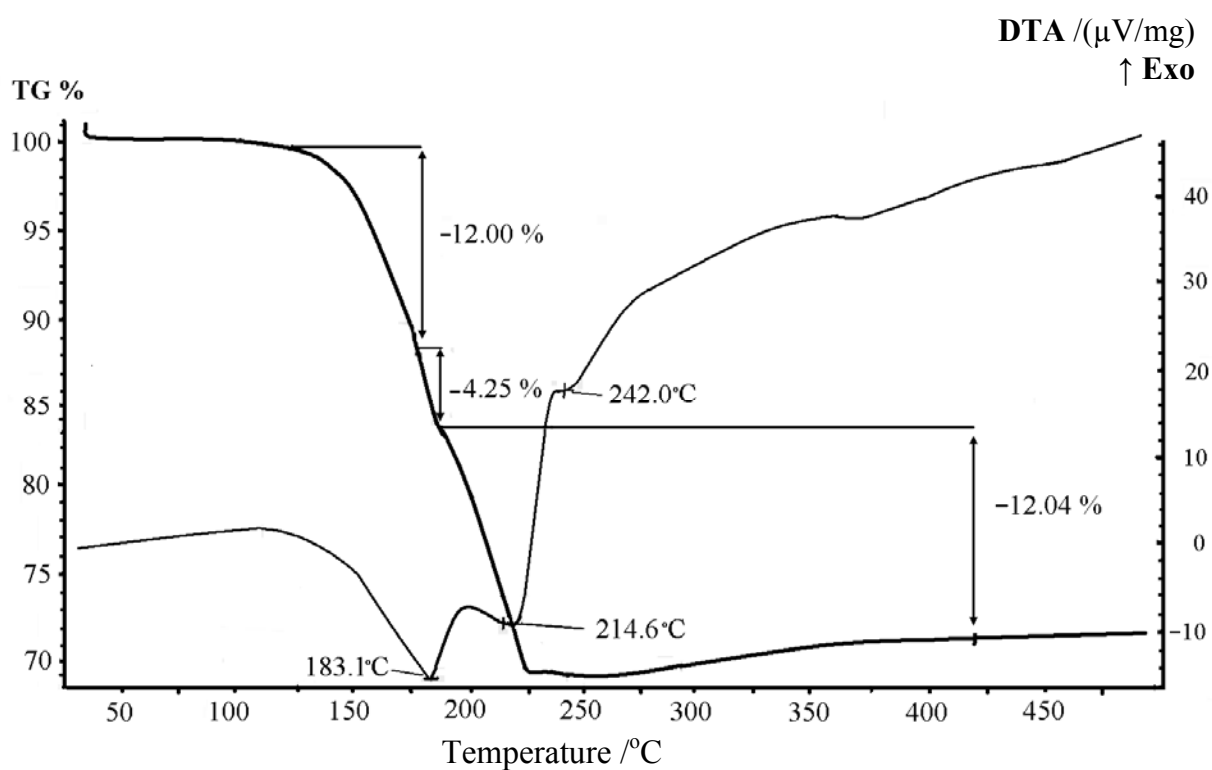


Fig. 21: DTA/TG diagram of $\text{Ni}(\text{H}_2\text{O})_6[\text{B}_{12}\text{H}_{12}] \cdot 6 \text{H}_2\text{O}$ from room temperature to 500 °C

3.2.3 Dioxonium Dodecahydro-*closo*-Dodecaborates with Divalent Transition Metal Cations

Most of the dodecahydro-*closo*-dodecaborate salts with inorganic cations were synthesized by reactions between oxides, hydroxides or carbonates of these cations and the free acid $(\text{H}_3\text{O})_2[\text{B}_{12}\text{H}_{12}]$ in aqueous solution. As described in the previous section, $\text{Ni}(\text{H}_2\text{O})_6[\text{B}_{12}\text{H}_{12}] \cdot 6 \text{H}_2\text{O}$ was obtained by neutralizing an aqueous solution of the free acid $(\text{H}_3\text{O})_2[\text{B}_{12}\text{H}_{12}]$ with NiCO_3 , for instance. Depending on the reaction conditions and the nature of the cation, however, mixed-ion dodecahydro-*closo*-dodecaborates can be formed. Well known examples are $\text{Cs}_3\text{Cl}[\text{B}_{12}\text{H}_{12}]$, $\text{Cs}_3[\text{BH}_4][\text{B}_{12}\text{H}_{12}]$ and $\text{Cs}_3(\text{NO}_3)[\text{B}_{12}\text{H}_{12}]$ [85]. Even mixed-anion and -cation $[\text{La}(\text{H}_2\text{O})_9](\text{H}_3\text{O})\text{Cl}_2[\text{B}_{12}\text{H}_{12}] \cdot \text{H}_2\text{O}$ has been published recently, but no mixed oxonium dodecahydro-*closo*-dodecaborate salts were not reported to date [91]. In this work the syntheses and crystal structures of the hydrated dioxonium dodecahydro-*closo*-dodecaborate of nickel(II) and isotopic compounds with other divalent transition metal cations of the composition $[\text{M}(\text{H}_2\text{O})_6](\text{H}_3\text{O})_2[\text{B}_{12}\text{H}_{12}]_2 \cdot 6 \text{H}_2\text{O}$ ($\text{M} = \text{Mn, Fe, Co, Ni, Cu, Zn}$ and Cd) are presented for the first time.

3.2.3.1 Synthesis of the Compounds $[\text{M}(\text{H}_2\text{O})_6](\text{H}_3\text{O})_2[\text{B}_{12}\text{H}_{12}]_2 \cdot 6 \text{H}_2\text{O}$ ($\text{M} = \text{Mn, Fe, Co, Ni, Cu, Zn}$ and Cd)

All compounds with the composition $[\text{M}(\text{H}_2\text{O})_6](\text{H}_3\text{O})_2[\text{B}_{12}\text{H}_{12}]_2 \cdot 6 \text{H}_2\text{O}$ ($\text{M} = \text{Mn, Fe, Co, Ni, Cu, Zn}$ and Cd) were synthesized by the reaction between carbonates or hydroxides of the corresponding M^{2+} cations and an excess amount of the free acid $(\text{H}_3\text{O})_2[\text{B}_{12}\text{H}_{12}]$. Single crystals are obtained by evaporating the resulting aqueous solution isothermally.

3.2.3.2 Structure Description of the Compounds $[\text{M}(\text{H}_2\text{O})_6](\text{H}_3\text{O})_2[\text{B}_{12}\text{H}_{12}]_2 \cdot 6 \text{H}_2\text{O}$ ($\text{M} = \text{Mn, Fe, Co, Ni, Cu, Zn}$ and Cd)

The title compounds with the composition $[\text{M}(\text{H}_2\text{O})_6](\text{H}_3\text{O})_2[\text{B}_{12}\text{H}_{12}]_2 \cdot 6 \text{H}_2\text{O}$ crystallize orthorhombically in space group Pnmm (no. 58) with two formula units per unit cell (Fig. 22). In all crystal structures the metal cations M^{2+} ($\text{M} = \text{Mn, Fe, Co, Ni, Cu, Zn}$ and Cd) occupy the special *Wyckoff* position $2a$ ($x/a = y/b = z/c = 0$; site symmetry: $..2/m$). The oxygen atoms

(O1 – O3) of crystal water molecules within the octahedral $[M(H_2O)_6]^{2+}$ coordination sphere are located at three crystallographically distinct *Wyckoff* sites: O1 at the *Wyckoff* site 4b ($x/a = y/b = 0, z/c$; site symmetry: $..2$), O2 and O3 at the *Wyckoff* site 4g ($x/a, y/b, z/c = 0$; site symmetry: $..m$). The oxygen atoms (O4a) of the oxonium cations H_3O^+ occupy the *Wyckoff* site 4g as well, while the oxygen atoms (O5w, O6w) of “zeolitic” water molecules reside at two crystallographically different *Wyckoff* sites 4g and 8h ($x/a, y/b, z/c$; site symmetry: 1), respectively. The boron and hydrogen atoms of the *quasi*-icosahedral $[B_{12}H_{12}]^{2-}$ -cluster anions also lie on the *Wyckoff* sites 4g and 8h. The crystal structure of the mixed-cation compounds $[M(H_2O)_6](H_3O)_2[B_{12}H_{12}]_2 \cdot 6 H_2O$ ($M = Mn, Fe, Co, Ni, Cu, Zn$ and Cd) is characterized as a layer-like arrangement with $[M(H_2O)_6]^{2+}$, $[B_{12}H_{12}]^{2-}$, H_2O and H_3O^+ layers alternatively stacked along $[001]$. While the crystal structures of $M(H_2O)_6[B_{12}H_{12}] \cdot 6 H_2O$ contain octahedral hexaaqua-dications $[M(H_2O)_6]^{2+}$ ($M = Mn, Fe, Co, Ni, Zn$ and Cd) or a discrete dimer cation $[M(H_2O)_{11}]^{4+}$ resulting from the corner-linkage of two highly distorted $[M(H_2O)_{4+1+1}]^{2+}$ octahedra ($M = Cu$), each M^{2+} cation is coordinated by six nearest water molecules forming an almost perfect octahedron in all corresponding dioxonium compounds (Fig. 23, *left*). Likewise, CN = 6 is also found for divalent transition metal cations in all these compounds. Comparing to the dodecahydro-*closo*-dodecaborate hydrates $M(H_2O)_6[B_{12}H_{12}] \cdot 6 H_2O$, the M–O bond lengths in the new compounds $[M(H_2O)_6](H_3O)_2[B_{12}H_{12}]_2 \cdot 6 H_2O$ ($M = Mn, Fe, Co, Ni, Cu, Zn$ and Cd) [85] cover the same interval for each metal dication (Table 19). The M–O bond lengths of the $[M(H_2O)_6]^{2+}$ octahedra are almost the same for all M^{2+} cations with an exception of Cu^{2+} . With the Jahn-Teller d^9 cation Cu^{2+} the apical coordinated oxygens of the distorted $[Cu(H_2O)_{4+2}]^{2+}$ octahedra bond to the central metal cation with significantly longer bond lengths ($d(Cu-O) = 226$ pm, $2\times$) than those of equatorial ones ($d(Cu-O) = 201 - 202$ pm, $4\times$) in the crystal structure of $[Cu(H_2O)_6](H_3O)_2[B_{12}H_{12}]_2 \cdot 6 H_2O$. The oxonium cations H_3O^+ connect to three neighbour “zeolitic” crystal water molecules with the shape of a tetrahedron via classical hydrogen bridging bonds ($d(O4a \cdots Ow) = 251 - 257$ pm) in all mixed-cation compounds $[M(H_2O)_6](H_3O)_2[B_{12}H_{12}]_2 \cdot 6 H_2O$ ($M = Mn, Fe, Co, Ni, Cu, Zn$ and Cd) (Fig. 23, *right*). Strong $O-H^{\delta+} \cdots \delta^-O$ hydrogen bridging bonds are also found between the hydrogen atoms of the water molecules within the $[M(H_2O)_6]^{2+}$ octahedra (O1 – O3) and those of the six “zeolitic” water molecules (O5w and O6w) to form distorted trigonal antiprisms with $d(O \cdots Ow) = 302 - 325$ pm as donor-acceptor distances (Fig. 24). No direct connection

between the *quasi*-icosahedral $[B_{12}H_{12}]^{2-}$ anions and the cationic $[M(H_2O)_6]^{2+}$ coordination spheres are found in the crystal structures of $[M(H_2O)_6](H_3O)_2[B_{12}H_{12}]_2 \cdot 6 H_2O$. There are non-classical hydrogen bridging bonds $B-H^{\delta-} \cdots \delta^+H-O$, however, between the hydrogen atoms of the *quasi*-icosahedral $[B_{12}H_{12}]^{2-}$ -cluster anions and the hydrogen atoms of oxonium cations (O4a + H4A and H4B (2 \times)) and free water molecules as well. The B–B and B–H bond lengths of the *quasi*-icosahedral $[B_{12}H_{12}]^{2-}$ -cluster anions in all compounds $[M(H_2O)_6](H_3O)_2[B_{12}H_{12}]_2 \cdot 6 H_2O$ (M = Mn, Fe, Co, Ni, Cu, Zn and Cd) are close to common intervals ($d(B-B) = 177$ pm, $d(B-H) = 110$ pm) (Fig. 25).

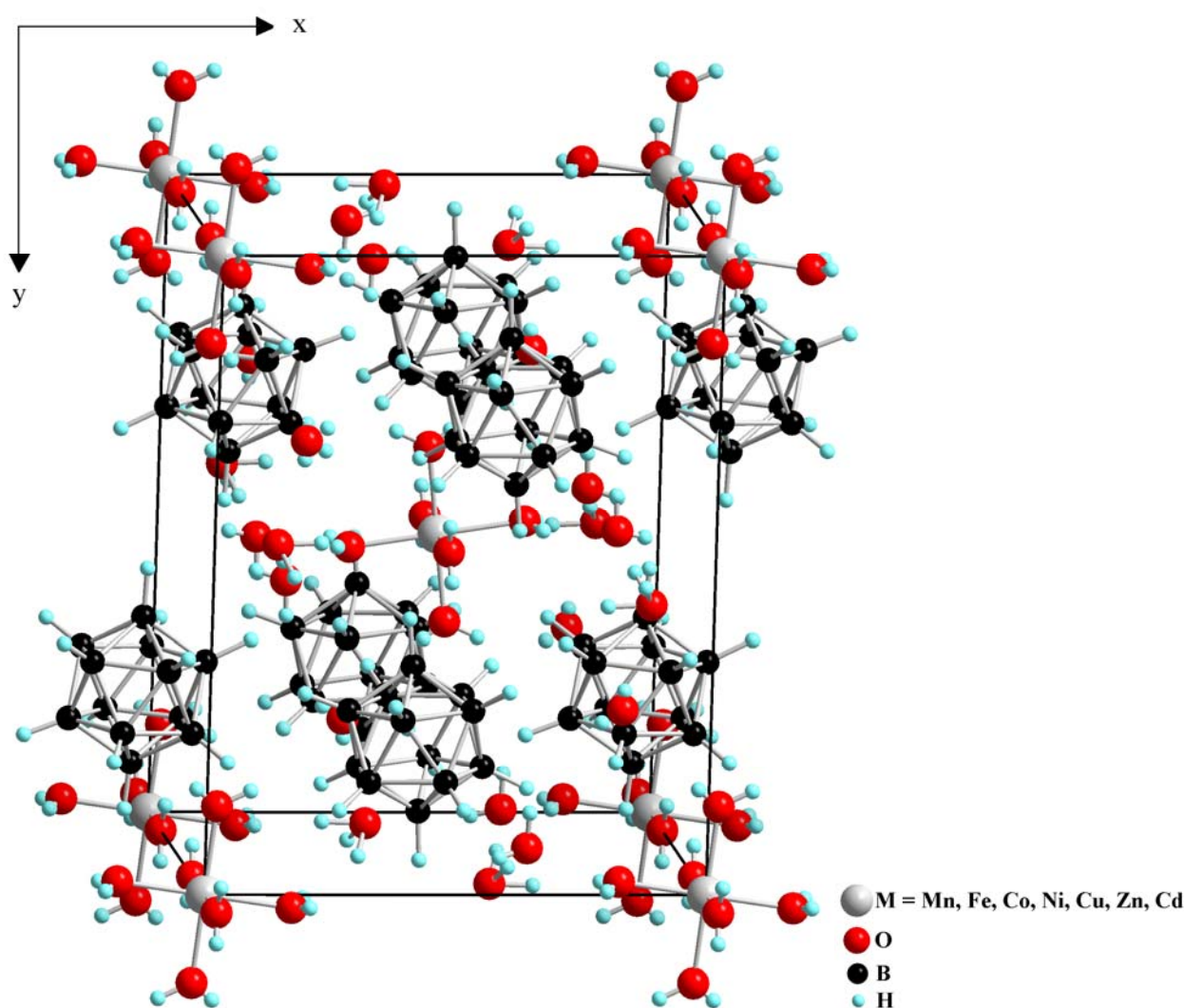


Fig. 22: View at a unit cell of the crystal structure of the mixed-cation compounds $[M(H_2O)_6](H_3O)_2[B_{12}H_{12}]_2 \cdot 6 H_2O$ (M = Mn, Fe, Co, Ni, Cu, Zn and Cd) along [001]

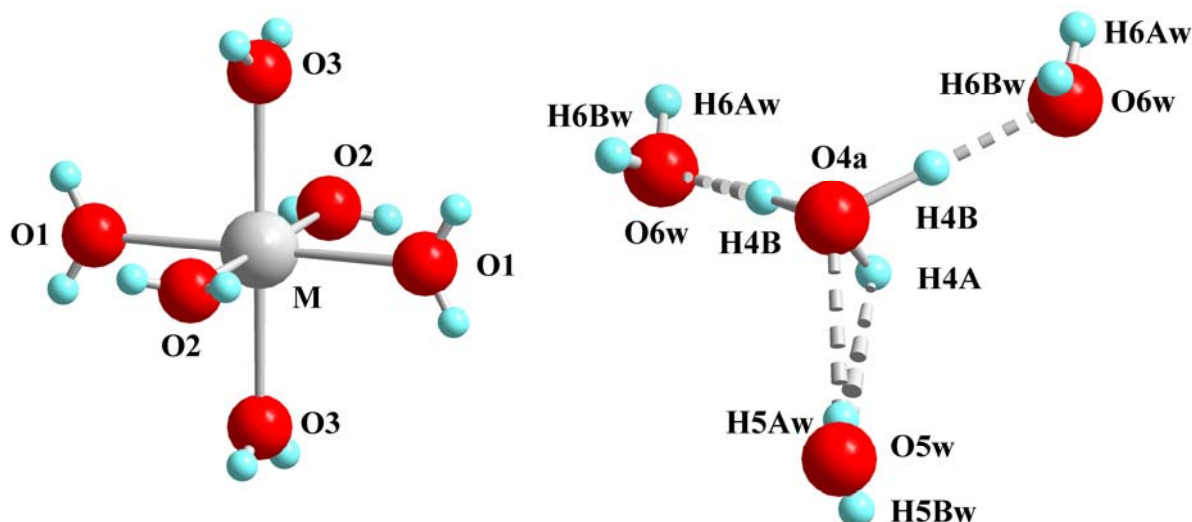


Fig. 23: View at the octahedral coordination sphere of the M^{2+} cations with their six nearest water molecules (*left*) and the $O-H^{\delta+}\cdots\delta^-O$ hydrogen bridges between hydrogen atoms of the oxonium cations (H_3O^+ : O4a + H4A and H4B, 2 \times) with those of “zeolitic” water molecules in the crystal structure of the mixed-cation compounds $[M(H_2O)_6](H_3O)_2[B_{12}H_{12}]_2 \cdot 6 H_2O$ ($M = Mn, Fe, Co, Ni, Cu, Zn$ and Cd) (*right*)

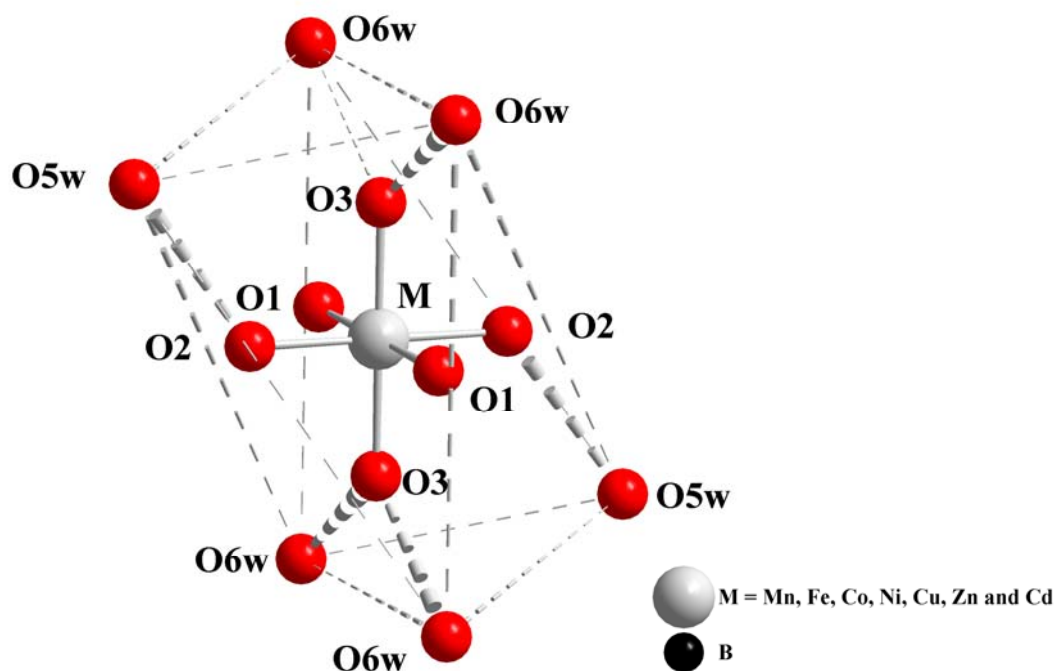


Fig. 24: Trigonal antiprismatic arrangement of the six “zeolitic” crystal water molecules (O5w and O6w) around each $[M(H_2O)_6]^{2+}$ octahedron in the crystal structure of the mixed-cation compounds $[M(H_2O)_6](H_3O)_2[B_{12}H_{12}]_2 \cdot 6 H_2O$ ($M = Mn, Fe, Co, Ni, Cu, Zn$ and Cd)

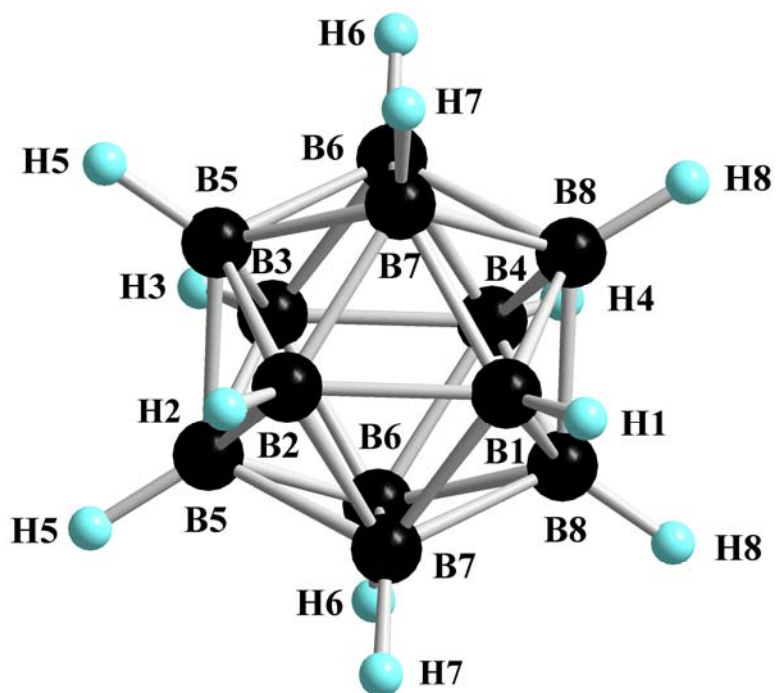


Fig. 25: View at the *quasi*-icosahedral $[B_{12}H_{12}]^{2-}$ -cluster anion in the crystal structure the of the mixed-cation compounds $[M(H_2O)_6](H_3O)_2[B_{12}H_{12}]_2 \cdot 6 H_2O$ ($M = Mn, Fe, Co, Ni, Cu, Zn$ and Cd)

Table 16: Crystallographic data for the mixed-cation compounds $[M(H_2O)_6](H_3O)_2[B_{12}H_{12}]_2 \cdot 6 H_2O$ (M = Mn, Fe, Co, Ni, Cu, Zn and Cd) and their determination

Crystallographic data	M = Mn	M = Fe	M = Co	M = Ni	
Crystal system	orthorhombic				
Space group	Pnmm (no. 58)				
Unit cell parameters:	a (pm)	1160.56(7)	1160.38(7)	1157.45(7)	1156.25(7)
	b (pm)	1512.86(9)	1504.89(9)	1495.14(9)	1488.47(9)
	c (pm)	925.55(6)	923.30(6)	924.68(6)	924.98(6)
Formula units per unit cell	2				
Calculated density ($D_x/g\text{ cm}^{-3}$)	1.212	1.225	1.239	1.245	
Molar volume ($V_m/cm^3\text{ mol}^{-1}$)	489.3	484.9	481.8	479.3	
Diffractometer	κ -CCD (Bruker-Nonius)				
Radiation	Mo-K α : $\lambda = 71.07\text{ pm}$, graphite monochromator				
Index range: $\pm h_{\max}, \pm k_{\max}, \pm l_{\max}$	14, 18, 10	15, 20, 12	15, 19, 12	14, 19, 12	
θ_{\max} (deg)	26.0	28.3	28.3	27.5	
F(000)	622	624	626	628	
Absorption coefficient (μ/mm^{-1})	0.45	0.51	0.58	0.66	
Absorption correction	numerical, Program X-SHAPE [64]				
Other data corrections	background, polarization and Lorentz factors				
Collected reflections	12882	17784	19806	19914	
Unique reflections	1655	2118	2114	1929	
$R_{\text{int}}, R_{\sigma}$	0.084, 0.067	0.060, 0.032	0.042, 0.023	0.058, 0.026	
Structure solution and refinement	Program SHELXS-97 and SHELXL-97 [68]				
Scattering factors	International Tables for Crystallography, Vol. C [87]				
R_1, R_1 with $ F_o \geq 4\sigma(F_o)$	0.093, 0.052	0.085, 0.065	0.060, 0.050	0.054, 0.042	
Reflections with $ F_o \geq 4\sigma(F_o)$	925	1685	1794	1617	
w R_2 , Goodness of fit (GooF)	0.135, 1.167	0.191, 1.129	0.155, 1.067	0.102, 1.108	
Extinction (g)	0.015(3)	0.0002(1)	0.020(5)	0.016(23)	
Residual electron density (<i>max.</i> , <i>min.</i> in $\rho/e^{-1}\text{ }10^6\text{ pm}$)	0.59, -0.29	0.97, -0.36	1.00, -0.36	0.34, -0.23	

Table 16: (*continued*)

Crystallographic data	M = Cu	M = Zn	M = Cd
Crystal system		orthorhombic	
Space group		Pnmm (no. 58)	
Unit cell parameters:			
a (pm)	1162.81(7)	1157.57(7)	1159.02(7)
b (pm)	1493.21(9)	1493.03(9)	1532.90(9)
c (pm)	921.60(6)	924.93(6)	923.90(6)
Number of formula units per unit cell		2	
Calculated density ($D_x/g\text{ cm}^{-3}$)	1.248	1.253	1.316
Molar volume ($V_m/\text{cm}^3\text{ mol}^{-1}$)	482.0	481.3	494.3
Diffractometer	κ -CCD (Bruker-Nonius)		
Radiation	Mo-K α : $\lambda = 71.07\text{ pm}$, graphite monochromator		
Index range: $\pm h_{\max}, \pm k_{\max}, \pm l_{\max}$	15, 19, 12	15, 19, 12	13, 17, 10
θ_{\max} (deg)	28.3	28.3	24.1
F(000)	630	632	668
Absorption coefficient (μ/mm^{-1})	0.73	0.81	0.71
Absorption correction	numerical, Program X-SHAPE [64]		
Other data corrections	background, polarization and <i>Lorentz</i> factors		
Collected reflections	17902	20319	10452
Unique reflections	2101	2095	1384
$R_{\text{int}}, R_{\sigma}$	0.062, 0.031	0.065, 0.031	0.102, 0.102
Structure solution and refinement	Program SHELXS-97 and SHELXL-97 [68]		
Scattering factors	International Tables for Crystallography, Vol. C [87]		
R_1, R_w with $ F_o \geq 4\sigma(F_o)$	0.077, 0.059	0.062, 0.042	0.110, 0.048
Reflections with $ F_o \geq 4\sigma(F_o)$	1674	1657	688
wR_2 , Goodness of fit (GooF)	0.191, 1.049	0.106, 1.081	0.085, 1.351
Extinction (g)	0.0002(1)	0.003(2)	0.02(6)
Residual electron densities (<i>max.</i> , <i>min.</i> in $\rho/e^{-1}\text{ 10}^6\text{ pm}$)	1.02, -0.45	0.35, -0.30	0.50, -0.41

Table 17: Atomic coordinates for $[M(H_2O)_6](H_3O)_2[B_{12}H_{12}]_2 \cdot 6 H_2O$ (M = Mn, Fe, Co, Ni, Cu, Zn and Cd)

Atom	Wyckoff position	x/a	y/b	z/c
Mn	2a	0	0	0
O1	4e	0	0	0.2322(4)
O2	4g	0.0191(3)	0.8546(2)	0
O3	4g	0.1857(3)	0.0196(2)	0
O4a	4g	0.1310(5)	0.4547(3)	0
O5w	4g	0.1816(3)	0.2949(3)	0
O6w	8h	0.3340(5)	0.0422(3)	0.2677(4)
B1	4g	0.2789(5)	0.7149(4)	0
B2	4g	0.4006(5)	0.6456(4)	0
B3	4g	0.4535(5)	0.2017(4)	0
B4	4g	0.4223(5)	0.8676(4)	0
B5	8h	0.4884(4)	0.2993(3)	0.0959(4)
B6	8h	0.0429(4)	0.3036(3)	0.3441(5)
B7	8h	0.1329(3)	0.2029(3)	0.3558(5)
B8	8h	0.1871(3)	0.3125(3)	0.4037(5)
H1	4g	0.195(3)	0.692(3)	0
H2	4g	0.390(4)	0.581(3)	0
H3	4g	0.360(4)	0.170(3)	0
H4	4g	0.425(4)	0.940(3)	0
H5	8h	0.434(3)	0.341(2)	0.155(4)
H6	8h	0.013(4)	0.335(2)	0.236(4)
H7	8h	0.163(3)	0.178(2)	0.248(4)
H8	8h	0.250(3)	0.350(2)	0.341(4)

Table 17: (continued)

Atom	Wyckoff position	x/a	y/b	z/c
Fe	2a	0	0	0
O1	4e	0	0	0.2267(4)
O2	4g	0.0196(3)	0.8580(2)	0
O3	4g	0.1812(3)	0.0181(2)	0
O4a	4g	0.1284(5)	0.4548(3)	0
O5w	4g	0.1820(3)	0.2958(3)	0
O6w	8h	0.3323(3)	0.0414(2)	0.2648(3)
B1	4g	0.2777(4)	0.7136(3)	0
B2	4g	0.4013(4)	0.6442(3)	0
B3	4g	0.4530(4)	0.2016(3)	0
B4	4g	0.4235(4)	0.8674(3)	0
B5	8h	0.4875(3)	0.3004(3)	0.0966(4)
B6	8h	0.0428(3)	0.3037(2)	0.3436(4)
B7	8h	0.1327(3)	0.2081(2)	0.3448(3)
B8	8h	0.1877(3)	0.3122(2)	0.4031(3)
H1	4g	0.201(5)	0.693(4)	0
H2	4g	0.388(3)	0.576(3)	0
H3	4g	0.357(3)	0.169(3)	0
H4	4g	0.424(4)	0.941(3)	0
H5	8h	0.417(3)	0.345(3)	0.164(3)
H6	8h	0.012(3)	0.339(3)	0.240(3)
H7	8h	0.161(3)	0.173(3)	0.255(3)
H8	8h	0.250(3)	0.350(2)	0.336(3)

Table 17: (*continued*)

Atom	Wyckoff position	x/a	y/b	z/c
Co	2a	0	0	0
O1	4e	0	0	0.2228(3)
O2	4g	0.0190(2)	0.8595(2)	0
O3	4g	0.1782(3)	0.0194(2)	0
O4a	4g	0.1275(4)	0.4538(2)	0
O5w	4g	0.1811(3)	0.2924(3)	0
O6w	8h	0.3318(2)	0.0399(2)	0.2654(3)
B1	4g	0.2766(3)	0.7128(2)	0
B2	4g	0.4011(4)	0.6435(2)	0
B3	4g	0.4540(3)	0.2002(2)	0
B4	4g	0.4220(3)	0.8685(2)	0
B5	8h	0.4876(2)	0.3000(2)	0.0963(3)
B6	8h	0.0437(2)	0.3044(2)	0.3443(3)
B7	8h	0.1333(2)	0.2076(2)	0.3448(3)
B8	8h	0.1890(2)	0.3121(2)	0.4036(3)
H1	4g	0.194(3)	0.690(2)	0
H2	4g	0.397(3)	0.574(2)	0
H3	4g	0.365(3)	0.173(2)	0
H4	4g	0.427(3)	0.929(2)	0
H5	8h	0.414(2)	0.337(2)	0.168(3)
H6	8h	0.016(2)	0.338(2)	0.248(3)
H7	8h	0.159(2)	0.175(2)	0.253(3)
H8	8h	0.258(2)	0.344(2)	0.334(3)

Table 17: (continued)

Atom	Wyckoff position	x/a	y/b	z/c
Ni	2a	0	0	0
O1	4e	0	0	0.2185(2)
O2	4g	0.0190(2)	0.8626(1)	0
O3	4g	0.1743(2)	0.0205(2)	0
O4a	4g	0.1252(3)	0.4526(2)	0
O5w	4g	0.1778(3)	0.2895(3)	0
O6w	8h	0.3290(2)	0.0387(2)	0.2652(2)
B1	4g	0.2769(2)	0.7119(2)	0
B2	4g	0.4024(4)	0.6427(2)	0
B3	4g	0.4539(3)	0.2002(2)	0
B4	4g	0.4207(3)	0.8696(2)	0
B5	8h	0.4870(2)	0.2998(2)	0.0957(2)
B6	8h	0.0439(2)	0.3048(2)	0.3449(3)
B7	8h	0.1325(2)	0.2074(2)	0.3453(3)
B8	8h	0.1898(2)	0.3122(1)	0.4041(2)
H1w	8h	0.495(2)	0.457(2)	0.239(3)
H2Aw	4g	0.086(5)	0.839(3)	0
H2Bw	4g	0.021(4)	0.165(3)	0
H3w	8h	0.201(3)	0.011(2)	0.063(4)
H4A	4g	0.213(2)	0.451(1)	0
H4B	8h	0.163(4)	0.493(3)	0.099(5)
H5Aw	4g	0.176(4)	0.360(4)	0
H5Bw	4g	0.226(6)	0.269(5)	0
H6Aw	8h	0.392(4)	0.024(3)	0.241(5)
H6Bw	8h	0.328(4)	0.094(4)	0.271(6)
H1	4g	0.188(3)	0.686(2)	0
H2	4g	0.392(3)	0.570(2)	0
H3	4g	0.362(3)	0.167(2)	0
H4	4g	0.426(3)	0.944(2)	0
H5	8h	0.422(2)	0.337(2)	0.167(3)
H6	8h	0.017(2)	0.339(2)	0.247(3)
H7	8h	0.159(2)	0.174(2)	0.250(3)
H8	8h	0.255(2)	0.348(2)	0.338(3)

Table 17: (continued)

Atom	Wyckoff position	x/a	y/b	z/c
Cu	2a	0	0	0
O1	4e	0	0	0.2180(4)
O2	4g	0.0180(3)	0.8493(2)	0
O3	4g	0.1725(3)	0.0160(3)	0
O4a	4g	0.1306(5)	0.4562(3)	0
O5w	4g	0.1836(5)	0.2954(3)	0
O6w	8h	0.3291(3)	0.0398(2)	0.2613(3)
B1	4g	0.2782(4)	0.7120(3)	0
B2	4g	0.4026(4)	0.6425(3)	0
B3	4g	0.4539(4)	0.2010(3)	0
B4	4g	0.4234(4)	0.8671(3)	0
B5	8h	0.4870(3)	0.3010(3)	0.0968(4)
B6	8h	0.0429(3)	0.3038(2)	0.3444(4)
B7	8h	0.1314(3)	0.2069(2)	0.3445(3)
B8	8h	0.1876(3)	0.3115(2)	0.4025(4)
H1	4g	0.189(4)	0.696(4)	0
H2	4g	0.407(4)	0.576(4)	0
H3	4g	0.398(4)	0.180(4)	0
H4	4g	0.441(4)	0.919(4)	0
H5	8h	0.423(4)	0.335(4)	0.167(4)
H6	8h	0.016(4)	0.328(4)	0.256(4)
H7	8h	0.161(4)	0.175(4)	0.247(4)
H8	8h	0.255(4)	0.344(4)	0.333(4)

Table 17: (continued)

Atom	Wyckoff position	x/a	y/b	z/c
Zn	2a	0	0	0
O1	4e	0	0	0.2219(2)
O2	4g	0.0198(3)	0.8602(2)	0
O3	4g	0.1769(2)	0.0200(2)	0
O4a	4g	0.1233(3)	0.4533(2)	0
O5w	4g	0.1788(3)	0.2912(3)	0
O6w	8h	0.3280(3)	0.0402(2)	0.2664(3)
B1	4g	0.2767(3)	0.7125(2)	0
B2	4g	0.4023(3)	0.6434(2)	0
B3	4g	0.4536(3)	0.2004(2)	0
B4	4g	0.4216(3)	0.8692(2)	0
B5	8h	0.4874(2)	0.2997(2)	0.0959(2)
B6	8h	0.0438(2)	0.3049(2)	0.3444(2)
B7	8h	0.1325(2)	0.2079(1)	0.3451(2)
B8	8h	0.1888(2)	0.3125(1)	0.4035(3)
H1w	8h	0.497(4)	0.410(3)	0.256(3)
H2Aw	4g	0.062(5)	0.841(4)	0
H2Bw	4g	0.017(4)	0.169(4)	0
H3w	8h	0.202(4)	0.021(3)	0.058(5)
H4A	4g	0.210(2)	0.453(1)	0
H4B	8h	0.161(4)	0.486(3)	0.088(5)
H5Aw	4g	0.183(9)	0.327(7)	0
H5Bw	4g	0.214(7)	0.276(6)	0
H6Aw	8h	0.379(3)	0.024(3)	0.246(5)
H6Bw	8h	0.364(4)	0.070(4)	0.254(8)
H1	4g	0.189(2)	0.685(2)	0
H2	4g	0.396(3)	0.574(2)	0
H3	4g	0.371(3)	0.172(2)	0
H4	4g	0.427(3)	0.943(2)	0
H5	8h	0.421(2)	0.337(2)	0.157(3)
H6	8h	0.021(2)	0.336(2)	0.246(3)
H7	8h	0.160(2)	0.176(2)	0.248(3)
H8	8h	0.253(2)	0.345(2)	0.343(3)

Table 17: (continued)

Atom	Wyckoff position	x/a	y/b	z/c
Cd	2a	0	0	0
O1	4e	0	0	0.2428(5)
O2	4g	0.0178(8)	0.8488(3)	0
O3	4g	0.1944(4)	0.0201(5)	0
O4a	4g	0.1331(7)	0.4547(4)	0
O5w	4g	0.1851(8)	0.2976(5)	0
O6w	8h	0.3395(4)	0.0429(3)	0.2691(5)
B1	4g	0.2757(11)	0.7167(7)	0
B2	4g	0.3984(10)	0.6461(8)	0
B3	4g	0.4548(10)	0.2038(8)	0
B4	4g	0.4225(10)	0.8666(9)	0
B5	8h	0.4890(11)	0.2993(5)	0.0955(7)
B6	8h	0.0447(6)	0.3021(5)	0.3444(4)
B7	8h	0.1343(7)	0.2111(5)	0.3467(9)
B8	8h	0.1880(7)	0.3108(5)	0.4041(9)
H1	4g	0.181(9)	0.685(5)	0
H2	4g	0.398(6)	0.572(6)	0
H3	4g	0.362(7)	0.178(5)	0
H4	4g	0.419(7)	0.947(6)	0
H5	8h	0.424(5)	0.330(3)	0.157(6)
H6	8h	0.011(6)	0.330(3)	0.246(5)
H7	8h	0.165(4)	0.191(3)	0.249(5)
H8	8h	0.243(4)	0.350(3)	0.352(6)

Table 18: Anisotropic thermal displacement coefficients^{a)} (U_{ij}/pm^2) for the mixed-cation compounds $[\text{M}(\text{H}_2\text{O})_6](\text{H}_3\text{O})_2[\text{B}_{12}\text{H}_{12}]_2 \cdot 6 \text{H}_2\text{O}$ (M = Mn, Fe, Co, Ni, Cu, Zn and Cd)

Atom	U_{11}	U_{22}	U_{33}	U_{23}	U_{13}	U_{12}
Mn	559(6)	454(6)	425(7)	0	0	-18(6)
O1	1454(36)	577(20)	409(23)	0	0	-163(25)
O2	643(23)	454(18)	703(23)	0	0	-22(16)
O3	553(20)	729(16)	811(29)	0	0	7(17)
O4a	1663(48)	735(27)	851(37)	0	0	89(29)
O5w	869(29)	796(25)	692(30)	0	0	151(21)
O6w	1136(25)	791(18)	827(25)	35(16)	-92(19)	-178(16)
B1	323(20)	405(22)	402(22)	0	0	-101(17)
B2	431(23)	327(21)	387(23)	0	0	3(18)
B3	326(20)	483(25)	409(23)	0	0	-99(26)
B4	473(34)	465(34)	609(42)	0	0	-23(26)
B5	510(22)	544(20)	451(25)	-44(17)	52(21)	39(22)
B6	521(21)	588(24)	465(29)	73(20)	2(18)	98(18)
B7	523(23)	546(22)	422(28)	-31(19)	4(18)	89(18)
B8	474(22)	505(22)	548(28)	70(19)	60(19)	3(18)
H1	383(111)					
H2	578(132)					
H3	637(139)					
H4	555(132)					
H5	598(95)					
H6	615(93)					
H7	669(103)					
H8	595(94)					

^{a)} For M, O and B defined as anisotropic temperature factor according to: $\exp[-2\pi^2 (U_{11}h^2a^{*2} + U_{22}k^2b^{*2} + U_{33}l^2c^{*2} + 2U_{23}klb^{*}c^{*} + 2U_{13}hla^{*}c^{*} + 2U_{13}hka^{*}b^{*})]$; for H isotropically defined as temperature factor in: $\exp[-8\pi^2(U_{\text{iso}}\sin^2\theta/\lambda^2)]$.

Table 18: (*continued*)

Atom	U ₁₁	U ₂₂	U ₃₃	U ₂₃	U ₁₃	U ₁₂
Fe	410(4)	317(4)	332(4)	0	0	-1(3)
O1	1172(32)	490(18)	344(16)	0	0	-115(19)
O2	484(17)	348(15)	613(19)	0	0	27(12)
O3	458(17)	644(22)	698(23)	0	0	-2(15)
O4a	1534(48)	638(27)	783(30)	0	0	63(30)
O5w	705(23)	711(23)	591(21)	0	0	151(19)
O6w	954(21)	693(17)	721(19)	30(15)	-48(17)	-147(15)
B1	323(20)	405(22)	402(22)	0	0	-101(17)
B2	431(23)	327(21)	387(23)	0	0	3(18)
B3	326(20)	483(25)	409(23)	0	0	-86(19)
B4	401(23)	341(22)	493(26)	0	0	-58(17)
B5	378(16)	476(18)	417(16)	-43(13)	38(13)	35(13)
B6	415(15)	481(18)	359(15)	53(14)	4(13)	84(14)
B7	415(15)	429(16)	314(14)	-20(13)	26(12)	64(13)
B8	365(15)	406(16)	439(16)	73(13)	50(13)	15(13)
H1	768(176)					
H2	595(148)					
H3	511(131)					
H4	538(137)					
H5	578(102)					
H6	611(109)					
H7	626(108)					
H8	568(100)					

Table 18: (continued)

Atom	U ₁₁	U ₂₂	U ₃₃	U ₂₃	U ₁₃	U ₁₂
Co	382(3)	291(3)	326(3)	0	0	-2(2)
O1	1125(25)	487(14)	312(12)	0	0	-139(12)
O2	489(12)	298(10)	611(15)	0	0	40(8)
O3	405(12)	590(14)	641(16)	0	0	-11(10)
O4a	1362(32)	651(20)	764(22)	0	0	55(21)
O5w	692(17)	688(17)	601(16)	0	0	143(14)
O6w	892(15)	668(13)	724(14)	17(11)	-24(12)	-125(11)
B1	328(14)	401(16)	387(16)	0	0	-77(12)
B2	444(17)	341(15)	396(17)	0	0	1(13)
B3	318(15)	457(18)	494(17)	0	0	-62(13)
B4	427(17)	309(15)	511(20)	0	0	-48(12)
B5	374(11)	470(13)	411(12)	-38(10)	43(9)	33(9)
B6	394(11)	454(12)	349(11)	65(10)	-8(10)	69(10)
B7	423(11)	423(11)	319(11)	-25(9)	23(9)	57(9)
B8	366(11)	393(11)	460(13)	59(10)	54(10)	-3(9)
H1	493(101)					
H2	606(116)					
H3	537(103)					
H4	743(138)					
H5	597(80)					
H6	462(72)					
H7	622(84)					
H8	696(89)					

Table 18: (continued)

Atom	U ₁₁	U ₂₂	U ₃₃	U ₂₃	U ₁₃	U ₁₂
Ni	414(3)	338(3)	373(3)	0	0	-7(2)
O1	1113(21)	473(13)	407(11)	0	0	-89(15)
O2	489(14)	378(10)	631(14)	0	0	7(10)
O3	457(11)	632(15)	617(15)	0	0	-9(10)
O4a	732(16)	710(15)	647(15)	0	0	141(13)
O5w	1208(29)	757(19)	857(21)	0	0	7(19)
O6w	923(16)	687(12)	780(14)	12(11)	-18(12)	-89(12)
B1	375(14)	452(16)	419(15)	0	0	-72(12)
B2	510(17)	370(15)	415(16)	0	0	6(13)
B3	371(14)	491(17)	475(17)	0	0	-66(13)
B4	460(16)	405(16)	529(18)	0	0	-67(13)
B5	447(11)	486(11)	447(11)	-46(9)	49(9)	32(9)
B6	446(11)	531(12)	407(11)	52(10)	21(9)	75(10)
B7	467(11)	467(11)	377(11)	-26(9)	13(9)	61(9)
B8	407(11)	447(11)	485(12)	52(9)	57(9)	12(9)
H1w	854(94)					
H2Aw	1191(186)					
H2Bw	994(95)					
H3w	1317(162)					
H4A	1041(140)					
H4B	1749(190)					
H5Aw	1436(204)					
H5Bw	1618(311)					
H6Aw	1289(176)					
H6Bw	2067(250)					
H1	351(62)					
H2	596(86)					
H3	529(77)					
H4	498(77)					
H5	597(58)					
H6	596(61)					
H7	563(58)					
H8	530(54)					

Table 18: (continued)

Atom	U ₁₁	U ₂₂	U ₃₃	U ₂₃	U ₁₃	U ₁₂
Cu	411(4)	364(4)	315(4)	0	0	-10(3)
O1	1041(32)	495(19)	358(17)	0	0	-120(17)
O2	465(17)	437(17)	558(20)	0	0	29(12)
O3	480(18)	660(22)	584(21)	0	0	52(15)
O4a	1297(41)	679(28)	763(30)	0	0	39(29)
O5w	630(21)	650(22)	559(20)	0	0	93(17)
O6w	883(20)	643(17)	763(30)	22(15)	41(17)	-105(15)
B1	299(19)	392(22)	338(21)	0	0	-66(16)
B2	423(23)	318(21)	353(22)	0	0	-6(17)
B3	279(19)	504(26)	379(23)	0	0	-60(19)
B4	413(23)	317(22)	478(27)	0	0	-83(18)
B5	346(15)	483(18)	372(16)	-31(13)	34(12)	34(12)
B6	383(15)	469(17)	307(15)	62(14)	-20(12)	81(13)
B7	391(14)	432(16)	273(14)	-24(12)	23(12)	41(12)
B8	351(14)	382(15)	410(16)	37(13)	62(12)	8(12)
H1	463(127)					
H2	573(149)					
H3	1011(258)					
H4	481(135)					
H5	623(110)					
H6	681(132)					
H7	718(123)					
H8	598(105)					

Table 18: (continued)

Atom	U ₁₁	U ₂₂	U ₃₃	U ₂₃	U ₁₃	U ₁₂
Zn	399(3)	319(3)	322(3)	0	0	-5(2)
O1	1129(24)	412(14)	290(11)	0	0	-115(15)
O2	419(16)	288(11)	277(14)	0	0	25(11)
O3	377(13)	598(15)	532(16)	0	0	-6(10)
O4a	1055(30)	701(19)	707(21)	0	0	9(19)
O5w	659(20)	637(20)	556(16)	0	0	161(16)
O6w	812(18)	625(13)	724(14)	14(11)	3(13)	-95(13)
B1	267(15)	537(15)	341(15)	0	0	-51(11)
B2	423(18)	290(14)	320(15)	0	0	-3(12)
B3	288(15)	459(17)	360(16)	0	0	-66(13)
B4	379(18)	311(15)	449(17)	0	0	-78(12)
B5	359(12)	415(11)	389(11)	-36(8)	52(9)	34(9)
B6	356(11)	417(11)	309(10)	64(9)	-4(9)	79(9)
B7	393(12)	380(10)	266(10)	-23(8)	8(8)	62(9)
B8	320(11)	355(10)	410(12)	48(9)	59(9)	-1(8)
H1w	795(119)					
H2Aw	902(218)					
H2Bw	683(197)					
H3w	1008(160)					
H4A	987(117)					
H4B	1335(174)					
H5A	1952(629)					
H5B	1335(403)					
H6Aw	543(115)					
H6Bw	2342(402)					
H1	264(67)					
H2	513(92)					
H3	424(82)					
H4	399(82)					
H5	545(66)					
H6	540(71)					
H7	469(62)					
H8	487(62)					

Table 18: (continued)

Atom	U ₁₁	U ₂₂	U ₃₃	U ₂₃	U ₁₃	U ₁₂
Cd	656(7)	597(7)	499(6)	0	0	-25(12)
O1	1873(62)	655(40)	393(21)	0	0	-219(85)
O2	595(55)	492(33)	752(35)	0	0	-105(55)
O3	449(46)	803(71)	1010(45)	0	0	23(40)
O4a	1703(79)	751(58)	774(51)	0	0	-23(47)
O5w	729(57)	816(51)	619(49)	0	0	137(49)
O6w	1112(41)	856(42)	872(37)	35(26)	-122(29)	-248(28)
B1	517(81)	459(78)	447(72)	0	0	-54(69)
B2	612(78)	366(74)	540(71)	0	0	-24(67)
B3	500(96)	556(86)	662(86)	0	0	-67(64)
B4	453(78)	527(90)	585(76)	0	0	-184(71)
B5	396(54)	525(45)	484(39)	-69(34)	142(61)	61(73)
B6	610(65)	607(57)	358(48)	34(39)	-29(36)	151(41)
B7	494(58)	553(60)	400(53)	-104(44)	-15(42)	61(47)
B8	416(55)	467(57)	463(58)	111(47)	122(45)	4(45)
H1	429(285)					
H2	591(223)					
H3	385(238)					
H4	1088(337)					
H5	449(187)					
H6	586(146)					
H7	429(154)					
H8	447(170)					

Table 19: Selected interatomic distances (d/pm) for the mixed-cation compounds $[M(H_2O)_6](H_3O)_2[B_{12}H_{12}]_2 \cdot 6 H_2O$ (M = Mn, Fe, Co, Ni, Cu, Zn and Cd)

[MnO ₆] polyhedron:			
	Mn – O1	214.9 (2×)	
	– O2	221.1 (2×)	
	– O3	217.5 (2×)	
[B ₁₂ H ₁₂] ²⁻ anion:			
B1 – B7	175.8 (2×)		B2 – B1 176.0
– B2	176.0		– B7 176.5 (2×)
– B8	176.8 (2×)		– B5 177.3 (2×)
– H1	103.8		– H2 98.2
B3 – B5	177.0 (2×)		B4 – B8 176.1 (2×)
– B6	178.0 (2×)		– B3 178.2
– B4	178.2		– B6 178.5 (2×)
– H3	118.7		– H4 110.0
B5 – B7	176.6		B6 – B8 176.7
– B6	176.9		– B7 176.8
– B3	177.0		– B5 176.9
– B2	177.3		– B3 178.0
– B5	177.6		– B4 178.5
– H5	111.7		– H6 116.5
B7 – B1	175.9		B8 – B4 176.1
– B2	176.5		– B7 176.6
– B8	176.6		– B6 176.7
– B5	176.6		– B1 176.8
– B6	176.8		– B8 178.2
– H7	108.6		– H8 109.0

Table 19: (*continued*)

[FeO ₆] polyhedron:			
	Fe – O1	208.9 (2×)	
	– O2	215.2 (2×)	
	– O3	211.8 (2×)	
[B ₁₂ H ₁₂] ²⁻ anion:			
B1 – B7	177.0 (2×)		B2 – B7 176.9 (2×)
– B2	177.3		– B1 177.3
– B8	178.0 (2×)		– B5 177.5 (2×)
– H1	94.2		– H2 104.3
B3 – B4	176.9		B4 – B3 177.0
– B6	178.0 (2×)		– B8 177.5 (2×)
– B5	178.1 (2×)		– B6 177.5 (2×)
– H3	121.3		– H4 111.5
B5 – B7	177.2		B6 – B8 177.1
– B2	177.6		– B4 177.5
– B3	178.1		– B7 177.8
– B5	178.1		– B3 178.0
– B6	178.3		– B5 178.3
– H5	122.7		– H6 115.4
B7 – B2	176.9		B8 – B6 177.1
– B1	177.0		– B4 177.5
– B5	177.2		– B7 177.7
– B8	177.7		– B1 178.0
– B6	177.8		– B8 178.6
– H7	103.2		– H8 110.8

Table 19: (continued)[CoO₆] polyhedron:

Co – O1	206.0 (2×)
– O2	211.2 (2×)
– O3	208.3 (2×)

[B₁₂H₁₂]²⁻ anion:

B1 – B2	177.4	B2 – B7	177.1 (2×)
– B7	177.6 (2×)	– B1	177.4
– B8	177.8 (2×)	– B5	177.9 (2×)
– H1	101.8	– H2	103.7
B3 – B4	176.5	B4 – B3	176.5
– B6	177.7 (2×)	– B6	177.4 (2×)
– B5	178.0 (2×)	– B8	177.6 (2×)
– H3	111.0	– H4	90.7
B5 – B7	177.6	B6 – B8	177.3
– B6	177.8	– B4	177.4
– B2	177.9	– B3	177.7
– B3	178.0	– B5	177.8
– B5	178.1	– B7	178.0
– H5	121.1	– H6	107.3
B7 – B2	177.1	B8 – B6	177.3
– B5	177.6	– B4	177.6
– B8	177.6	– B7	177.6
– B1	177.6	– B1	177.8
– B6	178.0	– B8	178.2
– H7	102.4	– H8	112.8

Table 19: (continued)[NiO₆] polyhedron:

Ni – O1	202.2 (2×)
– O2	205.8 (2×)
– O3	203.8 (2×)

[B₁₂H₁₂]²⁻ anion:

B1 – B7	177.4 (2×)	B2 – B7	177.1 (2×)
– B2	177.7	– B5	177.6 (2×)
– B8	178.1 (2×)	– B1	177.7
– H1	110.3	– H2	108.6
B3 – B5	177.2 (2×)	B4 – B8	177.5 (2×)
– B6	177.5 (2×)	– B6	177.7 (2×)
– B4	178.2	– B3	178.2
– H3	116.3	– H4	110.0
B5 – B7	177.0	B6 – B3	177.5
– B5	177.2	– B7	177.5
– B3	177.3	– B8	177.6
– B2	177.6	– B5	177.7
– B6	177.7	– B4	177.7
– H5	116.0	– H6	108.5
B7 – B5	177.0	B8 – B4	177.5
– B2	177.1	– B6	177.6
– B1	177.4	– B8	177.8
– B6	177.5	– B7	178.0
– B8	178.0	– B1	178.1
– H7	106.4	– H8	110.0

Table 19: (continued)[CuO₄₊₂] polyhedron:

Cu – O1	200.9 (2×)
– O2	226.1 (2×)
– O3	202.0 (2×)

[B₁₂H₁₂]²⁻ anion:

B1 – B7	177.9 (2×)	B2 – B7	177.1 (2×)
– B2	177.9	– B5	177.7 (2×)
– B8	178.1 (2×)	– B1	177.9
– H1	106.0	– H2	99.6
B3 – B4	175.3	B4 – B3	175.3
– B6	177.0 (2×)	– B6	176.2 (2×)
– B5	178.2 (2×)	– B8	177.9 (2×)
– H3	72.5	– H4	80.0
B5 – B7	176.9	B6 – B4	176.2
– B2	177.7	– B3	176.9
– B6	177.9	– B8	177.0
– B3	178.2	– B7	177.6
– B5	178.5	– B5	177.9
– H5	110.8	– H6	94.7
B7 – B5	176.9	B8 – B6	177.0
– B2	177.0	– B7	177.5
– B8	177.5	– B4	177.9
– B6	177.6	– B1	178.1
– B1	177.9	– B8	179.8
– H7	107.9	– H8	112.8

Table 19: (continued)[ZnO₆] polyhedron:

Zn – O1	205.0 (2×)
– O2	210.0 (2×)
– O3	206.8 (2×)

[B₁₂H₁₂]²⁻ anion:

B1 – B7	177.9 (2×)	B2 – B7	177.0 (2×)
– B2	178.3	– B5	177.2 (2×)
– B8	178.5 (2×)	– B1	178.3
– H1	109.5	– H2	103.8
B3 – B5	177.1 (2×)	B4 – B8	177.4 (2×)
– B4	177.7	– B6	177.5 (2×)
– B6	177.8 (2×)	– B3	177.7
– H3	104.3	– H4	110.7
B5 – B7	176.7	B6 – B8	177.0
– B3	177.1	– B4	177.5
– B2	177.2	– B7	177.5
– B5	177.4	– B5	177.7
– B6	177.7	– B3	177.7
– H5	110.5	– H6	105.3
B7 – B5	176.7	B8 – B6	177.0
– B2	177.9	– B4	177.4
– B6	177.5	– B7	177.7
– B8	177.7	– B8	178.3
– B1	177.9	– B1	178.5
– H7	106.6	– H8	104.8

Table 19: (*continued*)[CdO₆] polyhedron:

Cd – O1	224.3 (2×)
– O2	232.6 (2×)
– O3	227.4 (2×)

[B₁₂H₁₂]²⁻ anion:

B1 – B8	174.4 (2×)	B2 – B7	177.2 (2×)
– B7	176.1 (2×)	– B5	178.4 (2×)
– B2	178.7	– B1	178.7
– H1	120.3	– H2	113.8
B3 – B5	175.4 (2×)	B4 – B8	177.7 (2×)
– B6	177.2 (2×)	– B6	178.1 (2×)
– B4	178.6	– B3	178.6
– H3	114.6	– H4	122.7
B5 – B3	175.4	B6 – B7	173.9
– B5	176.5	– B8	175.3
– B6	176.9	– B5	176.9
– B7	177.4	– B3	177.2
– B2	178.4	– B4	178.1
– H5	105.2	– H6	107.7
B7 – B8	173.3	B8 – B7	173.3
– B6	173.9	– B1	174.4
– B1	176.1	– B6	175.3
– B2	177.2	– B8	177.2
– B5	177.4	– B4	177.7
– H7	102.0	– H8	100.0

3.2.3.3 Thermal Analysis of $[\text{Ni}(\text{H}_2\text{O})_6](\text{H}_3\text{O})_2[\text{B}_{12}\text{H}_{12}]_2 \cdot 6 \text{H}_2\text{O}$

To investigate the thermal stability of dioxonium dodecahydro-*closo*-dodecaborate hydrates with divalent transition metal cations, $[\text{Ni}(\text{H}_2\text{O})_6](\text{H}_3\text{O})_2[\text{B}_{12}\text{H}_{12}]_2 \cdot 6 \text{H}_2\text{O}$ was chosen to be analyzed exemplarily by DTA/TG methods in argon atmosphere. The thermal dehydration of the investigated sample occurred at 100 °C with an endothermic signal in the DTA curve and a peak in the TG curve corresponding to the dehydration (Fig. 26). After the loss of 5.5 to 6.0 mol of “zeolitic” water, the second stage of dehydration is followed by another endothermic signal in DTA at 161 °C. This rather continuous process is ending up at 657 °C with the total dehydration of 12 mol of water in $[\text{Ni}(\text{H}_2\text{O})_6](\text{H}_3\text{O})_2[\text{B}_{12}\text{H}_{12}]_2 \cdot 6 \text{H}_2\text{O}$. There are no more changes in the TG curve when heating the sample up to 1200 °C. This shows that the solvent-free form of the studied compound is thermally very stable in argon atmosphere.

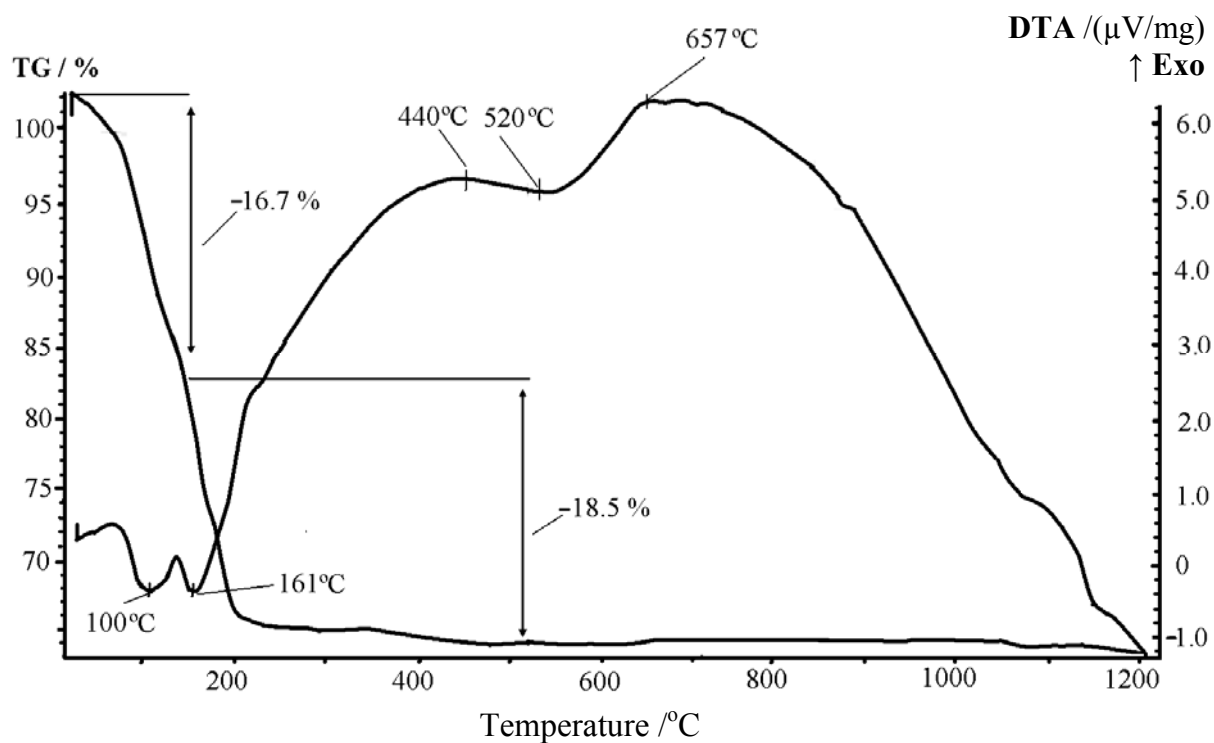


Fig. 26: DTA/TG diagram of $[\text{Ni}(\text{H}_2\text{O})_6](\text{H}_3\text{O})_2[\text{B}_{12}\text{H}_{12}]_2 \cdot 6 \text{H}_2\text{O}$ from room temperature to 1200 °C

3.2.4 Hexaaqua-Iron(II) Dodecahydro-*closo*-Dodecaborate

Although many crystal structures of dodecahydro-*closo*-dodecaborates of hydrated divalent transition metals such as Cu^{2+} , Co^{2+} , Zn^{2+} and Mn^{2+} have been elucidated, that one with iron(II) among the dodecahydro-*closo*-dodecaborate hydrates was not available in literature [16, 85]. Growing suitable single crystals for a crystal structure determination of these reported salts was successful in the form of their aqua-complexes, followed by recrystallization from water. The synthesis methods for the dodecahydro-*closo*-dodecaborate salts of iron(II) and iron(III), however, had not been published. In addition to normal crystal growth problems (twinning, decomposition, hydrolysis), the unstable oxidation state of the Fe^{2+} cation might also be a reason for the absence of single crystal structure data for iron(II) dodecahydro-*closo*-dodecaborates so far.

3.2.4.1 Synthesis of $\text{Fe}(\text{H}_2\text{O})_6[\text{B}_{12}\text{H}_{12}]$

The title compound was prepared by the reaction of iron powder with an aqueous solution of the free acid $(\text{H}_3\text{O})_2[\text{B}_{12}\text{H}_{12}]$ for 24 h under argon atmosphere in order to stabilize the divalent oxidation state of iron. The resulting solution is then filtered off and subsequently evaporated at room temperature by steady argon bubbling. Almost colourless, very pale bluish green, polyhedrally shaped single crystals were obtained and a suitable one was selected for X-ray single crystal diffraction measurements.

3.2.4.2 Structure Description of $\text{Fe}(\text{H}_2\text{O})_6[\text{B}_{12}\text{H}_{12}]$

Monoclinic hexaaqua-iron(II) dodecahydro-*closo*-dodecaborate $\text{Fe}(\text{H}_2\text{O})_6[\text{B}_{12}\text{H}_{12}]$ crystallizes in space group $C2/m$ (no. 12) with the lattice constants $a = 1393.45(9)$, $b = 1449.78(9)$, $732.00(5)$ pm, $\beta = 95.879(3)^\circ$ and four formula units per unit cell (Fig. 27). The crystal structure of $\text{Fe}(\text{H}_2\text{O})_6[\text{B}_{12}\text{H}_{12}]$ is basically isostructural to that one reported for $\text{Cd}(\text{H}_2\text{O})_6[\text{B}_{12}\text{H}_{12}]$ [85]. The crystal structure analysis revealed that the Fe^{2+} cations occupy two crystallographically different *Wyckoff* positions (Fe1 at $2a$: $x/a = y/b = z/c = 0$ and Fe2 at $2b$: $x/a = 0$, $y/b = 1/2$, $z/c = 0$; site symmetry: $2/m$ for both). The oxygen atoms of the water molecules that coordinate all to the Fe^{2+} cations are located at six crystallographically distinct sites. Particularly, O2 and O3 reside at the *Wyckoff* $4i$ site (x/a , $y/b = 0$, z/c ; site

symmetry: m), O4 in 4g ($x/a = 0$, y/b , $z/c = 0$; site symmetry: 2) and O1 at the general *Wyckoff* position 8j (x/a , y/b , z/c ; site symmetry: 1). The two oxygen atoms O5 and O6 are located at two different half-occupied 8j sites with site occupancies of 0.62 and 0.38, respectively, as split positions. All of the boron and hydrogen atoms of the *quasi*-icosahedral $[\text{B}_{12}\text{H}_{12}]^{2-}$ -cluster anions are found at the general *Wyckoff* positions 8j. Similar to the non-disordered aristotype $\text{Cd}(\text{H}_2\text{O})_6[\text{B}_{12}\text{H}_{12}]$, the structure of $\text{Fe}(\text{H}_2\text{O})_6[\text{B}_{12}\text{H}_{12}]$ can be addressed as a monoclinic distortion variant of the CsCl-type structure. The center of gravity of the *quasi*-icosahedral $[\text{B}_{12}\text{H}_{12}]^{2-}$ -cluster anion originates at the *Wyckoff* position 4f ($x/a = y/b = z/c = 1/2$; site symmetry: $\bar{1}$). Both the Fe1 and the Fe2 cations are octahedrally coordinated by oxygen atoms of six nearest water molecules (Fig. 28). These coordination spheres, which differ in their relative orientation within the crystal lattice, are slightly distorted from a perfect octahedron with $d(\text{Fe}-\text{O}) = 208 - 214$ pm and $\angle(\text{O}-\text{Fe}-\text{O}) = 87 - 93^\circ$. Due to the absence of “zeolitic” crystal water molecules and in contrast to the reported dodecahydrate phases $\text{M}(\text{H}_2\text{O})_6[\text{B}_{12}\text{H}_{12}] \cdot 6 \text{H}_2\text{O}$ ($\text{M} = \text{Co}, \text{Ni}, \text{Zn}, \text{Mn}$ and Mg), a strong $\text{O}-\text{H}^{\delta+} \cdots \delta^-\text{O}$ hydrogen bonding system, which connects the oxygen atoms of coordinating water molecules to those of crystalline “zeolitic” ones, can not be found in this compound. With the shortest $\text{Fe} \cdots \text{H}$ distance of 380 pm, there is no direct contact between the dication Fe^{2+} and hydrogen atoms of the anionic boron cages. There are weak, non-classical $\text{B}-\text{H}^{\delta-} \cdots \delta^+\text{H}-\text{O}$ hydrogen bridging bonds between hydrogen atoms of coordinating water molecules and hydrogen atoms of the $[\text{B}_{12}\text{H}_{12}]^{2-}$ cage judging from the short indirect junction lines $d(\text{B} \cdots \text{O}) = 345 - 406$ pm. Each hydrated iron(II) cation is cubically coordinated by eight surrounding $[\text{B}_{12}\text{H}_{12}]^{2-}$ -cluster anions via these weak hydrogen bonds, forming a network that stabilizes the crystal structure of $\text{Fe}(\text{H}_2\text{O})_6[\text{B}_{12}\text{H}_{12}]$ (Fig. 29). The interatomic B–B distances of the *quasi*-icosahedral $[\text{B}_{12}\text{H}_{12}]^{2-}$ boron cage range from 176 to 179 pm and the B–H distances were fixed deliberately at 110 pm (Fig. 30).

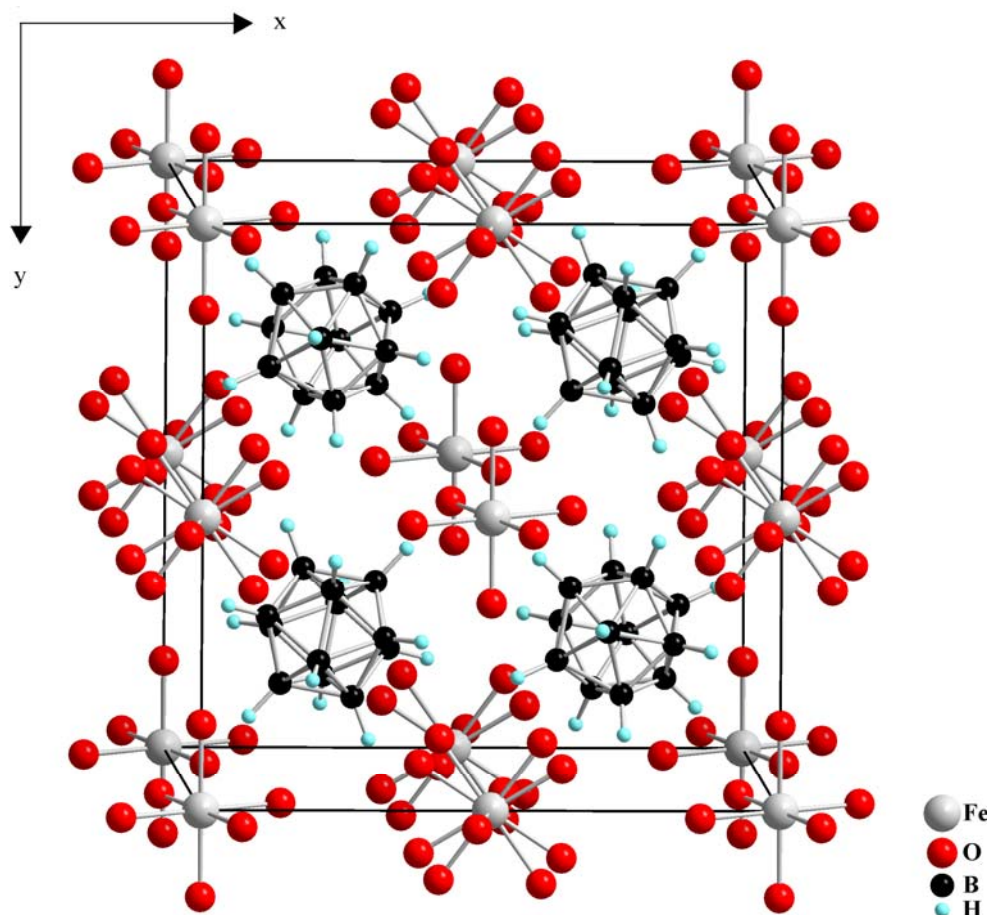


Fig. 27: Perspective view of the crystal structure of $\text{Fe}(\text{H}_2\text{O})_6[\text{B}_{12}\text{H}_{12}]$ along [001]

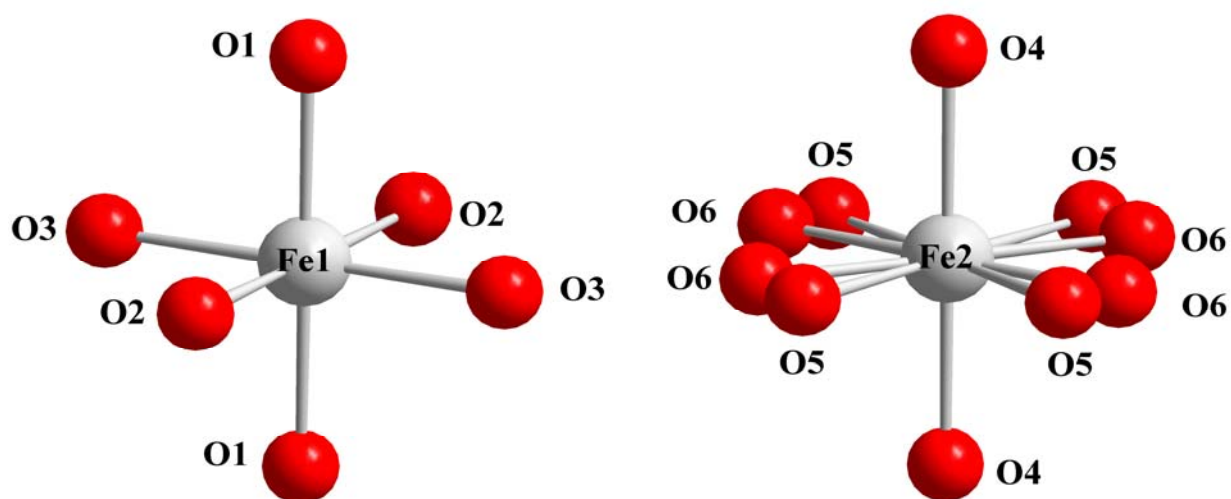


Fig. 28: View at the octahedral coordination spheres about the $(\text{Fe}1)^{2+}$ (left, ordered) and the $(\text{Fe}2)^{2+}$ cation (right, disordered)

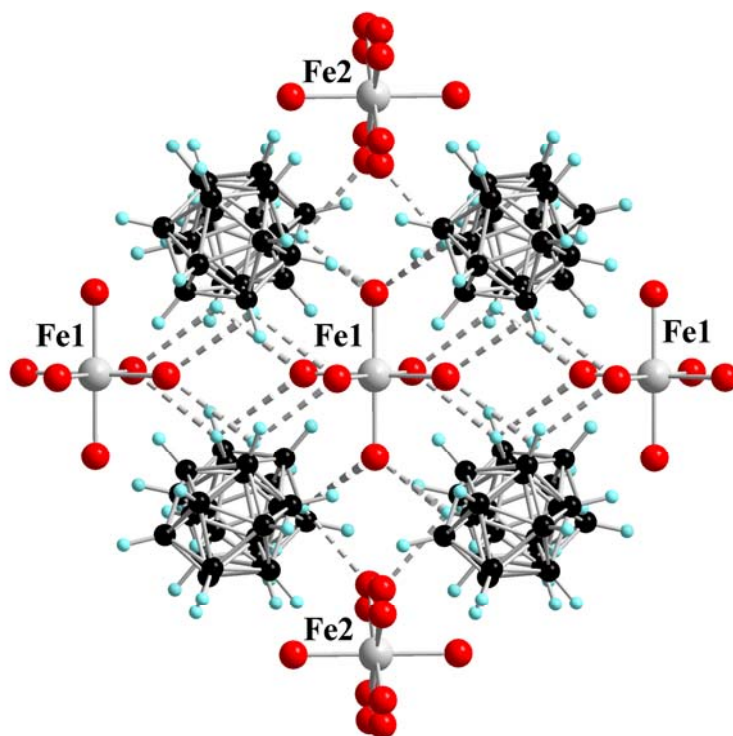


Fig. 29: Scheme of the $B-H^{\delta-}\cdots\delta^+H-O$ hydrogen bridging bonds in the crystal structure of $Fe(H_2O)_6[B_{12}H_{12}]$

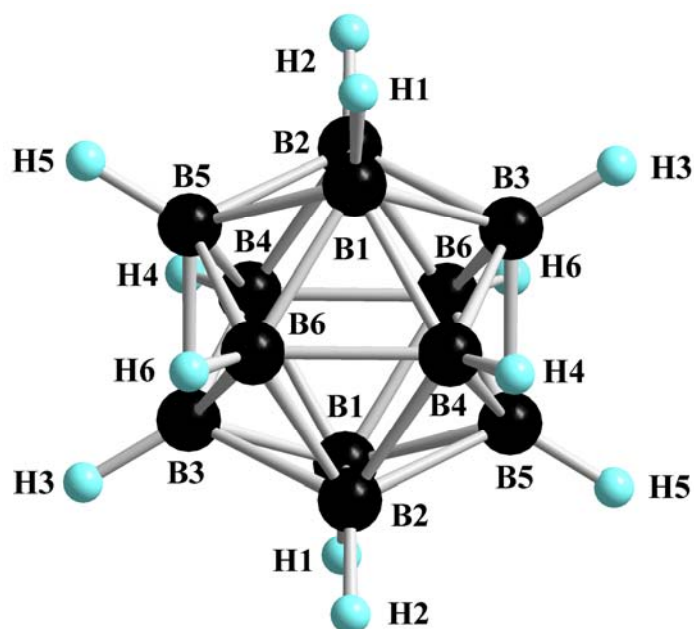


Fig. 30: View at the *quasi*-icosahedral $[B_{12}H_{12}]^{2-}$ -cluster anion in the crystal structure of $Fe(H_2O)_6[B_{12}H_{12}]$

Table 20: Crystallographic data for $\text{Fe}(\text{H}_2\text{O})_6[\text{B}_{12}\text{H}_{12}]$ and their determination

Crystallographic data	
Crystal system	monoclinic
Space group	C2/m (no. 12)
Unit cell parameters:	
a (pm)	1393.45(9)
b (pm)	1449.78(9)
c (pm)	732.00(5)
β (deg)	95.879(3)
Number of formula units per unit cell	Z = 4
Calculated density ($D_x/\text{g cm}^{-3}$)	1.381
Molar volume ($V_m/\text{cm}^3 \text{ mol}^{-1}$)	221.5
Diffractometer	κ -CCD (Bruker-Nonius)
Radiation	Mo-K α : $\lambda = 71.07$ pm, graphite monochromator
Index range	$\pm h_{\max} = 18, \pm k_{\max} = 18, \pm l_{\max} = 9$
θ_{\max} (deg)	27.4
F(000)	632
Absorption coefficient (μ/mm^{-1})	1.03
Absorption correction	numerical, Program X-SHAPE [64]
Other data corrections	background, polarization and Lorentz factors
Collected reflections	14965
Unique reflections	1745
$R_{\text{int}}, R_{\sigma}$	0.092, 0.040
Structure solution and refinement	Program SHELXS-97 and SHELXL-97 [68]
Scattering factors	International Tables for Crystallography, Vol. C [87]
R_1, R_w with $ F_o \geq 4\sigma(F_o)$	0.096, 0.086
Reflections with $ F_o \geq 4\sigma(F_o)$	1454
wR_2 , Goodness of fit (GooF)	0.072, 1.039
Extinction (g)	0.0016(3)
Residual electron density (<i>max.</i> ; <i>min.</i> in $\rho/e^{-1} 10^6$ pm)	2.73, -0.65

Table 21: Atomic coordinates for Fe(H₂O)₆[B₁₂H₁₂]

Atom	Wyckoff position	x/a	y/b	z/c
Fe1	2a	0	0	0
Fe2	2b	0	1/2	0
O1	4g	0	0.1467(4)	0
O2	4i	0.0549(5)	0	0.7401(8)
O3	4i	0.5414(4)	0	0.1188(8)
O4	4i	0.0413(4)	1/2	0.2907(6)
O5 ^{a)}	8j	0.0870(20)	0.3801(20)	0.9684(11)
O6 ^{a)}	8j	0.1209(14)	0.4245(23)	0.9623(16)
B1	8j	0.1609(5)	0.2454(4)	0.6388(9)
B2	8j	0.1652(4)	0.1682(4)	0.4535(8)
B3	8j	0.2519(4)	0.1611(4)	0.6479(9)
B4	8j	0.2802(4)	0.2753(5)	0.7227(8)
B5	8j	0.1399(4)	0.2867(5)	0.4091(8)
B6	8j	0.2120(5)	0.3519(4)	0.5744(9)
H1 ^{b)}	8j	0.103	0.242	0.730
H2 ^{b)}	8j	0.110	0.115	0.422
H3 ^{b)}	8j	0.203	0.103	0.745
H4 ^{b)}	8j	0.300	0.292	0.868
H5 ^{b)}	8j	0.068	0.311	0.350
H6 ^{b)}	8j	0.187	0.419	0.623

^{a)} s.o.f. of O5: 0.62(5), s.o.f. of O6: 0.38(5);

^{b)} refinement with DFIX constraint ($d(\text{B-H}) = 110 \text{ pm}$); $U_{\text{iso}}(\text{H}) = 1.2 \cdot U_{\text{iso}}(\text{B})$.

Table 22: Anisotropic thermal displacement coefficients^{a)} (U_{ij}/pm^2) for $\text{Fe}(\text{H}_2\text{O})_6[\text{B}_{12}\text{H}_{12}]$

Atom	U_{11}	U_{22}	U_{33}	U_{23}	U_{13}	U_{12}
Fe1	383(8)	312(7)	340(7)	0	32(5)	0
Fe2	390(8)	323(7)	270(7)	0	27(5)	0
O1	938(52)	395(29)	930(52)	0	-176(39)	0
O2	592(35)	971(50)	410(28)	0	143(24)	0
O3	483(29)	586(33)	550(31)	0	-46(23)	0
O4	562(30)	353(30)	306(22)	0	12(20)	0
O5	1092(118)	560(145)	458(39)	-73(42)	13(45)	487(108)
O6	598(82)	359(113)	399(53)	-20(48)	-8(43)	184(72)
B1	369(28)	581(39)	376(29)	77(21)	92(22)	9(21)
B2	412(27)	442(20)	438(28)	23(23)	-24(21)	-167(22)
B3	395(26)	464(31)	512(31)	224(25)	-25(22)	-29(23)
B4	441(29)	603(33)	328(25)	-20(25)	-1(21)	-78(27)
B5	324(24)	466(32)	482(29)	128(25)	17(20)	18(22)
B6	521(32)	396(29)	610(37)	-149(28)	96(27)	36(25)
H1	526					
H2	522					
H3	554					
H4	552					
H5	511					
H6	608					

^{a)} For Fe, O and B defined as anisotropic temperature factor according to: $\exp[-2\pi^2(U_{11}h^2a^{*2} + U_{22}k^2b^{*2} + U_{33}l^2c^{*2} + 2U_{23}klb^{*}c^{*} + 2U_{13}hla^{*}c^{*} + 2U_{13}hka^{*}b^{*})]$; for H isotropically defined as temperature factor in: $\exp[-8\pi^2(U_{\text{iso}}\sin^2\theta/\lambda^2)]$.

Table 23: Selected interatomic distances (d/pm) for Fe(H₂O)₆[B₁₂H₁₂]

[FeO ₆] polyhedron:			
Fe1	– O3	211.7 (2×)	
	– O2	212.2 (2×)	
	– O1	212.7 (2×)	
			Fe2 – O6
			– O5
			– O4
			205.2 (4/2×)
			214.5 (4/2×)
			214.7 (2×)
[B ₁₂ H ₁₂] ²⁻ anion:			
B1	– B3	175.6	
	– B2	176.4	
	– B4	176.5	
	– B5	178.1	
	– B6	178.3	
	– H1	110.0	
			B2 – B1
			– B4
			– B6
			– B3
			– B5
			– H2
			176.4
			176.4
			176.8
			177.3
			177.7
			110.0
B3	– B1	175.7	
	– B6	176.2	
	– B2	177.3	
	– B4	177.6	
	– B5	177.6	
	– H3	110.0	
			B4 – B6
			– B2
			– B1
			– B3
			– B5
			– H4
			176.1
			176.4
			176.5
			177.6
			178.9
			110.0
B5	– B6	176.6	
	– B3	177.6	
	– B2	177.7	
	– B1	178.1	
	– B4	178.8	
	– H5	110.0	
			B6 – B4
			– B3
			– B5
			– B2
			– B1
			– H6
			176.1
			176.2
			176.6
			176.8
			178.3
			110.0

3.2.5 Triaqua-Lead(II) Dodecahydro-*closo*-Dodecaborate Trihydrate $\text{Pb}(\text{H}_2\text{O})_3[\text{B}_{12}\text{H}_{12}] \cdot 3 \text{H}_2\text{O}$

Although dodecahydro-*closo*-dodecaborates have been studied very systematically, the crystal structures of some salts with divalent metals are not yet elucidated. One of these examples is the dodecahydro-*closo*-dodecaborate of Pb^{2+} , which has a lone-pair electron $6s^2$, even though the synthesis of this salt was published fifty years ago [16]. Hence, we here present the synthesis and crystal structure of lead(II) dodecahydro-*closo*-dodecaborate hydrate for the first time.

3.2.5.1 Synthesis of $\text{Pb}(\text{H}_2\text{O})_3[\text{B}_{12}\text{H}_{12}] \cdot 3 \text{H}_2\text{O}$

Lead(II) dodecahydro-*closo*-dodecaborate hydrate was synthesized by the reaction of PbCO_3 (Merck: 99.9 %) with an aqueous solution of the free acid $(\text{H}_3\text{O})_2[\text{B}_{12}\text{H}_{12}]$. After heating this reacting mixture at about 90 °C for 12 h, the residual solids were filtered off. Colourless, lath-shaped single crystals of hydrated lead(II) dodecahydro-*closo*-dodecaborate were obtained by isothermal evaporation of resulting solution.

3.2.5.2 Structure Description of $\text{Pb}(\text{H}_2\text{O})_3[\text{B}_{12}\text{H}_{12}] \cdot 3 \text{H}_2\text{O}$

The title compound $\text{Pb}(\text{H}_2\text{O})_3[\text{B}_{12}\text{H}_{12}] \cdot 3 \text{H}_2\text{O}$ crystallizes in the orthorhombic crystal system with the non-centrosymmetric space group $\text{Pna}2_1$ (no. 33) and four formula units per unit cell (Fig. 31). The crystal structure of $\text{Pb}(\text{H}_2\text{O})_3[\text{B}_{12}\text{H}_{12}] \cdot 3 \text{H}_2\text{O}$ is characterized as a layer-like arrangement, in which Pb^{2+} and $[\text{B}_{12}\text{H}_{12}]^{2-}$ are alternatively stacked. In this crystal structure the lead(II) cations, the oxygen atoms of water molecules and all boron and hydrogen atoms of the boron cages occupy the general *Wyckoff* position $4a$ ($x/a, y/b, z/c$; site symmetry: 1). Each Pb^{2+} cation is coordinated with only three nearest oxygen atoms of water molecules ($\angle(\text{O}-\text{Pb}-\text{O}) = 74 - 77^\circ$) (Fig. 32, *left*). The Pb–O bond lengths are in the range of 247 – 249 pm and thus similar to those found in other compounds containing Pb^{2+} such as $\text{Pb}(\text{OH})\text{Br}$ ($d(\text{Pb}-\text{O}) = 239 - 248$ pm) [92]. The Pb^{2+} cations are also connected to three nearest $[\text{B}_{12}\text{H}_{12}]^{2-}$ -cluster anions via one hydrogen atom per each cage ($d(\text{Pb}-\text{H}) = 250 - 268$ pm). As a result, Pb^{2+} has a coordination number of six with three coordinated oxygen atoms of H_2O molecules and three hydrogen atoms that form an irregular polyhedron (Fig. 32, *right*). The distances from the lead(II) cation to other hydrogen atoms of $[\text{B}_{12}\text{H}_{12}]^{2-}$ -cluster anions range

from 295 to 335 pm and a second coordination sphere is formed. In this coordination sphere, the central cation is coordinated to the same three nearest $[\text{B}_{12}\text{H}_{12}]^{2-}$ -cluster anions as before, but now via three hydrogen atoms originating from one triangular face of each $[\text{B}_{12}\text{H}_{12}]^{2-}$ cage and the coordination number of Pb^{2+} is thus extended to 12 (Fig. 33, *left* and *right*). It is, hence,

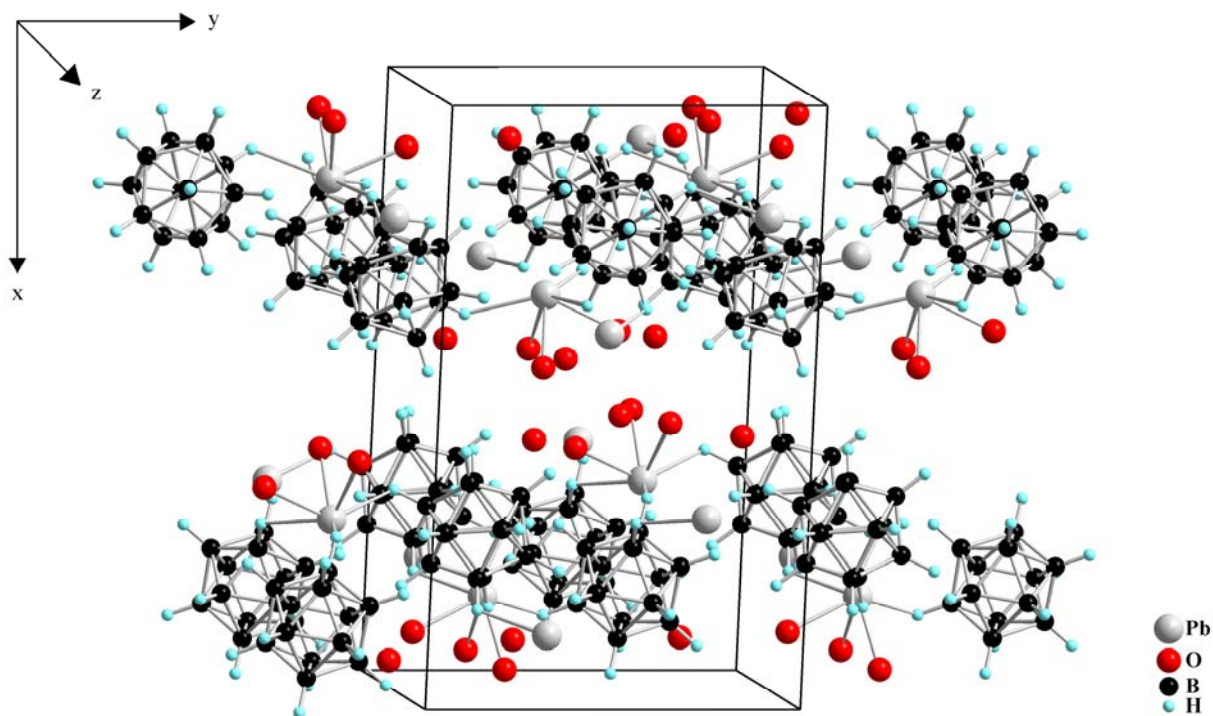


Fig. 31: View at the unit cell of $\text{Pb}(\text{H}_2\text{O})_3[\text{B}_{12}\text{H}_{12}] \cdot 3 \text{H}_2\text{O}$ along $[001]$

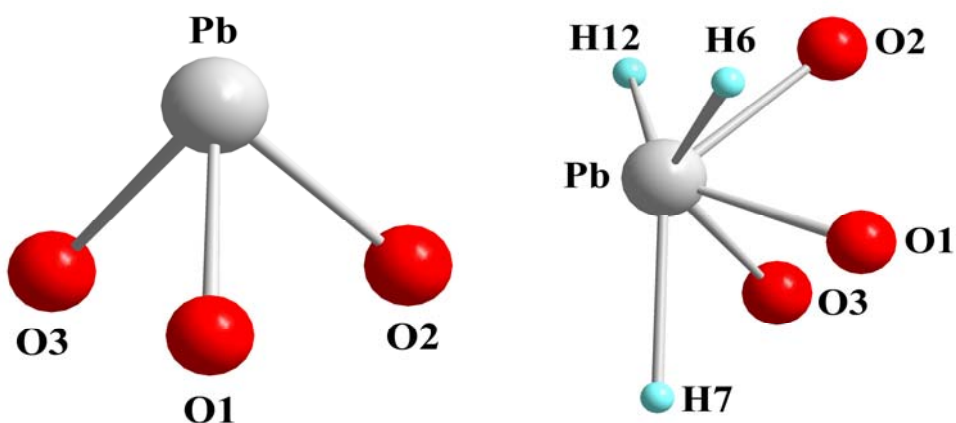


Fig. 32: The non-spherical coordination polyhedron $[\text{Pb}(\text{H}_2\text{O})_3]^{2+}$ of Pb^{2+} with three coordinating water molecules (*left*) and the mixed coordination sphere of Pb^{2+} with three water molecules and three hydrogen atoms of $[\text{B}_{12}\text{H}_{12}]^{2-}$ anions (*right*)

obvious that in the crystal structure of $\text{Pb}(\text{H}_2\text{O})_3[\text{B}_{12}\text{H}_{12}] \cdot 3 \text{H}_2\text{O}$ the Pb^{2+} cations coordinate to both the oxygen atoms of coordinating water molecules and the hydrogen atoms of $[\text{B}_{12}\text{H}_{12}]^{2-}$ -cluster anions to form a “mixed” anionic coordination sphere. A coordination number of twelve is also found in the crystal structure of $\text{Ba}(\text{H}_2\text{O})_6[\text{B}_{12}\text{H}_{12}]$, in which Ba^{2+} is linked to six neighbouring oxygen atoms of water molecules [93], but there are only two $[\text{B}_{12}\text{H}_{12}]^{2-}$ -cluster anions connected to every Ba^{2+} cation via three hydrogen atoms belonging to one triangular face per each. This coordination environment again differs from that one of the Na^+ cations in the partially disordered room temperature crystal phase of $\text{Na}_2(\text{H}_2\text{O})_4[\text{B}_{12}\text{H}_{12}]$, in which Na^+ is coordinated by four nearest oxygen atoms of water molecules [81, 94]. Furthermore, two hydrogen atoms from two different $[\text{B}_{12}\text{H}_{12}]^{2-}$ -cluster anions connect to each Na^+ cation with relative short distances. Thus four nearest oxygen atoms of water molecules and two hydrogen atoms from two $[\text{B}_{12}\text{H}_{12}]^{2-}$ -cluster anions form a distorted octahedral coordination sphere and the Na^+ cations exhibit a coordination number of six. Although the crystal structure of $\text{Pb}(\text{H}_2\text{O})_3[\text{B}_{12}\text{H}_{12}] \cdot 3 \text{H}_2\text{O}$ is similar to that of $\text{Ba}(\text{H}_2\text{O})_6[\text{B}_{12}\text{H}_{12}]$ in some aspects, the Pb^{2+} cations show rather non-spherical coordination environment owing to a strong stereochemical lone-pair activity $6sp$ rather than $6s^2$. The *quasi*-icosahedral $[\text{B}_{12}\text{H}_{12}]^{2-}$ -cluster anions connect to the pyramidal $[\text{Pb}(\text{H}_2\text{O})_3]^{2+}$ units in a way that one-dimensional chains along $[010]$ can form. The chains are separated from each other by “zeolitic” crystal water molecules and then the layer-structure (Fig. 31) is generated. There are both classical $\text{O}-\text{H}^{\delta+} \cdots \delta^-\text{O}$ and non-classical $\text{B}-\text{H}^{\delta-} \cdots \delta^+\text{H}-\text{O}$ hydrogen bridging bonds that stabilize the crystal structure of $\text{Pb}(\text{H}_2\text{O})_3[\text{B}_{12}\text{H}_{12}] \cdot 3 \text{H}_2\text{O}$. The strong hydrogen bridging bonds are not only found among the oxygen atoms of water molecules of the $[\text{Pb}(\text{H}_2\text{O})_3]^{2+}$ units themselves, but also between each of them and to “free” crystal water molecules as well. The $\text{O}_{\text{Donor}}-\text{O}_{\text{Acceptor}}$ distances from coordinated oxygen atoms belonging to $[\text{Pb}(\text{H}_2\text{O})_3]^{2+}$ cations to each other range from 298 to 311 pm, while those between coordinated oxygen atoms to oxygen atoms of “zeolitic” crystal water molecules are found in the interval 273 – 284 pm. The B–B and B–H bond lengths of the *quasi*-icosahedral $[\text{B}_{12}\text{H}_{12}]^{2-}$ cluster anions are in the common range for dodecahydro-*closo*-dodecaborates ($d(\text{B}-\text{B}) = 174 - 179$ pm; $d(\text{B}-\text{H}) = 110$ pm) (Fig. 34). The distances from center of gravity of each $[\text{B}_{12}\text{H}_{12}]^{2-}$ anion to its twelve boron atoms are about 170 pm, providing an inner diameter for the $[\text{B}_{12}\text{H}_{12}]^{2-}$ cage of 340 pm.

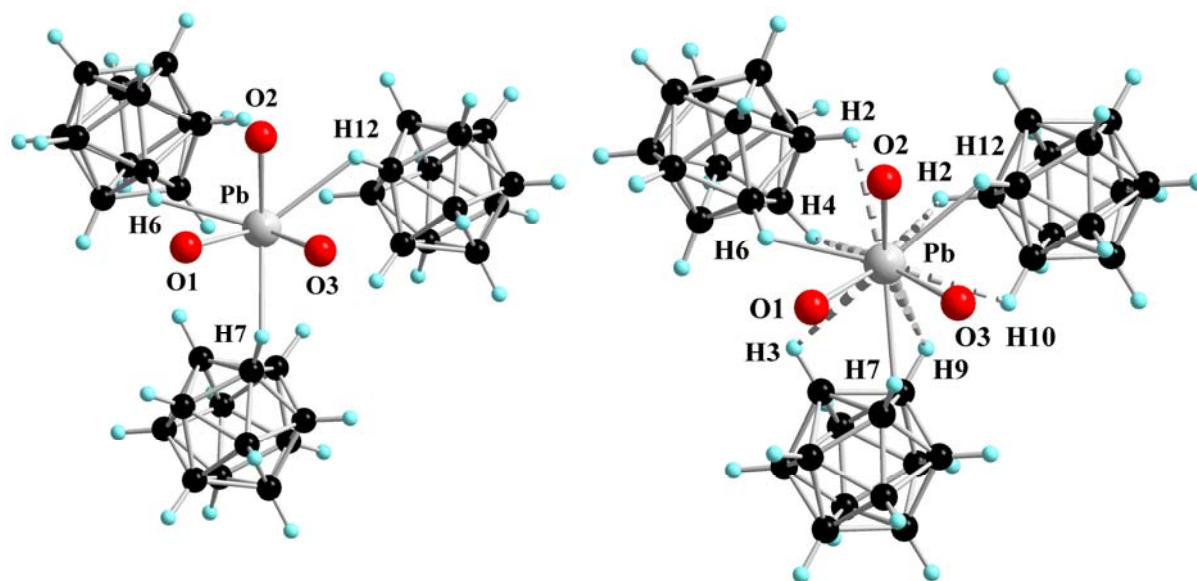


Fig. 33: The first (*left*) and the second coordination sphere (*right*) of the Pb^{2+} cations with three nearest *quasi*-icosahedral $[\text{B}_{12}\text{H}_{12}]^{2-}$ anions in the crystal structure of $\text{Pb}(\text{H}_2\text{O})_3[\text{B}_{12}\text{H}_{12}] \cdot 3 \text{H}_2\text{O}$

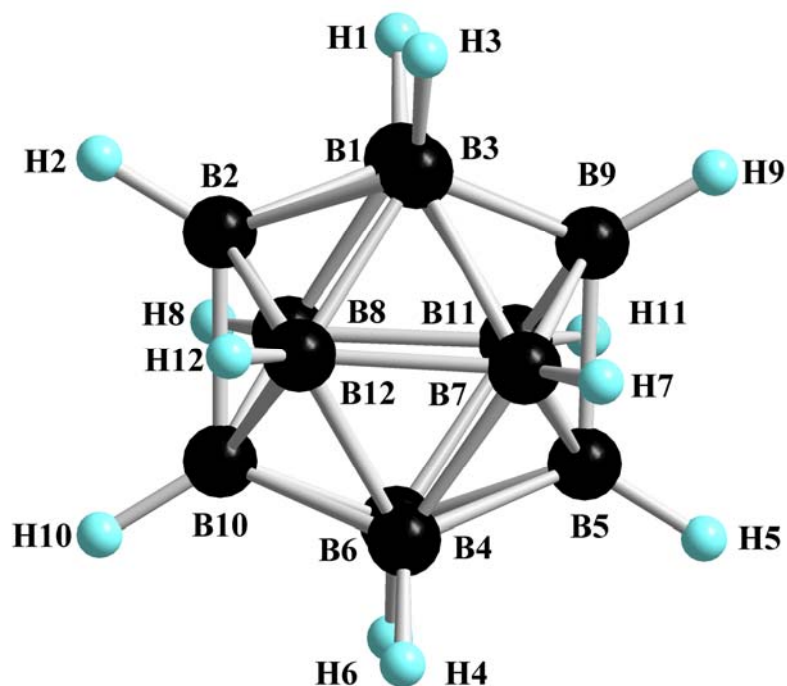


Fig. 34: The *quasi*-icosahedral $[\text{B}_{12}\text{H}_{12}]^{2-}$ -cluster anion in $\text{Pb}(\text{H}_2\text{O})_3[\text{B}_{12}\text{H}_{12}] \cdot 3 \text{H}_2\text{O}$

Table 24: Crystallographic data for $\text{Pb}(\text{H}_2\text{O})_3[\text{B}_{12}\text{H}_{12}] \cdot 3 \text{H}_2\text{O}$ and their determination

Crystallographic data	
Crystal system	orthorhombic
Space group	Pna2 ₁ (no. 33)
Unit cell parameters:	
a (pm)	1839.08(9)
b (pm)	1166.52(6)
c (pm)	717.27(4)
Number of formula units per unit cell	Z = 4
Calculated density ($D_x/\text{g cm}^{-3}$)	1.976
Molar volume ($V_m/\text{cm}^3 \text{ mol}^{-1}$)	231.3
Diffractometer	κ -CCD (Bruker-Nonius)
Radiation	Mo-K α : $\lambda = 71.07 \text{ pm}$, graphite monochromator
Index range	$\pm h_{\text{max}} = 11, \pm k_{\text{max}} = 16, \pm l_{\text{max}} = 15$
θ_{max} (deg)	27.4
F(000)	808
Absorption coefficient (μ/mm^{-1})	10.97
Absorption correction	numerical, Program X-SHAPE [64]
Other data corrections	background, polarization and Lorentz factors
Collected reflections	25544
Unique reflections	3489
$R_{\text{int}}, R_{\sigma}$	0.056, 0.037
Structure solution and refinement	Program SHELXS-97 and SHELXL-97 [68]
Scattering factors	International Tables for Crystallography, Vol. C [87]
R_1, R_w with $ F_o \geq 4\sigma(F_o)$	0.039, 0.030
Reflections with $ F_o \geq 4\sigma(F_o)$	3015
wR ₂ , Goodness of fit (GooF)	0.072, 1.039
Extinction (g)	0.0081(4)
Flack-x-parameter	-0.02(1)
Residual electron density	
(<i>max.</i> , <i>min.</i> in $\rho/e^{-1} 10^6 \text{ pm}$)	1.47, -1.31

Table 25: Atomic coordinates for $\text{Pb}(\text{H}_2\text{O})_3[\text{B}_{12}\text{H}_{12}] \cdot 3 \text{H}_2\text{O}$

Atom	Wyckoff position	x/a	y/b	z/c
Pb	4a	0.32972(1)	0.31566(1)	0.24998(1)
O1	4a	0.4276(3)	0.3183(3)	0.0143(7)
O2	4a	0.4420(3)	0.2806(4)	0.4318(8)
O3	4a	0.1140(3)	0.0068(3)	0.8022(6)
O4w	4a	0.4341(2)	0.1424(3)	0.7408(9)
O5w	4a	0.0703(2)	0.1989(3)	0.2461(9)
O6w	4a	0.4697(3)	0.4671(3)	0.7195(9)
B1	4a	0.2576(5)	0.4441(5)	0.8960(9)
B2	4a	0.2245(5)	0.3059(5)	0.8319(9)
B3	4a	0.2703(3)	0.3938(5)	0.6632(9)
B4	4a	0.2541(4)	0.0367(5)	0.2043(9)
B5	4a	0.3159(4)	0.0382(5)	0.3922(9)
B6	4a	0.1708(5)	0.3966(6)	0.9703(9)
B7	4a	0.3950(4)	0.9652(6)	0.3242(9)
B8	4a	0.6298(4)	0.1811(6)	0.7863(9)
B9	4a	0.1916(5)	0.3167(7)	0.5943(9)
B10	4a	0.2059(5)	0.4595(6)	0.5214(9)
B11	4a	0.3947(5)	0.0472(7)	0.1638(9)
B12	4a	0.6183(4)	0.0873(6)	0.5966(9)
H1 ^{a)}	4a	0.303	0.455	0.994
H2 ^{a)}	4a	0.248	0.227	0.888
H3 ^{a)}	4a	0.324	0.307	0.610
H4 ^{a)}	4a	0.216	0.108	0.177
H5 ^{a)}	4a	0.318	0.111	0.490
H6 ^{a)}	4a	0.160	0.376	0.117
H7 ^{a)}	4a	0.449	0.990	0.375
H8 ^{a)}	4a	0.592	0.252	0.813
H9 ^{a)}	4a	0.194	0.244	0.496
H10 ^{a)}	4a	0.218	0.481	0.375
H11 ^{a)}	4a	0.371	0.127	0.109
H12 ^{a)}	4a	0.572	0.098	0.500

^{a)} refinement with DFIX constraint ($d(\text{B-H}) = 110 \text{ pm}$); $U_{\text{iso}}(\text{H}) = 1.2 \cdot U_{\text{iso}}(\text{B})$.

Table 26: Anisotropic thermal displacement coefficients^{a)} (U_{ij}/pm^2) for $\text{Pb}(\text{H}_2\text{O})_3[\text{B}_{12}\text{H}_{12}] \cdot 3 \text{H}_2\text{O}$

Atom	U_{11}	U_{22}	U_{33}	U_{23}	U_{13}	U_{12}
Pb	294(1)	303(1)	330(1)	-6(3)	6839	-16(1)
O1	423(35)	312(25)	336(29)	19(18)	94(24)	-8(20)
O2	333(30)	423(24)	452(33)	46(24)	-7(24)	-51(24)
O3	525(31)	274(19)	599(38)	-25(19)	91(23)	46(19)
O4w	441(24)	480(20)	392(21)	36(42)	-13(41)	40(17)
O5w	399(25)	632(25)	671(30)	24(45)	143(57)	-91(18)
O6w	607(31)	498(23)	365(39)	49(22)	-94(26)	-152(20)
B1	517(49)	300(31)	328(67)	78(26)	71(35)	117(27)
B2	349(42)	275(36)	312(44)	-61(27)	-31(36)	38(28)
B3	532(60)	287(38)	329(39)	-11(27)	-38(40)	89(35)
B4	330(38)	277(29)	401(58)	67(24)	37(28)	69(25)
B5	320(46)	274(36)	270(40)	-27(28)	2(31)	17(31)
B6	394(50)	189(32)	493(45)	1(29)	-15(39)	-93(34)
B7	348(44)	344(36)	176(31)	11(27)	-66(30)	17(31)
B8	258(42)	393(39)	420(42)	113(33)	-55(34)	-16(31)
B9	537(59)	382(40)	235(36)	-15(30)	109(33)	-92(37)
B10	386(46)	370(36)	192(32)	54(27)	-10(31)	-44(34)
B11	260(43)	502(47)	551(49)	-274(37)	-42(34)	-12(35)
B12	294(43)	413(42)	271(32)	-2(31)	24(31)	63(33)
H1	458					
H2	374					
H3	459					
H4	404					
H5	346					
H6	430					
H7	347					
H8	428					
H9	462					
H10	379					
H11	525					
H12	391					

^{a)} For Pb, O and B defined as anisotropic temperature factor according to: $\exp[-2\pi^2(U_{11}h^2a^{*2} + U_{22}k^2b^{*2} + U_{33}l^2c^{*2} + 2U_{23}klb^{*}c^{*} + 2U_{13}hla^{*}c^{*} + 2U_{13}hka^{*}b^{*})]$; for H isotropically defined as temperature factor in: $\exp[-8\pi^2(U_{\text{iso}}\sin^2\theta/\lambda^2)]$.

Table 27: Selected interatomic distances (d/pm) and angles (\sphericalangle /deg) for $\text{Pb}(\text{H}_2\text{O})_3[\text{B}_{12}\text{H}_{12}] \cdot 3 \text{H}_2\text{O}$

[PbO ₃ H ₃] polyhedron:					
Pb – O1	247.3	O2–Pb–O3	74.0	Pb – H3	250.3
– O2	247.9	O1–Pb–O2	75.9	– H10	253.0
– O3	248.8	O1–Pb–O3	76.6	– H5	267.9
[B ₁₂ H ₁₂] ²⁻ anion:					
B1 – B9	177.7	B2 – B8	175.8	B3 – B12	176.6
– B2	178.0	– B12	177.0	– B7	177.3
– B8	178.4	– B10	177.1	– B9	177.8
– B3	178.9	– B1	178.0	– B1	178.9
– B11	179.0	– B3	179.0	– B2	179.0
– H1	110.0	– H2	110.0	– H3	110.0
B4 – B12	174.5	B5 – B6	173.5	B6 – B5	173.5
– B6	174.9	– B7	174.0	– B11	173.5
– B7	175.1	– B11	174.7	– B10	174.8
– B10	175.2	– B9	175.3	– B4	174.9
– B5	176.4	– B4	176.4	– B8	175.7
– H4	110.0	– H5	110.0	– H6	110.0
B7 – B5	174.0	B8 – B6	175.7	B9 – B5	175.3
– B4	175.1	– B2	175.9	– B7	177.3
– B12	176.1	– B10	176.7	– B11	177.7
– B9	177.3	– B1	178.4	– B1	177.7
– B3	177.3	– B11	179.1	– B3	177.8
– H7	110.0	– H8	110.0	– H9	110.0
B10 – B6	174.8	B11 – B6	173.5	B12 – B4	174.5
– B12	175.0	– B5	174.7	– B10	175.0
– B4	175.2	– B9	177.7	– B7	176.1
– B8	176.7	– B8	179.1	– B3	176.6
– B2	177.1	– B1	179.1	– B2	177.0
– H10	110.0	– H11	110.0	– H12	110.0

3.3 Dodecahydro-*closo*-Dodecaborate Salts with Trivalent Cations

3.3.1 Crystal Structure of Diaqua-Monohydroxo-Bismuth(III) Dodecahydro-*closo*-Dodecaborate

The counter-cation in dodecahydro-*closo*-dodecaborate salts may exhibit a spherical or non-spherical coordination environment. The spherical one may possess the connection to the $[\text{B}_{12}\text{H}_{12}]^{2-}$ anions directly (e. g. in $\text{Hg}[\text{B}_{12}\text{H}_{12}]$), or absolutely not at all (e. g. in $[\text{Ni}(\text{H}_2\text{O})_6]_2[\text{B}_{12}\text{H}_{12}] \cdot 6 \text{H}_2\text{O}$). The non-spherical one can be expected to exist in dodecahydro-*closo*-dodecaborates with Tl^+ , Pb^{2+} and Bi^{3+} cations that possess lone-pair $6s^2$ electrons. In our recent work, the crystal structures of dodecahydro-*closo*-dodecaborate salts of Tl^+ and Pb^{2+} have been elucidated [95, 96]. The synthesis and crystal structure of a dodecahydro-*closo*-dodecaborate salt with Bi^{3+} cations was not published so far. In order to obtain crystallographic data and to investigate the effect of lone-pair electrons at the Bi^{3+} cation, the first synthesis and crystal structure determination for a dodecahydro-*closo*-dodecaborate salt of bismuth(III) was carried out.

3.3.1.1 Synthesis of $\text{Bi}(\text{H}_2\text{O})_2(\text{OH})[\text{B}_{12}\text{H}_{12}]$

The title compound was synthesized by the reaction of Bi_2O_3 (Merck: 99.9 %) with the aqueous solution of the free acid $(\text{H}_3\text{O})_2[\text{B}_{12}\text{H}_{12}]$, followed by isothermal evaporation of the resulting solution at room temperature. Light yellow, polyhedrally shaped single crystals emerged and were then selected for X-ray diffraction measurements.

3.3.1.2 Structure Description of $\text{Bi}(\text{H}_2\text{O})_2(\text{OH})[\text{B}_{12}\text{H}_{12}]$

The results of a crystal structure determination showed that the compound under consideration has a chemical formula like $\text{Bi}(\text{H}_2\text{O})_2(\text{OH})[\text{B}_{12}\text{H}_{12}]$. Its existence might be due to the strong tendency for hydrolysis of inorganic salts with Bi^{3+} cations [97]. $\text{Bi}(\text{H}_2\text{O})_2(\text{OH})[\text{B}_{12}\text{H}_{12}]$ crystallizes orthorhombically in space group Pnma (no. 62) with four formula units in the unit cell (Fig. 35). In the crystal structure the bismuth(III) cations occupy the special *Wyckoff* site $4c$ ($x/a, y/b = 1/4, z/c$; site symmetry: .m.). The oxygen atoms of the hydroxide anions are also located at the *Wyckoff* position $4c$, while those of the crystal water molecules reside at the general *Wyckoff* site $8d$ ($x/a, y/b, z/c$; site symmetry: 1). All boron and

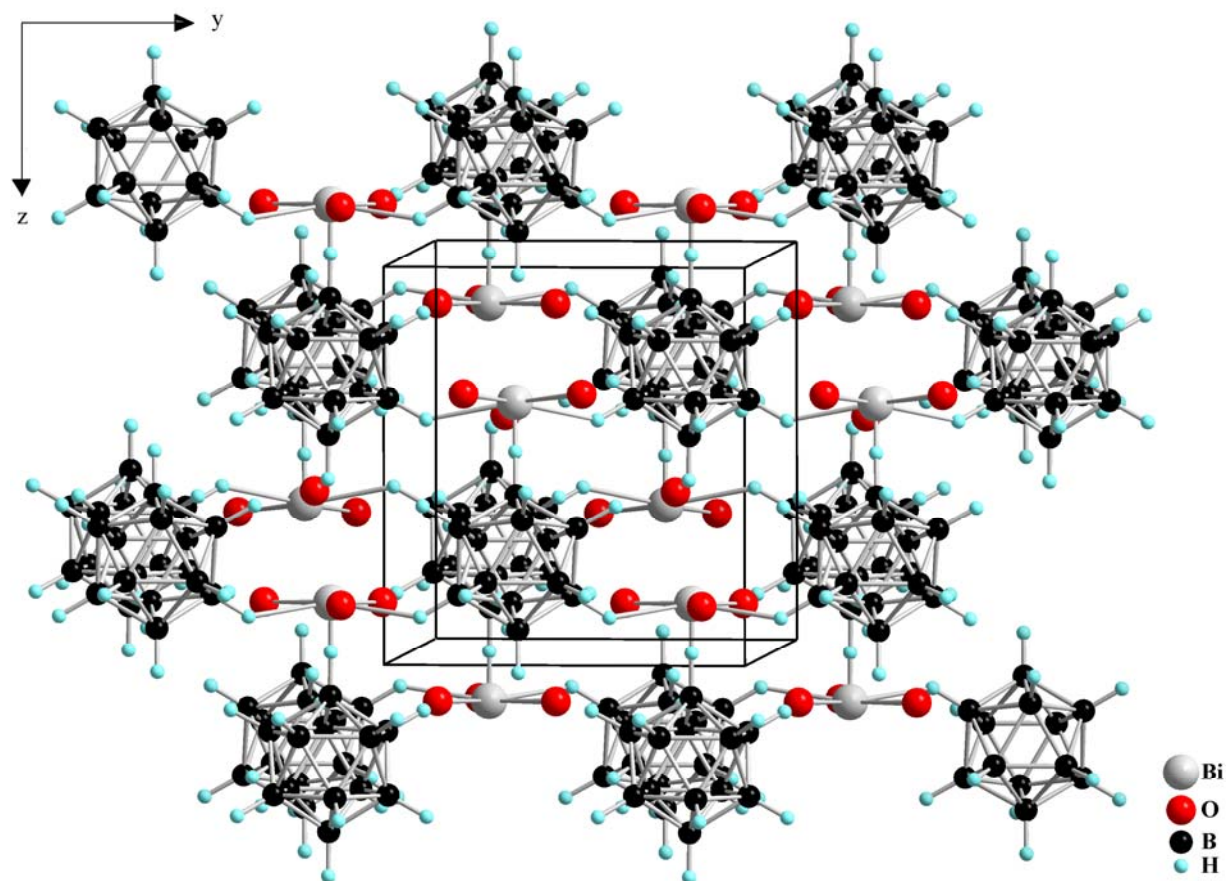


Fig. 35: View at the unit cell of $\text{Bi}(\text{H}_2\text{O})_2(\text{OH})[\text{B}_{12}\text{H}_{12}]$ along $[100]$

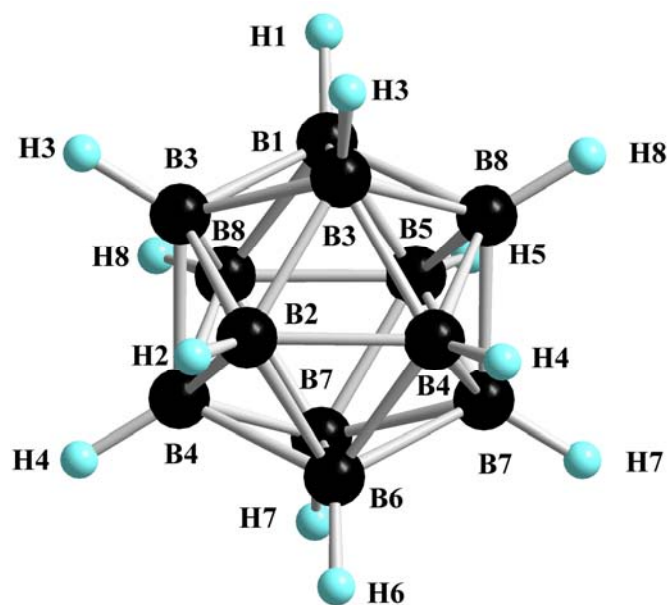


Fig. 36: The *quasi*-icosahedral $[\text{B}_{12}\text{H}_{12}]^{2-}$ -cluster anion in the crystal structure of $\text{Bi}(\text{H}_2\text{O})_2(\text{OH})[\text{B}_{12}\text{H}_{12}]$

hydrogen atoms of the *quasi*-icosahedral $[\text{B}_{12}\text{H}_{12}]^{2-}$ -cluster anions are found at the *Wyckoff* positions *4c* and *8d* (see Table 29). The B–B and B–H bond lengths of the boron cage are in the common range with $d(\text{B–B}) = 175 - 181$ pm and $d(\text{B–H}) = 110$ pm. The centers of gravity of the $[\text{B}_{12}\text{H}_{12}]^{2-}$ -cluster anions occupy the *Wyckoff* position *4c* and the distances from each center of gravity to the twelve boron atoms of 170 pm provides an inner diameter of 340 pm for the boron cage (Fig. 36). Each Bi^{3+} cation is nearly coplanar coordinated by three neighbouring oxygen atoms with two oxygen atoms of coordinated crystal water and one of a hydroxide anion with Bi–O bond length of 252 (2 \times) and 259 pm, respectively (Fig. 37, *left*). This coordination sphere is different from that of the Pb^{2+} cation in $\text{Pb}(\text{H}_2\text{O})_3[\text{B}_{12}\text{H}_{12}] \cdot 3 \text{H}_2\text{O}$, in which Pb^{2+} forms with three oxygen atoms a slightly distorted tetrahedron. Moreover, the Bi^{3+} cation is surrounded by three nearest *quasi*-icosahedral $[\text{B}_{12}\text{H}_{12}]^{2-}$ -cluster anions to form a first hydrogen coordination sphere (Fig. 38, *left*). Two *quasi*-icosahedral $[\text{B}_{12}\text{H}_{12}]^{2-}$ anions connect to each Bi^{3+} cation via one hydrogen atom per boron cage with a Bi–H distance of 232 pm (2 \times). The bismuth(III) cations link to one boron atom (B1) of a third $[\text{B}_{12}\text{H}_{12}]^{2-}$ anion with a significant short Bi–H1–B1 bridge ($d(\text{Bi–B1}) = 233$ pm). To elucidate whether a Bi–B1 direct bond exists or not, a further spectroscopic investigation is required. All Bi^{3+} cations connect to a fourth $[\text{B}_{12}\text{H}_{12}]^{2-}$ anion via one hydrogen atom of this cage with the longest Bi \cdots H distance of 320 pm. As a result, Bi^{3+} is coordinated to four nearest *quasi*-icosahedral $[\text{B}_{12}\text{H}_{12}]^{2-}$ -cluster anions to form a strongly distorted tetrahedral second coordination sphere (Fig. 38, *right*). The distances of the Bi^{3+} cation to centers of gravity of the first two, the third and the fourth $[\text{B}_{12}\text{H}_{12}]^{2-}$ anions are 398 (2 \times), 478 and 589 pm, respectively. So the coordination sphere of each Bi^{3+} cation, which has the coordination number of seven with three oxygen atoms and four hydrogen atoms, represents an irregular polyhedron. (Fig. 37, *right*). Hence, among the known dodecahydro-*closo*-dodecaborate salts with inorganic cations, and together with $\text{Pb}(\text{H}_2\text{O})_3[\text{B}_{12}\text{H}_{12}] \cdot 3 \text{H}_2\text{O}$, $\text{Ba}(\text{H}_2\text{O})_6[\text{B}_{12}\text{H}_{12}]$ and crystal phase $\text{Na}_2(\text{H}_2\text{O})_4[\text{B}_{12}\text{H}_{12}]$, $\text{Bi}(\text{H}_2\text{O})_2(\text{OH})[\text{B}_{12}\text{H}_{12}]$ is the fourth example, in which the central cations have a mixed coordination sphere consisting of both oxygen and hydrogen atoms. Similar to the Pb^{2+} cation in $\text{Pb}(\text{H}_2\text{O})_3[\text{B}_{12}\text{H}_{12}] \cdot 3 \text{H}_2\text{O}$, the Bi^{3+} cation in $\text{Bi}(\text{H}_2\text{O})_2(\text{OH})[\text{B}_{12}\text{H}_{12}]$ has a non-spherical coordination environment, indicating a strong stereochemically active lone-pair 6sp electron. In the crystal structure of $\text{Bi}(\text{H}_2\text{O})_2(\text{OH})[\text{B}_{12}\text{H}_{12}]$ the existence of both of strong $\text{O–H}^{\delta+}\cdots\delta^-\text{O}$ and weak $\text{B–H}^{\delta-}\cdots\delta^+\text{H–O}$ hydrogen bridging bonds are found. The $\text{O}_{\text{Donor}} - \text{O}_{\text{Acceptor}}$ distances within the $[\text{Bi}(\text{H}_2\text{O})_2(\text{OH})]^{2+}$ fragment are in the common range for

classical hydrogen bonds ($d(\text{O2}\cdots\text{O2}') = 293 \text{ pm}$). The non-classical $\text{B}-\text{H}^{\delta-}\cdots\delta^+\text{H}-\text{O}$ hydrogen bridging bonds are found between the oxygen atoms of coordinated OH^- anions and water molecules to hydrogen atoms of the boron cages ($d(\text{O}\cdots\text{H}) = 276 - 329 \text{ pm}$). Hence, although there are no “zeolitic” crystal water molecules in $\text{Bi}(\text{H}_2\text{O})_2(\text{OH})[\text{B}_{12}\text{H}_{12}]$, the crystal structure is obviously very much stabilized by these hydrogen bridging bonds.

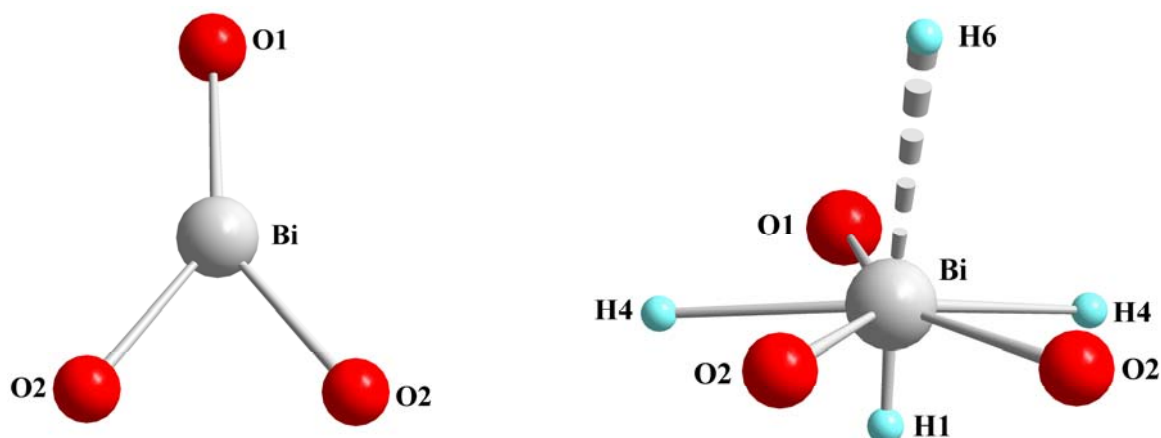


Fig. 37: Coordination environment of the Bi^{3+} cation with three coplanar nearest oxygen atoms (*left*) and with both oxygen and hydrogen atoms (*right*)

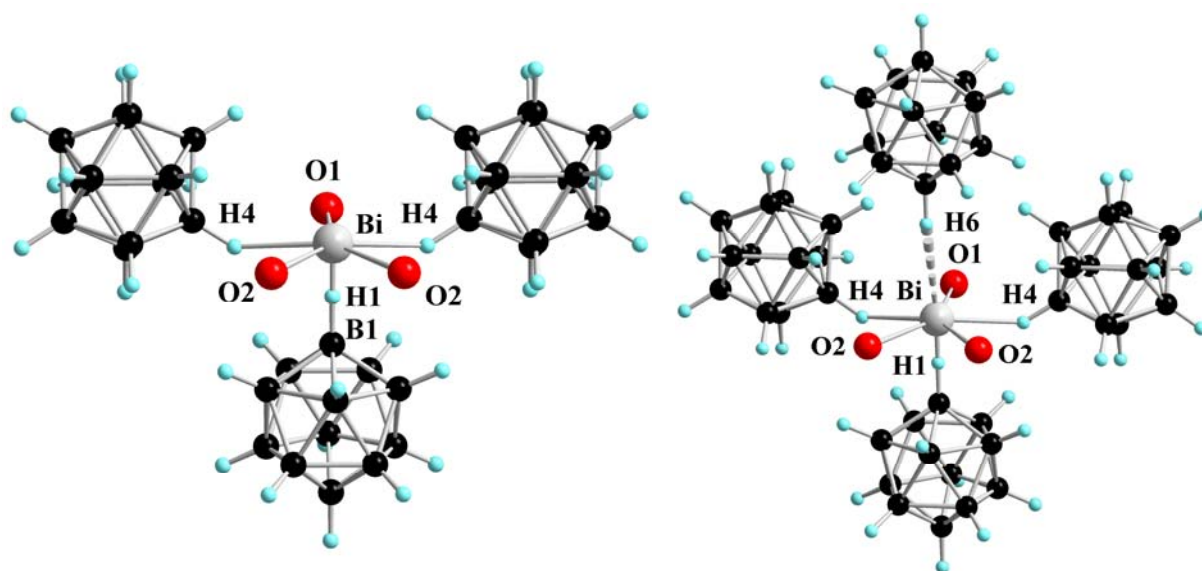


Fig. 38: The first (*left*) and the second coordination sphere (*right*) of each Bi^{3+} cation with three or four nearest *quasi*-icosahedral $[\text{B}_{12}\text{H}_{12}]^{2-}$ -cluster anions in the crystal structure of $\text{Bi}(\text{H}_2\text{O})_2(\text{OH})[\text{B}_{12}\text{H}_{12}]$

Table 28: Crystallographic data of $\text{Bi}(\text{H}_2\text{O})_2(\text{OH})[\text{B}_{12}\text{H}_{12}]$ and their determination

Crystal system	orthorhombic
Space group	Pnma (no. 62)
Unit cell parameters:	
a (pm)	1382.29(9)
b (pm)	892.78(6)
c (pm)	982.47(7)
Number of formula units per unit cell	Z = 4
Calculated density ($D_x/\text{g cm}^{-3}$)	2.213
Molar volume ($V_m/\text{cm}^3 \text{ mol}^{-1}$)	182.5
Diffractometer	κ -CCD (Bruker-Nonius)
Radiation	Mo-K α : $\lambda = 71.07$ pm, graphite monochromator
Index range	$\pm h_{\text{max}} = 18, \pm k_{\text{max}} = 11, \pm l_{\text{max}} = 13$
θ_{max} (deg)	28.3
F(000)	736
Absorption coefficient (μ/mm^{-1})	14.51
Absorption correction	numerical, Program X-SHAPE [64]
Other data corrections	background, polarization and <i>Lorentz</i> factors
Collected reflections	19763
Unique reflections	1588
$R_{\text{int}}, R_{\sigma}$	0.067, 0.024
Structure solution and refinement	Program SHELXS-97 and SHELXL-97 [68]
Scattering factors	International Tables for Crystallography, Vol. C [87]
R_1, R_w with $ F_o \geq 4\sigma(F_o)$	0.045, 0.041
Reflections with $ F_o \geq 4\sigma(F_o)$	1496
w R_2 , Goodness of fit (GooF)	0.090, 1.257
Extinction (g)	0.0028(3)
Residual electron density (<i>max.</i> , <i>min.</i> in $\rho/e^{-1} 10^6$ pm)	1.62, -1.02

Table 29: Atomic coordinates for Bi(H₂O)₂(OH)[B₁₂H₁₂]

Atom	Wyckoff position	x/a	y/b	z/c
Bi	4 <i>c</i>	0.2161(1)	1/4	0.3913(1)
O1	4 <i>c</i>	0.4026(6)	1/4	0.4115(9)
O2	8 <i>d</i>	0.0679(4)	0.0861(8)	0.3802(6)
B1	4 <i>c</i>	0.1979(7)	1/4	0.6264(9)
B2	4 <i>c</i>	0.2840(7)	1/4	0.8899(9)
B3	8 <i>d</i>	0.2767(5)	0.1505(8)	0.7333(7)
B4	8 <i>d</i>	0.2078(5)	0.0917(8)	0.8764(7)
B5	4 <i>c</i>	0.0791(7)	1/4	0.6959(9)
B6	4 <i>c</i>	0.1664(7)	1/4	0.9656(9)
B7	8 <i>d</i>	0.0858(5)	0.1493(8)	0.8534(7)
B8	8 <i>d</i>	0.1551(5)	0.0879(8)	0.7111(7)
H1 ^{a)}	4 <i>c</i>	0.209	1/4	0.516
H2 ^{a)}	4 <i>c</i>	0.350	1/4	0.951
H3 ^{a)}	8 <i>d</i>	0.338	0.085	0.694
H4 ^{a)}	8 <i>d</i>	0.225	-0.012	0.931
H5 ^{a)}	4 <i>c</i>	0.014	1/4	0.632
H6 ^{a)}	4 <i>c</i>	0.156	1/4	0.077
H7 ^{a)}	8 <i>d</i>	0.024	0.084	0.892
H8 ^{a)}	8 <i>d</i>	0.138	-0.017	0.658

^{a)} refinement with DFIX constraint (d(B–H) = 110 pm); U_{iso}(H) = 1.2 · U_{iso}(B).

Table 30: Anisotropic thermal displacement coefficients^{a)} (U_{ij}/pm^2) for $\text{Bi}(\text{H}_2\text{O})_2(\text{OH})[\text{B}_{12}\text{H}_{12}]$

Atom	U_{11}	U_{22}	U_{33}	U_{23}	U_{13}	U_{12}
Bi	267(2)	308(2)	187(2)	0	-12(2)	0
O1	257(38)	322(39)	583(55)	0	-109(37)	0
O2	316(29)	363(38)	573(39)	-282(33)	14(27)	-58(27)
B1	180(45)	157(40)	120(40)	0	-23(34)	0
B2	246(49)	225(45)	193(47)	0	-73(46)	0
B3	219(33)	195(28)	158(30)	-2(26)	-20(26)	38(28)
B4	252(36)	194(31)	190(32)	29(27)	-22(28)	9(27)
B5	144(44)	249(48)	247(51)	0	14(39)	0
B6	497(69)	154(43)	61(40)	0	-60(43)	0
B7	210(33)	224(32)	229(34)	32(28)	65(27)	-50(28)
B8	231(34)	165(31)	221(34)	1(26)	29(28)	-40(27)
H1	183					
H2	265					
H3	229					
H4	255					
H5	256					
H6	285					
H7	265					
H8	247					

^{a)} For Bi, O and B defined as anisotropic temperature factor according to: $\exp[-2\pi^2(U_{11}h^2a^{*2} + U_{22}k^2b^{*2} + U_{33}l^2c^{*2} + 2U_{23}klb^*c^* + 2U_{13}hla^*c^* + 2U_{12}hka^*b^*)]$; for H isotropically defined as temperature factor in: $\exp[-8\pi^2(U_{\text{iso}}\sin^2\theta/\lambda^2)]$.

Table 31: Selected interatomic distances (d/pm) for $\text{Bi}(\text{H}_2\text{O})_2(\text{OH})[\text{B}_{12}\text{H}_{12}]$ [BiO_3H_4] polyhedron:

Bi – O1	258.5	Bi – H4	230.7 (2×)
– O2	252.0 (2×)	– H6	319.9
– B1	232.7		

[$\text{B}_{12}\text{H}_{12}$]²⁻ anion:

B1 – B3	175.2 (2×)	B2 – B4	176.8 (2×)
– B8	177.0 (2×)	– B3	177.9 (2×)
– B5	177.6	– B6	178.8
– H1	110.0	– H2	110.0
– Bi	232.7		
B3 – B1	175.2	B4 – B6	175.8
– B3	177.6	– B2	176.8
– B4	177.7	– B7	177.6
– B2	177.9	– B3	177.7
– B8	178.5	– B8	177.9
– H3	110.0	– H4	110.0
B5 – B1	177.6	B6 – B4	175.8 (2×)
– B7	179.2 (2×)	– B2	178.8
– B8	179.4 (2×)	– B7	180.6 (2×)
– H5	110.0	– H6	110.0
B7 – B4	177.6	B8 – B1	177.0
– B8	178.0	– B7	180.0
– B5	179.2	– B4	177.9
– B7	179.8	– B3	178.5
– B6	180.6	– B5	179.4
– H7	110.0	– H8	110.0

3.3.2 Bis-Hexaaqua-Chromium(III) and Bis-Hexaaqua-Indium(III) Tris-Dodecahydro-*closo*-Dodecaborate Pentadecahydrate

The synthesis of hydrated dodecahydro-*closo*-dodecaborate salts of trivalent metal cations has been studied since the 1960s, but their crystallographic data sets were not fully described at all [16]. The crystal structures of trigonal dodecahydro-*closo*-dodecaborate hydrates of the trivalent rare-earth metals (e. g. $[\text{La}(\text{H}_2\text{O})_9]_2[\text{B}_{12}\text{H}_{12}]_3 \cdot 15 \text{H}_2\text{O}$) with 33 water molecules in the entire formula were elucidated [91], however. In these compounds, comparing to $\text{Bi}(\text{H}_2\text{O})_2(\text{OH})[\text{B}_{12}\text{H}_{12}]$, there is no direct contact between trications and the $[\text{B}_{12}\text{H}_{12}]^{2-}$ anions, in which the $[\text{B}_{12}\text{H}_{12}]^{2-}$ units are arranged according to the stacking sequence of the α -Sm-type structure, while the hydrated M^{3+} cations fill the interlayer region in the fashion of a (doubled) Cu-type structure. However, no crystallographic data of dodecahydro-*closo*-dodecaborate salts with trivalent transition metal d-block cations, which have a much smaller ionic radius and are expected to exhibit smaller coordination numbers with respect to trivalent rare-earth element ones are yet available in literature. Particularly in the case of Cr^{3+} cations, only bis-hexaammine-chromium(III) tris-dodecahydro-*closo*-dodecaborate heptahydrate, $[\text{Cr}(\text{NH}_3)_6]_2[\text{B}_{12}\text{H}_{12}]_3 \cdot 7 \text{H}_2\text{O}$ has been synthesized and characterized by only elemental analysis. However, no crystal structures of any dodecahydro-*closo*-dodecaborate with Cr^{3+} cations in the form of aqua or ammine complexes were reported. In the case of indium(III) dodecahydro-*closo*-dodecaborate hydrates, neither crystal structures nor syntheses or even chemical compositions have entered the literature yet.

3.3.2.1 Synthesis of $[\text{M}(\text{H}_2\text{O})_6]_2[\text{B}_{12}\text{H}_{12}]_3 \cdot 15 \text{H}_2\text{O}$ (M = Cr and In)

Single crystals of bis-hexaaqua-chromium(III) tris-dodecahydro-*closo*-dodecaborate pentadecahydrate are obtained by neutralization of an aqueous solution of the free acid $(\text{H}_3\text{O})_2[\text{B}_{12}\text{H}_{12}]$ with chromium(III) hydroxide $\text{Cr}(\text{OH})_3$. By using freshly precipitated chromium(III) hydroxide prepared from a stoichiometric reaction between chromium(III) chloride CrCl_3 (Strem: 99 %) and sodium hydroxide NaOH (Merck: 99 %) in aqueous solution, other by-products than dissolved NaCl are avoided and good quality single crystals of the title compound were obtained. The reaction mixture was left 24 h at room temperature and the crude product then was filtered off. By isothermal evaporation of the resulting concentrated solution at room temperature, hygroscopic, green, bead-shaped single crystals

are formed and selected for X-ray single crystal diffraction measurements at room temperature.

The analogous indium(III) compound, on the other hand, was prepared by neutralization of an aqueous solution of the free acid $(\text{H}_3\text{O})_2[\text{B}_{12}\text{H}_{12}]$ with indium(III) oxide In_2O_3 (Strem: 99.999 %). The reaction mixture was left several days at room temperature and the crude product then was filtered off. Colourless, bead-shaped single crystals are obtained by isothermal evaporation of the filtrate at room temperature. The isotopic crystal structures of $[\text{Cr}(\text{H}_2\text{O})_6]_2[\text{B}_{12}\text{H}_{12}]_3 \cdot 15 \text{H}_2\text{O}$ and $[\text{In}(\text{H}_2\text{O})_6]_2[\text{B}_{12}\text{H}_{12}]_3 \cdot 15 \text{H}_2\text{O}$ were both solved based on the data collected from single crystal X-ray diffraction measurements.

3.3.2.2 Structure Description of $[\text{M}(\text{H}_2\text{O})_6]_2[\text{B}_{12}\text{H}_{12}]_3 \cdot 15 \text{H}_2\text{O}$ (M = Cr and In)

The two isostructural salts $[\text{Cr}(\text{H}_2\text{O})_6]_2[\text{B}_{12}\text{H}_{12}]_3 \cdot 15 \text{H}_2\text{O}$ and $[\text{In}(\text{H}_2\text{O})_6]_2[\text{B}_{12}\text{H}_{12}]_3 \cdot 15 \text{H}_2\text{O}$ crystallize in the trigonal space group $R\bar{3}c$ ($a = 1157.62(3)$, $c = 6730.48(9)$ pm for the chromium, and $a = 1171.71(3)$, $c = 6740.05(9)$ pm for the indium compound) with six formula units per unit cell (Fig. 39, *left*). In these crystal structures, the metal trications are located at the *Wyckoff* position $12c$ ($x/a = y/b = 0$, z/c ; site symmetry: $3.$), while all boron and hydrogen atoms of $[\text{B}_{12}\text{H}_{12}]^{2-}$ -cluster anions reside at the general position $36f$. The *quasi*-icosahedral anionic $[\text{B}_{12}\text{H}_{12}]^{2-}$ units have distances of 170 pm from their center of gravity to the twelve cage boron atoms providing them an inner diameter of 340 pm. The centers of gravity of the $[\text{B}_{12}\text{H}_{12}]^{2-}$ -cluster anions occupy two different crystallographic positions at the *Wyckoff* positions $6b$ ($x/a = y/b = z/c = 0$; site symmetry: $\bar{3}.$) and $12c$, respectively. Each Cr^{3+} or In^{3+} cation is coordinated by six oxygen atoms of crystal water molecules to provide a slightly distorted octahedral coordination sphere ($d(\text{Cr}-\text{O}) = 199 - 200$ pm; $d(\text{In}-\text{O}) = 212 - 215$ pm) (Fig. 40). The remaining fifteen water molecules are situated in the unit cell as “zeolitic” water particles. In the crystal structure of $[\text{Cr}(\text{H}_2\text{O})_6]_2[\text{B}_{12}\text{H}_{12}]_3 \cdot 15 \text{H}_2\text{O}$ and $[\text{In}(\text{H}_2\text{O})_6]_2[\text{B}_{12}\text{H}_{12}]_3 \cdot 15 \text{H}_2\text{O}$ the O–H distances of the water molecules ($d(\text{O}-\text{H}) = 66 - 87$ pm and $59 - 103$ pm), the intramolecular H···H distances range ($d(\text{H}\cdots\text{H}) = 108 - 140$ pm and $107 - 148$ pm) and the H–O–H angles ($\angle(\text{H}-\text{O}-\text{H}) = 101 - 115^\circ$ and $81 - 111^\circ$) could be determined without any problems. These values are deviating considerably from the ideal ones of “free” water molecules in the gas phase ($d(\text{O}-\text{H}) = 96$ pm, $d(\text{H}\cdots\text{H}) = 151$ pm, $\angle(\text{H}-\text{O}-\text{H}) = 104.5^\circ$) of course. With the shortest value of 457 pm for both $\text{Cr}\cdots\text{H}_{\text{cluster}}$

distances and the analogous $\text{In}\cdots\text{H}_{\text{Cluster}}$ ones for these trigonal hexaaqua-dodecahydro-*closo*-dodecaborate hydrates, no direct contact between $[\text{B}_{12}\text{H}_{12}]^{2-}$ anion and counter-trication is found in both title compounds. With respect to the ideal icosahedral symmetry, the boron cages in $[\text{In}(\text{H}_2\text{O})_6]_2[\text{B}_{12}\text{H}_{12}]_3 \cdot 15 \text{H}_2\text{O}$ are more distorted than that ones in $[\text{Cr}(\text{H}_2\text{O})_6]_2[\text{B}_{12}\text{H}_{12}]_3 \cdot 15 \text{H}_2\text{O}$ with B–B distances in intervals of 177 – 180 pm (12 \times) and 177 – 178 pm (12 \times), respectively (Fig. 41). The B–H distances of the *quasi*-icosahedral anionic $[\text{B}_{12}\text{H}_{12}]^{2-}$ units in $[\text{Cr}(\text{H}_2\text{O})_6]_2[\text{B}_{12}\text{H}_{12}]_3 \cdot 15 \text{H}_2\text{O}$ ($d(\text{B}-\text{H}) = 107 - 110$ pm, 12 \times) are close to the ideal value (110 pm) found for this bond type, whereas those of $[\text{In}(\text{H}_2\text{O})_6]_2[\text{B}_{12}\text{H}_{12}]_3 \cdot 15 \text{H}_2\text{O}$ cover a larger range ($d(\text{B}-\text{H}) = 106 - 115$ pm, 12 \times). The crystal structure of both salts $[\text{M}(\text{H}_2\text{O})_6]_2[\text{B}_{12}\text{H}_{12}]_3 \cdot 15 \text{H}_2\text{O}$ ($\text{M} = \text{Cr}$ and In) can be described as two independent interpenetrating layered motifs, namely the complex $[\text{M}(\text{H}_2\text{O})_6]^{3+}$ cations and the $[\text{B}_{12}\text{H}_{12}]^{2-}$ -cluster anions, as lattice components. The chromium(III) and the indium(III) cations arrange in a cubic closest packed fashion with a stacking sequence *abc* just like the Cu-type structure and the $[\text{B}_{12}\text{H}_{12}]^{2-}$ anions form a 9-layer stacking sequences like *ABCCABBCA* (Fig. 39, *right*). These stacking sequences differ strongly from those of the hydrated rare-earth metal trications (stacking sequence: *aa bb cc*) and the $[\text{B}_{12}\text{H}_{12}]^{2-}$ -cluster anions (stacking sequences: *ABABCBCAC*) in trigonal $[\text{La}(\text{H}_2\text{O})_9]_2[\text{B}_{12}\text{H}_{12}]_3 \cdot 15 \text{H}_2\text{O}$ [85]. The chromium or indium trications, in comparison to the rare-earth metal cations in $[\text{La}(\text{H}_2\text{O})_9]_2[\text{B}_{12}\text{H}_{12}]_3 \cdot 15 \text{H}_2\text{O}$, no longer reside at the octahedral voids in between two different stacking layers of the $[\text{B}_{12}\text{H}_{12}]^{2-}$ anions in an alternative manner. Instead, they are located at two thirds of the trigonal prismatic voids between each two identical stacking layers of the *quasi*-icosahedral $[\text{B}_{12}\text{H}_{12}]^{2-}$ units. Nonetheless, the crystal structure of the title compounds, quite similar to this one of the dodecahydro-*closo*-dodecaborate hydrates with the trivalent rare-earth metals, is stabilized by bridging hydrogen bonds. Each coordinating water molecule connects to two other neighbouring “zeolitic” crystal water molecules via classical $\text{O}-\text{H}^{\delta+}\cdots\delta-\text{O}$ hydrogen bridges with donor-acceptor distances like $d(\text{O}\cdots\text{Ow}) = 257 - 277$ pm ($\angle(\text{O}\cdots\text{Ow}) = 169 - 176^\circ$) (Fig. 40). Considering two stacking layers of complex cations $[\text{M}(\text{H}_2\text{O})_6]^{3+}$ ($\text{M} = \text{Cr}$ and In), coordination spheres that reside in between each of the two identical stacking layers of $[\text{B}_{12}\text{H}_{12}]^{2-}$ units, each two nearest $[\text{M}(\text{H}_2\text{O})_6]^{3+}$ aqua-complex spheres are linked via strong $\text{O}-\text{H}^{\delta+}\cdots\delta-\text{O}$ hydrogen bridging bonds between their own water molecules and one “free” water molecule represented by Ow. As a result, these coordination spheres are linked in zigzag chains parallel to the *a* and *b* axes via hydrogen bridges and a

stable two-dimensional polymeric network is formed. These zigzag chains are not found in the trigonal dodecahydro-*closo*-dodecaborate hydrates of the rare-earth metals. The zigzag chains are separated by layers of boron-cage anions and no connection between these chains via hydrogen bridges is found. Together with these strong classical hydrogen bonds, there are two types of non-classical B–H^{δ-}...^{δ+}H–O hydrogen bonds existing in the title compounds. The first type is the one between negatively polarized hydrogen atoms of the boron cages and those positively polarized ones of the twelve surrounding “zeolitic” crystal water molecules with $d(\text{H}^{\delta-} \dots \delta^+ \text{H}) = 248 - 287$ pm, which are forming distorted dodecahedra. The second type of non-classical B–H^{δ-}...^{δ+}H–O hydrogen bonds exists between hydrogen atoms of the boron cages and those of water molecules coordinated to the M³⁺ cations. The strength of this second type of non-classical B–H^{δ-}...^{δ+}H–O hydrogen bonds of [Cr(H₂O)₆]₂[B₁₂H₁₂]₃ · 15 H₂O and [In(H₂O)₆]₂[B₁₂H₁₂]₃ · 15 H₂O is comparable to that one of the trigonal dodecahydro-*closo*-dodecaborate hydrates with the rare-earth metals ($d(\text{H}^{\delta-} \dots \text{O}) = 320 - 448$ pm and 305 – 396 pm).

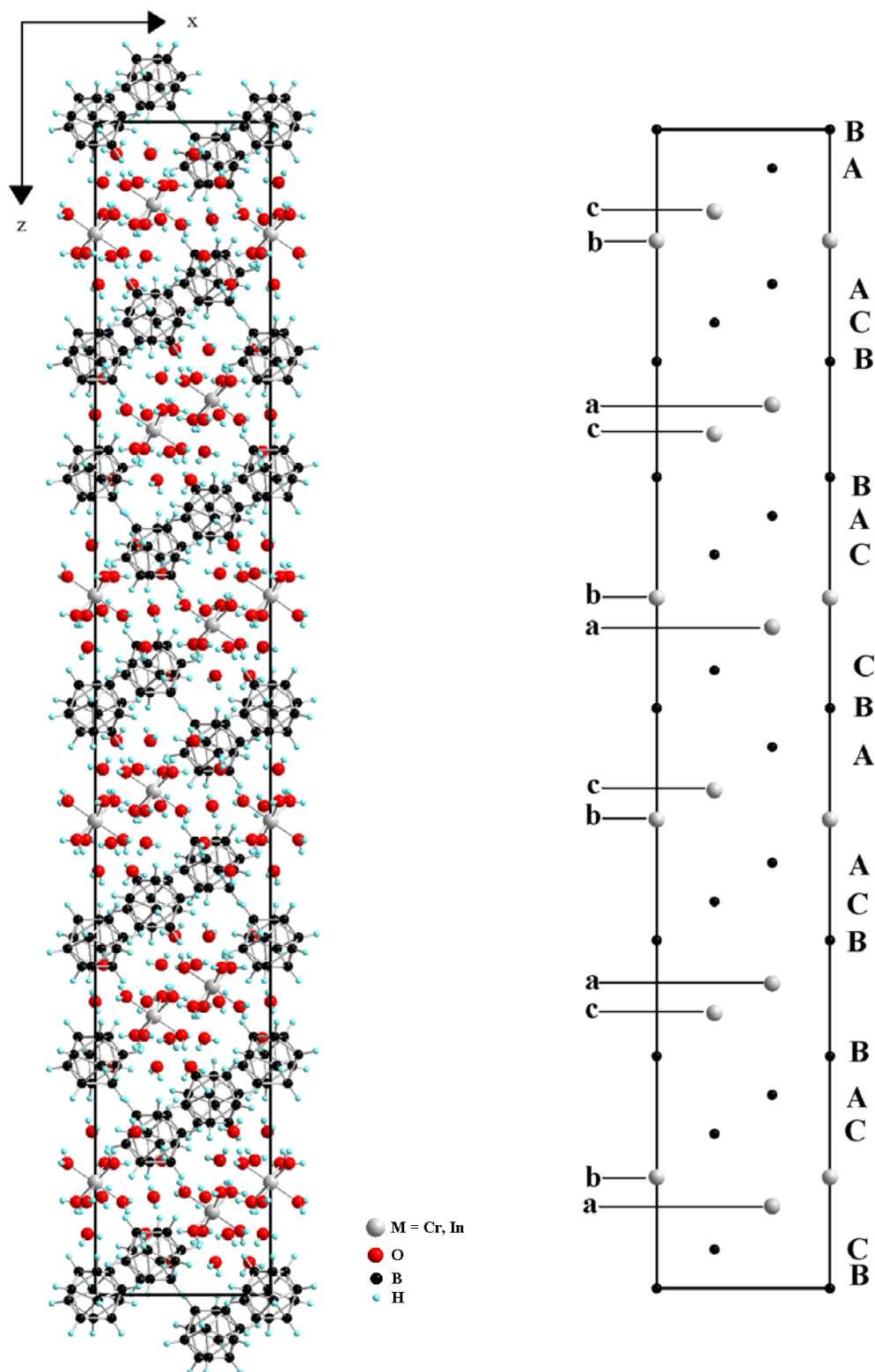


Fig. 39: Crystal structure of the salts $[M(H_2O)_6]_2[B_{12}H_{12}]_3 \cdot 15 H_2O$ ($M = Cr$ and In) as viewed along $[010]$ (*left*) and the arrangement of the M^{3+} cations (grey spheres, stacking sequence: *abc*) and the centers of gravity of the $[B_{12}H_{12}]^{2-}$ -cluster anions (black spheres, stacking sequence: *ABCCABBCA*) (*right*)

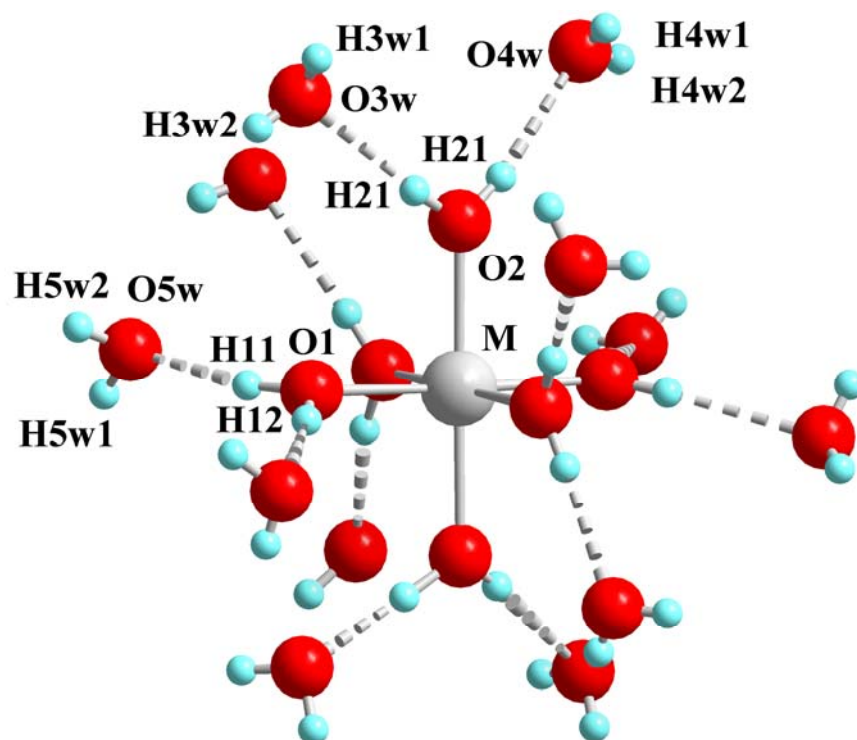


Fig. 40: First (octahedral, O1 and O2) and second (cuboctahedral, O3w, O4w and O5w) coordination sphere of the M^{3+} cations in the salts $[M(H_2O)_6]_2[B_{12}H_{12}]_3 \cdot 15 H_2O$ ($M = Cr$ and In)

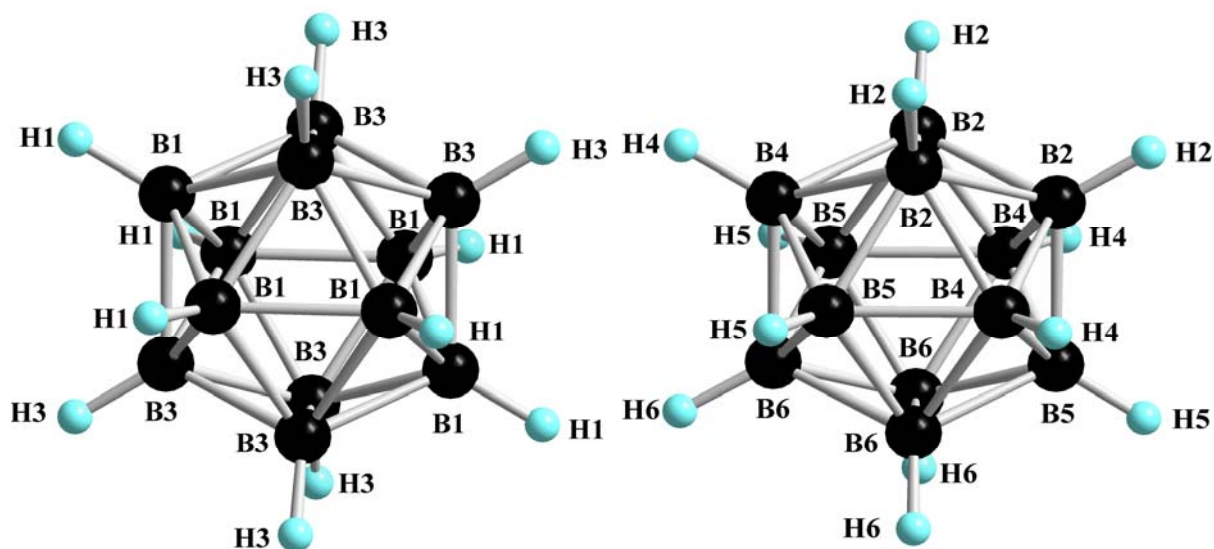


Fig. 41: View at the *quasi*-icosahedral $[B_{12}H_{12}]^{2-}$ -cluster anions with their centers of gravity at $6b$ ($x/a = y/b = z/c = 0$) (*left*) and at $12c$ ($x/a = y/b = 0, z/c$) (*right*) in the crystal structure of the salts $[M(H_2O)_6]_2[B_{12}H_{12}]_3 \cdot 15 H_2O$ ($M = Cr$ and In)

Table 32: Crystallographic data for the salts $[M(H_2O)_6]_2[B_{12}H_{12}]_3 \cdot 15 H_2O$ (M = Cr and In) and their determination

Crystallographic data	M = Cr	M = In
Crystal system	trigonal	
Space group	$R\bar{3}c$ (no. 167)	
Unit cell parameters:		
a (pm)	1157.62(3)	1171.71(3)
c (pm)	6730.48(9)	6740.05(9)
Number of formula units per unit cell	6	
Calculated density ($D_x/g\text{ cm}^{-3}$)	1.296	1.419
Molar volume ($V_m/cm^3\text{ mol}^{-1}$)	784.1	804.6
Diffractometer	κ -CCD (Bruker-Nonius)	
Radiation	Mo-K α : $\lambda = 71.07$ pm, graphite monochromator	
Index range: $\pm h_{\max}, \pm k_{\max}, \pm l_{\max}$	15, 15, 88	15, 15, 88
θ_{\max} (deg)	28.3	28.3
F(000)	3204	3504
Absorption coefficient (μ/mm^{-1})	0.49	0.93
Absorption correction	numerical, Program X-SHAPE [64]	
Other data corrections	background, polarization and <i>Lorentz</i> factors	
Collected reflections	34342	26373
Unique reflections	2158	2202
$R_{\text{int}}, R_{\sigma}$	0.065, 0.021	0.202, 0.074
Structure solution and refinement	Program SHELXS-97 and SHELXL-97 [68]	
Scattering factors	International Tables for Crystallography, Vol. C [87]	
R_1, R_w with $ F_o \geq 4\sigma(F_o)$	0.105, 0.091	0.114, 0.081
Reflections with $ F_o \geq 4\sigma(F_o)$	1967	1701
wR_2 , Goodness of fit (GooF)	0.082, 1.152	0.131, 1.287
Extinction (g)	0.0001(1)	0.0001(1)
Residual electron density (<i>max.</i> , <i>min.</i> in $\rho/e^{-1}\text{ 10}^6\text{ pm}$)	0.23, -0.25	0.94, -0.97

Table 33: Atomic coordinates for $[\text{Cr}(\text{H}_2\text{O})_6]_2[\text{B}_{12}\text{H}_{12}]_3 \cdot 15 \text{H}_2\text{O}$

Atom	Wyckoff position	x/a	y/b	z/c
Cr	12c	0	0	0.0960(1)
O1	36f	0.1592(1)	0.0543(1)	0.1122(1)
O2	36f	0.1084(1)	0.1566(1)	0.0791(1)
O3w	18e	0	0.2945(1)	$\frac{1}{4}$
O4w	36f	0.0439(1)	0.2867(1)	0.0520(1)
O5w	36f	0.2306(1)	0.2120(1)	0.3611(1)
B1	36f	0.0154(1)	0.1512(1)	0.0047(1)
B2	36f	0.0932(1)	0.0834(1)	0.0199(1)
B3	36f	0.0211(1)	0.0973(1)	0.1802(1)
B4	36f	0.0354(1)	0.1573(1)	0.2048(1)
B5	36f	0.1582(1)	0.1230(1)	0.1953(1)
B6	36f	0.0976(1)	0.0758(1)	0.2800(1)
H11	36f	0.193(2)	0.009(2)	0.112(1)
H12	36f	0.174(2)	0.103(2)	0.122(1)
H21	36f	0.082(2)	0.184(2)	0.071(1)
H22	36f	0.185(2)	0.199(2)	0.080(1)
H3w	36f	0.015(2)	0.268(2)	0.258(1)
H4w1	36f	-0.024(2)	0.272(2)	0.050(1)
H4w2	36f	0.077(2)	0.278(2)	0.044(1)
H5w1	36f	0.271(2)	0.282(2)	0.358(1)
H5w2	36f	0.211(2)	0.175(2)	0.351(1)
H1	36f	0.027(2)	0.248(2)	0.007(1)
H2	36f	0.151(2)	0.137(2)	0.033(1)
H3	36f	0.031(2)	0.159(2)	0.168(1)
H4	36f	0.061(2)	0.259(2)	0.208(1)
H5	36f	0.262(2)	0.204(2)	0.193(1)
H6	36f	0.161(2)	0.125(2)	0.232(1)

Table 34: Anisotropic thermal displacement coefficients^{a)} (U_{ij}/pm^2) for $[\text{Cr}(\text{H}_2\text{O})_6]_2[\text{B}_{12}\text{H}_{12}]_3 \cdot 15 \text{H}_2\text{O}$

Atom	U_{11}	U_{22}	U_{33}	U_{23}	U_{13}	U_{12}
Cr	197(1)	= U_{11}	210(2)	0	0	= $\frac{1}{2} U_{11}$
O1	281(5)	310(5)	341(5)	-56(5)	-88(5)	176(5)
O2	278(5)	311(5)	350(5)	126(5)	49(5)	102(5)
O3w	482(9)	313(5)	497(9)	= $\frac{1}{2} U_{13}$	-134(5)	= $\frac{1}{2} U_{11}$
O4w	562(9)	384(5)	381(9)	-67(5)	-145(5)	279(5)
O5w	454(7)	347(5)	394(7)	-18(5)	106(5)	123(5)
B1	275(9)	199(7)	368(9)	-14(5)	-1(5)	129(5)
B2	234(9)	231(7)	318(9)	-25(5)	-22(5)	104(5)
B3	317(9)	341(7)	310(9)	64(5)	16(5)	161(5)
B4	306(9)	232(7)	407(9)	-26(5)	3(5)	142(5)
B5	227(9)	255(7)	430(9)	10(5)	25(5)	95(5)
B6	336(9)	339(7)	315(9)	-62(5)	73(5)	166(5)
H11	553(65)					
H12	852(65)					
H21	499(65)					
H22	536(65)					
H3w	968(120)					
H4w1	956(120)					
H4w2	924(120)					
H5w1	690(87)					
H5w2	703(87)					
H1	421(49)					
H2	390(49)					
H3	490(49)					
H4	493(49)					
H5	459(49)					
H6	534(49)					

^{a)} For Cr, O and B defined as anisotropic temperature factor according to: $\exp[-2\pi^2(U_{11}h^2a^{*2} + U_{22}k^2b^{*2} + U_{33}l^2c^{*2} + 2U_{23}klb^*c^* + 2U_{13}hla^*c^* + 2U_{12}hka^*b^*)]$; for H isotropically defined as temperature factor in: $\exp[-8\pi^2(U_{\text{iso}}\sin^2\theta/\lambda^2)]$.

Table 35: Selected interatomic distances (d/pm) for $[\text{Cr}(\text{H}_2\text{O})_6]_2[\text{B}_{12}\text{H}_{12}]_3 \cdot 15 \text{H}_2\text{O}$

[CrO ₆] polyhedron:					
		Cr – O1	195.5 (3×)		
		– O2	196.7 (3×)		
[B ₁₂ H ₁₂] ²⁻ anions:					
B1 – B3	177.5	B2 – B4	176.8	B3 – B1	177.5
– B3'	180.0	– B5	177.3	– B3	177.8 (2×)
– B2	178.4	– B2	177.9 (2×)	– B1'	180.0
– B3''	178.4 (2×)	– B4'	178.1	– B1''	184.4
– H1	108.1	– H2	107.8	– H3	108.1
B4 – B2	176.8	B5 – B6	176.8	B6 – B5	176.7
– B5	177.7	– B6'	177.2	– B5'	177.1
– B6	177.9	– B2	177.3	– B4	177.9
– B2'	178.1	– B4	177.7	– B6	180.0 (2×)
– B5'	178.3	– B4'	178.3	– H6	108.7
– H4	109.6	– H5	105.8		
Hydrogen bridging bonds ^{a)} :					
D–H...A		d(D–H)	d(H...A)	d(D...A)	∠ (D–H...A)
O1–H11...O5w	(3×)	86.6	170.0	255.7	169.4
O5w–H5w1...O1	(3×)	75.6	302.0	255.7	46.3
O5w–H5w2...O1	(3×)	75.4	299.0	255.7	48.8
O1–H12...O4w	(3×)	79.6	196.8	276.4	175.6
O4w–H4w2...O1	(3×)	77.8	295.0	276.4	114.7
O2–H21...O3w	(3×)	77.8	193.9	270.9	169.8
O3w–H3w...O2	(3×)	66.2	308.6	284.5	50.0
O3w–H3w'...O2	(3×)	66.2	301.7	284.5	56.6
O2–H22...O4w	(3×)	77.7	193.2	270.0	169.8
O4w–H4w1...O2	(3×)	68.2	288.8	270.0	67.4
O4w–H4w2'...O2	(3×)	75.1	318.8	270.0	41.1

^{a)} D = Donor, A = Acceptor

Table 36: Atomic coordinates for $[\text{In}(\text{H}_2\text{O})_6]_2[\text{B}_{12}\text{H}_{12}]_3 \cdot 15 \text{H}_2\text{O}$

Atom	Wyckoff position	x/a	y/b	z/c
In	12 <i>c</i>	0	0	0.0966(1)
O1	36 <i>f</i>	0.1724(4)	0.0623(4)	0.1135(1)
O2	36 <i>f</i>	0.1160(4)	0.1668(4)	0.0782(1)
O3w	18 <i>e</i>	0	0.2893(4)	$\frac{1}{4}$
O4w	36 <i>f</i>	0.0434(4)	0.2585(4)	0.0510(1)
O5w	36 <i>f</i>	0.2370(4)	0.2173(4)	0.3603(1)
B1	36 <i>f</i>	0.0183(2)	0.1501(2)	0.0047(1)
B2	36 <i>f</i>	0.0937(2)	0.0817(2)	0.0199(1)
B3	36 <i>f</i>	0.0200(2)	0.0960(2)	0.1798(1)
B4	36 <i>f</i>	0.0336(2)	0.1550(2)	0.2044(1)
B5	36 <i>f</i>	0.1560(2)	0.1219(2)	0.1949(1)
B6	36 <i>f</i>	0.0966(2)	0.0752(2)	0.2195(1)
H11	36 <i>f</i>	0.207(2)	0.026(2)	0.114(1)
H12	36 <i>f</i>	0.189(3)	0.118(3)	0.126(1)
H21	36 <i>f</i>	0.097(2)	0.201(2)	0.069(1)
H22	36 <i>f</i>	0.196(2)	0.194(2)	0.077(1)
H3w	36 <i>f</i>	0.013(2)	0.259(2)	0.258(1)
H4w1	36 <i>f</i>	-0.007(2)	0.275(2)	0.049(1)
H4w2	36 <i>f</i>	0.097(2)	0.293(2)	0.041(1)
H5w1	36 <i>f</i>	0.229(2)	0.191(2)	0.347(1)
H5w2	36 <i>f</i>	0.281(3)	0.277(2)	0.356(1)
H1	36 <i>f</i>	0.027(2)	0.244(2)	0.007(1)
H2	36 <i>f</i>	0.154(2)	0.133(2)	0.034(1)
H3	36 <i>f</i>	0.036(2)	0.162(2)	0.168(1)
H4	36 <i>f</i>	0.063(2)	0.252(2)	0.208(1)
H5	36 <i>f</i>	0.259(2)	0.196(2)	0.193(1)
H6	36 <i>f</i>	0.156(2)	0.122(2)	0.233(1)

Table 37: Anisotropic thermal displacement coefficients^{a)} (U_{ij}/pm^2) for $[\text{In}(\text{H}_2\text{O})_6]_2[\text{B}_{12}\text{H}_{12}]_3 \cdot 15 \text{H}_2\text{O}$

Atom	U_{11}	U_{22}	U_{33}	U_{23}	U_{13}	U_{12}
In	229(2)	= U_{11}	303(2)	0	0	= $\frac{1}{2} U_{11}$
O1	346(21)	410(21)	481(21)	-85(21)	-135(21)	246(21)
O2	322(21)	370(21)	450(21)	218(21)	30(21)	108(21)
O3w	591(37)	342(21)	493(37)	= $\frac{1}{2} U_{13}$	-173(28)	= $\frac{1}{2} U_{11}$
O4w	716(37)	440(21)	498(29)	-72(21)	-218(21)	357(21)
O5w	438(37)	363(21)	508(21)	-68(21)	102(21)	104(21)
B1	269(28)	222(24)	387(36)	-34(21)	-44(21)	109(21)
B2	207(21)	235(21)	373(21)	20(21)	-25(21)	67(21)
B3	293(28)	325(21)	405(31)	115(21)	30(21)	130(21)
B4	296(25)	232(25)	504(36)	-34(21)	-23(21)	146(21)
B5	218(25)	263(25)	471(36)	60(21)	25(21)	80(21)
B6	382(35)	355(30)	396(31)	-24(21)	-53(21)	194(21)
H11	341(162)					
H12	785(216)					
H21	343(161)					
H22	1137(322)					
H3w	681(232)					
H4w1	552(327)					
H4w2	995(323)					
H5w1	728(224)					
H5w2	383(187)					
H1	277(116)					
H2	291(120)					
H3	312(124)					
H4	484(189)					
H5	431(144)					
H6	443(146)					

^{a)} For In, O and B defined as anisotropic temperature factor according to: $\exp[-2\pi^2(U_{11}h^2a^{*2} + U_{22}k^2b^{*2} + U_{33}l^2c^{*2} + 2U_{23}klb^{*}c^{*} + 2U_{13}hla^{*}c^{*} + 2U_{13}hka^{*}b^{*})]$; for H isotropically defined as temperature factor in: $\exp[-8\pi^2(U_{\text{iso}}\sin^2\theta/\lambda^2)]$.

Table 38: Selected interatomic distances (d/pm) for $[\text{In}(\text{H}_2\text{O})_6]_2[\text{B}_{12}\text{H}_{12}]_3 \cdot 15 \text{H}_2\text{O}$

[InO ₆] polyhedron:								
		In	– O1	211.8 (3×)				
			– O2	214.7 (3×)				
[B ₁₂ H ₁₂] ²⁻ anion:								
B1	– B3	177.1	B2	– B4	177.1	B3	– B1	176.8
	– B1	177.7 (2×)		– B5	177.5		– B1'	177.8
	– B3'	177.8		– B2	178.3 (2×)		– B1''	178.6
	– B3''	178.6		– B4'	178.5		– B3	179.5 (2×)
	– H1	109.3		– H2	105.5		– H3	113.3
B4	– B6	176.9	B5	– B6	176.3	B6	– B5	176.3
	– B2	177.1		– B6'	177.2		– B4	176.9
	– B5	177.2		– B4	177.2		– B4'	177.2
	– B5'	178.0		– B2	177.3		– B6	179.1 (2×)
	– B2'	178.5		– B4'	178.0		– H6	115.0
	– H4	112.2		– H5	108.2			
Hydrogen bridging bonds ^{a)} :								
D–H...A		d(D–H)	d(H...A)	d(D...A)	∠(D–H...A)			
O1–H11...O5w	(3×)	102.4	155.6	255.5	163.6			
O5w–H5w1...O1	(3×)	92.1	325.1	255.5	35.2			
O5w–H5w2...O1	(3×)	70.7	303.6	255.5	42.0			
O1–H12...O4w	(3×)	73.1	300.0	269.2	58.9			
O4w–H4w2...O1	(3×)	63.3	267.2	269.2	85.0			
O2–H21...O3w	(3×)	63.3	302.8	269.2	60.6			
O3w–H3w...O2	(3×)	88.2	215.1	284.5	135.2			
O3w–H3w'...O2	(3×)	66.3	321.0	284.5	51.5			
O2–H22...O4w	(3×)	71.6	199.1	264.4	151.9			
O4w–H4w1...O2	(3×)	71.6	302.2	264.4	52.2			
O4w–H4w2'...O2	(3×)	63.3	342.2	290.2	31.6			

^{a)} D = Donor, A = Acceptor

3.3.3 Hexaaqua-Chromium(III) Aqua-Oxonium Bis-Dodecahydro-*closo*-Dodecaborate Hexahydrate

Mixed oxonium dodecahydro-*closo*-dodecaborate salts with monooxonium cation (H_3O^+) are formed with certain cations (e. g. $[\text{M}(\text{H}_2\text{O})_6](\text{H}_3\text{O})_2[\text{B}_{12}\text{H}_{12}]_2 \cdot 6 \text{H}_2\text{O}$; M = Mn, Fe, Co, Ni, Cu, Zn and Cd). For polyoxonium dodecahydro-*closo*-dodecaborate derivatives, only crystallographic data for $(\text{H}_5\text{O}_2)[\text{CHB}_{11}\text{Cl}_{11}]$ and $(\text{H}_9\text{O}_4)[\text{CHB}_{11}\text{H}_5\text{Br}_6]$ had been reported [98]. No mixed-cation polyoxonium dodecahydro-*closo*-dodecaborate salts have been published to date, although the existence of such kind of salt would be understandable. In the reaction between oxides, hydroxides or salts with inorganic cations and the free acid $(\text{H}_3\text{O})_2[\text{B}_{12}\text{H}_{12}]$ in aqueous solution, several types of oxonium cations can exist such as H_3O^+ , H_5O_2^+ (Zundel-type), H_7O_3^+ and H_9O_4^+ (Eigen-type). This may lead to the formation of mixed-cation polyoxonium dodecahydro-*closo*-dodecaborate salts. In this work, the synthesis and crystal structure of hexaaqua-chromium(III) aqua-oxonium bis-dodecahydro-*closo*-dodecaborate hexahydrate, $[\text{Cr}(\text{H}_2\text{O})_6](\text{H}_5\text{O}_2)[\text{B}_{12}\text{H}_{12}]_2 \cdot 6 \text{H}_2\text{O}$, was studied.

3.3.3.1 Synthesis of $[\text{Cr}(\text{H}_2\text{O})_6](\text{H}_5\text{O}_2)[\text{B}_{12}\text{H}_{12}]_2 \cdot 6 \text{H}_2\text{O}$

$[\text{Cr}(\text{H}_2\text{O})_6](\text{H}_5\text{O}_2)[\text{B}_{12}\text{H}_{12}]_2 \cdot 6 \text{H}_2\text{O}$ was synthesized by the reaction of $[\text{Cr}(\text{H}_2\text{O})_6]_2[\text{B}_{12}\text{H}_{12}]_3 \cdot 15 \text{H}_2\text{O}$ with an excess amount of the free acid $(\text{H}_3\text{O})_2[\text{B}_{12}\text{H}_{12}]$. Green, polyhedrally shaped single crystals were obtained by isothermal evaporation of the resulting aqueous solution at room temperature. The chemical composition of the single crystals was examined by electron beam microanalysis.

3.3.3.2 Structure Description of $[\text{Cr}(\text{H}_2\text{O})_6](\text{H}_5\text{O}_2)[\text{B}_{12}\text{H}_{12}]_2 \cdot 6 \text{H}_2\text{O}$

The title compound crystallizes orthorhombically in space group Pnmm (no. 58) with two formula units per unit cell (Fig. 42). The chromium(III) cations occupy the special *Wyckoff* position $2a$ ($x/a = y/b = z/c = 0$; site symmetry: $..2/m$) and the oxygen atoms (O1 – O3) of crystal water molecules within the octahedral $[\text{Cr}(\text{H}_2\text{O})_6]^{3+}$ coordination sphere are located at three crystallographically distinct *Wyckoff* sites: O1 at the *Wyckoff* site $4b$ ($x/a = y/b = 0$, z/c ; site symmetry: $..2$), O2 and O3 at the *Wyckoff* site $4g$ (x/a , y/b , $z/c = 0$; site symmetry: $..m$). The oxygen atoms of the aqua-oxonium cations (O4a) reside at the *Wyckoff* site $4g$ as well,

while the oxygen atoms of “zeolitic” water molecules (O5w and O6w) occupy two crystallographically distinct *Wyckoff* sites 4g and 8h (x/a, y/b, z/c; site symmetry: 1), respectively. The boron and hydrogen atoms of the *quasi*-icosahedral $[B_{12}H_{12}]^{2-}$ -cluster anions reside at the *Wyckoff* sites 4g and 8h. The distances from the center of gravity of the $[B_{12}H_{12}]^{2-}$ cages, which is found at the *Wyckoff* site 4g, to twelve boron atoms range from 169 to 170 pm providing each cage an inner diameter of about 340 pm. Similar to the salts $[M(H_2O)_6](H_3O)_2[B_{12}H_{12}]_2 \cdot 6 H_2O$ (M = Mn, Fe, Co, Ni, Cu, Zn and Cd), the crystal structure of $[Cr(H_2O)_6](H_5O_2)[B_{12}H_{12}]_2 \cdot 6 H_2O$ is characterized as a layer-like construction with $[Cr(H_2O)_6]^{3+}$ cation, $[B_{12}H_{12}]^{2-}$ anion and $H_5O_2^+$ layers alternatively arranged along [001]. Each Cr^{3+} cation is coordinated by six nearest oxygen atoms of water molecules forming an almost perfect octahedron ($d(Cr-O) = 195 - 197$ pm, $6 \times$, $\angle(O-Cr-O) = 90 - 91^\circ$) (Fig. 43, *left*). The O...O distance of the aqua-oxonium cation $H_5O_2^+$ is 242 pm and therefore in the typical range (240 – 245 pm) found for $H_5O_2^+$ in literature [99–101]. Two symmetry-related oxygen atoms (O4a and O4a') of this Zundel-type cation are connected to each other via a bridging hydrogen atom. As a result of this symmetrical constraint, it is possible to locate the hydrogen atom residing at the middle point (*Wyckoff* site 2c: x/a = z/c = 0, y/b = $1/2$; site symmetry: $..2/m$) of the O...O distance, although its crystallographic position could actually not be refined properly. Thus the crystal structure of $[Cr(H_2O)_6](H_5O_2)[B_{12}H_{12}]_2 \cdot 6 H_2O$ possesses a central equidistant hydrogen bond ($d(O4a-H) = 121$ pm) between two oxygen atoms similar to the situation in $(H_5O_2)[Mn(H_2O)_2(SO_4)_2]$ [102]. Each Zundel-type cation connects to six nearest crystal water molecules with the shape of a distorted trigonal antiprism via strong $O-H^{\delta+} \cdots \delta^-O$ hydrogen bridging bonds ($d(O4a \cdots Ow) = 276 - 293$ pm) (Fig. 44, *left*). Strong $O-H^{\delta+} \cdots \delta^-O$ hydrogen bridging bonds are also found between the hydrogen atoms of water molecules within the $[Cr(H_2O)_6]^{3+}$ cations and those of the “free” water molecules ($d(O \cdots Ow) = 269 - 276$ pm) (Fig. 43, *right*). No direct connection between the *quasi*-icosahedral $[B_{12}H_{12}]^{2-}$ -cluster anions and the $[Cr(H_2O)_6]^{3+}$ coordination spheres is found in the crystal structure of $[Cr(H_2O)_6](H_5O_2)[B_{12}H_{12}]_2 \cdot 6 H_2O$. Instead, there are non-classical hydrogen bridging bonds $B-H^{\delta-} \cdots \delta^+H-O$ between the hydrogen atoms of the *quasi*-icosahedral $[B_{12}H_{12}]^{2-}$ anions and the hydrogen atoms of the “free” crystal water molecules ($d(H^{\delta-} \cdots O) = 265 - 315$ pm) and the aqua-oxonium cations ($d(H^{\delta-} \cdots O) = 331 - 351$ pm) as well. Via these weak hydrogen bonds, each aqua-oxonium cation $H_5O_2^+$ is octahedrally surrounded by six boron cages (Fig. 44, *right*). The B–B and B–H bond lengths of the *quasi*-

icosahedral $[\text{B}_{12}\text{H}_{12}]^{2-}$ -cluster anions are similar to those in $[\text{Cr}(\text{H}_2\text{O})_6]_2[\text{B}_{12}\text{H}_{12}]_3 \cdot 15 \text{H}_2\text{O}$ within the common interval ($d(\text{B}-\text{B}) = 177 - 178 \text{ pm}$, $d(\text{B}-\text{H}) = 102 - 115 \text{ pm}$) (Fig. 45).

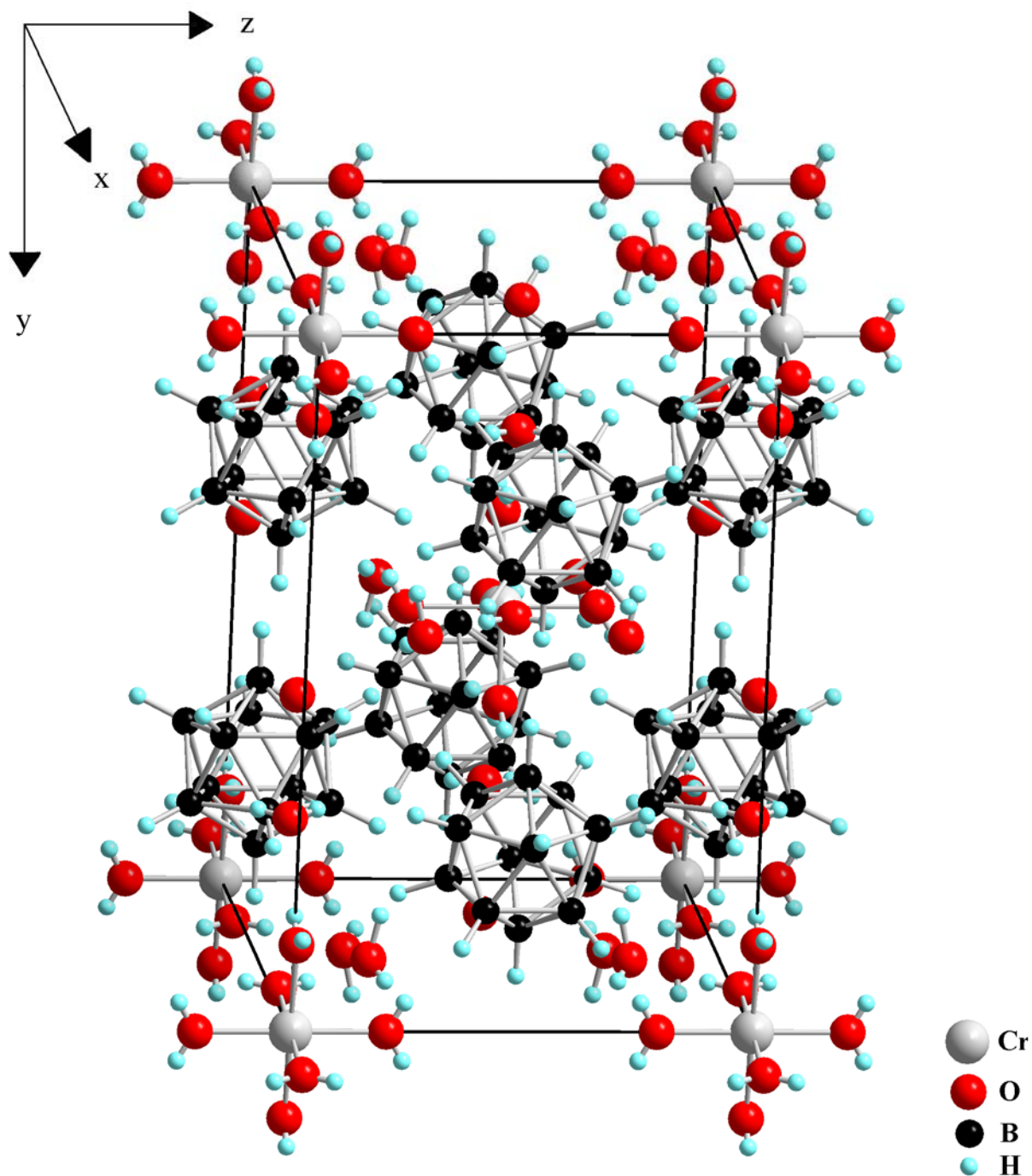


Fig. 42: View at the unit cell of the crystal structure of $[\text{Cr}(\text{H}_2\text{O})_6](\text{H}_5\text{O}_2)[\text{B}_{12}\text{H}_{12}]_2 \cdot 6 \text{H}_2\text{O}$ along $[100]$

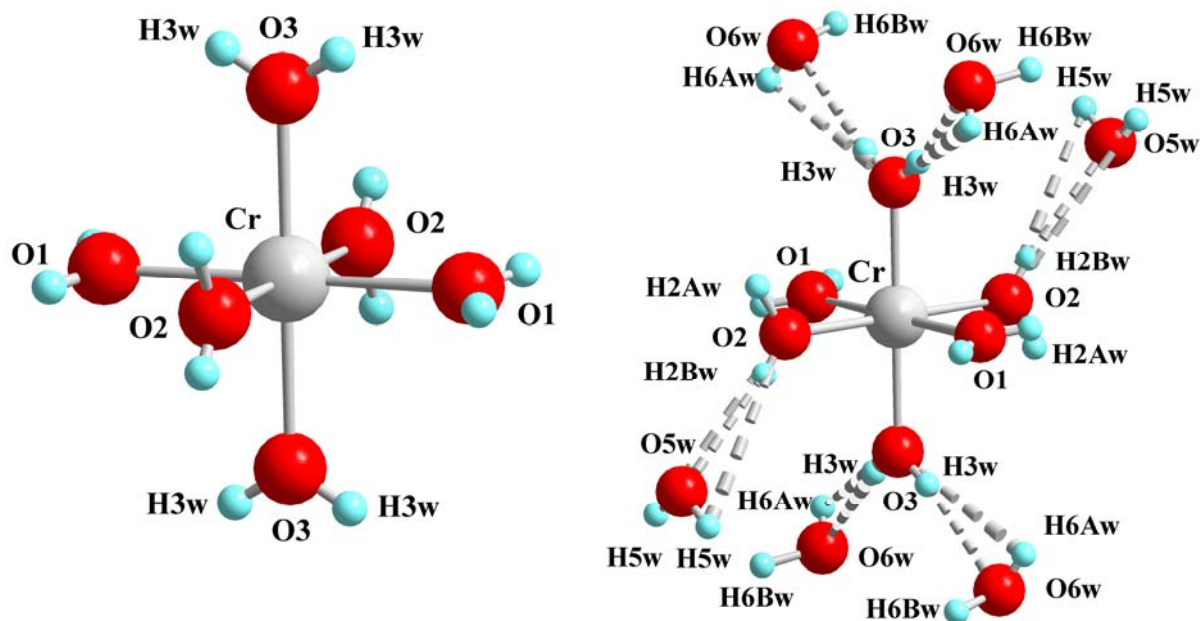


Fig. 43: View at the coordination sphere of the Cr^{3+} cation with its six nearest oxygen atoms of water molecules (*left*) and the $\text{O}-\text{H}^{\delta+}\cdots\delta^-\text{O}$ hydrogen bridges between hydrogen atoms of these water molecules of $[\text{Cr}(\text{H}_2\text{O})_6]^{3+}$ complex cations and those oxygen atoms of crystal water molecules (*right*)

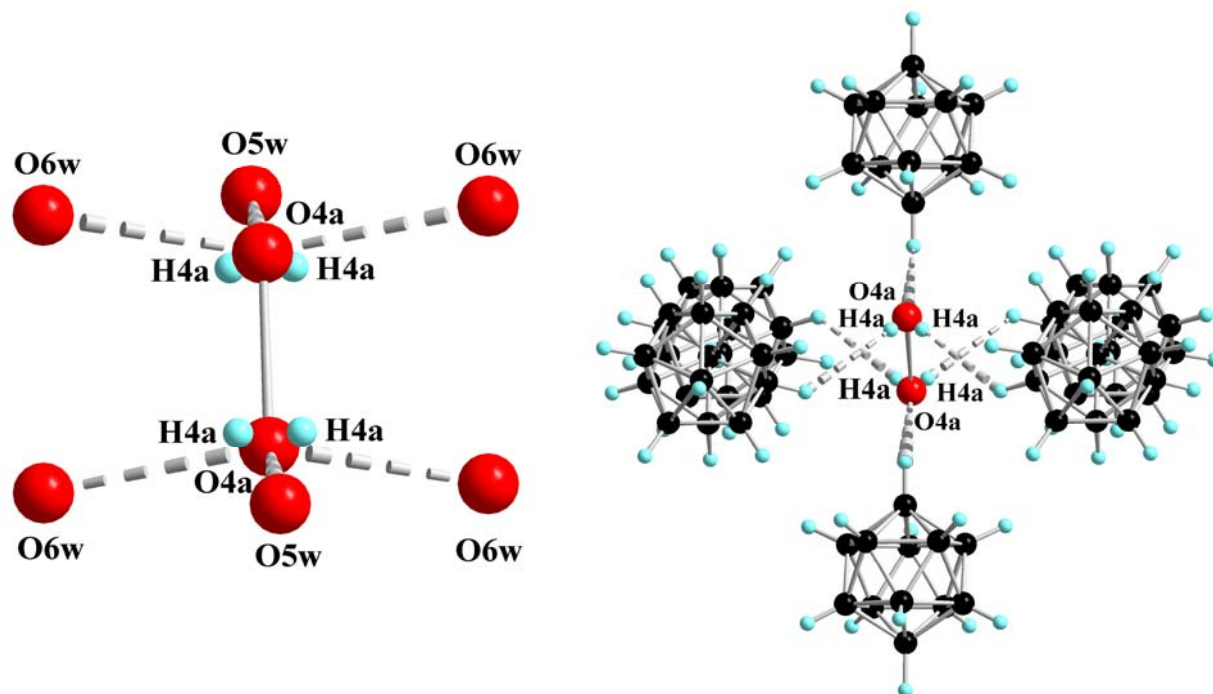


Fig. 44: Coordination sphere of the Zundel-type cation $(\text{H}_5\text{O}_2)^+$ with six nearest crystal water molecules (*left*) and with six surrounded *quasi*-icosahedral $[\text{B}_{12}\text{H}_{12}]^{2-}$ anions (*right*) in the crystal structure of $[\text{Cr}(\text{H}_2\text{O})_6](\text{H}_5\text{O}_2)[\text{B}_{12}\text{H}_{12}]_2 \cdot 6 \text{H}_2\text{O}$

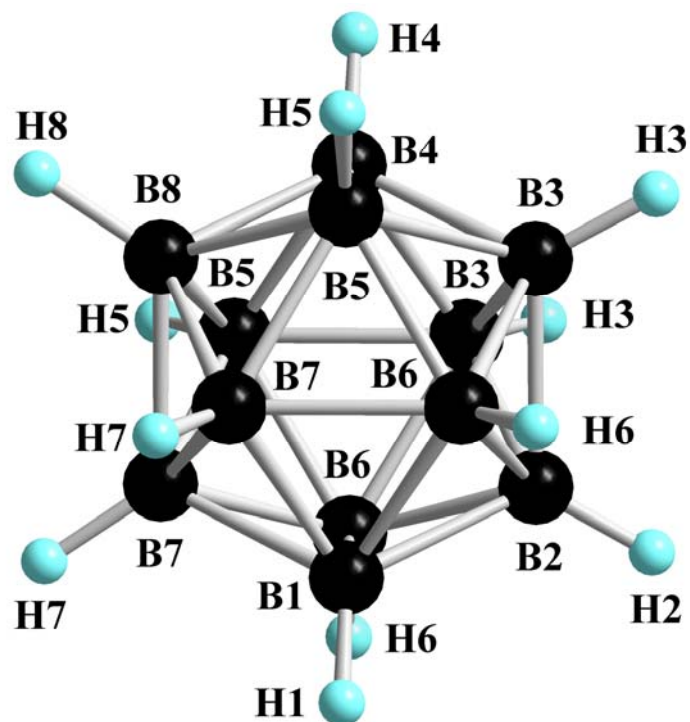


Fig. 45: View at the *quasi*-icosahedral $[B_{12}H_{12}]^{2-}$ -cluster anion in the crystal structure of $[Cr(H_2O)_6](H_5O_2)[B_{12}H_{12}]_2 \cdot 6 H_2O$

Table 39: Crystallographic data for $[\text{Cr}(\text{H}_2\text{O})_6](\text{H}_5\text{O}_2)[\text{B}_{12}\text{H}_{12}]_2 \cdot 6 \text{H}_2\text{O}$ and their determination

Crystal system	orthorhombic
Space group	Pnnm (no. 58)
Unit cell parameters:	
a (pm)	1086.55(7)
b (pm)	1483.17(9)
c (pm)	949.24(6)
Number of formula units per unit cell	$Z = 2$
Calculated density ($D_x/\text{g cm}^{-3}$)	1.279
Molar volume ($V_m/\text{cm}^3 \text{mol}^{-1}$)	460.7
Diffractometer	κ -CCD (Bruker-Nonius)
Radiation	Mo-K α : $\lambda = 71.07 \text{ pm}$, graphite monochromator
Index range	$\pm h_{\text{max}} = 14, \pm k_{\text{max}} = 19, \pm l_{\text{max}} = 12$
θ_{max} (deg)	28.3
F(000)	618
Absorption coefficient (μ/mm^{-1})	0.42
Absorption correction	numerical, Program X-SHAPE [64]
Other data corrections	background, polarization and Lorentz factors
Collected reflections	16424
Unique reflections	2004
$R_{\text{int}}, R_{\sigma}$	0.100, 0.041
Structure solution and refinement	Program SHELXS-97 and SHELXL-97 [68]
Scattering factors	International Tables for Crystallography, Vol. C [87]
R_1, R_w with $ F_o \geq 4\sigma(F_o)$	0.061, 0.050
Reflections with $ F_o \geq 4\sigma(F_o)$	1718
wR_2 , Goodness of fit (GooF)	0.132, 1.121
Extinction (g)	0.0151(3)
Residual electron density (<i>max.</i> , <i>min.</i> in $\rho/e^{-1} 10^6 \text{ pm}$)	0.47, -0.31

Table 40: Atomic coordinates for $[\text{Cr}(\text{H}_2\text{O})_6](\text{H}_5\text{O}_2)[\text{B}_{12}\text{H}_{12}]_2 \cdot 6 \text{H}_2\text{O}$

Atom	Wyckoff position	x/a	y/b	z/c
Cr	2a	0	0	0
O1	4e	0	0	0.2069(2)
O2	4g	0.0320(2)	0.8693(2)	0
O3	4g	0.1765(2)	0.0230(2)	0
O4a	4g	0.0978(2)	0.4613(2)	0
O5w	4g	0.1227(2)	0.2788(2)	0
O6w	8h	0.3352(2)	0.0299(2)	0.2176(3)
B1	4g	0.0955(3)	0.1268(2)	$\frac{1}{2}$
B2	4g	0.2235(3)	0.2021(2)	$\frac{1}{2}$
B3	4g	0.0576(3)	0.3530(2)	$\frac{1}{2}$
B4	4g	0.9306(3)	0.2786(2)	$\frac{1}{2}$
B5	8h	0.0253(2)	0.2868(2)	0.3488(2)
B6	8h	0.1277(2)	0.3935(1)	0.3489(2)
B7	8h	0.9733(2)	0.1796(2)	0.4071(2)
B8	8h	0.1799(2)	0.3004(1)	0.4066(2)
H1w	8h	-0.002(3)	0.042(2)	0.244(3)
H2w1	4g	0.107(5)	0.846(3)	0
H2w2	4g	-0.011(4)	0.838(3)	0
H3w	8h	0.212(3)	0.025(2)	0.065(3)
H4a	8h	0.086(4)	0.444(3)	0.044(4)
H5w	8h	0.161(4)	0.284(3)	0.064(4)
H6w1	8h	0.292(2)	0.009(2)	0.248(2)
H6w2	8h	0.335(7)	0.093(6)	0.239(7)
H1	4g	0.104(3)	0.058(2)	$\frac{1}{2}$
H2	4g	0.314(2)	0.181(3)	$\frac{1}{2}$
H3	4g	0.049(3)	0.426(2)	$\frac{1}{2}$
H4	4g	0.833(3)	0.308(2)	$\frac{1}{2}$
H5	8h	-0.009(2)	0.313(2)	0.250(3)
H6	8h	0.160(2)	0.164(2)	0.247(2)
H7	8h	0.910(2)	0.138(2)	0.349(3)
H8	8h	0.247(2)	0.335(2)	0.348(3)

Table 41: Anisotropic thermal displacement coefficients^{a)} (U_{ij}/pm^2) for $[\text{Cr}(\text{H}_2\text{O})_6](\text{H}_5\text{O}_2)[\text{B}_{12}\text{H}_{12}]_2 \cdot 6 \text{H}_2\text{O}$

Atom	U_{11}	U_{22}	U_{33}	U_{23}	U_{13}	U_{12}
Cr	253(3)	179(3)	230(3)	0	0	-17(2)
O1	611(9)	291(9)	232(8)	0	0	-47(8)
O2	304(9)	197(9)	507(8)	0	0	2(8)
O3	252(9)	402(9)	352(8)	0	0	-44(8)
O4a	825(19)	476(16)	1037(35)	0	0	46(12)
O5w	474(13)	609(16)	638(17)	0	0	102(12)
O6w	767(15)	548(12)	652(13)	49(10)	-171(12)	-51(11)
B1	327(12)	325(13)	378(14)	0	0	18(11)
B2	255(13)	310(14)	416(15)	0	0	33(11)
B3	312(14)	215(12)	398(15)	0	0	36(10)
B4	233(13)	304(14)	383(14)	0	0	25(10)
B5	400(11)	339(10)	282(9)	29(8)	-16(8)	76(8)
B6	397(11)	330(10)	286(10)	-25(8)	29(8)	74(8)
B7	333(10)	300(10)	404(11)	-63(8)	-90(8)	-16(8)
B8	311(10)	304(10)	433(11)	72(8)	86(8)	-15(8)
H1w	679(100)					
H2w1	826(149)					
H2w2	437(114)					
H3w	629(90)					
H4a	321(94)					
H5w	1138(165)					
H6w1	144(56)					
H6w2	2267(339)					
H1	439(91)					
H2	525(97)					
H3	512(66)					
H4	422(87)					
H5	560(74)					
H6	465(64)					
H7	510(68)					
H8	407(84)					

^{a)} For Cr, O and B defined as anisotropic temperature factor according to: $\exp[-2\pi^2(U_{11}h^2a^{*2} + U_{22}k^2b^{*2} + U_{33}l^2c^{*2} + 2U_{23}klb^{*}c^{*} + 2U_{13}hla^{*}c^{*} + 2U_{13}hka^{*}b^{*})]$; for H isotropically defined as temperature factor in: $\exp[-8\pi^2(U_{\text{iso}}\sin^2\theta/\lambda^2)]$.

Table 42: Selected interatomic distances (d/pm) and angles (\angle /deg) for $[\text{Cr}(\text{H}_2\text{O})_6](\text{H}_5\text{O}_2)[\text{B}_{12}\text{H}_{12}]_2 \cdot 6 \text{H}_2\text{O}$

[CrO ₆] polyhedron:					
Cr	– O1	196.4 (2×)	O1–Cr–O1	180.0	
	– O2	197.0 (2×)	O1–Cr–O2	90.0 (2×)	
	– O3	194.8 (2×)	O1–Cr–O3	90.0 (2×)	
			O2–Cr–O2	180.0	
			O2–Cr–O3	90.1	
			O2–Cr–O3'	89.0	
			O3–Cr–O3'	180.0	
[B ₁₂ H ₁₂] ²⁻ anion:					
B1	– B2	177.4	B2	– B1	177.4
	– B7	177.6 (2×)		– B6	177.5 (2×)
	– B6	177.7 (2×)		– B8	178.4 (2×)
	– H1	103.2		– H2	102.5
B3	– B4	176.7	B4	– B3	176.7
	– B5	177.5 (2×)		– B5	177.0 (2×)
	– B8	178.4 (2×)		– B7	177.5 (2×)
	– H3	108.5		– H4	114.7
B5	– B4	177.0	B6	– B8	177.0
	– B3	177.5		– B5	177.5
	– B6	177.5		– B2	177.5
	– B7	177.6		– B1	177.7
	– B8	177.9		– B7	177.8
	– H5	107.8		– H6	111.9
B7	– B7	176.3	B8	– B6	177.0
	– B4	177.5		– B8	177.4
	– B5	177.5		– B3	177.8
	– B1	177.6		– B5	177.9
	– B6	177.8		– B2	178.4
	– H7	107.2		– H8	105.9

Table 42: (continued)

Hydrogen bridging bonds ^{a)} :					
D–H...A		d(D–H)	d(H...A)	d(D...A)	∠ (D–H...A)
O2–H2w2...O5w	(2×)	66.3	211.0	276.6	170.3
O5w–H5w...O2	(2×)	73.8	315.0	276.6	52.7
O3–H3...O6w	(2×)	73.1	197.0	269.2	169.3
O3–H3'...O6w	(2×)	73.1	300.0	269.2	58.9
O6w–H6w1...O3	(2×)	63.3	267.2	269.2	85.0
O6w–H6w2...O3	(2×)	63.3	302.8	269.2	60.6
O2–H2w1...H3	(2×)	88.2	215.1	284.5	135.2
O2–H2w2...H3	(2×)	66.3	321.0	284.5	51.5
O1–H1w...H7	(2×)	71.6	199.1	264.4	151.9
O1–H1w'...H7	(2×)	71.6	302.2	264.4	52.2
O6w–H6w1...H5	(2×)	63.3	342.2	290.2	31.6
O6w–H6w2...H5	(2×)	95.2	220.7	290.2	129.1
O5w–H5w...H8	(2×)	73.8	239.4	262.5	100.0

^{a)} D = Donor, A = Acceptor

3.3.4 Bis-Hexaaqua-Aluminium(III) Oxosulfate Bis-Dodecahydro-*closo*-Dodecaborate Pentadecahydrate

The synthesis of hydrated aluminium dodecahydro-*closo*-dodecaborate salts by the reaction of $\text{Al}_2(\text{SO}_4)_3$ and $\text{Ba}[\text{B}_{12}\text{H}_{12}]$ has been reported in literature, but crystal structure data were still not known [16]. Using this procedure, however, the mixed-anion compound $[\text{Al}(\text{H}_2\text{O})_6]_2(\text{SO}_4)[\text{B}_{12}\text{H}_{12}]_2 \cdot 15 \text{H}_2\text{O}$ was now obtained instead of a pure aluminium dodecahydro-*closo*-dodecaborate hydrate.

3.3.4.1 Synthesis of $[\text{Al}(\text{H}_2\text{O})_6]_2(\text{SO}_4)[\text{B}_{12}\text{H}_{12}]_2 \cdot 15 \text{H}_2\text{O}$

Colourless, polyhedral single crystals of $[\text{Al}(\text{H}_2\text{O})_6]_2(\text{SO}_4)[\text{B}_{12}\text{H}_{12}]_2 \cdot 15 \text{H}_2\text{O}$ were obtained by the stoichiometric reaction between $\text{Al}_2(\text{SO}_4)_3 \cdot 18 \text{H}_2\text{O}$ (Strem: 98 %) and $\text{Ba}(\text{H}_2\text{O})_6[\text{B}_{12}\text{H}_{12}]$ [85]. The resulting aqueous solution was then filtered and subsequently evaporated at room temperature within several days.

3.3.4.2 Structure Description of $[\text{Al}(\text{H}_2\text{O})_6]_2(\text{SO}_4)[\text{B}_{12}\text{H}_{12}]_2 \cdot 15 \text{H}_2\text{O}$

The title compound crystallizes in the trigonal crystal system with space group $R\bar{3}c$ (no. 167) and $Z = 6$ (Fig. 46, *left*). In this crystal structure, the aluminium(III) cations reside at the *Wyckoff* position $12c$ ($x/a = y/b = 0, z/c$; site symmetry: $3.$), while the sulfur atoms of the SO_4^{2-} anions are surprisingly located at the special *Wyckoff* position $6b$ ($x/a = y/b = z/c = 0$; site symmetry: $\bar{3}$). All coordinated oxygen atoms of the octahedral Al^{3+} coordination sphere occupy the general *Wyckoff* site $36f$ ($x/a, y/b, z/c$; site symmetry: 1), while those belonging to the SO_4^{2-} anion are located at two almost half-occupied *Wyckoff* positions $36f$ ($x/a, y/b, z/c$; site occupancy: 0.46) and $12c$ ($x/a = y/b = 0, z/c$; site occupancy: 0.38). The oxygen atoms of the “free” crystal water molecules occupy one crystallographic $18e$ site ($x/a, y/b, z/c = 3/4$; site symmetry: $.2$) and two different $36f$ sites. All boron atoms (B1 – B4) and hydrogen atoms (H1 – H4) of the *quasi*-icosahedral $[\text{B}_{12}\text{H}_{12}]^{2-}$ -cluster anions are located at the *Wyckoff* positions $36f$. The centers of gravity of the *quasi*-icosahedral $[\text{B}_{12}\text{H}_{12}]^{2-}$ -cluster anions are found at the *Wyckoff* position $12c$ ($x/a = 1/3, y/b = 2/3, z/c$; site symmetry: $3.$) and the distances from the center of gravity to the twelve boron atoms of each cluster anion range from 168 to 177 pm providing them an inner diameter of 336 – 354 pm. The coordination of each Al^{3+} cation with

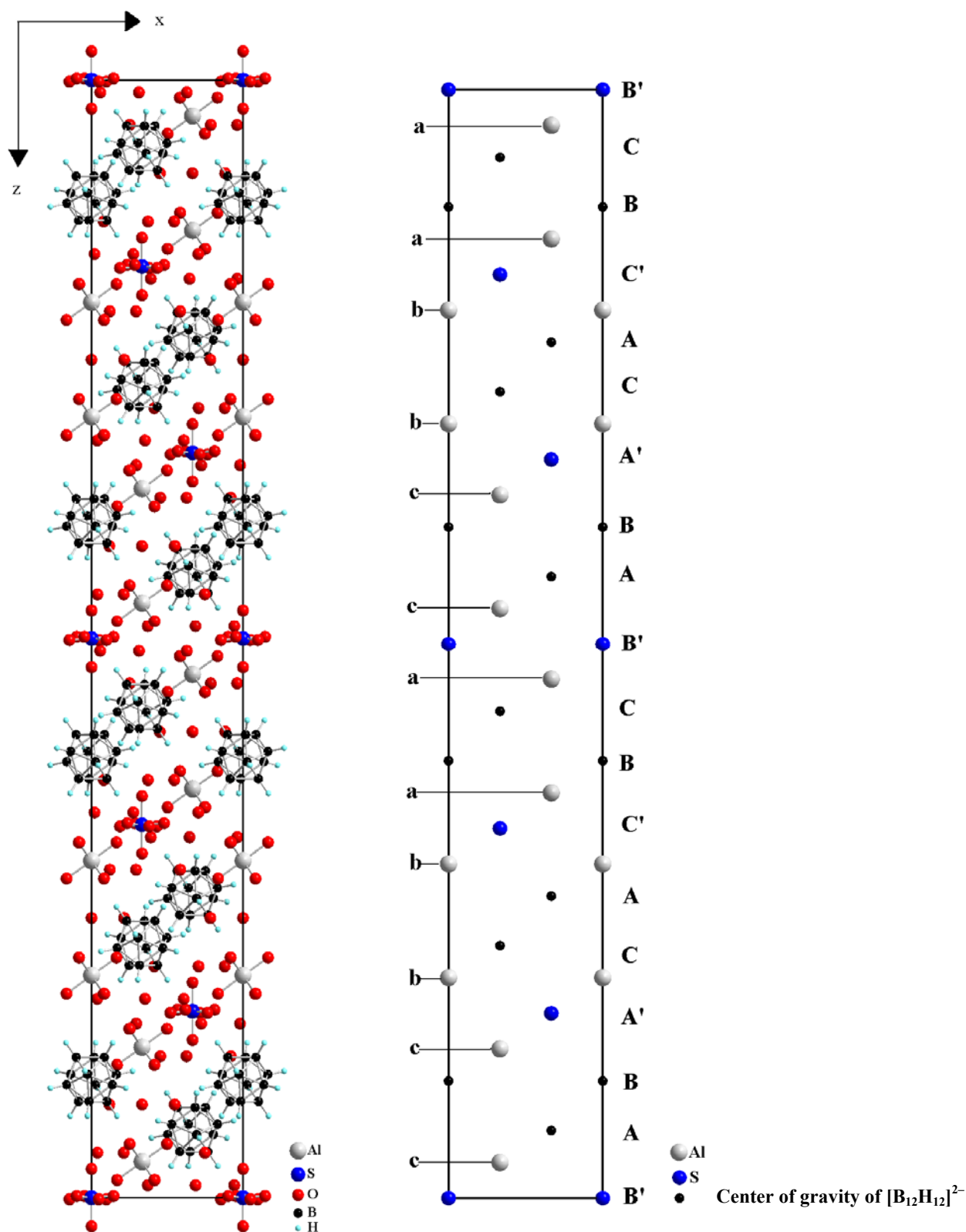


Fig. 46: View at a unit cell of the crystal structure of $[\text{Al}(\text{H}_2\text{O})_6]_2(\text{SO}_4)[\text{B}_{12}\text{H}_{12}]_2 \cdot 15 \text{H}_2\text{O}$ as viewed along $[010]$ (*left*) and the arrangement of Al^{3+} cations, SO_4^{2-} anions and the centers of gravity of the $[\text{B}_{12}\text{H}_{12}]^{2-}$ -cluster anions (*right*) as stacking scheme

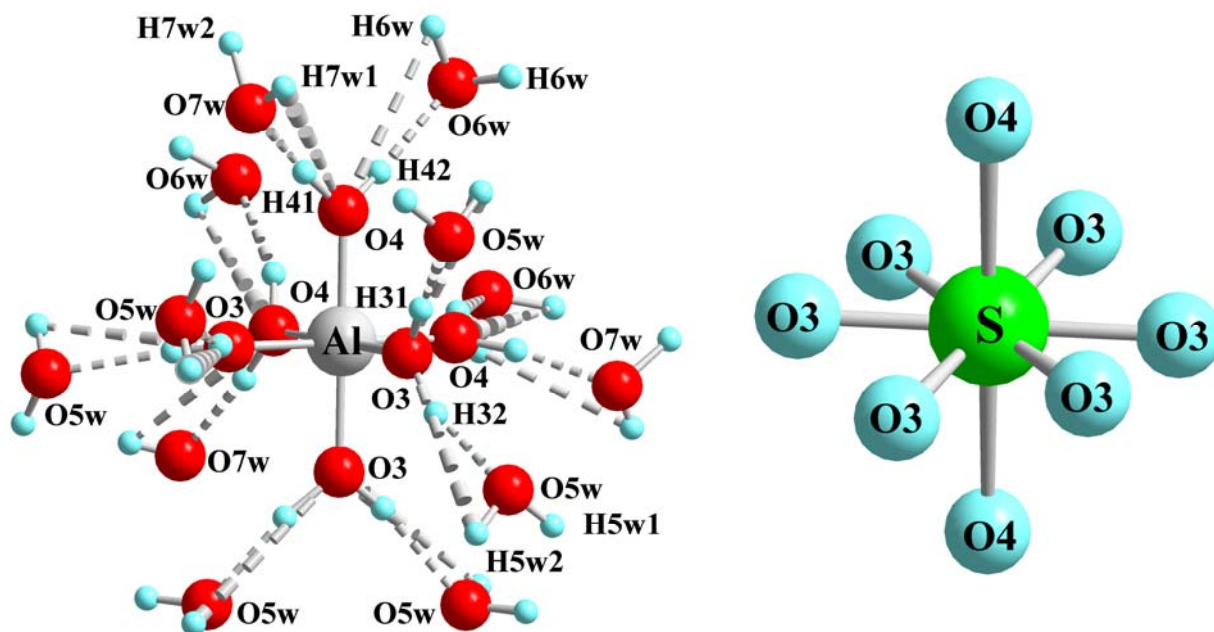


Fig. 47: View of the first coordination sphere of Al^{3+} with six neighbour water molecules (*left*) and the disordered SO_4^{2-} anion (*right*) in the crystal structure of $[\text{Al}(\text{H}_2\text{O})_6]_2(\text{SO}_4)[\text{B}_{12}\text{H}_{12}]_2 \cdot 15 \text{H}_2\text{O}$

oxygen atoms of the six nearest coordinating water molecules results in a slightly distorted octahedron $d(\text{Al}-\text{O}) = 188 - 191 \text{ pm}$, $\angle(\text{O}-\text{Al}-\text{O}) = 90 - 91^\circ$ (Fig. 47, *left*). The peculiar shape of the SO_4^{2-} anions, with sulfur-coordinated oxygen atoms located at two half-occupied *Wyckoff* sites, is a distorted hexagonal scalenohedron rather than a common tetrahedron (Fig. 47, *right*). The central sulfur atom bonds to *six* equatorial oxygen atoms with common bond lengths ($d(\text{S}-\text{O}) = 140 \text{ pm}$) and to *two* other apical ones at significantly longer distances ($d(\text{S}-\text{O}) = 174 \text{ pm}$). Of course this picture results from a superposition of two independently oriented SO_4^{2-} tetrahedra as shown in Figure 47 (*right*). The crystal structure of $[\text{Al}(\text{H}_2\text{O})_6]_2(\text{SO}_4)[\text{B}_{12}\text{H}_{12}]_2 \cdot 15 \text{H}_2\text{O}$ can be described by three different motifs, namely Al^{3+} cations along with SO_4^{2-} and $[\text{B}_{12}\text{H}_{12}]^{2-}$ anions as non-aqueous lattice components. The arrangement of both the $[\text{B}_{12}\text{H}_{12}]^{2-}$ and the SO_4^{2-} anions follows the cubic closest packed fashion with a stacking sequence of *ABC* and *A'B'C'*, respectively (Fig. 46, *right*). The stacking sequence of the aluminium(III) cations is *aa bb cc* of the (double-layer) copper structure type, quite the same to that one of the La^{3+} cations in trigonal $[\text{La}(\text{H}_2\text{O})_9]_2[\text{B}_{12}\text{H}_{12}]_3 \cdot 15 \text{H}_2\text{O}$ [91]. There are strong and weak hydrogen bridging bonds in the crystal structure of

$[\text{Al}(\text{H}_2\text{O})_6]_2(\text{SO}_4)[\text{B}_{12}\text{H}_{12}]_2 \cdot 15 \text{H}_2\text{O}$. Each oxygen atom of the octahedral coordination sphere of Al^{3+} is linked to oxygen atoms of crystal water molecules via strong classical $\text{O}-\text{H}^{\delta+}\cdots\delta^-\text{O}$ hydrogen bridging bonds with $d(\text{O}\cdots\text{O}) = 256 - 274 \text{ pm}$ as donor-acceptor distances (Fig. 48, *left*). In addition, there are also non-classical $\text{B}-\text{H}^{\delta-}\cdots\delta^+\text{H}-\text{O}$ hydrogen bonds between hydrogen atoms of the boron cage and hydrogen atoms of water molecules coordinated to the Al^{3+} cations with $d(\text{H}^{\delta-}\cdots\text{O}) = 307 - 336 \text{ pm}$ as donor-acceptor distances. All Al^{3+} cations are tetrahedrally surrounded by and linked via these weak bonds to four nearest $[\text{B}_{12}\text{H}_{12}]^{2-}$ cages. Such weak hydrogen bonds are also found between hydrogen atoms of the boron cages and hydrogen atoms of neighbouring “free” crystal water molecules ($d(\text{H}^{\delta-}\cdots\text{O}) = 285 - 324 \text{ pm}$). In the crystal structure of $[\text{Al}(\text{H}_2\text{O})_6]_2(\text{SO}_4)[\text{B}_{12}\text{H}_{12}]_2 \cdot 15 \text{H}_2\text{O}$ the *quasi*-icosahedral $[\text{B}_{12}\text{H}_{12}]^{2-}$ -cluster anions are not very much distorted from the ideal icosahedron ($d(\text{B}-\text{B}) = 176 - 178 \text{ pm}$, $d(\text{B}-\text{H}) = 110 \text{ pm}$) (Fig. 48, *right*).

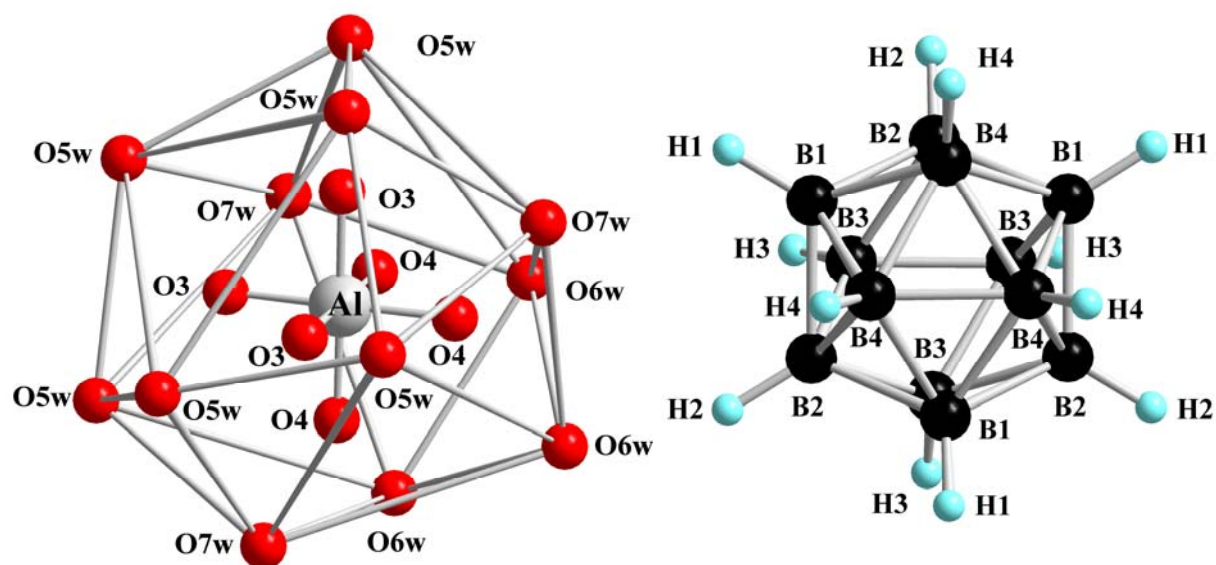


Fig. 48: *Quasi*-icosahedral arrangement of twelve “zeolitic” crystal water molecules (O2w) around each $[\text{Al}(\text{H}_2\text{O})_6]^{3+}$ octahedron (*left*) and the *quasi*-icosahedral $[\text{B}_{12}\text{H}_{12}]^{2-}$ -cluster anion (*right*) in the crystal structure of $[\text{Al}(\text{H}_2\text{O})_6]_2(\text{SO}_4)[\text{B}_{12}\text{H}_{12}]_2 \cdot 15 \text{H}_2\text{O}$

Table 43 Crystallographic data for $[\text{Al}(\text{H}_2\text{O})_6]_2(\text{SO}_4)[\text{B}_{12}\text{H}_{12}]_2 \cdot 15 \text{H}_2\text{O}$ and their determination

Crystal system	trigonal
Space group	$R\bar{3}c$ (no. 167)
Unit cell parameters:	
a (pm)	1083.82(2)
c (pm)	6776.56(9)
Number of formula units per unit cell	Z = 6
Calculated density ($D_x/\text{g cm}^{-3}$)	1.330
Molar volume ($V_m/\text{cm}^3 \text{mol}^{-1}$)	691.9
Diffractometer	IPDS (Stoe)
Radiation	Mo-K α : $\lambda = 71.07$ pm, graphite monochromator
Index range	$\pm h_{\max} = 11, \pm k_{\max} = 11, \pm l_{\max} = 72$
θ_{\max} (deg)	22.4
F(000)	2928
Absorption coefficient (μ/mm^{-1})	0.19
Absorption correction	numerical, Program X-SHAPE [64]
Other data corrections	background, polarization and <i>Lorentz</i> factors
Collected reflections	10979
Unique reflections	988
$R_{\text{int}}, R_{\sigma}$	0.145, 0.124
Structure solution and refinement	Program SHELXS-97 and SHELXL-97 [68]
Scattering factors	International Tables for Crystallography, Vol. C [87]
R_1, R_1 with $ F_o \geq 4\sigma(F_o)$	0.134, 0.051
Reflections with $ F_o \geq 4\sigma(F_o)$	404
w R_2 , Goodness of fit (GooF)	0.129, 0.775
Extinction (g)	0.0002(1)
Residual electron density (<i>max.</i> , <i>min.</i> in $\rho/e^{-1} 10^6$ pm)	0.29, -0.30

Table 44: Atomic coordinates for $[\text{Al}(\text{H}_2\text{O})_6]_2(\text{SO}_4)[\text{B}_{12}\text{H}_{12}]_2 \cdot 15 \text{H}_2\text{O}$

Atom	Wyckoff position	x/a	y/b	z/c
Al	12 <i>c</i>	0	0	0.1988(1)
S	6 <i>b</i>	0	0	0
O1 ^{a)}	12 <i>c</i>	0	0	0.0257(1)
O2 ^{a)}	36 <i>f</i>	0.0983(9)	0.9525(9)	0.0014(1)
O3	36 <i>f</i>	0.5822(4)	0.4136(4)	0.0157(1)
O4	36 <i>f</i>	0.7486(4)	0.4980(3)	0.0480(1)
O5w	36 <i>f</i>	0.3136(4)	0.3712(4)	0.0111(1)
O6w	18 <i>e</i>	0.2158(5)	0.2158(5)	³ / ₄
O7w	36 <i>f</i>	0.7874(5)	0.7479(5)	0.0402(1)
B1	36 <i>f</i>	0.3068(7)	0.5028(7)	0.0564(1)
B2	36 <i>f</i>	0.1692(7)	0.5292(7)	0.0657(1)
B3	36 <i>f</i>	0.3169(7)	0.5649(7)	0.0807(1)
B4	36 <i>f</i>	0.4182(7)	0.6502(7)	0.0412(1)
H31	36 <i>f</i>	0.501(4)	0.393(4)	0.017(1)
H32	36 <i>f</i>	0.597(4)	0.426(4)	0.010(1)
H41	36 <i>f</i>	0.767(4)	0.569(4)	0.045(1)
H42	36 <i>f</i>	0.772(1)	0.495(4)	0.055(1)
H5w1	36 <i>f</i>	0.277(4)	0.396(4)	0.022(1)
H5w2	36 <i>f</i>	0.253(4)	0.297(4)	0.009(1)
H6w	36 <i>f</i>	0.280(4)	0.228(4)	0.748(1)
H7w1	36 <i>f</i>	0.858(4)	0.787(4)	0.040(1)
H7w2	36 <i>f</i>	0.768(4)	0.778(4)	0.048(1)
H1	36 <i>f</i>	0.297(4)	0.391(4)	0.053(1)
H2	36 <i>f</i>	0.063(4)	0.441(4)	0.069(1)
H3	36 <i>f</i>	0.318(4)	0.507(4)	0.093(1)
H4	36 <i>f</i>	0.474(4)	0.643(4)	0.030(1)

^{a)} s.o.f. of O1: 0.39(1); s.o.f. of O2: 0.45(1).

Table 45: Anisotropic thermal displacement coefficients^{a)} (U_{ij}/pm^2) for $[\text{Al}(\text{H}_2\text{O})_6]_2(\text{SO}_4)[\text{B}_{12}\text{H}_{12}]_2 \cdot 15 \text{H}_2\text{O}$

Atom	U_{11}	U_{22}	U_{33}	U_{23}	U_{13}	U_{12}
Al	393(10)	= U_{11}	358(15)	0	0	= $\frac{1}{2} U_{11}$
S	410(16)	= U_{11}	1288(40)	0	0	= $\frac{1}{2} U_{11}$
O1	451(69)	= U_{11}	1034(74)	0	0	= $\frac{1}{2} U_{11}$
O2	451(75)	681(66)	1066(74)	306(49)	127(50)	497(51)
O3	533(26)	506(25)	439(19)	30(21)	-47(21)	280(19)
O4	526(26)	460(22)	443(19)	-102(17)	-48(21)	241(24)
O5w	561(27)	562(26)	547(24)	3(21)	61(21)	255(21)
O6w	547(25)	= U_{11}	422(30)	1(14)	= $-U_{23}$	197(30)
O7w	1138(39)	682(32)	738(29)	45(25)	121(27)	553(20)
B1	518(44)	431(42)	498(38)	9(36)	63(38)	263(36)
B2	449(43)	502(44)	570(39)	54(37)	38(36)	226(37)
B3	601(51)	565(44)	452(34)	102(36)	4(35)	312(38)
B4	492(48)	512(46)	420(44)	-21(32)	-16(33)	283(42)
H31	915(78)					
H32	935(65)					
H41	1032(93)					
H42	987(89)					
H5w1	966(105)					
H5w2	957(97)					
H6w	896(72)					
H7w1	1121(64)					
H7w2	1082(59)					
H1	500(98)					
H2	331(98)					
H3	330(98)					
H4	504(98)					

^{a)} For Al, S, O and B defined as anisotropic temperature factor according to: $\exp[-2\pi^2(U_{11}h^2a^{*2} + U_{22}k^2b^{*2} + U_{33}l^2c^{*2} + 2U_{23}klb^{*}c^{*} + 2U_{13}hla^{*}c^{*} + 2U_{13}hka^{*}b^{*})]$; for H defined isotropically in the expression: $\exp[-8\pi^2(U_{\text{iso}}\sin^2\theta/\lambda^2)]$.

Table 46: Selected interatomic distances (d/pm) for $[\text{Al}(\text{H}_2\text{O})_6]_2(\text{SO}_4)[\text{B}_{12}\text{H}_{12}]_2 \cdot 15 \text{H}_2\text{O}$

[AlO ₆] polyhedron:			
	Al – O3	188.9	(3×)
	– O4	188.7	(3×)
[SO ₄] ²⁻ anion:			
	S – O2	139.9	(6/2×)
	– O1	174.1	(2/2×)
[B ₁₂ H ₁₂] ²⁻ anion:			
B1 – B3	175.7	B2 – B3	176.6
– B2	176.7	– B3'	176.6
– B4	177.5	– B1	176.7
– B4'	177.5	– B4	176.7
– H1	116.7	– B4'	177.8
		– H2	109.0
B3 – B1	175.7	B4 – B4	176.9
– B2	176.6	– B4'	176.9
– B2'	176.7	– B1	177.5
– B3	177.6	– B1'	177.5
– B3'	177.6	– B2	177.8
– H3	101.3	– H4	101.3

3.3.5 Bis-Enneaqua-Lanthanum(III) Tris-Dodecahydro-*closo*-Dodecaborate Heptahydrate $[\text{La}(\text{H}_2\text{O})_9]_2[\text{B}_{12}\text{H}_{12}]_3 \cdot 7 \text{H}_2\text{O}$

The synthesis and crystal structure of the trigonal hydrated dodecahydro-*closo*-dodecaborate salt with La^{3+} , $[\text{La}(\text{H}_2\text{O})_9]_2[\text{B}_{12}\text{H}_{12}]_3 \cdot 15 \text{H}_2\text{O}$ namely, was published recently [91]. This compound is obtained by neutralizing the aqueous solution of the free acid $(\text{H}_3\text{O})_2[\text{B}_{12}\text{H}_{12}]$ with lanthanum(III) oxide, La_2O_3 , or lanthanum(III) hydroxide, $\text{La}(\text{OH})_3$. In other words, $[\text{La}(\text{H}_2\text{O})_9]_2[\text{B}_{12}\text{H}_{12}]_3 \cdot 15 \text{H}_2\text{O}$ will always be the only product, regardless of whether $(\text{H}_3\text{O})_2[\text{B}_{12}\text{H}_{12}]$ is neutralized by the oxide or the hydroxide of lanthanum. Furthermore, if $[\text{La}(\text{H}_2\text{O})_9]_2[\text{B}_{12}\text{H}_{12}]_3 \cdot n \text{H}_2\text{O}$ with $n < 15$ is target product, it should be obtained by controlled thermal dehydration of $[\text{La}(\text{H}_2\text{O})_9]_2[\text{B}_{12}\text{H}_{12}]_3 \cdot 15 \text{H}_2\text{O}$. However, when neutralizing the aqueous solution of $(\text{H}_3\text{O})_2[\text{B}_{12}\text{H}_{12}]$ with $\text{La}(\text{NO}_3)_3 \cdot 6 \text{H}_2\text{O}$ (Merck: 99.9 %), which was used as an alternative starting material, triclinic $[\text{La}(\text{H}_2\text{O})_9]_2[\text{B}_{12}\text{H}_{12}]_3 \cdot 7 \text{H}_2\text{O}$ with lower water content became the dominating hydrate.

3.3.5.1 Synthesis of $[\text{La}(\text{H}_2\text{O})_9]_2[\text{B}_{12}\text{H}_{12}]_3 \cdot 7 \text{H}_2\text{O}$

The title compound was synthesized by the reaction of lanthanum(III) nitrate $\text{La}(\text{NO}_3)_3 \cdot 6 \text{H}_2\text{O}$ (Merck: 99.9 %) with the free acid $(\text{H}_3\text{O})_2[\text{B}_{12}\text{H}_{12}]$ and subsequent evaporation of the resulting aqueous solution at room temperature. The colourless, polyhedrally shaped single crystals were grown and then selected, before getting subject to single crystal X-ray diffraction measurements at low temperature ($T = 100 \text{ K}$). The crystal structure was able to be determined with all of the atoms refined freely.

3.3.5.2 Structure Description of $[\text{La}(\text{H}_2\text{O})_9]_2[\text{B}_{12}\text{H}_{12}]_3 \cdot 7 \text{H}_2\text{O}$

$[\text{La}(\text{H}_2\text{O})_9]_2[\text{B}_{12}\text{H}_{12}]_3 \cdot 7 \text{H}_2\text{O}$ crystallizes in the triclinic space group $P\bar{1}$ (no. 2) with two formula units per unit cell (Fig. 49). All of the atoms in this crystal structure occupy the general *Wyckoff* position $2i$ (x/a , y/b , z/c ; site symmetry: 1). Both of the two crystallographically distinct La^{3+} cations are ninefold coordinated by oxygen atoms of the nearest water molecules, forming a distorted monocapped square antiprism with La–O distances ranging from 248 to 259 pm (Fig. 50). The centers of gravity of the *quasi*-

icosahedral $[\text{B}_{12}\text{H}_{12}]^{2-}$ -cluster anions are found at four crystallographically different *Wyckoff* positions. Two of them occupy special *Wyckoff* sites (1e: $x/a = y/b = 1/2$, $z/c = 0$ and 1g: $x/a = 0$, $y/b = z/c = 1/2$; site symmetry: $\bar{1}$ for both). Two others are located at two independent general *Wyckoff* positions 2i (x/a , y/b , z/c). The distances from the centers of gravity to the twelve boron atoms at the vertices of each *quasi*-icosahedral $[\text{B}_{12}\text{H}_{12}]^{2-}$ -cluster anion range from 169 to 170 pm providing inner cage diameters from 338 to 340 pm. The boron cages $[\text{B}_{12}\text{H}_{12}]^{2-}$, with B–B and B–H bond lengths in the intervals of 176 – 179 pm and 106 – 114 pm, respectively, are slightly distorted from an ideal icosahedron (Fig. 51). Six out of nine coordinated oxygen atoms of the La1 trication link to oxygen atoms of the nearest “zeolitic” water molecules and coordinated oxygen atoms of another La1 trication via strong hydrogen bridging bonds with $d(\text{O}\cdots\text{O}) = 266 - 287$ pm as donor-acceptor distances. Particularly, two of these six coordinated oxygen atoms are connected to two coordinated oxygen atoms of another La1 trication and the four others are linked to oxygen atoms of “free” crystal water molecules. Similarly, with the La2 trication only eight out of nine coordinated oxygen atoms take part in a classical hydrogen bonding system; two are linked to two coordinated oxygen atoms of another La2 trication with O \cdots O distances of 329 pm, while the other six oxygen atoms bond to those of the nearest “zeolitic” crystal water molecules with $d(\text{O}\cdots\text{O}) = 270 - 276$ pm. These strong hydrogen bridging bonds differ remarkably from those of $[\text{La}(\text{H}_2\text{O})_9]_2[\text{B}_{12}\text{H}_{12}]_3 \cdot 15 \text{H}_2\text{O}$, in which all oxygen atoms of water molecules of the $[\text{La}(\text{H}_2\text{O})_9]^{3+}$ coordination sphere link to oxygen atoms of “zeolitic” crystal water molecules only. In addition, there are weak hydrogen bridging bonds between the hydrogen atoms of boron cages $[\text{B}_{12}\text{H}_{12}]^{2-}$ and hydrogen atoms of the surrounding “zeolitic” crystal and the coordinating water molecules ($d(\text{H}^{\delta-}\cdots\text{O}) = 272 - 299$ pm) as non-classical B–H $^{\delta-}\cdots\delta^+$ H–O or sometimes even called “dihydrogen” bonds.

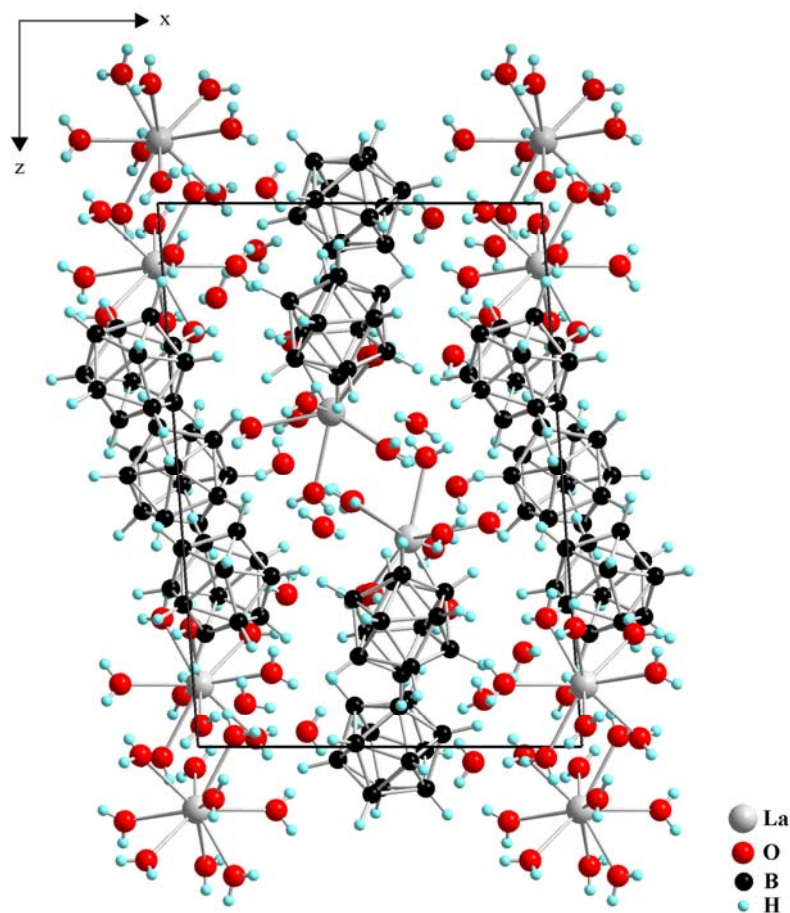


Fig. 49: Perspective view at a unit cell of the crystal structure of $[\text{La}(\text{H}_2\text{O})_9]_2[\text{B}_{12}\text{H}_{12}]_3 \cdot 7 \text{H}_2\text{O}$ as viewed along $[010]$

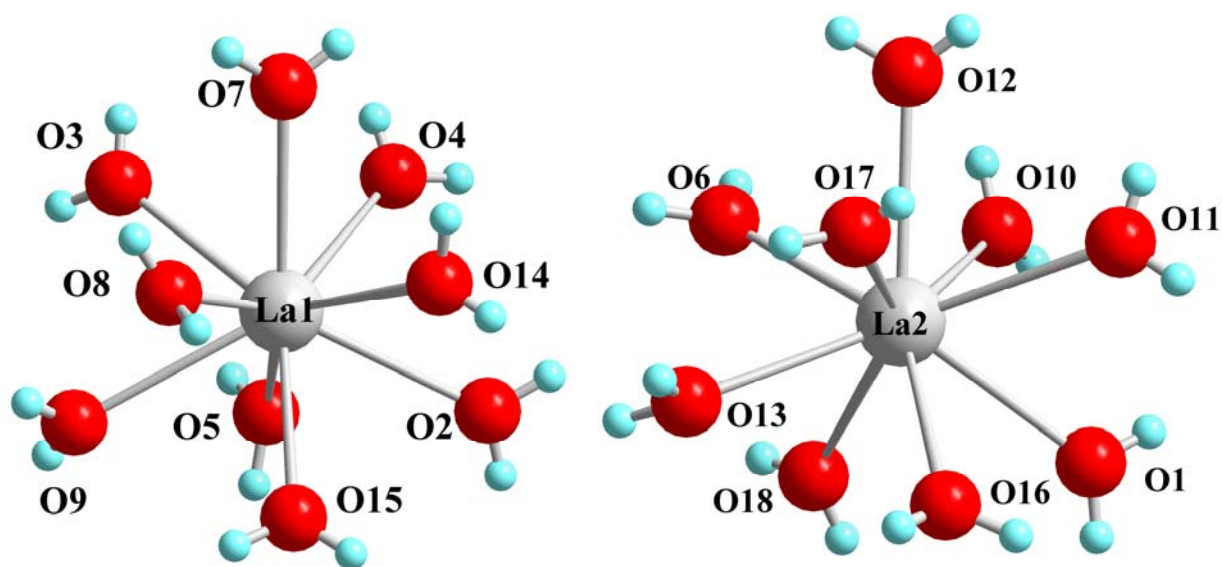


Fig. 50: View at the coordination spheres of the La1 (*left*) and La2 trications (*right*)

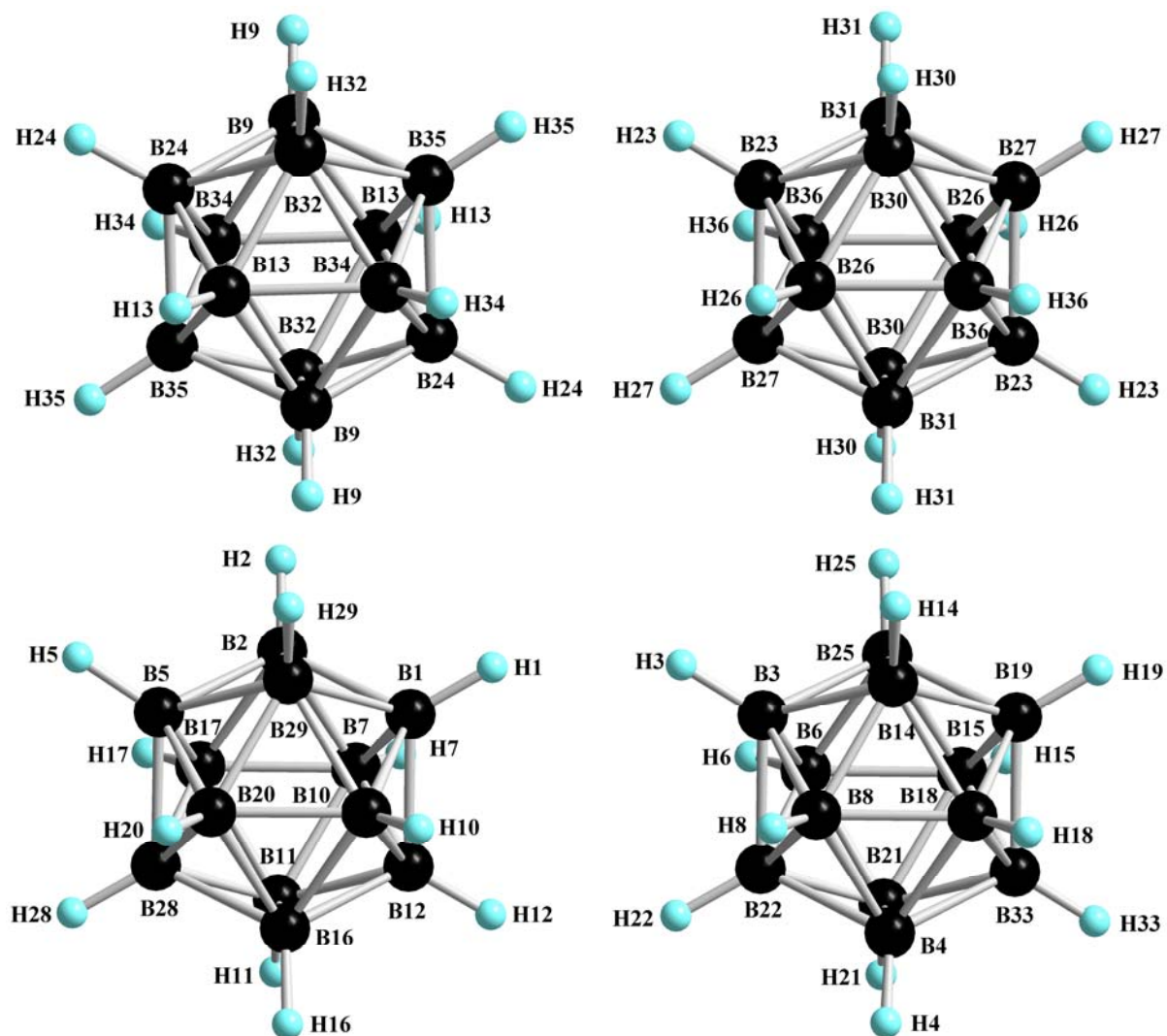


Fig. 51: View of the four crystallographic distinct *quasi*-icosahedral $[\text{B}_{12}\text{H}_{12}]^{2-}$ -cluster anions in the crystal structure of $[\text{La}(\text{H}_2\text{O})_9]_2[\text{B}_{12}\text{H}_{12}]_3 \cdot 7 \text{H}_2\text{O}$ (*top left*: center of gravity at $x/a = y/b = 1/2$, $z/c = 0$; *top right*: center of gravity at $x/a = 0$, $y/b = z/c = 1/2$; *bottom left*: center of gravity at $x/a \approx 0.446$, $y/b \approx 0.845$, $z/c \approx 0.226$; *bottom right*: center of gravity at $x/a \approx 0.091$, $y/b \approx 0.102$, $z/c \approx 0.303$)

Table 47: Crystallographic data for $[\text{La}(\text{H}_2\text{O})_9]_2[\text{B}_{12}\text{H}_{12}]_3 \cdot 7 \text{H}_2\text{O}$ and their determination

Crystal system	triclinic
Space group	$P\bar{1}$ (no. 2)
Unit cell parameters:	
a (pm)	1186.54(6)
b (pm)	1277.09(7)
c (pm)	1789.15(9)
α (deg)	70.492(3)
β (deg)	85.201(3)
γ (deg)	87.633(3)
Number of formula units per unit cell	$Z = 2$
Calculated density ($D_x/\text{g cm}^{-3}$)	1.505
Molar volume ($V_m/\text{cm}^3 \text{ mol}^{-1}$)	766.7
Diffractometer	κ -CCD (Bruker-Nonius)
Measuring temperature (T/K)	100(2)
Radiation	Mo-K α : $\lambda = 71.07$ pm, graphite monochromator
Index range	$\pm h_{\max} = 15, \pm k_{\max} = 17, \pm l_{\max} = 23$
θ_{\max} (deg)	28.3
F(000)	1160
Absorption coefficient (μ/mm^{-1})	1.72
Absorption correction	numerical, Program X-SHAPE [64]
Other data corrections	background, polarization and <i>Lorentz</i> factors
Collected reflections	83565
Unique reflections	12609
$R_{\text{int}}, R_{\sigma}$	0.041, 0.022
Structure solution and refinement	Program SHELXS-97 and SHELXL-97 [68]
Scattering factors	International Tables for Crystallography, Vol. C [87]
R_1, R_1 with $ F_o \geq 4\sigma(F_o)$	0.022, 0.019
Reflections with $ F_o \geq 4\sigma(F_o)$	1434
wR_2 , Goodness of fit (GooF)	0.040, 1.061
Extinction (g)	0.002(1)
Residual electron density (<i>max.</i> , <i>min.</i> in $\rho/e^{-1} 10^6$ pm)	0.53, -0.62

Table 48: Atomic coordinates for $[\text{La}(\text{H}_2\text{O})_9]_2[\text{B}_{12}\text{H}_{12}]_3 \cdot 7 \text{H}_2\text{O}$

Atom	Wyckoff position	x/a	y/b	z/c
La1	2i	0.98329(1)	0.74617(1)	0.11501(1)
La2	2i	0.41139(1)	0.25102(1)	0.28323(1)
O1	2i	0.1989(1)	0.2441(1)	0.4127(1)
O2	2i	0.0945(1)	0.2253(1)	0.9802(1)
O3	2i	0.8428(1)	0.8015(1)	0.2085(1)
O4	2i	0.0297(1)	0.9455(1)	0.0961(1)
O5	2i	0.8482(1)	0.8712(1)	0.0159(1)
O6	2i	0.5357(1)	0.3912(1)	0.2795(1)
O7	2i	0.0685(1)	0.7669(1)	0.2371(1)
O8	2i	0.9960(1)	0.5560(1)	0.2193(1)
O9	2i	0.7944(1)	0.6422(1)	0.1368(1)
O10	2i	0.3220(1)	0.3080(1)	0.2545(1)
O11	2i	0.3233(1)	0.0656(1)	0.3919(1)
O12	2i	0.5176(1)	0.1706(1)	0.2827(1)
O13	2i	0.5489(1)	0.3248(1)	0.4524(1)
O14	2i	0.1910(1)	0.6817(1)	0.1161(1)
O15	2i	0.9874(1)	0.6153(1)	0.0387(1)
O16	2i	0.3504(1)	0.1803(1)	0.5331(1)
O17	2i	0.5543(1)	0.0970(1)	0.4515(1)
O18	2i	0.3487(1)	0.4519(1)	0.3664(1)
O1w	2i	0.2865(1)	0.9861(1)	0.9721(1)
O2w	2i	0.8694(1)	0.4188(1)	0.0800(1)
O3w	2i	0.7406(1)	0.4748(1)	0.2806(1)
O4w	2i	0.1336(1)	0.4038(1)	0.1746(1)
O5w	2i	0.7237(1)	0.1868(1)	0.5214(1)
O6w	2i	0.7540(1)	0.8016(1)	0.9121(1)
O7w	2i	0.6318(1)	0.8539(1)	0.4043(1)
B1	2i	0.4620(1)	0.8867(1)	0.3051(1)
B2	2i	0.3928(1)	0.9721(1)	0.2208(1)
B3	2i	0.8136(1)	0.1806(1)	0.2405(1)
B4	2i	0.8981(1)	0.9616(1)	0.3274(1)
B5	2i	0.3249(1)	0.8838(1)	0.1806(1)

Table 48: (continued)

Atom	Wyckoff position	x/a	y/b	z/c
B6	2i	0.9593(1)	0.1712(1)	0.2091(1)
B7	2i	0.5415(1)	0.9464(1)	0.2120(1)
B8	2i	0.7765(1)	0.0509(1)	0.3144(1)
B9	2i	0.5844(1)	0.4633(1)	0.0764(1)
B10	2i	0.4356(1)	0.7451(1)	0.3174(1)
B11	2i	0.5640(1)	0.8408(1)	0.1673(1)
B12	2i	0.5676(1)	0.8062(1)	0.2724(1)
B13	2i	0.4431(1)	0.5130(1)	0.0872(1)
B14	2i	0.8060(1)	0.1671(1)	0.3427(1)
B15	2i	0.0404(1)	0.1518(1)	0.2920(1)
B16	2i	0.4999(1)	0.7169(1)	0.2321(1)
B17	2i	0.4564(1)	0.9445(1)	0.1352(1)
B18	2i	0.8580(1)	0.0316(1)	0.3970(1)
B19	2i	0.9457(1)	0.1493(1)	0.3753(1)
B20	2i	0.3520(1)	0.7435(1)	0.2403(1)
B21	2i	0.0113(1)	0.0366(1)	0.2624(1)
B22	2i	0.8706(1)	0.0543(1)	0.2306(1)
B23	2i	0.9555(1)	0.5795(1)	0.4111(1)
B24	2i	0.6385(1)	0.5296(1)	0.9766(1)
B25	2i	0.9188(1)	0.2409(1)	0.2783(1)
B26	2i	0.9008(1)	0.4442(1)	0.4620(1)
B27	2i	0.0431(1)	0.4605(1)	0.4210(1)
B28	2i	0.4306(1)	0.8027(1)	0.1472(1)
B29	2i	0.3276(1)	0.8483(1)	0.2853(1)
B30	2i	0.1310(1)	0.4451(1)	0.5001(1)
B31	2i	0.0091(1)	0.3607(1)	0.5170(1)
B32	2i	0.5896(1)	0.3903(1)	0.0066(1)
B33	2i	0.0033(1)	0.0222(1)	0.3656(1)
B34	2i	0.5489(1)	0.6050(1)	0.0265(1)
B35	2i	0.4691(1)	0.3800(1)	0.0747(1)
B36	2i	0.9007(1)	0.4199(1)	0.5661(1)
H1A	2i	0.160(2)	0.268(2)	0.441(1)

Table 48: (continued)

Atom	Wyckoff position	x/a	y/b	z/c
H1B	2i	0.164(2)	0.225(2)	0.388(1)
H2A	2i	0.151(2)	0.860(2)	0.973(1)
H2B	2i	0.082(2)	0.825(2)	0.940(1)
H3A	2i	0.777(2)	0.799(2)	0.209(1)
H3B	2i	0.855(2)	0.831(2)	0.234(1)
H4A	2i	0.060(2)	0.999(2)	0.060(1)
H4B	2i	0.026(2)	0.963(2)	0.128(1)
H5A	2i	0.804(2)	0.913(2)	0.029(1)
H5B	2i	0.821(2)	0.846(2)	-0.014(1)
H6A	2i	0.521(2)	0.420(2)	0.234(1)
H6B	2i	0.598(2)	0.410(2)	0.284(1)
H7A	2i	0.119(2)	0.802(2)	0.236(1)
H7B	2i	0.049(2)	0.731(2)	0.282(1)
H8A	2i	0.035(2)	0.510(2)	0.208(1)
H8B	2i	0.993(2)	0.543(2)	0.263(1)
H9A	2i	0.785(2)	0.595(2)	0.1768(1)
H9B	2i	0.741(2)	0.664(2)	0.116(1)
H10A	2i	0.357(2)	0.306(2)	0.219(1)
H10B	2i	0.266(2)	0.338(2)	0.240(1)
H11A	2i	0.272(2)	0.040(2)	0.414(1)
H11B	2i	0.339(2)	0.036(2)	0.367(1)
H12A	2i	0.503(2)	0.121(2)	0.274(1)
H12B	2i	0.578(2)	0.194(2)	0.264(1)
H13A	2i	0.598(2)	0.286(2)	0.475(1)
H13B	2i	0.572(2)	0.391(2)	0.440(1)
H14A	2i	0.227(2)	0.678(2)	0.153(1)
H14B	2i	0.229(2)	0.678(2)	0.085(1)
H15A	2i	0.950(2)	0.562(2)	0.056(1)
H15B	2i	0.033(2)	0.610(2)	0.007(1)
H16A	2i	0.292(2)	0.149(2)	0.551(1)
H16B	2i	0.387(2)	0.179(2)	0.564(1)
H17A	2i	0.608(2)	0.110(2)	0.472(1)

Table 48: (continued)

Atom	Wyckoff position	x/a	y/b	z/c
H17B	2i	0.543(2)	0.054(2)	0.450(1)
H18A	2i	0.378(2)	0.501(2)	0.338(1)
H18B	2i	0.295(2)	0.470(2)	0.383(1)
H1w1	2i	0.326(2)	0.959(2)	0.934(1)
H1w2	2i	0.320(2)	0.924(2)	0.006(1)
H2w1	2i	0.806(2)	0.430(2)	0.073(1)
H2w2	2i	0.874(2)	0.374(2)	0.119(1)
H3w1	2i	0.724(2)	0.505(2)	0.316(1)
H3w2	2i	0.788(2)	0.431(2)	0.295(1)
H4w1	2i	0.167(2)	0.430(2)	0.128(1)
H4w2	2i	0.103(2)	0.344(2)	0.176(1)
H5w1	2i	0.733(2)	0.188(2)	0.562(1)
H5w2	2i	0.786(2)	0.191(2)	0.499(1)
H6w1	2i	0.698(2)	0.766(2)	0.929(1)
H6w2	2i	0.738(2)	0.850(2)	0.880(1)
H7w1	2i	0.589(2)	0.593(2)	0.392(1)
H7w2	2i	0.680(2)	0.561(2)	0.431(1)
H1	2i	0.472(1)	0.911(1)	0.356(1)
H2	2i	0.357(1)	0.056(1)	0.217(1)
H3	2i	0.751(1)	0.231(1)	0.201(1)
H4	2i	0.890(1)	0.872(1)	0.341(1)
H5	2i	0.242(1)	0.911(1)	0.152(1)
H6	2i	0.996(1)	0.218(1)	0.145(1)
H7	2i	0.602(1)	0.011(1)	0.202(1)
H8	2i	0.690(1)	0.017(1)	0.325(1)
H9	2i	0.636(1)	0.438(1)	0.125(1)
H10	2i	0.428(1)	0.679(1)	0.376(1)
H11	2i	0.641(1)	0.838(1)	0.129(1)
H12	2i	0.645(1)	0.782(1)	0.304(1)
H13	2i	0.405(1)	0.522(1)	0.143(1)
H14	2i	0.738(1)	0.213(1)	0.368(1)
H15	2i	0.127(1)	0.185(1)	0.282(1)

Table 48: (continued)

Atom	Wyckoff position	x/a	y/b	z/c
H16	2 <i>i</i>	0.538(1)	0.631(1)	0.236(1)
H17	2 <i>i</i>	0.463(1)	0.007(1)	0.077(1)
H18	2 <i>i</i>	0.826(1)	-0.015(1)	0.459(1)
H19	2 <i>i</i>	0.970(1)	0.179(1)	0.421(1)
H20	2 <i>i</i>	0.294(1)	0.674(1)	0.251(1)
H21	2 <i>i</i>	0.080(1)	-0.003(1)	0.235(1)
H22	2 <i>i</i>	0.841(1)	0.025(1)	0.185(1)
H23	2 <i>i</i>	0.925(1)	0.628(1)	0.385(1)
H24	2 <i>i</i>	0.731(1)	0.550(1)	0.961(1)
H25	2 <i>i</i>	0.924(1)	0.333(1)	0.261(1)
H26	2 <i>i</i>	0.835(1)	0.408(1)	0.437(1)
H27	2 <i>i</i>	0.070(1)	0.434(1)	0.371(1)
H28	2 <i>i</i>	0.419(1)	0.778(1)	0.095(1)
H29	2 <i>i</i>	0.251(1)	0.852(1)	0.321(1)
H30	2 <i>i</i>	0.218(1)	0.410(1)	0.499(1)
H31	2 <i>i</i>	0.021(1)	0.269(1)	0.527(1)
H32	2 <i>i</i>	0.649(1)	0.317(1)	0.012(1)
H33	2 <i>i</i>	0.064(1)	-0.027(1)	0.405(1)
H34	2 <i>i</i>	0.583(1)	0.672(1)	0.043(1)
H35	2 <i>i</i>	0.450(1)	0.301(1)	0.122(1)
H36	2 <i>i</i>	0.834(1)	0.368(1)	0.610(1)

Table 49: Anisotropic thermal displacement coefficients^{a)} (U_{ij}/pm^2) for $[\text{La}(\text{H}_2\text{O})_9]_2[\text{B}_{12}\text{H}_{12}]_3 \cdot 7 \text{H}_2\text{O}$

Atom	U_{11}	U_{22}	U_{33}	U_{23}	U_{13}	U_{12}
La1	52(1)	52(1)	52(1)	-17(1)	-1(1)	-5(1)
La2	61(1)	65(1)	59(1)	-10(1)	-1(1)	-4(1)
O1	84(6)	168(6)	180(6)	-108(5)	-4(5)	6(5)
O2	138(6)	151(6)	79(6)	-28(5)	-1(5)	-43(5)
O3	77(6)	193(6)	176(6)	-120(5)	2(5)	-10(5)
O4	182(6)	84(6)	84(6)	-28(5)	19(5)	-35(5)
O5	101(6)	149(6)	116(6)	-41(5)	-21(5)	-2(5)
O6	158(6)	195(6)	96(6)	-22(5)	3(5)	-87(5)
O7	96(6)	130(6)	88(6)	-25(5)	-14(4)	-33(5)
O8	154(6)	104(6)	102(6)	-23(5)	-11(5)	3(5)
O9	96(6)	123(6)	144(6)	-95(5)	-17(5)	-24(5)
O10	98(6)	238(7)	101(6)	-44(5)	4(5)	-3(5)
O11	161(7)	123(6)	260(7)	-96(5)	74(5)	-25(5)
O12	129(6)	160(6)	220(7)	-108(5)	14(5)	-3(5)
O13	212(7)	238(7)	153(7)	-22(6)	-76(5)	-66(6)
O14	86(6)	231(7)	102(6)	-70(5)	-12(5)	16(5)
O15	170(6)	145(6)	151(6)	-90(5)	73(5)	-79(5)
O16	164(7)	312(8)	97(6)	-13(5)	-7(5)	-84(6)
O17	247(7)	155(7)	207(7)	18(5)	-26(6)	31(6)
O18	182(7)	108(6)	240(7)	-37(5)	-73(6)	4(5)
O1w	116(6)	200(7)	142(7)	-10(5)	8(5)	-23(5)
O2w	97(6)	122(6)	126(6)	-5(5)	12(5)	8(5)
O3w	140(6)	203(7)	215(7)	-14(6)	-2(5)	-13(5)
O4w	156(6)	164(7)	193(7)	-7(5)	29(5)	-1(5)
O5w	189(7)	385(9)	120(7)	-111(6)	-3(6)	-81(6)
O6w	300(8)	212(8)	250(8)	-6(6)	-151(7)	-75(6)
O7w	243(7)	195(7)	354(8)	-97(6)	-164(6)	32(6)
B1	77(8)	126(8)	93(8)	-56(7)	-21(6)	3(6)
B2	100(8)	99(8)	97(8)	-49(6)	-22(6)	11(6)
B3	77(8)	83(8)	121(8)	-26(7)	-2(6)	9(6)
B4	142(9)	86(8)	101(8)	-19(7)	-25(7)	-32(6)
B5	69(8)	115(8)	73(8)	-23(6)	-13(6)	4(6)

Table 49: (continued)

Atom	U ₁₁	U ₂₂	U ₃₃	U ₂₃	U ₁₃	U ₁₂
B6	93(8)	105(8)	96(8)	-23(7)	1(6)	3(6)
B7	86(8)	111(8)	106(8)	-34(7)	-13(6)	-22(6)
B8	96(8)	95(8)	95(8)	-11(6)	-5(6)	-25(6)
B9	101(8)	149(9)	92(8)	-37(7)	-5(6)	21(7)
B10	87(8)	114(8)	84(8)	-16(6)	-17(6)	1(6)
B11	65(8)	125(8)	113(8)	-39(7)	2(6)	6(6)
B12	72(8)	129(8)	97(8)	-39(7)	-23(6)	15(6)
B13	108(8)	128(9)	85(8)	-38(7)	18(6)	10(6)
B14	100(8)	111(8)	111(8)	-42(7)	26(7)	-19(7)
B15	89(8)	134(9)	105(8)	-48(7)	-6(6)	-18(7)
B16	95(8)	93(8)	112(8)	-44(7)	-6(6)	6(6)
B17	75(8)	113(8)	88(8)	-25(7)	-8(6)	-4(7)
B18	133(9)	133(9)	85(8)	-20(7)	4(7)	-27(7)
B19	137(9)	160(9)	95(8)	-79(7)	9(7)	-38(7)
B20	94(8)	106(8)	95(8)	-29(7)	-13(6)	-17(6)
B21	106(8)	104(8)	107(8)	-46(7)	-9(6)	14(6)
B22	113(8)	84(8)	98(8)	-31(7)	-23(6)	1(6)
B23	125(8)	96(8)	76(8)	-9(6)	-4(6)	21(7)
B24	104(8)	147(9)	82(8)	-34(7)	14(6)	5(7)
B25	109(8)	95(8)	125(8)	-47(7)	23(7)	-22(6)
B26	163(9)	111(9)	133(9)	-30(7)	-60(7)	-3(7)
B27	164(9)	175(9)	95(8)	-68(7)	-22(7)	77(7)
B28	83(8)	149(9)	92(8)	-61(7)	-1(6)	-20(7)
B29	70(8)	125(8)	83(8)	-42(7)	-6(6)	-5(6)
B30	121(8)	172(9)	85(8)	-29(7)	-20(7)	51(7)
B31	214(9)	95(8)	132(9)	-36(7)	-65(7)	20(7)
B32	110(8)	126(8)	87(8)	-30(7)	14(6)	29(7)
B33	113(8)	138(9)	108(8)	-30(7)	-27(7)	-4(7)
B34	95(8)	137(9)	99(8)	-46(7)	5(6)	7(7)
B35	111(8)	117(8)	84(8)	-13(7)	8(6)	15(7)
B36	128(9)	173(9)	108(9)	13(7)	-5(6)	-20(7)

Table 49: (continued)

Atom	U_{iso}	Atom	U_{iso}	Atom	U_{iso}
H1A	388(78)	H15B	315(69)	H9	126(49)
H1B	534(98)	H16A	560(94)	H10	182(53)
H2A	301(68)	H16B	401(82)	H11	161(52)
H2B	329(75)	H17A	1033(161)	H12	125(49)
H3A	364(75)	H17B	2072(360)	H13	126(49)
H3B	422(86)	H18A	483(91)	H14	201(55)
H4A	316(69)	H18B	452(88)	H15	187(54)
H4B	433(87)	H1w1	373(78)	H16	224(57)
H5A	364(73)	H1w2	400(83)	H17	111(48)
H5B	328(69)	H2w1	276(66)	H18	310(64)
H6A	383(77)	H2w2	338(76)	H19	179(53)
H6B	368(74)	H3w1	277(65)	H20	86(46)
H7A	569(98)	H3w2	385(80)	H21	216(57)
H7B	543(94)	H4w1	483(83)	H22	138(50)
H8A	285(67)	H4w2	513(90)	H23	175(53)
H8B	373(78)	H5w1	380(80)	H24	149(51)
H9A	252(63)	H5w2	446(85)	H25	190(54)
H9B	313(72)	H6w1	613(106)	H26	205(55)
H10A	300(70)	H6w2	739(122)	H27	170(52)
H10B	316(71)	H7w1	729(113)	H28	112(48)
H11A	880(144)	H7w2	787(119)	H29	143(50)
H11B	848(150)	H1	113(48)	H30	171(52)
H12A	824(134)	H2	128(49)	H31	170(52)
H12B	818(133)	H3	206(55)	H32	201(55)
H13A	303(71)	H4	148(51)	H33	184(53)
H13B	744(15)	H5	127(49)	H34	138(50)
H14A	322(70)	H6	132(49)	H35	210(56)
H14B	434(89)	H7	195(54)	H36	234(58)
H15A	321(69)	H8	190(54)		

^{a)} For La, O and B defined as anisotropic temperature factor according to: $\exp[-2\pi^2 (U_{11}h^2a^{*2} + U_{22}k^2b^{*2} + U_{33}l^2c^{*2} + 2U_{23}klb^{*}c^{*} + 2U_{13}hla^{*}c^{*} + 2U_{13}hka^{*}b^{*})]$; for H isotropically defined as temperature factor in: $\exp[-8\pi^2(U_{iso}\sin^2\theta/\lambda^2)]$.

Table 50: Selected interatomic distances (d/pm) for $[\text{La}(\text{H}_2\text{O})_9]_2[\text{B}_{12}\text{H}_{12}]_3 \cdot 7 \text{H}_2\text{O}$

[LaO ₉] polyhedra:					
La1 – O15	248.4			La2 – O10	248.8
– O3	251.1			– O13	251.5
– O8	252.9			– O6	252.2
– O4	253.2			– O1	253.1
– O14	256.7			– O18	256.7
– O2	256.7			– O12	257.5
– O7	257.8			– O16	257.7
– O5	258.1			– O11	258.1
– O9	258.9			– O17	259.1
[B ₁₂ H ₁₂] ²⁻ anions:					
B1 – B12	177.2	B2 – B5	177.8	B3 – B14	177.4
– B29	177.9	– B1	179.9	– B22	178.0
– B10	178.3	– B29	178.0	– B25	178.4
– B10	178.5	– B17	178.4	– B8	178.4
– B7	178.6	– B7	178.5	– B6	178.7
– H1	108.9	– H2	110.3	– H3	109.5
B4 – B21	178.1	B5 – B2	177.8	B6 – B22	177.8
– B8	178.3	– B29	177.8	– B25	177.8
– B18	178.8	– B17	177.9	– B15	177.9
– B22	178.8	– B28	178.4	– B21	177.9
– B33	178.9	– B20	178.6	– B3	178.7
– H4	109.5	– H5	111.3	– H6	114.0
B7 – B17	177.9	B8 – B14	177.6	B9 – B35	177.7
– B11	178.4	– B18	177.7	– B24	177.8
– B12	178.4	– B22	178.2	– B34	177.9
– B2	178.5	– B4	178.3	– B13	178.5
– B1	178.6	– B3	178.4	– B32	178.7
– H7	109.8	– H8	110.4	– H9	105.9

Table 50: (continued)

B10 – B20	177.2	B11 – B28	177.3	B12 – B1	177.2
– B29	178.4	– B16	177.6	– B7	178.4
– B1	178.5	– B7	178.4	– B10	178.5
– B12	178.5	– B17	178.4	– B11	178.7
– B16	178.9	– B12	178.7	– B16	178.7
– H10	110.5	– H11	109.2	– H12	109.5
B13 – B24	178.3	B14 – B25	176.8	B15 – B21	177.8
– B34	178.4	– B3	177.4	– B6	177.9
– B32	178.4	– B8	177.6	– B33	178.2
– B9	178.5	– B19	178.6	– B19	178.2
– B35	179.6	– B18	179.1	– B25	178.3
– H13	110.0	– H14	112.5	– H15	113.3
B16 – B11	177.6	B17 – B5	177.9	B18 – B8	177.7
– B20	177.8	– B7	177.9	– B19	177.9
– B12	178.7	– B2	178.4	– B33	178.1
– B10	178.9	– B11	178.4	– B4	178.8
– B28	179.1	– B28	178.6	– B14	179.1
– H16	112.8	– H17	107.1	– H18	110.1
B19 – B18	177.9	B20 – B10	177.2	B21 – B15	177.8
– B15	178.2	– B16	177.8	– B6	177.9
– B25	178.5	– B29	178.2	– B4	178.1
– B14	178.6	– B28	178.2	– B33	178.7
– B33	179.1	– B5	178.6	– B22	179.0
– H19	107.1	– H20	111.4	– H21	110.1
B22 – B6	177.8	B23 – B30	176.2	B24 – B9	177.8
– B3	178.0	– B27	177.0	– B35	178.1
– B8	178.2	– B26	178.3	– B13	178.3
– B4	178.8	– B31	178.6	– B34	178.4
– B21	179.0	– B36	178.8	– B32	178.7
– H22	110.0	– H23	103.1	– H24	116.8

Table 50: (continued)

B25	– B14	176.8	B26	– B27	177.4	B27	– B23	177.0
	– B6	177.9		– B31	177.7		– B26	177.4
	– B15	178.3		– B30	178.0		– B30	178.1
	– B3	178.4		– B23	178.3		– B36	178.3
	– B19	178.5		– B36	178.4		– B21	178.8
	– H25	111.7		– H26	112.6		– H27	110.2
B28	– B11	177.3	B29	– B5	177.8	B30	– B23	176.2
	– B20	178.2		– B2	178.0		– B26	178.0
	– B5	178.4		– B20	178.2		– B27	178.1
	– B17	178.6		– B1	178.3		– B31	178.2
	– B16	179.1		– B10	178.4		– B36	178.4
	– H28	110.4		– H29	107.9		– H30	111.9
B31	– B26	177.7	B32	– B35	177.7	B33	– B18	178.1
	– B36	178.1		– B13	178.4		– B15	178.2
	– B30	178.2		– B34	178.5		– B21	178.7
	– B23	178.6		– B9	178.7		– B4	178.9
	– B27	178.8		– B24	178.8		– B19	179.1
	– H31	110.8		– H32	112.5		– H33	109.1
B34	– B9	177.9	B35	– B9	177.7	B36	– B31	178.1
	– B13	178.4		– B32	177.7		– B27	178.3
	– B24	178.4		– B24	178.1		– B26	178.4
	– B32	178.5		– B34	178.5		– B30	178.4
	– B35	178.5		– B13	179.6		– B23	178.8
	– H34	110.5		– H35	109.2		– H36	113.1

3.3.6 Bis-Enneaqua-Praseodymium(III) and Bis-Enneaqua-Holmium(III) Tris-Dodecahydro-*closo*-Dodecaborate Pentadecahydrate

The syntheses and crystal structures of dodecahydro-*closo*-dodecaborate hydrates of rare-earth metals with the composition $[M(H_2O)_9]_2[B_{12}H_{12}]_3 \cdot 15 H_2O$ ($M = La$ and Eu), which crystallize trigonally in space group $R\bar{3}c$ (no. 167), have been published recently [85, 91]. These salts were prepared by neutralization reactions between the free acid $(H_3O)_2[B_{12}H_{12}]$ and rare-earth metal(III) oxides or hydroxides. Although it can be expected that the crystal structures of hydrated dodecahydro-*closo*-dodecaborate salts of other rare-earth metals are isostructural to those of $[M(H_2O)_9]_2[B_{12}H_{12}]_3 \cdot 15 H_2O$ ($M = La$ and Eu), the detailed crystallographic data of the whole lanthanoid series are not available in literature.

3.3.6.1 Synthesis of $[M(H_2O)_9]_2[B_{12}H_{12}]_3 \cdot 15 H_2O$ ($M = Pr$ and Ho)

The hydrated dodecahydro-*closo*-dodecaborate salts with praseodymium(III) and holmium(III) are prepared by the reaction of free acid $(H_3O)_2[B_{12}H_{12}]$ with Pr_6O_{11} (Merck: 99.9 %) and Ho_2O_3 (Merck: 99.9 %), respectively. Single crystals of both compounds were obtained by isothermal evaporation of the resulting aqueous filtrates at room temperature.

3.3.6.2 Structure Description of $[M(H_2O)_9]_2[B_{12}H_{12}]_3 \cdot 15 H_2O$ ($M = Pr$ and Ho)

The title compounds crystallize trigonally in space group $R\bar{3}c$ (no. 167) with six formula units per unit cell (Fig. 52, *left*). The rare-earth metal(III) cations are located at the crystallographic *Wyckoff* position $12c$ ($x/a = y/b = 0, z/c$; site symmetry: $3.$), while the oxygen atoms of water molecules occupy two crystallographically distinct *Wyckoff* sites: $1 \times 18e$ ($x/a, y/b = 0, z/c = 1/4$; site symmetry: $.2$) and $5 \times 36f$ ($x/a, y/b, z/c$; site symmetry: 1). The lanthanoid trications M^{3+} are coordinated by nine oxygen atoms from water molecules with the shape of a tricapped trigonal prism ($d(Pr-O) = 249 - 259$ pm, $d(Ho-O) = 217 - 241$ pm) (Fig. 53). All boron and hydrogen atoms of the $[B_{12}H_{12}]^{2-}$ cage reside in two compounds at the general *Wyckoff* site $36f$. The centers of gravity of the *quasi*-icosahedral $[B_{12}H_{12}]^{2-}$ cluster anions occupy two different *Wyckoff* positions: $6b$ ($x/a = y/b = z/c = 0$; site symmetry: $\bar{3}$) and $12c$ ($x/a = y/b = 0, z/c$). The distances from their centers of gravity to the twelve boron atoms are about 170 pm for both cluster anions providing them inner diameters of around 340

pm (Fig. 54). These crystal structures are isotopic to that one of the salts $[M(H_2O)_9]_2[B_{12}H_{12}]_3 \cdot 15 H_2O$ ($M = La$ and Eu) and can be described with two independent interpenetrating layered motifs, namely the $[M(H_2O)_9]^{3+}$ cations and the $[B_{12}H_{12}]^{2-}$ -cluster anions, as lattice components [85]. The arrangement of rare-earth metal trications exhibits a cubic closest packed fashion with the stacking sequence of *aa bb cc*, while the $[B_{12}H_{12}]^{2-}$ -cluster anions form a 9-layer stack *ABABCBCAC*, according to the α -Sm-type structure (Fig. 52, *right*). Each coordinating water molecule of the $[M(H_2O)_9]^{3+}$ cations connects to two other neighbouring “zeolitic” crystal water molecules via classical $O-H^{\delta+} \cdots \delta^-O$ hydrogen bonds with $d(O \cdots Ow) = 274 - 336$ pm and $257 - 303$ pm as donor-acceptor distances for $[Pr(H_2O)_9]_2[B_{12}H_{12}]_3 \cdot 15 H_2O$ and $[Ho(H_2O)_9]_2[B_{12}H_{12}]_3 \cdot 15 H_2O$, respectively. In addition, there are two types of non-classical $B-H^{\delta-} \cdots \delta^+H-O$ “dihydrogen bonds” existing in the title compounds between the negatively polarized hydrogen atoms of the $[B_{12}H_{12}]^{2-}$ -cluster anions and the positively polarized ones of water molecules coordinated to the M^{3+} cations ($d(H \cdots O) = 291 - 338$ pm for $[Pr(H_2O)_9]_2[B_{12}H_{12}]_3 \cdot 15 H_2O$ and $296 - 346$ pm for $[Ho(H_2O)_9]_2[B_{12}H_{12}]_3 \cdot 15 H_2O$) as well as those of the surrounding “zeolitic” crystal water molecules ($d(H \cdots Ow) = 272 - 326$ pm for $[Pr(H_2O)_9]_2[B_{12}H_{12}]_3 \cdot 15 H_2O$ and $278 - 329$ pm for $[Ho(H_2O)_9]_2[B_{12}H_{12}]_3 \cdot 15 H_2O$).

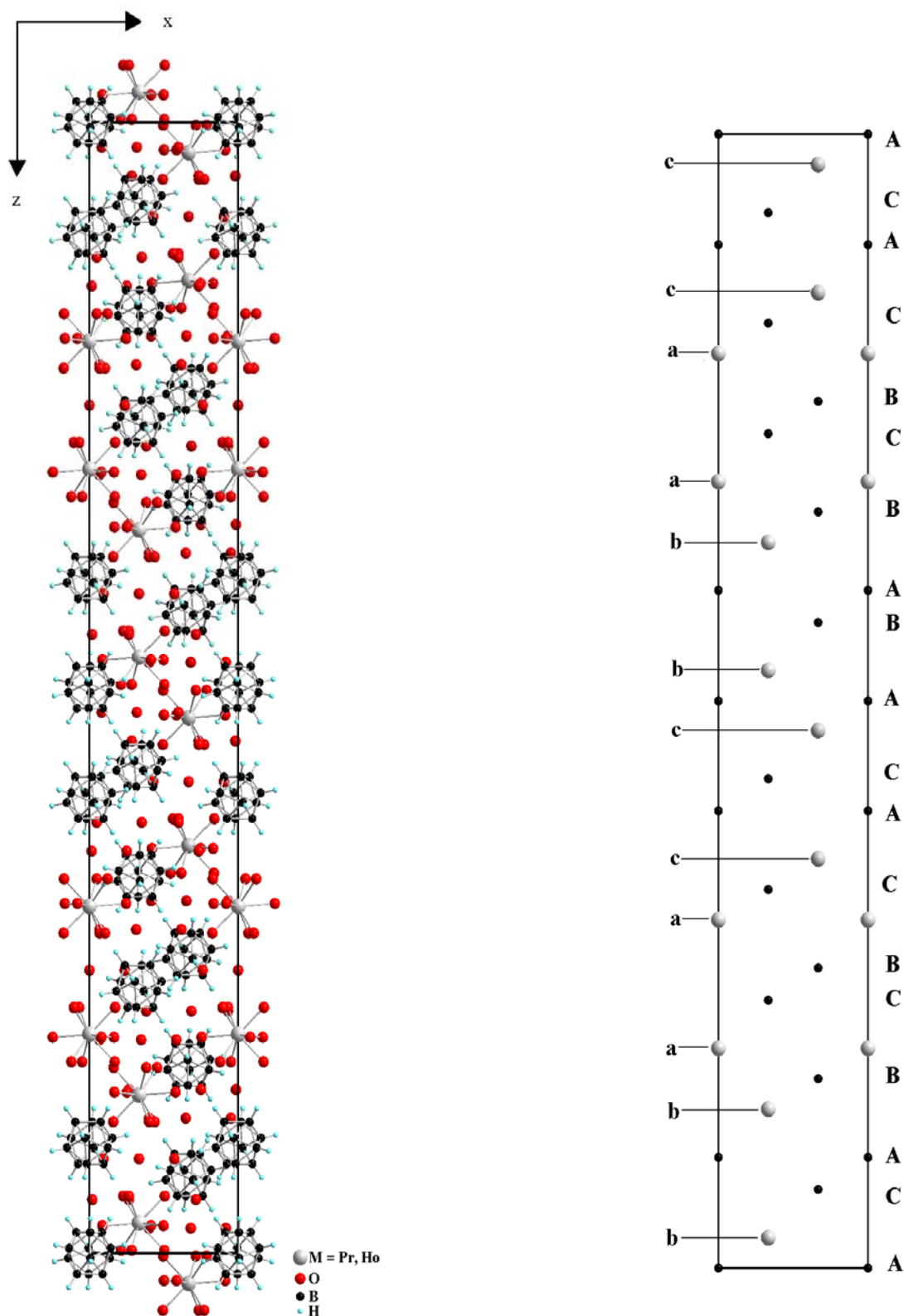


Fig. 52: Unit cell of the crystal structure of the salts $[M(\text{H}_2\text{O})_9]_2[\text{B}_{12}\text{H}_{12}]_3 \cdot 15 \text{H}_2\text{O}$ ($M = \text{Pr}$ and Ho) as viewed along $[010]$ (*left*) and the arrangement of the M^{3+} cations (grey spheres, stacking sequence: *aa bb cc*) and the centers of gravity of the $[\text{B}_{12}\text{H}_{12}]^{2-}$ cluster anions (black spheres, stacking sequence: *ABABCBCAC*) (*right*)

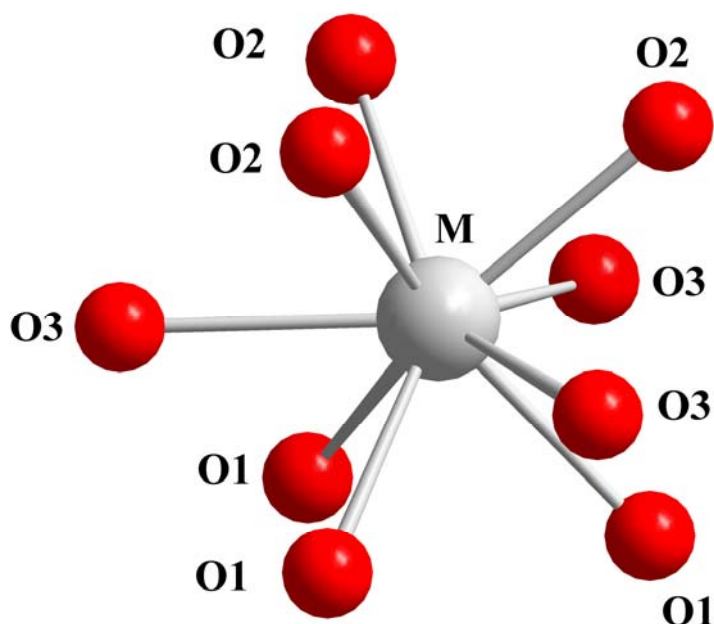


Fig. 53: View at the aqueous coordination spheres of the trications M^{3+} in the crystal structure of the salts $[M(H_2O)_9]_2[B_{12}H_{12}]_3 \cdot 15 H_2O$ ($M = Pr$ and Ho)

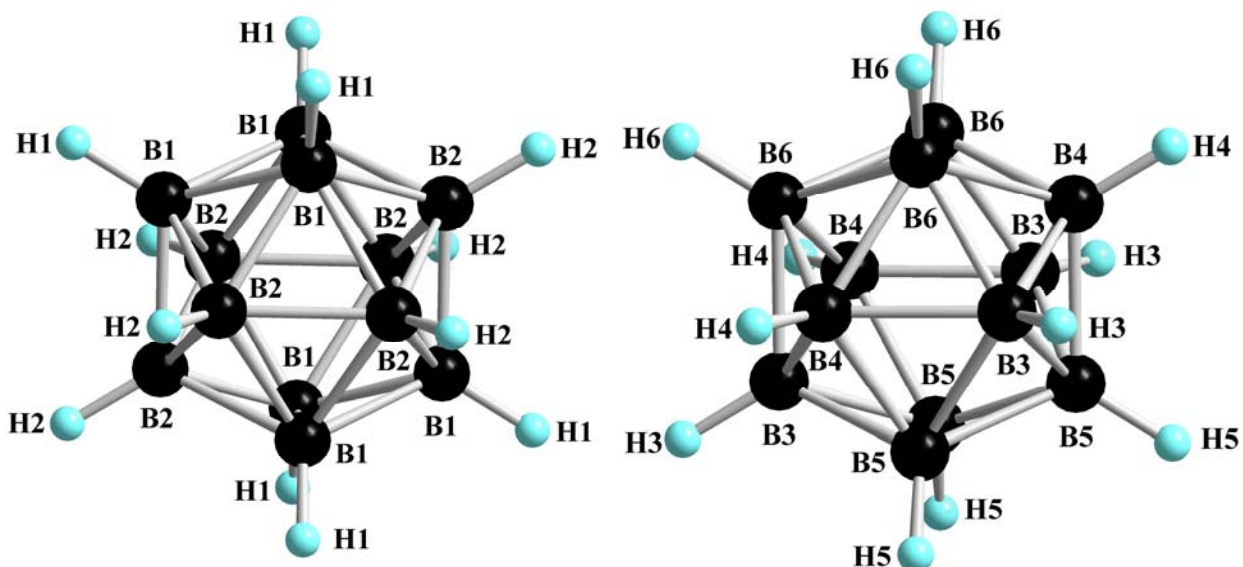


Fig. 54: View at the *quasi*-icosahedral $[B_{12}H_{12}]^{2-}$ -cluster anions with their centers of gravity at $6b$ ($x/a = y/b = z/c = 0$) (*left*) and at $12c$ ($x/a = y/b = 0, z/c$) (*right*) in the isotypic crystal structures of the salts $[M(H_2O)_9]_2[B_{12}H_{12}]_3 \cdot 15 H_2O$ ($M = Pr$ and Ho)

Table 51: Crystallographic data for the isotypic salts $[M(H_2O)_9]_2[B_{12}H_{12}]_3 \cdot 15 H_2O$ (M = Pr and Ho) and their determination

Crystallographic data	M = Pr	M = Ho
Crystal system	trigonal	
Space group	$R\bar{3}c$ (no. 167)	
Unit cell parameters:		
a (pm)	1187.80(2)	1172.65(2)
c (pm)	7290.76(9)	7204.12(9)
Number of formula units per unit cell	6	
Calculated density ($D_x/g\text{ cm}^{-3}$)	1.456	1.525
Molar volume ($V_m/\text{cm}^3\text{ mol}^{-1}$)	894.2	885.1
Diffractionmeter	κ -CCD (Bruker-Nonius)	
Measuring temperature (T/K)	100(2)	293(2)
Radiation	Mo-K α : $\lambda = 71.07$ pm, graphite monochromator	
Index range: $\pm h_{\max}, \pm k_{\max}, \pm l_{\max}$	15, 15, 96	15, 15, 98
θ_{\max} (deg)	27.9	28.3
F(000)	3984	4080
Absorption coefficient (μ/mm^{-1})	1.70	2.75
Absorption correction	numerical, Program X-SHAPE [64]	
Other data corrections	background, polarization and Lorentz factors	
Collected reflections	36554	39331
Unique reflections	2388	2442
$R_{\text{int}}, R_{\sigma}$	0.108, 0.038	0.073, 0.021
Structure solution and refinement	Program SHELXS-97 and SHELXL-97 [68]	
Scattering factors	International Tables for Crystallography, Vol. C [87]	
R_1, R_w with $ F_o \geq 4\sigma(F_o)$	0.104, 0.091	0.105, 0.088
Reflections with $ F_o \geq 4\sigma(F_o)$	2101	1989
wR_2 , Goodness of fit (GooF)	0.189, 1.263	0.237, 1.298
Extinction (g)	0.0001(1)	0.0011(3)
Residual electron density (<i>max.</i> , <i>min.</i> in $\rho/e^{-1} 10^6$ pm)	2.94, -1.97	3.26, -1.41

Table 52: Atomic coordinates for $[\text{Pr}(\text{H}_2\text{O})_9]_2[\text{B}_{12}\text{H}_{12}]_3 \cdot 15 \text{H}_2\text{O}$

Atom	Wyckoff position	x/a	y/b	z/c
Pr	12 <i>c</i>	0	0	0.19349(1)
O1	36 <i>f</i>	0.0485(7)	0.1703(7)	0.1691(2)
O2	36 <i>f</i>	0.0679(6)	0.1722(6)	0.2169(2)
O3	36 <i>f</i>	0.2459(6)	0.1654(6)	0.1910(1)
O4w	18 <i>e</i>	0.2374(8)	0	$\frac{1}{4}$
O5w	36 <i>f</i>	0.0182(7)	0.2847(6)	0.4527(1)
O6w	36 <i>f</i>	0.0680(6)	0.4162(6)	0.3111(1)
B1	36 <i>f</i>	0.0887(9)	0.0840(9)	0.0179(1)
B2	36 <i>f</i>	0.0058(8)	0.1428(8)	0.0040(1)
B3	36 <i>f</i>	0.0768(9)	0.0951(9)	0.0795(1)
B4	36 <i>f</i>	0.1227(9)	0.1525(9)	0.1017(1)
B5	36 <i>f</i>	0.0942(8)	0.0155(8)	0.1162(1)
B6	36 <i>f</i>	0.1509(9)	0.0274(9)	0.0932(1)
H1 ^{a)}	36 <i>f</i>	0.146	0.138	0.031
H2 ^{a)}	36 <i>f</i>	0.087	0.237	0.006
H3 ^{a)}	36 <i>f</i>	0.127	0.158	0.069
H4 ^{a)}	36 <i>f</i>	0.201	0.253	0.104
H5 ^{a)}	36 <i>f</i>	0.155	0.032	0.129
H6 ^{a)}	36 <i>f</i>	0.251	0.046	0.091

^{a)} refinement with DFIX constraint ($d(\text{B}-\text{H}) = 110 \text{ pm}$); $U_{\text{iso}}(\text{H}) = 1.2 \cdot U_{\text{iso}}(\text{B})$.

Table 53: Atomic coordinates for $[\text{Ho}(\text{H}_2\text{O})_9]_2[\text{B}_{12}\text{H}_{12}]_3 \cdot 15 \text{H}_2\text{O}$

Atom	Wyckoff position	x/a	y/b	z/c
Ho	12 <i>c</i>	0	0	0.19832(1)
O1	36 <i>f</i>	0.0812(8)	0.1642(8)	0.2117(2)
O2	36 <i>f</i>	0.1043(8)	0.2058(8)	0.1902(2)
O3	36 <i>f</i>	0.2281(8)	0.1390(8)	0.1943(2)
O4w	18 <i>e</i>	0.2310(6)	0	$\frac{1}{4}$
O5w	36 <i>f</i>	0.0250(6)	0.2851(5)	0.4518(1)
O6w	36 <i>f</i>	0.0868(4)	0.4284(5)	0.3154(1)
B1	36 <i>f</i>	0.0928(6)	0.0819(6)	0.0183(1)
B2	36 <i>f</i>	0.0170(6)	0.1503(6)	0.0043(1)
B3	36 <i>f</i>	0.0796(6)	0.0951(6)	0.0803(1)
B4	36 <i>f</i>	0.1264(6)	0.1530(6)	0.1029(1)
B5	36 <i>f</i>	0.0953(6)	0.0154(6)	0.1167(1)
B6	36 <i>f</i>	0.1538(6)	0.0274(6)	0.0941(1)
H1 ^{a)}	36 <i>f</i>	0.153	0.135	0.031
H2 ^{a)}	36 <i>f</i>	0.029	0.248	0.007
H3 ^{a)}	36 <i>f</i>	0.132	0.157	0.069
H4 ^{a)}	36 <i>f</i>	0.208	0.252	0.106
H5 ^{a)}	36 <i>f</i>	0.156	0.025	0.128
H6 ^{a)}	36 <i>f</i>	0.253	0.045	0.091

^{a)} refinement with DFIX constraint ($d(\text{B-H}) = 110 \text{ pm}$); $U_{\text{iso}}(\text{H}) = 1.2 \cdot U_{\text{iso}}(\text{B})$.

Table 54: Anisotropic thermal displacement coefficients^{a)} (U_{ij}/pm^2) for $[\text{Pr}(\text{H}_2\text{O})_9]_2[\text{B}_{12}\text{H}_{12}]_3 \cdot 15 \text{H}_2\text{O}$

Atom	U_{11}	U_{22}	U_{33}	U_{23}	U_{13}	U_{12}
Pr	130(3)	= U_{11}	230(4)	0	0	= $\frac{1}{2} U_{11}$
O1	267(34)	288(35)	264(33)	99(28)	53(27)	147(29)
O2	185(34)	249(34)	294(32)	-117(27)	38(28)	51(27)
O3	183(31)	166(29)	249(31)	-83(24)	-25(25)	79(26)
O4w	153(28)	209(43)	104(35)	21(31)	= $\frac{1}{2} U_{23}$	= $\frac{1}{2} U_{22}$
O5w	192(32)	137(30)	210(30)	-62(24)	-35(25)	90(25)
O6w	175(32)	218(32)	227(32)	78(25)	105(26)	106(28)
B1	131(40)	99(39)	151(41)	-87(32)	-68(33)	65(34)
B2	157(39)	101(39)	98(36)	17(27)	17(32)	77(33)
B3	125(43)	108(40)	102(42)	-14(34)	11(32)	48(32)
B4	109(38)	96(38)	88(33)	-49(29)	18(29)	36(33)
B5	72(37)	61(37)	167(38)	24(29)	19(31)	25(32)
B6	110(41)	157(42)	117(38)	-13(33)	22(32)	81(36)
H1	152					
H2	99					
H3	169					
H4	104					
H5	123					
H6	144					

^{a)} For Pr, O and B defined as anisotropic temperature factor according to: $\exp[-2\pi^2(U_{11}h^2a^{*2} + U_{22}k^2b^{*2} + U_{33}l^2c^{*2} + 2U_{23}klb^{*}c^{*} + 2U_{13}hla^{*}c^{*} + 2U_{13}hka^{*}b^{*})]$; for H isotropically defined as temperature factor in: $\exp[-8\pi^2(U_{\text{iso}}\sin^2\theta/\lambda^2)]$.

Table 55: Anisotropic thermal displacement coefficients^{a)} (U_{ij}/pm^2) for $[\text{Ho}(\text{H}_2\text{O})_9]_2[\text{B}_{12}\text{H}_{12}]_3 \cdot 15 \text{H}_2\text{O}$

Atom	U_{11}	U_{22}	U_{33}	U_{23}	U_{13}	U_{12}
Ho	485(6)	= U_{11}	870(8)	0	0	= $\frac{1}{2} U_{11}$
O1	1294(101)	1056(99)	1543(91)	-174(71)	302(49)	264(50)
O2	1314(104)	1001(125)	2305(197)	266(111)	-521(126)	-69(87)
O3	1007(81)	1372(77)	2762(199)	-231(144)	157(76)	459(64)
O4w	623(27)	1192(56)	1174(58)	501(51)	= $\frac{1}{2} U_{23}$	= $\frac{1}{2} U_{22}$
O5w	711(27)	528(23)	749(25)	-73(19)	-197(22)	366(23)
O6w	581(26)	707(30)	775(27)	111(24)	261(22)	298(23)
B1	417(37)	403(32)	257(24)	-7(27)	-8(27)	205(35)
B2	448(41)	421(37)	295(29)	11(26)	29(27)	227(32)
B3	479(43)	486(48)	366(33)	51(32)	50(31)	253(38)
B4	381(41)	407(42)	488(41)	-7(34)	-18(33)	149(35)
B5	383(41)	462(43)	439(37)	-26(32)	-18(31)	206(39)
B6	355(38)	454(43)	450(36)	18(31)	-11(29)	199(34)
H1	473					
H2	455					
H3	536					
H4	542					
H5	521					
H6	514					

^{a)} For Ho, O and B defined as anisotropic temperature factor according to: $\exp[-2\pi^2(U_{11}h^2a^{*2} + U_{22}k^2b^{*2} + U_{33}l^2c^{*2} + 2U_{23}klb^{*}c^{*} + 2U_{13}hla^{*}c^{*} + 2U_{13}hka^{*}b^{*})]$; for H isotropically defined as temperature factor in: $\exp[-8\pi^2(U_{\text{iso}}\sin^2\theta/\lambda^2)]$.

Table 56: Selected interatomic distances (d/pm) for the isotypic salts $[M(H_2O)_9]_2[B_{12}H_{12}]_3 \cdot 15 H_2O$ (M = Pr and Ho)[PrO₉] polyhedron:

Pr – O1	252.4 (3×)
– O2	249.4 (3×)
– O3	258.7 (3×)

[B₁₂H₁₂]²⁻ anion:

B1 – B2	176.9	B2 – B1	176.8
– B2'	177.3	– B2'	177.4
– B1	178.1 (2×)	– B1'	177.8 (2×)
– B2''	179.0	– B1''	179.0
– H1	110.0	– H2	110.0
B3 – B4	177.3	B4 – B6	175.3
– B6	177.5	– B3	177.3
– B6'	179.2	– B5	177.7
– B3''	180.5	– B5'	178.4
– H3	110.0	– B6	179.2
		– H4	110.0
B5 – B6	176.5	B6 – B4	175.2
– B4	177.7	– B5	176.5
– B5	178.3 (2×)	– B3	177.3
– B4'	178.4	– B3'	179.1
– H5	110.0	– B4	179.2
		– H6	110.0

Table 56: (continued)[HoO₉] polyhedron:

Ho	– O1	235.1 (3×)
	– O2	217.4 (3×)
	– O3	240.5 (3×)

[B₁₂H₁₂]²⁻ anion:

B1	– B1	178.5 (2×)	B2	– B2	178.6 (2×)
	– B2	178.6		– B1	178.6
	– B2'	178.7		– B1'	178.9
	– B2''	179.5		– B1''	179.5
	– H1	110.0		– H2	110.0
B3	– B6	177.2	B4	– B5	176.6
	– B6'	178.0		– B6	178.1
	– B4	178.5		– B3	178.5
	– B3	178.8 (2×)		– B5'	178.8
	– H3	110.0		– B6'	179.3
				– H4	110.0
B5	– B4	176.6	B6	– B3	175.2
	– B4'	178.8		– B3'	178.0
	– B6	179.1		– B4	178.1
	– B5	180.1 (2×)		– B5	179.1
	– H5	110.0		– B4'	179.3
				– H6	110.0

3.3.7 Enneaqua-Holmium(III) Tris-Oxonium Tris-Dodecahydro-*closo*-Dodecaborate Enneahydrate $[\text{Ho}(\text{H}_2\text{O})_9](\text{H}_3\text{O})_3[\text{B}_{12}\text{H}_{12}]_3 \cdot 9 \text{H}_2\text{O}$

The syntheses and crystal structures of mixed oxonium rare-earth metal(III) dodecahydro-*closo*-dodecaborates, similar to those with divalent cations, have not been studied up to date. Only the synthesis and the crystallographic data of cation-and-anion-mixed salt $[\text{La}(\text{H}_2\text{O})_9](\text{H}_3\text{O})\text{Cl}_2[\text{B}_{12}\text{H}_{12}] \cdot \text{H}_2\text{O}$ containing both H_3O^+ and $[\text{La}(\text{H}_2\text{O})_9]^{3+}$ cations along with Cl^- and $[\text{B}_{12}\text{H}_{12}]^{2-}$ anions had been reported recently [91]. Its crystal structure can be described as a layer-like structure, in which $[\text{B}_{12}\text{H}_{12}]^{2-}$ -cluster anions and H_3O^+ cations are arranged alternatively with layers of $[\text{La}(\text{H}_2\text{O})_9]^{3+}$ cations and Cl^- anions. In our work, the synthesis of a mixed oxonium rare-earth metal(III) dodecahydro-*closo*-dodecaborate hydrate was carried out and the crystal structure of $[\text{Ho}(\text{H}_2\text{O})_9](\text{H}_3\text{O})_3[\text{B}_{12}\text{H}_{12}]_3 \cdot 9 \text{H}_2\text{O}$ has been elucidated.

3.3.7.1 Synthesis of $[\text{Ho}(\text{H}_2\text{O})_9](\text{H}_3\text{O})_3[\text{B}_{12}\text{H}_{12}]_3 \cdot 9 \text{H}_2\text{O}$

The mixed-cationic oxonium holmium(III) dodecahydro-*closo*-dodecaborate hydrate under consideration was synthesized by the reaction of $[\text{Ho}(\text{H}_2\text{O})_9]_2[\text{B}_{12}\text{H}_{12}]_3 \cdot 15 \text{H}_2\text{O}$ and the free acid $(\text{H}_3\text{O})_2[\text{B}_{12}\text{H}_{12}]$ from aqueous solution. Pale yellow, polyhedrally shaped single crystals were obtained by evaporating the resulting solution at room temperature isothermally.

3.3.7.2 Structure Description of $[\text{Ho}(\text{H}_2\text{O})_9](\text{H}_3\text{O})_3[\text{B}_{12}\text{H}_{12}]_3 \cdot 9 \text{H}_2\text{O}$

The title compound crystallizes trigonally in the non-centrosymmetric space group R3c (no. 161) with six formula units per unit cell (Fig. 55). The holmium(III) cations occupy the special *Wyckoff* position 6a ($x/a = y/b = 0, z/c$; site symmetry: 3.), while the oxygen atoms of the oxonium cations, as well as of coordinating and “zeolitic” water molecules reside at the general crystallographic *Wyckoff* position 18b ($x/a, y/b, z/c$; site symmetry: 1) in this crystal structure. All boron and hydrogen atoms of the *quasi*-icosahedral $[\text{B}_{12}\text{H}_{12}]^{2-}$ -cluster anions and the centers of gravity of these *quasi*-icosahedral boron cages are found at the *Wyckoff* positions 18b. The B–B bond lengths of $[\text{B}_{12}\text{H}_{12}]^{2-}$ anions are in the common interval of 176 – 181 pm, whereas the B–H bond lengths were fixed at 110 pm (Fig. 56). The distances from the centers of gravity to the twelve boron atoms of each $[\text{B}_{12}\text{H}_{12}]^{2-}$ -cluster anion range from 165 to 173 pm providing inner diameters in the range of 330 to 346 pm for the boron icosahedra. Comparing to $[\text{Ho}(\text{H}_2\text{O})_9]_2[\text{B}_{12}\text{H}_{12}]_3 \cdot 15 \text{H}_2\text{O}$, the holmium(III) cations are also

coordinated by nine nearest oxygen atoms of crystal water molecules, but these are forming more distorted tricapped trigonal prisms ($d(\text{Ho}-\text{O}) = 224 - 239 \text{ pm}$) here (Fig. 57). Each oxonium cation H_3O^+ is tetrahedrally surrounded by four boron cages via non-classical hydrogen bridging bonds between its three hydrogen atoms and those of the $[\text{B}_{12}\text{H}_{12}]^{2-}$ anions ($d(\text{H}\cdots\text{H}) = 198 - 270 \text{ pm}$) (Fig. 58). The crystal structure of $[\text{Ho}(\text{H}_2\text{O})_9](\text{H}_3\text{O})_3[\text{B}_{12}\text{H}_{12}]_3 \cdot 9 \text{ H}_2\text{O}$ can be described with three independent interpenetrating layered motifs, namely the $[\text{Ho}(\text{H}_2\text{O})_9]^{3+}$ and H_3O^+ cations and the $[\text{B}_{12}\text{H}_{12}]^{2-}$ -cluster anions, as lattice components (Fig. 59). All these motifs alternatively arrange in a cubic closest packed fashion with the same stacking sequence (*abc*). This arrangement is different from that one of $[\text{Ho}(\text{H}_2\text{O})_9]_2[\text{B}_{12}\text{H}_{12}]_3 \cdot 15 \text{ H}_2\text{O}$ (Ho^{3+} cations: stacking sequence of *aa bb cc*, $[\text{B}_{12}\text{H}_{12}]^{2-}$ anions: stacking sequence of *ABABCBCAC*) and that one of $[\text{In}(\text{H}_2\text{O})_6]_2[\text{B}_{12}\text{H}_{12}]_3 \cdot 15 \text{ H}_2\text{O}$ as well (In^{3+} cations: stacking sequence of *abc*, $[\text{B}_{12}\text{H}_{12}]^{2-}$ anions: stacking sequence of *ABCCABBCA*). This arrangement is also not comparable with the layer-like structure of $[\text{La}(\text{H}_2\text{O})_9](\text{H}_3\text{O})\text{Cl}_2[\text{B}_{12}\text{H}_{12}] \cdot \text{H}_2\text{O}$ [91], in which the $[\text{B}_{12}\text{H}_{12}]^{2-}$ anions and the H_3O^+ cations are alternatively stacked with layers of $[\text{La}(\text{H}_2\text{O})_9]^{3+}$ cations and Cl^- anions. There are strong $\text{O}-\text{H}^{\delta+}\cdots\delta^-\text{O}$ classical hydrogen bridging bonds between the oxygen atoms of the $[\text{Ho}(\text{H}_2\text{O})_9]^{3+}$ coordination sphere and those of the “free” water molecules ($d(\text{O}\cdots\text{Ow}) = 262 - 289 \text{ pm}$). No classical hydrogen bond between hydrogen atoms of the H_3O^+ cation and those of the “zeolitic” crystal water is detected. Instead, the H_3O^+ cation, similar to that one in $[\text{La}(\text{H}_2\text{O})_9](\text{H}_3\text{O})\text{Cl}_2[\text{B}_{12}\text{H}_{12}] \cdot \text{H}_2\text{O}$, forms non-classical hydrogen bridging bonds with neighbour *quasi*-icosahedral $[\text{B}_{12}\text{H}_{12}]^{2-}$ -cluster anions in this compound via the relative strong interaction between the oxonium cations and the $[\text{B}_{12}\text{H}_{12}]^{2-}$ anions with the shortest donor-acceptor distance of 275 pm. In addition, the existence of a non-classical hydrogen bridging bonds in this compound is also detected between hydrogen atoms of the *quasi*-icosahedral $[\text{B}_{12}\text{H}_{12}]^{2-}$ -cluster anions and those of crystal and “zeolitic” water molecules with $d(\text{H}^{\delta-}\cdots\text{O}) = 271 - 298 \text{ pm}$ and $d(\text{H}^{\delta-}\cdots\text{Ow}) = 262 - 278 \text{ pm}$, respectively, as donor-acceptor distances.

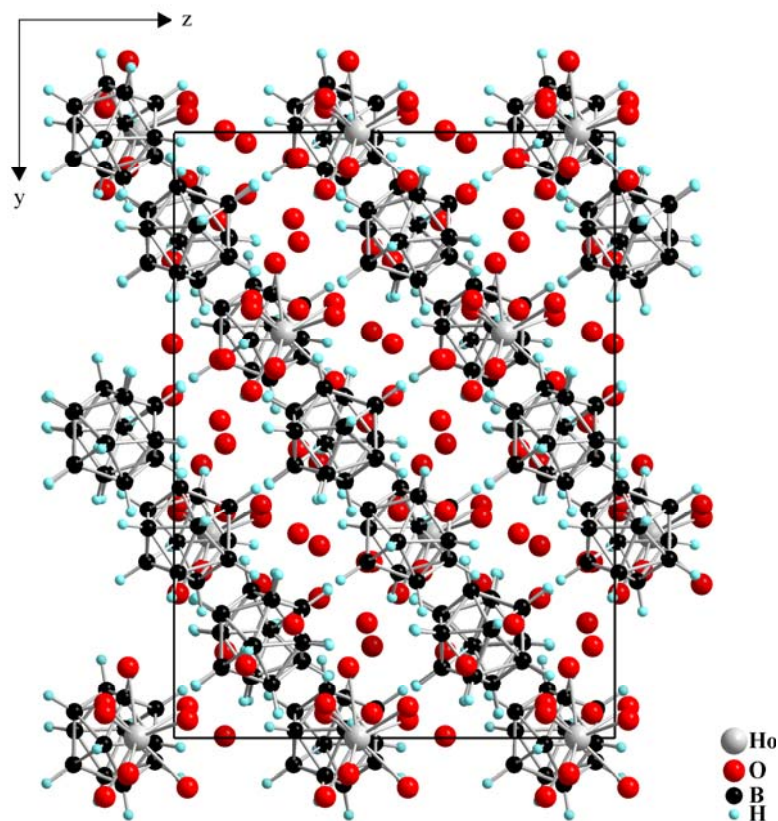


Fig. 55: View at the unit cell of the crystal structure of $[\text{Ho}(\text{H}_2\text{O})_9](\text{H}_3\text{O})_3[\text{B}_{12}\text{H}_{12}]_3 \cdot 9 \text{H}_2\text{O}$ along $[100]$

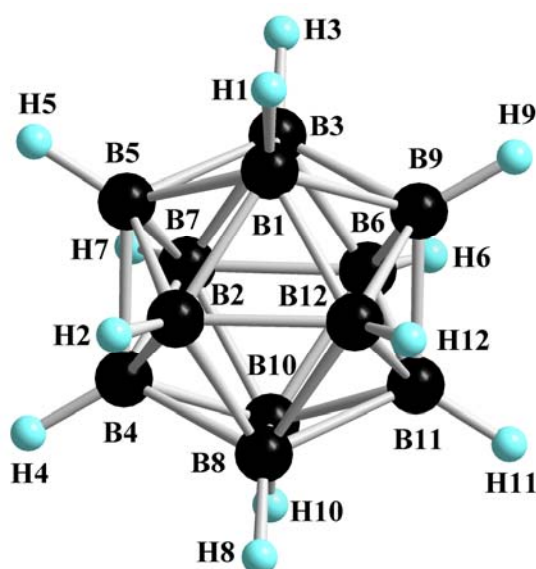


Fig. 56: View at the *quasi*-icosahedral $[\text{B}_{12}\text{H}_{12}]^{2-}$ -cluster anion in the crystal structure of $[\text{Ho}(\text{H}_2\text{O})_9](\text{H}_3\text{O})_3[\text{B}_{12}\text{H}_{12}]_3 \cdot 9 \text{H}_2\text{O}$

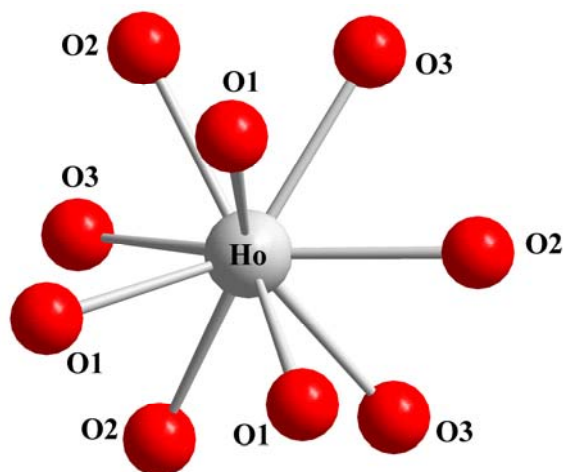


Fig. 57: View at the aqueous coordination sphere of the Ho^{3+} cation in the crystal structure of $[\text{Ho}(\text{H}_2\text{O})_9](\text{H}_3\text{O})_3[\text{B}_{12}\text{H}_{12}]_3 \cdot 9 \text{H}_2\text{O}$

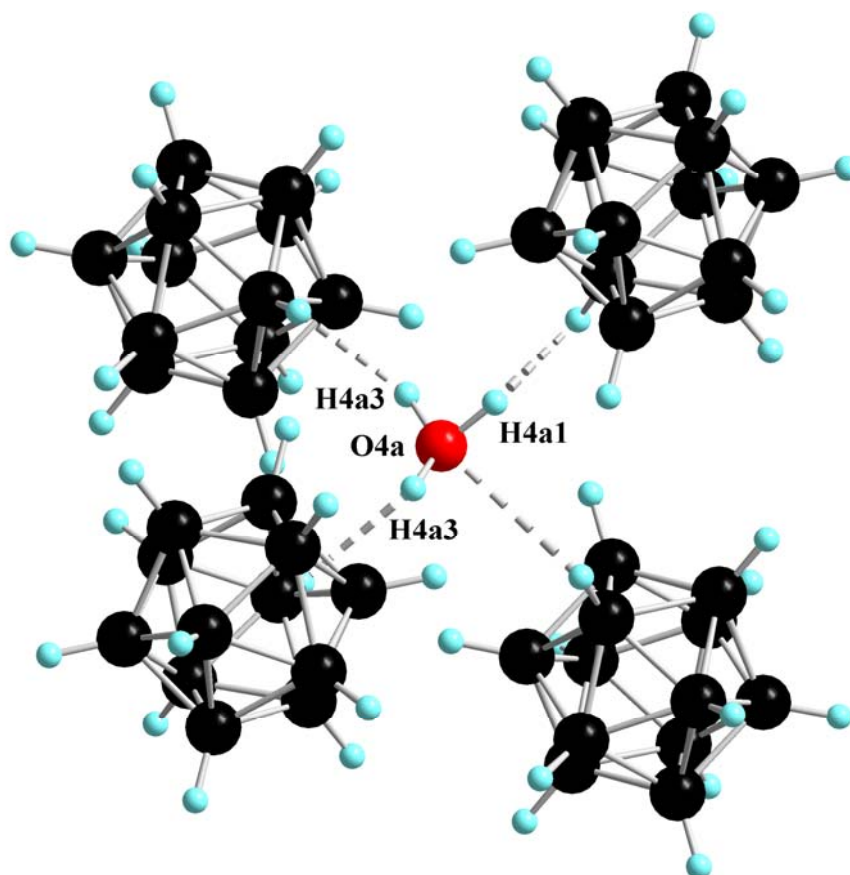


Fig. 58: Tetrahedral coordination sphere of the oxonium cation (H_3O^+) with four neighbour *quasi*-icosahedral $[\text{B}_{12}\text{H}_{12}]^{2-}$ -cluster anions in the crystal structure of $[\text{Ho}(\text{H}_2\text{O})_9](\text{H}_3\text{O})_3[\text{B}_{12}\text{H}_{12}]_3 \cdot 9 \text{H}_2\text{O}$

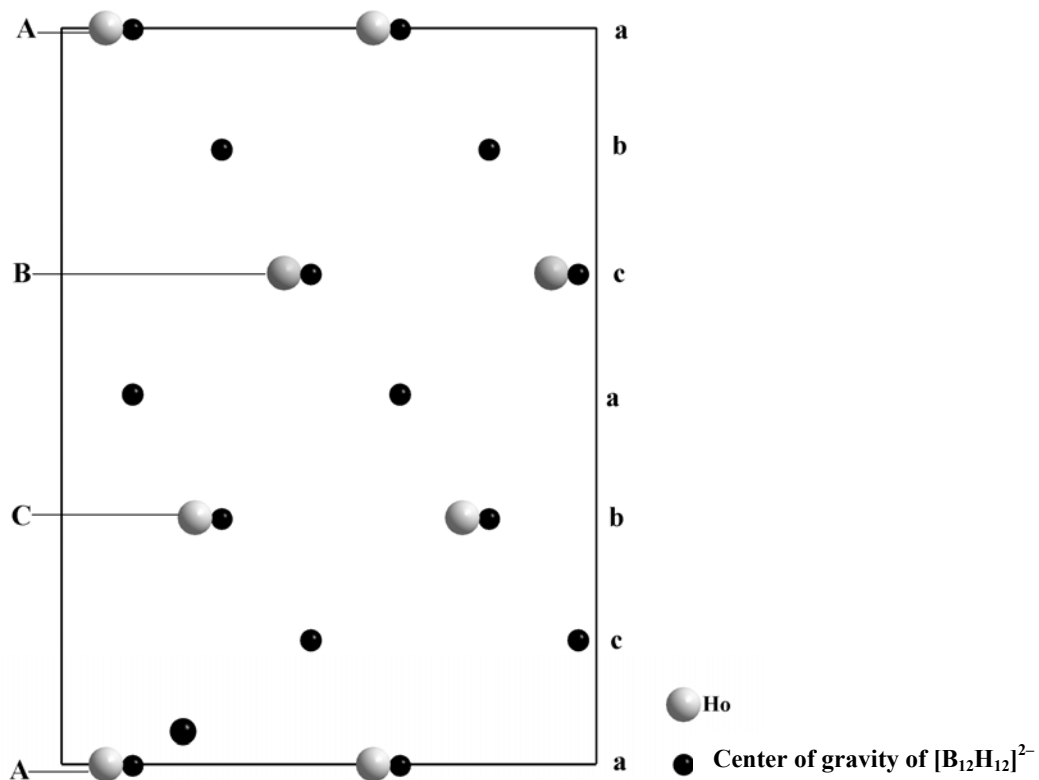


Fig. 59: The arrangement of the Ho³⁺ cations (grey spheres, stacking sequence: *ABC*) and the centers of gravity of the *quasi*-icosahedral [B₁₂H₁₂]²⁻-cluster anions (black spheres, stacking sequence: *abc*) in the crystal structure of [Ho(H₂O)₉](H₃O)₃[B₁₂H₁₂]₃ · 9 H₂O

Table 57: Crystallographic data for $[\text{Ho}(\text{H}_2\text{O})_9](\text{H}_3\text{O})_3[\text{B}_{12}\text{H}_{12}]_3 \cdot 9 \text{H}_2\text{O}$ and their determination

Crystal system	trigonal
Space group	R3c (no. 161)
Unit cell parameters:	
a (pm)	2351.04(9)
c (pm)	1472.73(6)
Number of formula units per unit cell	Z = 6
Calculated density ($D_x/\text{g cm}^{-3}$)	1.374
Molar volume ($V_m/\text{cm}^3 \text{mol}^{-1}$)	707.6
Diffractometer	κ -CCD (Bruker-Nonius)
Radiation	Mo-K α : $\lambda = 71.07 \text{ pm}$, graphite monochromator
Index range	$\pm h_{\text{max}} = 31, \pm k_{\text{max}} = 31, \pm l_{\text{max}} = 19$
θ_{max} (deg)	28.3
F(000)	3156
Absorption coefficient (μ/mm^{-1})	1.74
Absorption correction	numerical, Program X-SHAPE [64]
Other data corrections	background, polarization and <i>Lorentz</i> factors
Collected reflections	57026
Unique reflections	3851
$R_{\text{int}}, R_{\sigma}$	0.061, 0.018
Structure solution and refinement	Program SHELXS-97 and SHELXL-97 [68]
Scattering factors	International Tables for Crystallography, Vol. C [87]
R_1, R_w with $ F_o \geq 4\sigma(F_o)$	0.063, 0.062
Reflections with $ F_o \geq 4\sigma(F_o)$	3720
w R_2 , Goodness of fit (GooF)	0.163, 1.061
Extinction (g)	0.0013(2)
<i>Flack</i> -x-parameter	0.362(3) (treatment as inversion twin)
Residual electron density (<i>max.</i> , <i>min.</i> in $\rho/e^{-1} 10^6 \text{ pm}$)	4.03, -1.38

Table 58: Atomic coordinates for $[\text{Ho}(\text{H}_2\text{O})_9](\text{H}_3\text{O})_3[\text{B}_{12}\text{H}_{12}]_3 \cdot 9 \text{H}_2\text{O}$

Atom	Wyckoff position	x/a	y/b	z/c
Ho	6a	0	0	0.41569(1)
O1	18b	0.6963(2)	0.4136(2)	0.3637(4)
O2	18b	0.0402(8)	0.9447(8)	0.3629(9)
O3	18b	0.1166(5)	0.0591(4)	0.3954(8)
O4a	18b	0.6234(2)	0.6261(2)	0.1151(4)
O5w	18b	0.7867(2)	0.4363(2)	0.4960(4)
O6w	18b	0.8539(2)	0.3763(2)	0.6040(4)
O7w	18b	0.7063(2)	0.5245(2)	0.2828(3)
B1	18b	0.6816(3)	0.7724(3)	0.2217(4)
B2	18b	0.7457(3)	0.8482(3)	0.1802(4)
B3	18b	0.6053(2)	0.7579(2)	0.1756(4)
B4	18b	0.7095(3)	0.8818(3)	0.1076(4)
B5	18b	0.6784(3)	0.7949(3)	0.1079(4)
B6	18b	0.5915(3)	0.8214(3)	0.2175(4)
B7	18b	0.6229(3)	0.8261(3)	0.1049(4)
B8	18b	0.7321(3)	0.9117(3)	0.2208(4)
B9	18b	0.6277(3)	0.7878(3)	0.2898(4)
B10	18b	0.6561(3)	0.8988(2)	0.1740(4)
B11	18b	0.6581(3)	0.8733(3)	0.2891(4)
B12	18b	0.7142(3)	0.8426(3)	0.2917(4)
H4a1	18b	0.598(4)	0.606(4)	0.174(6)
H4a2	18b	0.676(4)	0.642(4)	0.114(6)
H4a3	18b	0.585(4)	0.590(4)	0.075(6)
H1 ^{a)}	18b	0.690	0.732	0.237
H2 ^{a)}	18b	0.796	0.857	0.169
H3 ^{a)}	18b	0.564	0.708	0.106
H4 ^{a)}	18b	0.736	0.912	0.049
H5 ^{a)}	18b	0.685	0.769	0.050
H6 ^{a)}	18b	0.541	0.813	0.230
H7 ^{a)}	18b	0.593	0.821	0.044
H8 ^{a)}	18b	0.773	0.961	0.235
H9 ^{a)}	18b	0.601	0.757	0.349
H10 ^{a)}	18b	0.648	0.940	0.158
H11 ^{a)}	18b	0.651	0.898	0.348
H12 ^{a)}	18b	0.744	0.847	0.352

^{a)} refinement with DFIX constraint ($d(\text{B-H}) = 110 \text{ pm}$); $U_{\text{iso}}(\text{H}) = 1.2 \cdot U_{\text{iso}}(\text{B})$.

Table 59: Anisotropic thermal displacement coefficients^{a)} (U_{ij}/pm^2) for $[\text{Ho}(\text{H}_2\text{O})_9](\text{H}_3\text{O})_3[\text{B}_{12}\text{H}_{12}]_3 \cdot 9 \text{H}_2\text{O}$

Atom	U_{11}	U_{22}	U_{33}	U_{23}	U_{13}	U_{12}
Ho	245(2)	= U_{11}	140(3)	0	0	= $\frac{1}{2} U_{11}$
O1	209(18)	194(21)	339(25)	-45(17)	-84(18)	113(17)
O2	557(49)	680(66)	680(72)	885(94)	586(43)	304(38)
O3	641(57)	852(68)	939(76)	-614(56)	408(55)	-277(44)
O4a	207(19)	218(19)	292(19)	-29(17)	25(17)	93(14)
O5w	128(15)	193(17)	269(19)	9(15)	-15(14)	61(14)
O6w	327(24)	182(20)	405(26)	-109(18)	135(20)	81(18)
O7w	186(17)	162(17)	257(20)	-36(15)	60(15)	42(15)
B1	116(22)	71(21)	173(27)	5(19)	13(18)	26(19)
B2	114(23)	193(26)	132(25)	67(20)	18(18)	119(21)
B3	61(19)	73(20)	164(24)	26(18)	19(17)	2(16)
B4	154(23)	135(23)	98(23)	45(18)	36(19)	76(20)
B5	193(25)	107(23)	123(23)	4(19)	9(20)	87(21)
B6	115(23)	66(21)	132(26)	-21(18)	-30(18)	-8(19)
B7	160(25)	90(22)	114(24)	-46(19)	-84(19)	78(20)
B8	209(26)	103(23)	146(26)	-34(19)	-34(20)	96(21)
B9	112(23)	169(26)	111(24)	-20(19)	-28(18)	94(20)
B10	101(22)	103(22)	166(25)	29(19)	1(19)	88(19)
B11	143(24)	153(25)	109(24)	-13(19)	-43(19)	93(21)
B12	130(25)	150(25)	95(24)	34(20)	7(19)	61(21)
H4a1	230(18)					
H4a2	361(18)					
H4a3	282(18)					
H1	156					
H2	153					
H3	109					
H4	153					
H5	162					
H6	154					
H7	137					
H8	173					
H9	144					
H10	129					
H11	152					
H12	155					

^{a)} For Ho, O and B defined as anisotropic temperature factor according to: $\exp[-2\pi^2(U_{11}h^2a^{*2} + U_{22}k^2b^{*2} + U_{33}l^2c^{*2} + 2U_{23}klb^{*}c^{*} + 2U_{13}hla^{*}c^{*} + 2U_{12}hka^{*}b^{*})]$; for H isotropically defined as temperature factor in: $\exp[-8\pi^2(U_{\text{iso}}\sin^2\theta/\lambda^2)]$.

Table 60: Selected interatomic distances (d/pm) for [Ho(H₂O)₉](H₃O)₃[B₁₂H₁₂]₃ · 9 H₂O

[HoO ₉] polyhedron:		Ho – O1	222.3 (3×)			
		– O2	236.4 (3×)			
		– O3	239.3 (3×)			
(H ₃ O) ⁺ cation:						
		O4a – H4a1	102.4			
		– H4a2	110.9			
		– H4a3	104.8			
[B ₁₂ H ₁₂] ²⁻ anion:						
B1	– B12	176.3	B2 – B8	177.0	B3 – B7	177.9
	– B5	176.9	– B12	177.8	– B1	178.4
	– B2	177.0	– B10	177.9	– B6	178.8
	– B3	178.4	– B1	178.0	– B5	179.2
	– B9	179.1	– B3	179.6	– B9	179.7
	– H1	110.0	– H2	110.0	– H3	110.0
B4	– B2	178.0	B5 – B1	176.9	B6 – B11	177.1
	– B8	178.4	– B7	178.9	– B9	177.4
	– B10	178.8	– B3	179.2	– B3	178.8
	– B7	178.8	– B4	179.4	– B7	179.6
	– B5	179.4	– B2	179.6	– B10	180.8
	– H4	110.0	– H5	110.0	– H6	110.0
B7	– B3	177.9	B8 – B2	177.8	B9 – B2	176.4
	– B4	178.8	– B4	178.4	– B4	177.4
	– B5	178.9	– B12	179.5	– B12	178.3
	– B6	179.6	– B10	179.5	– B10	179.1
	– B10	179.8	– B11	181.1	– B11	179.7
	– H7	110.0	– H8	110.0	– H9	110.0
B10	– B4	178.8	B11 – B9	176.4	B12 – B4	176.3
	– B8	179.5	– B6	177.1	– B2	177.9
	– B7	179.8	– B12	179.3	– B9	178.3
	– B11	180.7	– B10	180.7	– B11	179.3
	– B6	180.8	– B8	181.3	– B8	179.5
	– H10	110.0	– H11	110.0	– H12	110.0

4 Partially Hydroxylated Dodecahydro-*closo*-Dodecaborate Derivatives

4.1 Bis-Oxonium Undecahydro-Monohydroxo-*closo*-Dodecaborate Monohydrate

The chemical properties of bis-oxonium dodecahydro-*closo*-dodecaborate $(\text{H}_3\text{O})_2[\text{B}_{12}\text{H}_{12}]$ and its partially hydroxylated derivatives $(\text{H}_3\text{O})_2[\text{B}_{12}\text{H}_{12-n}(\text{OH})_n]$ ($n = 1$ and 2) had been studied since the 1960s [16]. $(\text{H}_3\text{O})_2[\text{B}_{12}\text{H}_{12}]$ and its halogenated derivatives provide strong acids and good water solubility [16, 85]. In the case of hydroxylated dodecahydro-*closo*-dodecaborates, however, the higher the degree of hydroxylation of $[\text{B}_{12}\text{H}_{12}]^{2-}$ the weaker is the acidity and the lower water solubility of the corresponding $(\text{H}_3\text{O})_2[\text{B}_{12}\text{H}_{12-n}(\text{OH})_n]$ or $\text{H}_2[\text{B}_{12}\text{H}_{12-n}(\text{OH})_n]$ acids [48]. Only the synthesis and crystal structure of the bis-oxonium acid $\text{H}_2[\text{B}_{12}(\text{OH})_{12}]$ with the perhydroxylated B_{12} cage has been published to date [103].

4.1.1 Synthesis of $(\text{H}_3\text{O})_2[\text{B}_{12}\text{H}_{11}(\text{OH})] \cdot \text{H}_2\text{O}$

Single crystals of $(\text{H}_3\text{O})_2[\text{B}_{12}\text{H}_{11}(\text{OH})] \cdot \text{H}_2\text{O}$ were obtained as a by-product by the reaction of dicesium dodecahydro-*closo*-dodecaborate $\text{Cs}_2[\text{B}_{12}\text{H}_{12}]$ with diluted hydrogen peroxide H_2O_2 at room temperature. 1 g $\text{Cs}_2[\text{B}_{12}\text{H}_{12}]$ is therefore stirred with 1.5 ml H_2O_2 (30 %) in aqueous solution at room temperature for 8 hours. Colourless, bead-shaped single crystals of $(\text{H}_3\text{O})_2[\text{B}_{12}\text{H}_{11}(\text{OH})] \cdot \text{H}_2\text{O}$ are obtained by isothermal evaporation of the resulting solution.

4.1.2 Structure Description of $(\text{H}_3\text{O})_2[\text{B}_{12}\text{H}_{11}(\text{OH})] \cdot \text{H}_2\text{O}$

The title compound crystallizes orthorhombically in the non-centrosymmetric space group Ama2 (no. 40) with four formula units per unit cell (Fig. 60). The oxygen atoms of the oxonium cations $(\text{H}_3\text{O}1\text{a})^+$ and $(\text{H}_3\text{O}2\text{a})^+$ are located at two different crystallographic *Wyckoff* sites $4a$ ($x/a = y/b = 0, z/c$; site symmetry: $\dots 2$) and $4b$ ($x/a = 1/4, y/b, z/c$; site symmetry: $m..$). The oxygen atoms of the single hydroxyl group at the boron cage and those of the crystal water molecule reside at the *Wyckoff* position $4b$. All boron and hydrogen atoms of the boron cage are located at the *Wyckoff* sites $8c$ ($x/a, y/b, z/c$; site symmetry: 1) and $4b$, respectively. Both oxygen atoms of the oxonium cations $(\text{H}_3\text{O}1\text{a})^+$ and $(\text{H}_3\text{O}2\text{a})^+$ exhibit the coordination numbers of twelve. Each $(\text{H}_3\text{O}1\text{a})^+$ cation is tetrahedrally coordinated with four nearest $[\text{B}_{12}\text{H}_{11}(\text{OH})]^{2-}$ -cluster anions via ten hydrogen and two oxygen atoms of the boron cages ($d(\text{O}\cdots\text{H}) = 278 - 350$ pm, $d(\text{O}\cdots\text{O}) = 283$ pm) (Fig. 61, *left*). Two of these $[\text{B}_{12}\text{H}_{11}(\text{OH})]^{2-}$ -

cluster anions link to the oxygen atoms of the oxonium cations via three hydrogen atoms originating from one triangular face per each. $(\text{H}_3\text{O}1\text{a})^+$ is connected to two other $[\text{B}_{12}\text{H}_{11}(\text{OH})]^{2-}$ anions via the hydroxyl oxygen and two hydrogen atoms originating from one triangular face per each. Each oxonium cation $(\text{H}_3\text{O}2\text{a})^+$, on the other hand, is tetrahedrally coordinated with four nearest $[\text{B}_{12}\text{H}_{11}(\text{OH})]^{2-}$ -cluster anions via three hydrogen atoms exclusively originating from one triangular face per each ($d(\text{O}\cdots\text{H}) = 269 - 309 \text{ pm}$) (Fig. 61, *right*). The B–B bond lengths within the *quasi*-icosahedral $[\text{B}_{12}\text{H}_{11}(\text{OH})]^{2-}$ -cluster anions are in the common range ($d(\text{B}–\text{B}) = 176 - 180 \text{ pm}$), but the distortion of the boron cage from an ideal icosahedron is pronounced with B–H and B–O bond lengths such as $d(\text{B}–\text{H}) = 100 - 121 \text{ pm}$ and $d(\text{B}–\text{O}) = 149 \text{ pm}$. A strong hydrogen bonding bridge is found between the hydroxyl oxygen atom at the boron cage (O3) and the one of the “zeolitic” crystal water molecule (Ow) ($d(\text{O}3\cdots\text{Ow}) = 255 \text{ pm}$) (Fig. 62). This classical hydrogen bond is much stronger than that one found in $\text{Cs}_2[\text{B}_{12}\text{H}_{11}(\text{OH})] \cdot \text{H}_2\text{O}$, which has $d(\text{O}\cdots\text{Ow}) = 297 \text{ pm}$ only. Strong hydrogen bridging bonds also exist between the oxygen atoms of the oxonium cations

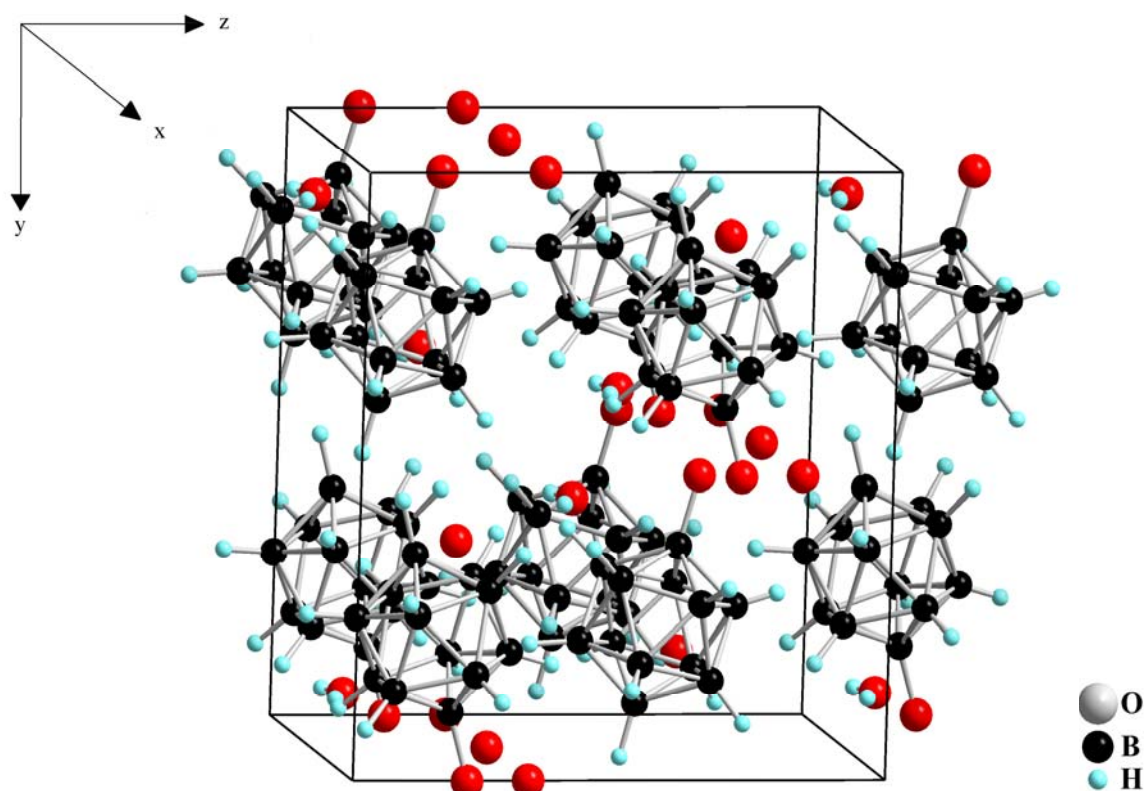


Fig. 60: View at the unit cell of the crystal structure of $(\text{H}_3\text{O})_2[\text{B}_{12}\text{H}_{11}(\text{OH})] \cdot \text{H}_2\text{O}$ along the $[100]$ direction

$(\text{H}_3\text{O1a})^+$ and those of the hydroxyl groups ($d(\text{O1a}\cdots\text{O3}) = 283 \text{ pm}$). The evidence of non-classical “dihydrogen” bridging bonds $\text{B}-\text{H}^{\delta-}\cdots\delta^+\text{H}-\text{O}$ in this crystal structure is obvious with linkages between the hydrogen atoms of the “zeolitic” crystal water molecules and the hydrogen atoms of the $[\text{B}_{12}\text{H}_{11}(\text{OH})]^{2-}$ -cluster anions ($d(\text{H}^{\delta-}\cdots\delta^+\text{H}) = 224 - 312 \text{ pm}$).

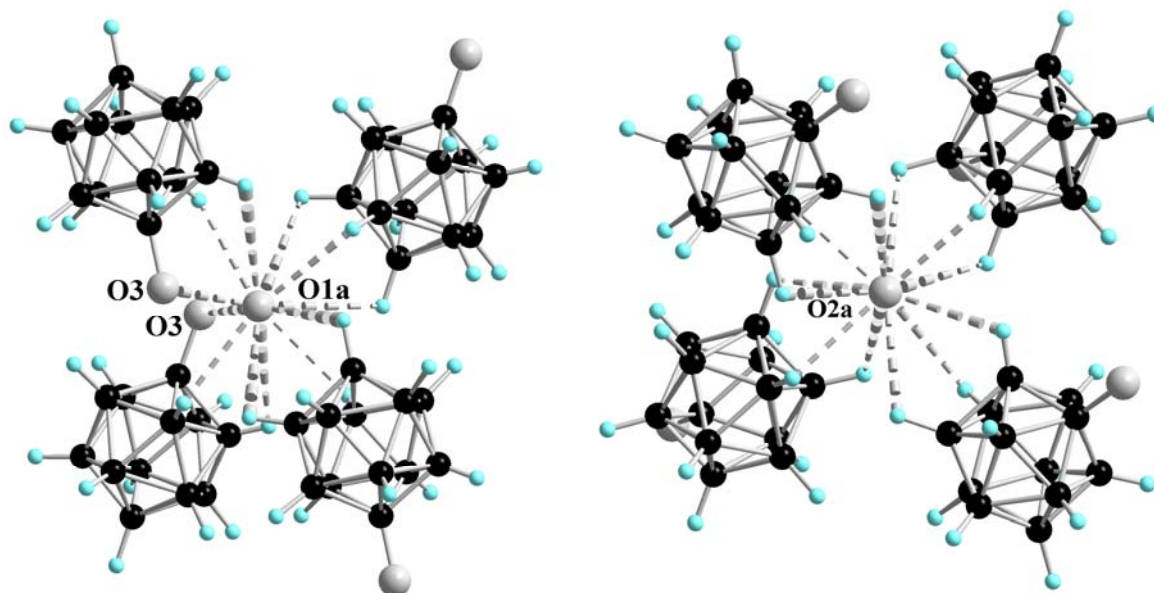


Fig. 61: View of the tetrahedral coordination sphere of the $(\text{H}_3\text{O1a})^+$ cation (*left*) and the $(\text{H}_3\text{O2a})^+$ cation (*right*)

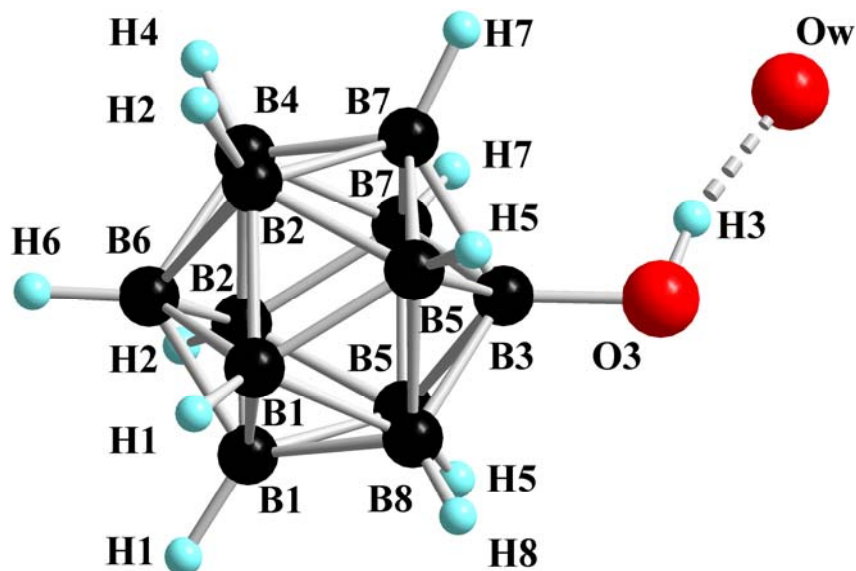


Fig. 62: The $\text{O}-\text{H}^{\delta+}\cdots\delta^-\text{O}$ hydrogen bond between the hydroxyl oxygen atom (O3) of the *quasi*-icosahedral $[\text{B}_{12}\text{H}_{11}(\text{OH})]^{2-}$ -cluster anion and the one of the “zeolitic” hydration water (Ow) in the crystal structure of $(\text{H}_3\text{O})_2[\text{B}_{12}\text{H}_{11}(\text{OH})] \cdot \text{H}_2\text{O}$

Table 61: Crystallographic data for $(\text{H}_3\text{O})_2[\text{B}_{12}\text{H}_{11}(\text{OH})] \cdot \text{H}_2\text{O}$ and their determination

Crystal system	orthorhombic
Space group	Ama2 (no. 40)
Unit cell parameters:	
a (pm)	868.60(6)
b (pm)	1252.16(9)
c (pm)	1149.29(8)
Number of formula units per unit cell	Z = 4
Calculated density ($D_x/\text{g cm}^{-3}$)	1.137
Molar volume ($V_m/\text{cm}^3 \text{ mol}^{-1}$)	188.2
Diffractometer	κ -CCD (Bruker-Nonius)
Radiation	Mo-K α : $\lambda = 71.07$ pm, graphite monochromator
Index range	$\pm h_{\max} = 11, \pm k_{\max} = 16, \pm l_{\max} = 15$
θ_{\max} (deg)	27.3
F(000)	448
Absorption coefficient (μ/mm^{-1})	0.07
Absorption correction	numerical, Program X-SHAPE [64]
Other data corrections	background, polarization and <i>Lorentz</i> factors
Collected reflections	8406
Unique reflections	1633
$R_{\text{int}}, R_{\sigma}$	0.052, 0.036
Structure solution and refinement	Program SHELXS-97 and SHELXL-97 [68]
Scattering factors	International Tables for Crystallography, Vol. C [87]
R_1, R_1 with $ F_o \geq 4\sigma(F_o)$	0.060, 0.050
Reflections with $ F_o \geq 4\sigma(F_o)$	1415
w R_2 , Goodness of fit (GooF)	0.126, 1.070
Extinction (g)	0.0002(3)
<i>Flack</i> -x-parameter	0.022(3)
Residual electron density (<i>max.</i> , <i>min.</i> in $\rho/e^{-1} 10^6$ pm)	0.22, -0.27

Table 62: Atomic coordinates for $(\text{H}_3\text{O})_2[\text{B}_{12}\text{H}_{11}(\text{OH})] \cdot \text{H}_2\text{O}$

Atom	Wyckoff position	x/a	y/b	z/c
O1a	4a	0	0	0.3294(2)
O2a	4b	$\frac{1}{4}$	0.3684(2)	0.2208(2)
O3	4b	$\frac{1}{4}$	0.4739(2)	0.6748(2)
Ow	4b	$\frac{1}{4}$	0.1168(4)	0.0164(4)
B1	8c	0.1470(3)	0.1486(2)	0.6897(2)
B2	8c	0.0838(3)	0.1824(2)	0.5469(2)
B3	4b	$\frac{1}{4}$	0.3601(2)	0.6390(3)
B4	4b	$\frac{1}{4}$	0.2082(3)	0.4583(3)
B5	8c	0.0848(3)	0.2805(3)	0.6590(2)
B6	4b	$\frac{1}{4}$	0.1007(2)	0.5652(3)
B7	8c	0.1479(3)	0.3147(2)	0.5160(2)
B8	4b	$\frac{1}{4}$	0.2602(3)	0.7475(3)
H1a1	4a	0	0	0.227(8)
H1a2	8c	-0.036(8)	-0.079(4)	0.376(7)
H2a1	4b	$\frac{1}{4}$	0.384(7)	0.291(9)
H2a2	8c	0.136(6)	0.367(4)	0.206(4)
H3	4b	$\frac{1}{4}$	0.508(5)	0.612(5)
Hw	8c	0.172(5)	0.121(4)	-0.004(5)
H1	8c	0.080(3)	0.084(2)	0.741(2)
H2	8c	-0.037(3)	0.148(2)	0.511(2)
H4	4b	$\frac{1}{4}$	0.199(3)	0.366(3)
H5	8c	-0.017(3)	0.315(2)	0.694(2)
H6	4b	$\frac{1}{4}$	0.012(3)	0.540(4)
H7	8c	0.088(3)	0.371(2)	0.453(2)
H8	4b	$\frac{1}{4}$	0.287(4)	0.830(6)

Table 63: Anisotropic thermal displacement coefficients^{a)} (U_{ij}/pm^2) for $(\text{H}_3\text{O})_2[\text{B}_{12}\text{H}_{11}(\text{OH})] \cdot \text{H}_2\text{O}$

Atom	U_{11}	U_{22}	U_{33}	U_{23}	U_{13}	U_{12}
O1a	387(12)	396(18)	338(15)	0	0	-55(18)
O2a	393(13)	605(16)	594(15)	243(12)	0	0
O3	721(16)	243(10)	418(12)	11(9)	0	0
Ow	457(19)	1095(30)	1010(28)	753(27)	0	0
B1	320(11)	301(10)	258(9)	28(8)	38(8)	-20(8)
B2	269(10)	345(11)	309(10)	-2(8)	-19(9)	-32(8)
B3	405(17)	219(14)	285(13)	14(11)	0	0
B4	352(17)	350(16)	227(13)	11(11)	0	0
B5	316(11)	320(10)	294(10)	14(8)	41(9)	21(8)
B6	336(15)	258(14)	281(13)	14(11)	0	0
B7	349(10)	299(11)	289(10)	38(8)	-9(9)	47(8)
B8	389(16)	294(14)	211(12)	4(11)	0	0
H1a1	1400(177)					
H1a2	1269(133)					
H2a1	1358(164)					
H2a2	1557(193)					
H3	832(168)					
Hw	1087(186)					
H1	362(62)					
H2	443(72)					
H4	432(99)					
H5	370(61)					
H6	483(103)					
H7	330(59)					
H8	893(176)					

^{a)} For O and B defined as anisotropic temperature factor according to: $\exp[-2\pi^2 (U_{11}h^2a^{*2} + U_{22}k^2b^{*2} + U_{33}l^2c^{*2} + 2U_{23}klb^*c^* + 2U_{13}hla^*c^* + 2U_{13}hka^*b^*)]$; for H isotropically defined as temperature factor in: $\exp[-8\pi^2(U_{\text{iso}}\sin^2\theta/\lambda^2)]$.

Table 64: Selected interatomic distances (d/pm) for $(\text{H}_3\text{O})_2[\text{B}_{12}\text{H}_{11}(\text{OH})] \cdot \text{H}_2\text{O}$

[(O1a)O ₂ H ₁₀] polyhedron:				[(O2a)H ₁₂] polyhedron:				
O1a	– O3/H3	282.6 (2×)		O2a	– H4	268.8		
	– H5	278.1 (2×)			– H6	275.4		
	– H2	286.0 (2×)			– H1	297.5 (2×)		
	– H6	324.7 (2×)			– H2	302.2 (2×)		
	– H4	332.3 (2×)			– H7	303.5 (2×)		
	– H8	349.8 (2×)			– H1'	306.7 (2×)		
					– H5	308.7 (2×)		
(H ₃ O1a) ⁺ cation:				(H ₃ O2a) ⁺ cation:				
O1a	– H1a1	117.1		O2a	– H2a1	83.0		
	– H1a2	117.7 (2×)			– H2a2	101.8 (2×)		
[B ₁₂ H ₁₁ (OH)] ²⁻ anion:								
B1	– B5	177.4	B2	– B5	178.0	B3	– B5	176.2 (2×)
	– B2	178.2		– B6	178.2		– B7	176.2 (2×)
	– B8	178.7		– B1	178.2		– B8	176.7
	– B1	178.9		– B7	178.3		– O3	148.3
	– B6	179.2		– B4	178.8			
	– H1	115.1		– H2	120.9			
B4	– B7	177.3 (2×)	B5	– B3	168.2	B6	– B2	178.2 (2×)
	– B6	178.6		– B1	177.4		– B4	178.6
	– B2	178.8 (2×)		– B8	177.8		– B1	179.2 (2×)
	– H4	106.5		– B2	178.0		– H6	114.9
				– B7	178.4			
				– H5	106.2			
B7	– B3	176.2				B8	– B3	176.7
	– B4	177.3					– B5	177.8 (2×)
	– B7	177.3					– B1	178.7 (2×)
	– B2	178.3					– H8	99.9
	– B5	178.4						
	– H7	113.5						

4.2 Dicesium Undecahydro-Monohydroxo-*closo*-Dodecaborate Monohydrate

Among the partially hydroxylated derivatives of $[\text{B}_{12}\text{H}_{12}]^{2-}$, undecahydro-monohydroxo-*closo*-dodecaborate $[\text{B}_{12}\text{H}_{11}(\text{OH})]^{2-}$ was the species studied in most detail as its preparation is the easiest. The synthesis of the $[\text{B}_{12}\text{H}_{11}(\text{OH})]^{2-}$ anion had been reported for the first time in 1964 [16] and has been significantly improved recently [30, 48]. However, there was no information on available crystal structures of its salt-like compounds with metal cations. The crystal structure of dicesium undecahydro-monohydroxo-*closo*-dodecaborate in particular has never entered literature so far, even though this salt is mostly used as starting material for further functionalization reactions of $[\text{B}_{12}\text{H}_{11}(\text{OH})]^{2-}$ [31, 32, 48].

4.2.1 Synthesis of $\text{Cs}_2[\text{B}_{12}\text{H}_{11}(\text{OH})] \cdot \text{H}_2\text{O}$

There are two methods for synthesizing this title compound. By the acid-catalyzed hydroxylation of the dodecahydro-*closo*-dodecaborate anion $[\text{B}_{12}\text{H}_{12}]^{2-}$ is the first one. 1 g $\text{Cs}_2[\text{B}_{12}\text{H}_{12}]$ was refluxed with 20 ml a 38 % aqueous solution of sulfuric acid H_2SO_4 at 90 °C for 45 minutes, leading to a clear liquid. This solution was slowly added with stirring to a slurry of 20 g of CaCO_3 in 200 ml of water. After the suspension was neutralized, the precipitated CaSO_4 was removed by filtration. Colourless, needle-shaped single crystals were obtained by recrystallization and subsequent isothermal evaporation of the filtrate. This synthesis method is time consuming, although it allows the controlled partial hydroxylation of the $[\text{B}_{12}\text{H}_{12}]^{2-}$ -cluster anion to proceed stepwise. An alternative preparation method was also used by stirring 1 g $\text{Cs}_2[\text{B}_{12}\text{H}_{12}]$ with 2 ml hydrogen peroxide H_2O_2 (30 %) in aqueous solution at room temperature for 12 h. Generally, by using this method, the hydroxylation of the $[\text{B}_{12}\text{H}_{12}]^{2-}$ -cluster anion does not process stepwise and the product consists of a number of isomers. This method, however, is simple and provides hydroxylated derivatives readily. Single crystals are again obtained by isothermal evaporation of the resulting solution. Those suitable for X-ray diffraction measurements were then selected and the data collection was carried out at $T = 100 \text{ K}$.

4.2.2 $^{11}\text{B}\{^1\text{H}\}$ -NMR Measurement of $\text{Cs}_2[\text{B}_{12}\text{H}_{11}(\text{OH})] \cdot \text{H}_2\text{O}$

In the $^{11}\text{B}\{^1\text{H}\}$ -NMR spectrum of $\text{Cs}_2[\text{B}_{12}\text{H}_{11}(\text{OH})] \cdot \text{H}_2\text{O}$, prepared by the acid-catalyzed hydroxylation method, in D_2O four signals at 6.7, -14.1, -16.3, and -22.3 ppm were able to

be detected having a 1:5:5:1 intensity ratio. This pattern of signals is typical for undeca-hydro-mono-hydroxo-*closo*-dodecaborate derivatives and therefore similar to that one reported by Hawthorne *et al.* [48]. There are three effects that influence the ^{11}B -NMR resonances of $[\text{B}_{12}\text{H}_{12-n}(\text{OH})_n]^{2-}$ ($n = 1 - 4$) species. The negative inductive effect ($-I$) of the hydroxyl group causes the downfield shift of the B–OH singlets and this effect diminishes rapidly with distance. The chemical shifts in the spectrum are influenced by the resonance effect ($+M$) that arises from substituents having lone-pairs. The $+M$ effect shields vertices of the boron cage due to the electron donation capacity of the substituent to the cluster as a whole. The antipodal effect describes the upfield shift of a signal of a vertex that is in *trans*-position to an *ipso*-boron atom. In $[\text{B}_{12}\text{H}_{11}(\text{OH})]^{2-}$, the $-I$ effect deshields the *ipso*-boron atom (-6.7 ppm) and causes the signals of the *ortho*-B–H vertices (-14.1 ppm) to be shifted downfield relative to the ones of the *meta*-B–H vertices (-16.3 ppm). The antipodal effect also causes the upfield shift of the *para*-B–H vertex (-22.3 ppm). Thus, NMR measurements reveal that $\text{Cs}_2[\text{B}_{12}\text{H}_{11}(\text{OH})] \cdot \text{H}_2\text{O}$ is synthesized with highly selective purity.

4.2.3 Structure Description of $\text{Cs}_2[\text{B}_{12}\text{H}_{11}(\text{OH})] \cdot \text{H}_2\text{O}$

The title compound $\text{Cs}_2[\text{B}_{12}\text{H}_{11}(\text{OH})] \cdot \text{H}_2\text{O}$ crystallizes orthorhombically in space group *Ama*2 (no. 40) with $Z = 4$ as inversion twin (Fig. 63). The crystal structure of $\text{Cs}_2[\text{B}_{12}\text{H}_{11}(\text{OH})] \cdot \text{H}_2\text{O}$ is basically isostructural to that one reported for $(\text{H}_3\text{O})_2[\text{B}_{12}\text{H}_{11}(\text{OH})] \cdot \text{H}_2\text{O}$. The X-ray crystal structure analysis at 100 K revealed that the cesium cations occupy three crystallographically distinct *Wyckoff* positions ($2 \times 4a + 1 \times 4b$), however, thus both $4a$ sites have to be half-occupied only. This is different from the structure of $(\text{H}_3\text{O})_2[\text{B}_{12}\text{H}_{11}(\text{OH})] \cdot \text{H}_2\text{O}$, in which the oxonium cations are only located at two crystallographically distinct *Wyckoff* positions $4a$ and $4b$. The Cs1 and Cs2 monocations (both in $4a$) are tetrahedrally surrounded by four *quasi*-icosahedral $[\text{B}_{12}\text{H}_{11}(\text{OH})]^{2-}$ -cluster anions each. The Cs1–H separations range from 302 to 316 pm ($8\times$) and CN = 12 is completed by four oxygen atoms ($d(\text{Cs1}-\text{O1}) = 299$ pm, $2\times$; $d(\text{Cs1}-\text{Ow}) = 310$ pm, $2\times$) (Fig. 64, *left*). A similar situation is realized for Cs2 with $d(\text{Cs2}-\text{H}) = 300 - 348$ pm ($10\times$) and $d(\text{Cs2}-\text{Ow}) = 332$ pm ($2\times$) (Fig. 64, *right*). The Cs3 cation in $4b$, however, is coordinated by five *quasi*-icosahedral boron cages arranged as trigonal bipyramid via hydrogen ($d(\text{Cs3}-\text{H}) = 313 - 350$ pm, $11\times$) and a single oxygen atom ($d(\text{Cs3}-\text{O1}) = 349$ pm) of the hydroxyl group (Fig. 65).

Another oxygen atom originating from the water molecule of hydration (Ow) at a distance of 319 pm completes the coordination sphere (CN = 13) of Cs3. In addition, all the Cs⁺ cations are linked together via Ow and O1 oxygen atoms to form a polymeric network in the crystal structure of Cs₂[B₁₂H₁₁(OH)] · H₂O. As a direct result Cs₂[B₁₂H₁₁(OH)] · H₂O displays a much lower water solubility than Cs₂[B₁₂H₁₂]. The B–B bond distances within the *quasi*-icosahedral [B₁₂H₁₁(OH)]²⁻-cluster anion cover the common interval (173 – 184 pm), but clearly reflect the distortion resulting from the monohydroxylation (d(B–H) = 109 – 111 pm; d(B–O1) = 129 pm). Among the known hydroxylated dodecahydro-*closo*-dodecaborates, this B–O bond length in the [B₁₂H₁₁(OH)]²⁻ anion in Cs₂[B₁₂H₁₁(OH)] · H₂O is significantly shorter than those in others (d(B–O) = 136 – 144 pm), despite a strong hydrogen bridge is found between the oxygen atom at the boron cage (O1) and the one of the water of hydration (Ow) (d(O1...Ow) = 297 pm) (Fig. 66).

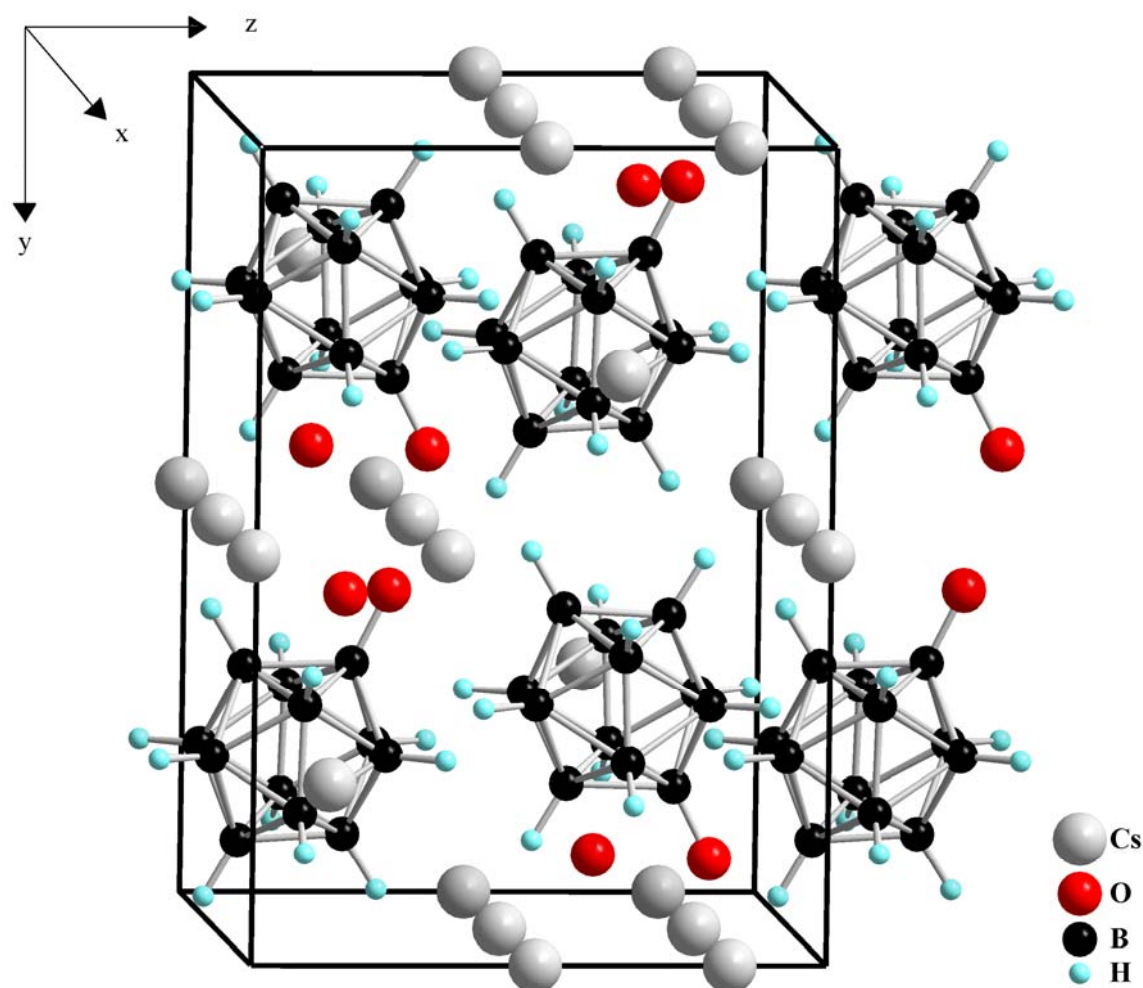


Fig. 63: Perspective view of the crystal structure of Cs₂[B₁₂H₁₁(OH)] · H₂O along [100]

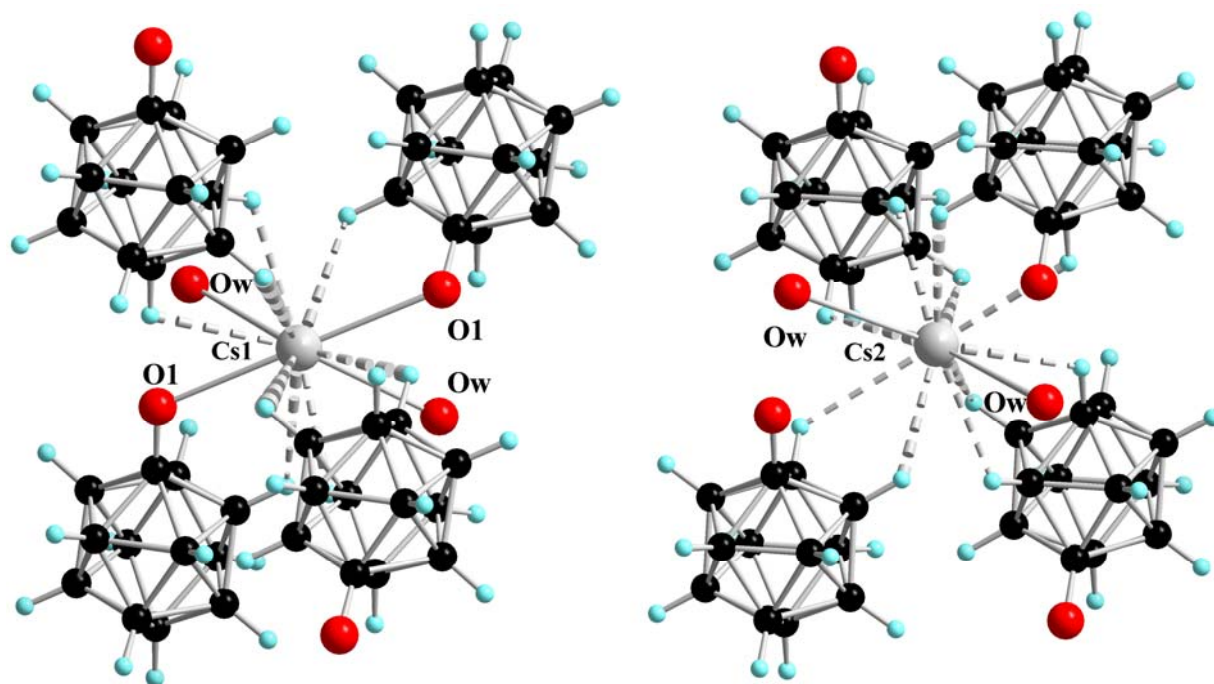


Fig. 64: View at the tetrahedral coordination spheres of boron cages around the Cs1 (CN = 12, *left*) and the Cs2 cations (CN = 12, *right*)

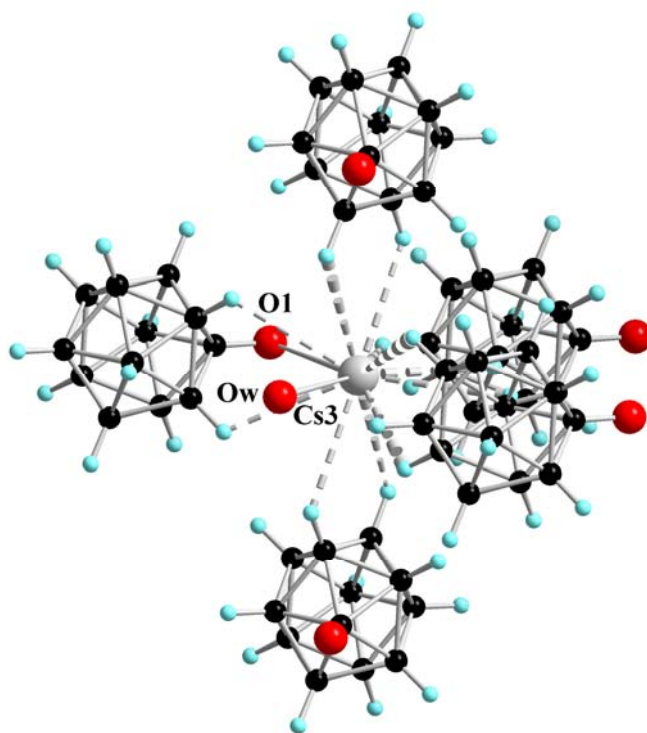


Fig. 65: View at the trigonal bipyramid of boron cages as coordination sphere of the Cs3 cation (CN = 13) in the crystal structure of $\text{Cs}_2[\text{B}_{12}\text{H}_{11}(\text{OH})] \cdot \text{H}_2\text{O}$

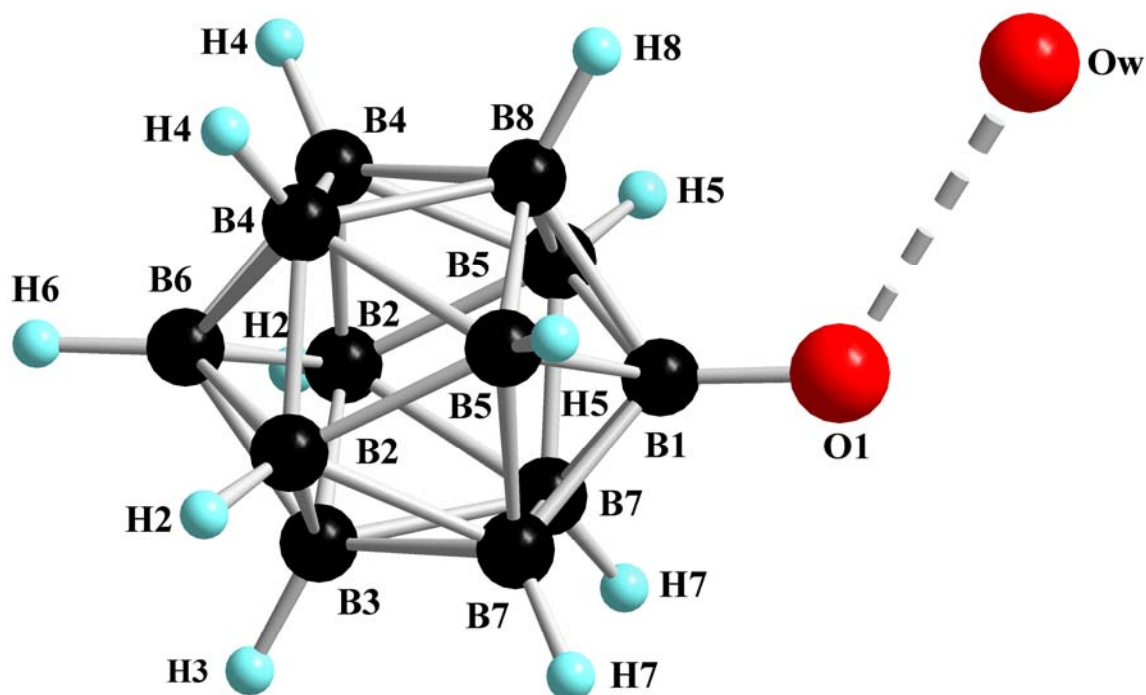


Fig. 66: The $O-H^{\delta+} \cdots \delta^-O$ hydrogen bond between the hydroxyl oxygen atom (O1) of the *quasi*-icosahedral $[B_{12}H_{11}(OH)]^{2-}$ -cluster anion and the one of the hydration water molecule (Ow) in the crystal structure of $Cs_2[B_{12}H_{11}(OH)] \cdot H_2O$

Table 65: Crystallographic data for $\text{Cs}_2[\text{B}_{12}\text{H}_{11}(\text{OH})] \cdot \text{H}_2\text{O}$ and their determination

Crystal system	orthorhombic
Space group	Ama2 (no. 40)
Unit cell parameters:	
a (pm)	1039.54(7)
b (pm)	1365.67(9)
c (pm)	958.16(6)
Number of formula units per unit cell	Z = 4
Calculated density ($D_x/\text{g cm}^{-3}$)	2.156
Molar volume ($V_m/\text{cm}^3 \text{ mol}^{-1}$)	204.8
Diffractometer	κ -CCD (Bruker-Nonius)
Radiation	Mo-K α : $\lambda = 71.07$ pm, graphite monochromator
Index range	$\pm h_{\max} = 13, \pm k_{\max} = 17, \pm l_{\max} = 12$
θ_{\max} (deg)	27.5
F(000)	800
Absorption coefficient (μ/mm^{-1})	5.33
Absorption correction	numerical, Program X-SHAPE [64]
Other data corrections	background, polarization and Lorentz factors
Collected reflections	10542
Unique reflections	1614
$R_{\text{int}}, R_{\sigma}$	0.081, 0.044
Structure solution and refinement	Program SHELXS-97 and SHELXL-97 [68]
Scattering factors	International Tables for Crystallography, Vol. C [87]
R_1, R_1 with $ F_o \geq 4\sigma(F_o)$	0.049, 0.039
Reflections with $ F_o \geq 4\sigma(F_o)$	1355
wR ₂ , Goodness of fit (GooF)	0.098, 1.071
Extinction (g)	0.0002(3)
Flack-x-parameter	0.369(2) (treatment as inversion twin)
Residual electron density (<i>max.</i> , <i>min.</i> in $\rho/e^{-1} 10^6$ pm)	1.41, -1.09

Table 66: Atomic coordinates for Cs₂[B₁₂H₁₁(OH)] · H₂O

Atom	Wyckoff position	x/a	y/b	z/c
Cs1 ^{a)}	4a	0	0	0.8355(1)
Cs2 ^{a)}	4a	0	0	0.4971(1)
Cs3	4b	1/4	0.1984(1)	0.1656(4)
O1	4b	1/4	0.1097(17)	0.8256(19)
Ow	4b	1/4	0.9321(6)	0.6767(45)
B1	4b	1/4	0.2044(18)	0.7589(43)
B2	4b	1/4	0.4119(15)	0.7545(35)
B3	8c	0.1094(6)	0.3684(5)	0.6566(30)
B4	8c	0.1651(19)	0.3047(11)	0.8175(24)
B5	8c	0.1636(17)	0.3029(9)	0.5153(14)
B6	8c	0.1109(6)	0.2373(5)	0.6735(30)
B7	4b	1/4	0.4044(21)	0.5713(37)
B8	4b	1/4	0.1932(16)	0.5707(43)
H2 ^{b)}	4b	1/4	0.481	0.812
H3 ^{b)}	8c	0.019	0.410	0.649
H4 ^{b)}	8c	0.111	0.306	0.916
H5 ^{b)}	8c	0.107	0.303	0.418
H6 ^{b)}	8c	0.027	0.194	0.618
H7 ^{b)}	4b	1/4	0.472	0.510
H8 ^{b)}	4b	1/4	0.125	0.510

^{a)} s.o.f. of Cs1: 0.58(6), s.o.f. of Cs2: 0.55(5);

^{b)} refinement with DFIX constraint ($d(\text{B-H}) = 110 \text{ pm}$); $U_{\text{iso}}(\text{H}) = 1.2 \cdot U_{\text{iso}}(\text{B})$.

Table 67: Anisotropic thermal displacement parameters^{a)} (U_{ij}/pm^2) for $\text{Cs}_2[\text{B}_{12}\text{H}_{11}(\text{OH})] \cdot \text{H}_2\text{O}$

Atom	U_{11}	U_{22}	U_{33}	U_{23}	U_{13}	U_{12}
Cs1	182(18)	289(16)	360(25)	0	0	86(9)
Cs2	257(21)	178(14)	409(25)	0	0	-47(9)
Cs3	181(3)	319(3)	280(30)	27(9)	0	0
O1	1202(149)	1331(148)	1195(137)	421(124)	0	0
Ow	345(38)	344(35)	806(129)	153(102)	0	0
B1	135(126)	185(99)	319(186)	-12(81)	0	0
B2	179(125)	57(67)	216(112)	-13(62)	0	0
B3	170(27)	183(26)	208(60)	25(61)	15(62)	24(21)
B4	129(92)	205(82)	583(126)	-17(73)	-1(83)	156(62)
B5	162(85)	229(76)	217(55)	-21(48)	2(52)	-83(52)
B6	127(26)	187(24)	229(53)	-24(63)	-37(70)	-9(21)
B7	183(131)	304(128)	223(141)	62(96)	0	0
B8	78(107)	68(81)	315(146)	-61(68)	0	0
H2	163					
H3	224					
H4	366					
H5	162					
H6	217					
H7	327					
H8	184					

^{a)} For Cs, O and B defined as anisotropic temperature factor according to: $\exp[-2\pi^2 (U_{11}h^2a^{*2} + U_{22}k^2b^{*2} + U_{33}l^2c^{*2} + 2U_{23}klb^*c^* + 2U_{13}hla^*c^* + 2U_{13}hka^*b^*)]$; for H isotropically defined as temperature factor in: $\exp[-8\pi^2(U_{\text{iso}}\sin^2\theta/\lambda^2)]$.

Table 68: Selected interatomic distances (d/pm) for Cs₂[B₁₂H₁₁(OH)] · H₂O

[(Cs1)O ₄ H ₈] polyhedron:			[(Cs2)O ₂ H ₁₀] polyhedron:			[(Cs3)O ₂ H ₁₁] polyhedron:		
Cs1	– O1	299.4 (2×)	Cs2	– Ow	332.0 (2×)	Cs3	– O1	346.9
	– Ow	309.6 (2×)		– H8	300.1 (2×)		– Ow	319.3
	– H4	302.0 (2×)		– H5	312.0 (2×)		– H4	313.3 (2×)
	– H5	310.4 (2×)		– H2	316.0 (2×)		– H3	316.1 (2×)
	– H6	311.2 (2×)		– H7	316.7 (2×)		– H5	318.7 (2×)
	– H3	333.8 (2×)		– H3	347.5 (2×)		– H8	319.4 (2×)
							– H6	329.2
							– H2	336.4
							– H7	349.6
[B ₁₂ H ₁₁ (OH)] ²⁻ anion:								
B1	– B4	172.4 (2×)	B2	– B7	175.8	B3	– B5	171.8
	– B6	172.2 (2×)		– B4	181.3 (2×)		– B7	174.4
	– B8	181.0		– B3	183.4 (2×)		– B6	179.8
	– O1	129.2		– H2	110.0		– B2	183.4
							– B4	186.2
							– H3	110.0
B4	– B1	172.4	B5	– B3	171.8	B6	– B1	172.1
	– B6	175.2		– B7	173.7		– B4	175.2
	– B4	176.6		– B5	179.7		– B3	179.8
	– B2	181.3		– B8	182.5		– B5	184.4
	– B3	186.2		– B6	184.4		– B8	185.1
	– H4	110.0		– H5	110.0		– H6	110.0
B7	– B5	173.7 (2×)				B8	– B1	181.0
	– B3	174.4 (2×)					– B5	182.5 (2×)
	– B2	175.8					– B6	185.1 (2×)
	– H7	110.0					– H8	110.0

4.2.4 Thermal Analysis of $\text{Cs}_2[\text{B}_{12}\text{H}_{11}(\text{OH})] \cdot \text{H}_2\text{O}$

The thermal stability of $\text{Cs}_2[\text{B}_{12}\text{H}_{11}(\text{OH})] \cdot \text{H}_2\text{O}$ was investigated by DTA/TG methods. The thermal dehydration of the investigated sample occurred at 125 °C with a small endothermic signal in the DTA and a peak in the TG curve corresponding to the complete dehydration (Fig. 67). After losing one crystal water molecule to form the dehydrated species $\text{Cs}_2[\text{B}_{12}\text{H}_{11}(\text{OH})]$, there is no change observed in the TG curve any more up to 906 °C, at which the boron cage begins to be destroyed. This reveals that the thermal stability of the monohydroxylated derivative $\text{Cs}_2[\text{B}_{12}\text{H}_{11}(\text{OH})]$ is very similar to that of $\text{Cs}_2[\text{B}_{12}\text{H}_{12}]$, which has a decomposition temperature of 908 °C [16, 85].

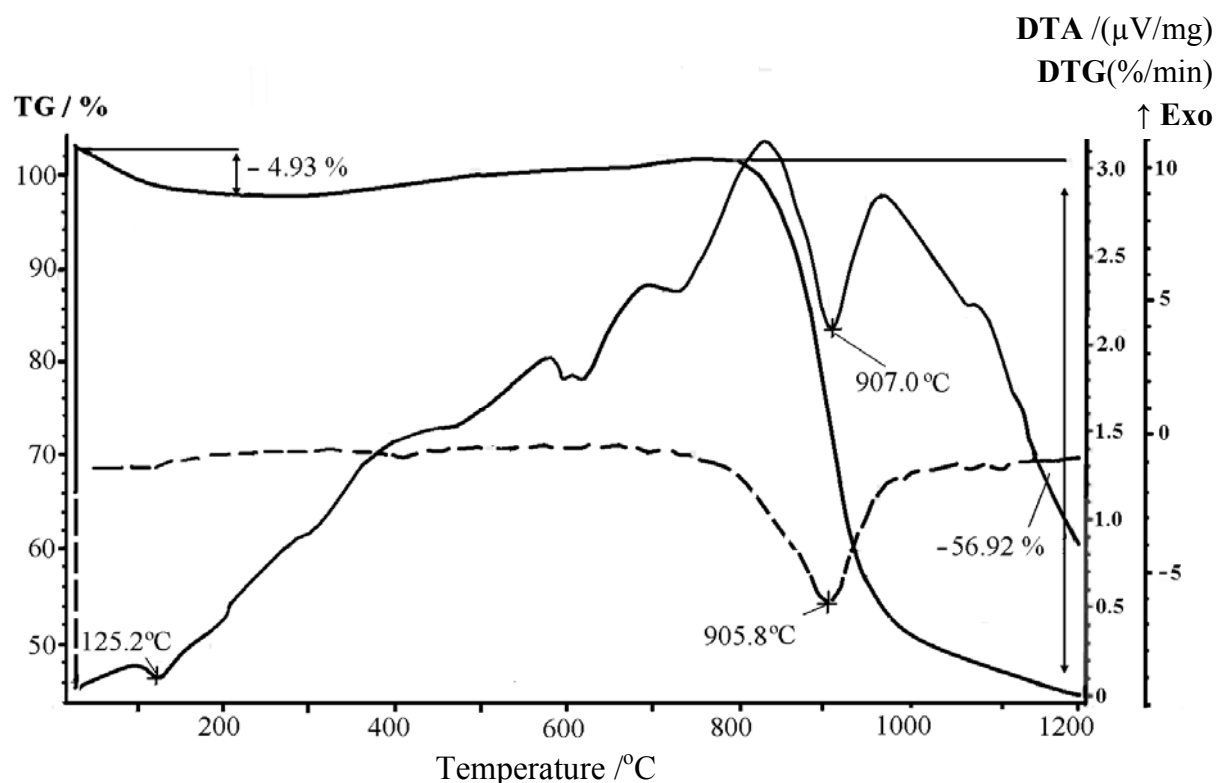


Fig. 67: DTA/TG diagram of $\text{Cs}_2[\text{B}_{12}\text{H}_{11}(\text{OH})] \cdot \text{H}_2\text{O}$ from room temperature up to 1200 °C

4.3 Dicesium 1,7-Dihydroxo-Decahydro-*closo*-Dodecaborate

The synthesis of dihydroxylated decahydro-*closo*-dodecaborate salts has been studied since the 1960s applying various preparation methods [16, 30, 48]. The aim of these investigations was not only to obtain the products with high yield, but also to prepare isomerically pure dihydroxylated decahydro-*closo*-dodecaborate species. Among them, the acid-catalyzed hydroxylation method of the *closo*-[B₁₂H₁₂]²⁻ anion pioneered by Hawthorne and coworkers is the only one that provides an isomer-pure [B₁₂H₁₀(OH)₂]²⁻-cluster anion [48]. Up to date, the syntheses and crystal structures of some functionalized derivatives of dihydroxylated *closo*-[B₁₂H₁₀(OH)₂]²⁻ anions were reported, such as dipyridinium 1,7-bis(methanesulfonyloxo)-decahydro-*closo*-dodecaborate and Cs₂[1,2-B₁₂H₁₀(ox)] · CH₃OH (ox: Oxalato) [21]. However, crystallographic data of dihydroxo-decahydro-*closo*-dodecaborate salts with both inorganic and organic cations in general and with the cesium cation in particular were not available in literature.

4.3.1 Synthesis of Cs₂[1,7-B₁₂H₁₀(OH)₂]

1 g dicesium dodecahydro-*closo*-dodecaborate, Cs₂[B₁₂H₁₂], is suspended in 20 ml water and 20 ml sulfuric acid (96 %) is added drop-wise to this mixture. The suspension is then stirred at 110 °C for 20 h, leading to a clear solution. This solution is slowly added with stirring to a slurry of 40 g CaCO₃ in 200 ml of water to neutralize the sulfuric acid. When the suspension is neutralized, the precipitated CaSO₄ is removed by filtration. The colourless, lath-shaped single crystals are obtained by evaporating the resulting filtrate at room temperature and double recrystallization from hot water. The result from the X-ray powder diffraction measurement shows that the dihydroxylated product of Cs₂[B₁₂H₁₂] using this preparation method contains only Cs₂[1,7-B₁₂H₁₀(OH)₂].

4.3.2 Structure Description of Cs₂[1,7-B₁₂H₁₀(OH)₂]

The title compound crystallizes in the orthorhombic space group Pnma (no. 62) with Z = 4 (Fig. 68). The cesium cations (Cs1 and Cs2) occupy two different crystallographic *Wyckoff* positions, namely 4c (x/a, y/b = 1/4, z/c; site symmetry: .m.) and half-occupied 8d (x/a, y/b, z/c; site symmetry: 1; site occupancy: 0.43). The oxygen atoms O1 and O2 also reside at the

two *Wyckoff* positions 4*c* and 8*d* (site occupancy: 0.58), respectively. The same holds for the boron and hydrogen atoms of the $[\text{B}_{12}\text{H}_{10}(\text{OH})_2]^{2-}$ -cluster anions occupying the *Wyckoff* positions 4*c* and 8*d* as well. The centers of gravity of the $[\text{B}_{12}\text{H}_{10}(\text{OH})_2]^{2-}$ -cluster anions are found at the *Wyckoff* position 4*c* with distances of 171 pm to each of the twelve boron atoms of the *quasi*-icosahedral B_{12} cage. The $(\text{Cs}1)^+$ cations located at the 4*c* site are surrounded by five neighbouring boron cages arranged as a trigonal pyramid, which coordinate via ten, in fact eleven hydrogen atoms and three, in fact only two hydroxyl oxygen atoms ($d(\text{Cs}1\text{--H}) = 307 - 327$ pm (10 \times), $d(\text{Cs}1\text{--O}) = 313 - 383$ pm (2 \times)) (Fig. 69, *left*). The two boron cages at the apical axis are coordinating to this cesium cation via one hydroxyl oxygen atom (mix occupied O2) and two hydrogen atoms per each. Moreover, the $(\text{Cs}1)^+$ cation is linked to two other boron cages located at equatorial positions each via three hydrogen atoms. Finally, one hydroxyl oxygen atom (O1) of the last equatorial boron cage with the longest Cs–O distance of 383 pm completes the coordination sphere (CN = 13) of $(\text{Cs}1)^+$. The half-occupied $(\text{Cs}2)^+$ cations, which have CN = 12, are nearly coplanar surrounded with four nearest boron cages via ten hydrogen atoms and two hydroxyl oxygen atoms ($d(\text{Cs}2\text{--H}) = 291 - 421$ pm (10 \times), $d(\text{Cs}2\text{--O}) = 288$ pm (2 \times)) (Fig. 69, *right*). All $(\text{Cs}2)^+$ cations are coordinated to two boron cages via three hydrogen atoms of a triangular face per each and to two others via two hydrogen atoms and one hydroxyl oxygen atom (mix occupied O2) per each. Similar to the case of $\text{Cs}_2[\text{B}_{12}\text{H}_{11}(\text{OH})] \cdot \text{H}_2\text{O}$, all Cs^+ cations are linked together via hydroxyl oxygen atoms to form a polymeric network in the crystal structure of $\text{Cs}_2[\text{B}_{12}\text{H}_{12}(\text{OH})_2]$. Each boron cage thereby connects to four neighbouring ones via strong $\text{O}\text{--H}^{\delta+}\cdots\delta^-\text{O}$ hydrogen bridges between their hydroxyl oxygen atoms as donors and acceptors to form a pyramid (Fig. 70, *left*). In this pyramid the center of gravity of a considered boron cage is slightly off from the plane of the four others. One hydroxyl oxygen atom (mix occupied O2) of each of two neighbouring boron cages is linked to another hydroxyl oxygen atom (O1) of the apical $[\text{B}_{12}\text{H}_{10}(\text{OH})_2]^{2-}$ -cluster anion. In contrast each two other boron cages have one hydroxyl oxygen atom (O1) per each connecting to one hydroxyl oxygen atom (mix occupied O2) of the apical $[\text{B}_{12}\text{H}_{10}(\text{OH})_2]^{2-}$ -cluster anion ($d(\text{O}1\cdots\text{O}2) = 292$ pm (4 \times)). Thus, the boron cages in this crystal structure are hydrogen-bond linked together to form layers that spread out perpendicular to the *a* axis. Comparing to other hydroxylated cesium salts $\text{Cs}_2[\text{B}_{12}\text{H}_{12-n}(\text{OH})_n] \cdot x \text{H}_2\text{O}$ ($n = 1 - 4, 12$), there are no strong hydrogen bridges between the hydroxyl oxygen atoms at the boron cage and for instance the ones of lacking “zeolitic” or coordinating crystal

water molecules in $\text{Cs}_2[\text{B}_{12}\text{H}_{10}(\text{OH})_2]$. The existence of a polymeric network consisting of hydrogen bonds between the boron cages and linkages between the Cs^+ cations in $\text{Cs}_2[\text{B}_{12}\text{H}_{10}(\text{OH})_2]$ is an explanation for the tendency of increasingly high lattice energy of the densely packed salts with the higher degree of hydroxylation of the *closo*- $[\text{B}_{12}\text{H}_{12}]^{2-}$ anions with respect to the hydration enthalpy of the ions upon solvation. This polymeric network might or might not include even “zeolitic” water molecules as observed in $\text{Cs}_2[\text{B}_{12}\text{H}_{11}(\text{OH})] \cdot \text{H}_2\text{O}$, but not so in $\text{Cs}_2[\text{B}_{12}\text{H}_{10}(\text{OH})_2]$, respectively. The *quasi*-icosahedral $[\text{B}_{12}\text{H}_{10}(\text{OH})_2]^{2-}$ -cluster anion is of course distorted in comparison to the parent $[\text{B}_{12}\text{H}_{12}]^{2-}$ species with B–B and B–O bond lengths in the range of 174 – 190 pm and 141 – 143 pm, respectively (Fig. 70, *right*). There are two possible orientations of 1,7-isomer obtained from the crystal structure analysis, due to the fact that the hydroxyl oxygen atoms O2 statistically bond to *two* boron atoms respected to the *ipso*-boron atom carrying O1. On the other hand, the $^{11}\text{B}\{^1\text{H}\}$ -NMR spectrum of $\text{Cs}_2[\text{B}_{12}\text{H}_{10}(\text{OH})_2]$ in D_2O consists of five signals in the intensity ratio 2:2:4:2:2 at 3.2, –15.1, –17.6, –20.2 and –23.7 ppm and the ^{11}B NMR spectrum indicates a singlet at 3.3 ppm along with four doublets. The first five signals, together with the relative intensity ratio between them, result from the C_{2v} point symmetry of the $[\text{B}_{12}\text{H}_{10}(\text{OH})_2]^{2-}$ -cluster anion. For such a cage, only two isomers, 1,2 and 1,7 namely, exhibit this point symmetry. Thus, there are two possible isomers obtained from the one-dimensional NMR measurement. The exact isomer of $\text{Cs}_2[\text{B}_{12}\text{H}_{10}(\text{OH})_2]$ is normally elucidated by two-dimensional NMR measurements. However, by combining the above results of crystal structure analysis and one-dimensional NMR measurements, the studied $\text{Cs}_2[\text{B}_{12}\text{H}_{10}(\text{OH})_2]$ is concluded to contain the 1,7-isomer exclusively.

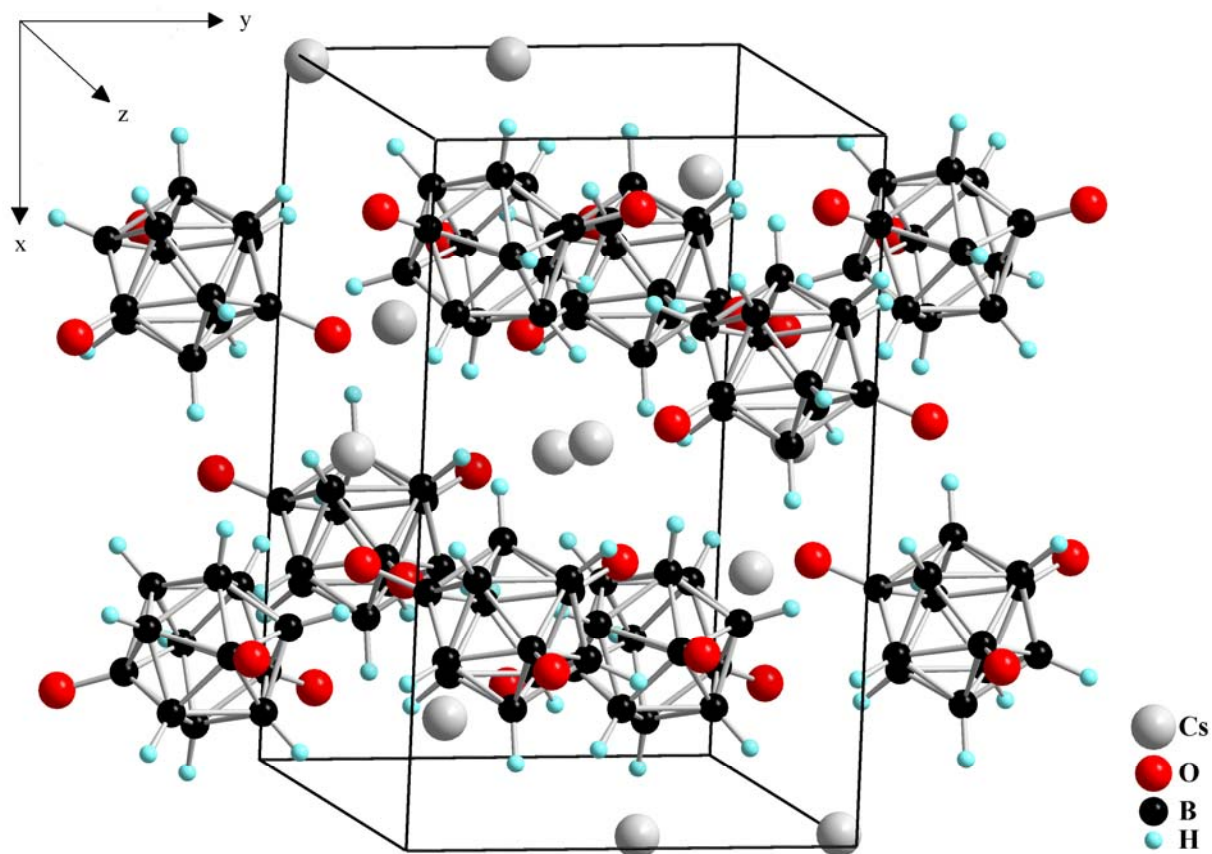


Fig. 68: Perspective view at the unit cell of $\text{Cs}_2[1,7\text{-B}_{12}\text{H}_{10}(\text{OH})_2]$ along $[001]$

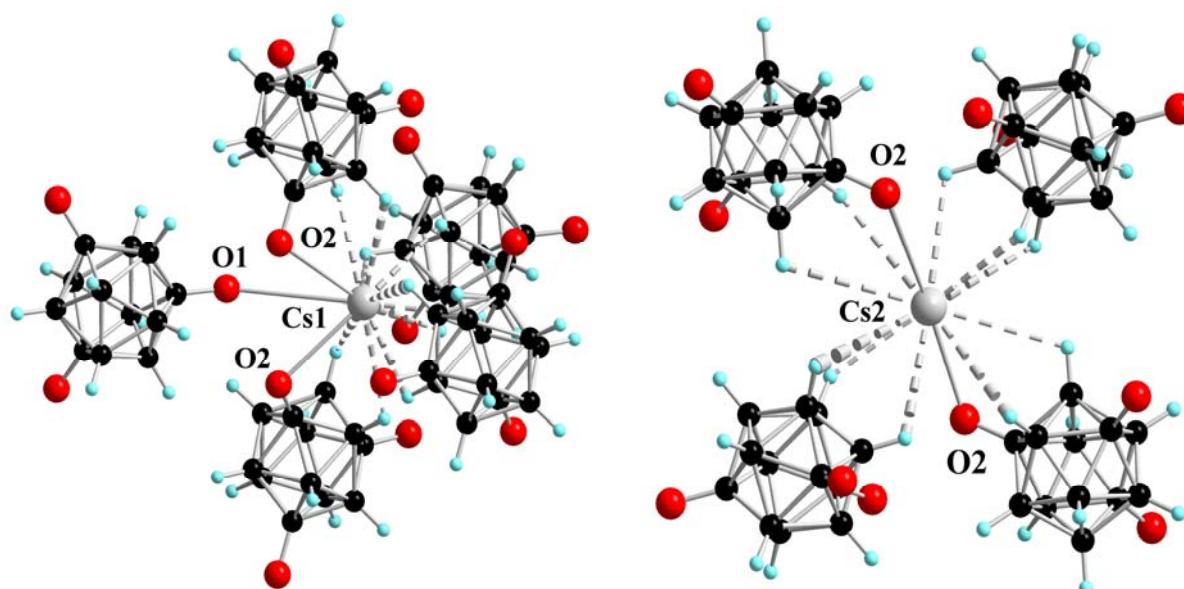


Fig. 69: View at the coordination spheres of the $(\text{Cs1})^+$ (left) and the $(\text{Cs2})^+$ cations (right) in the crystal structure of $\text{Cs}_2[1,7\text{-B}_{12}\text{H}_{10}(\text{OH})_2]$

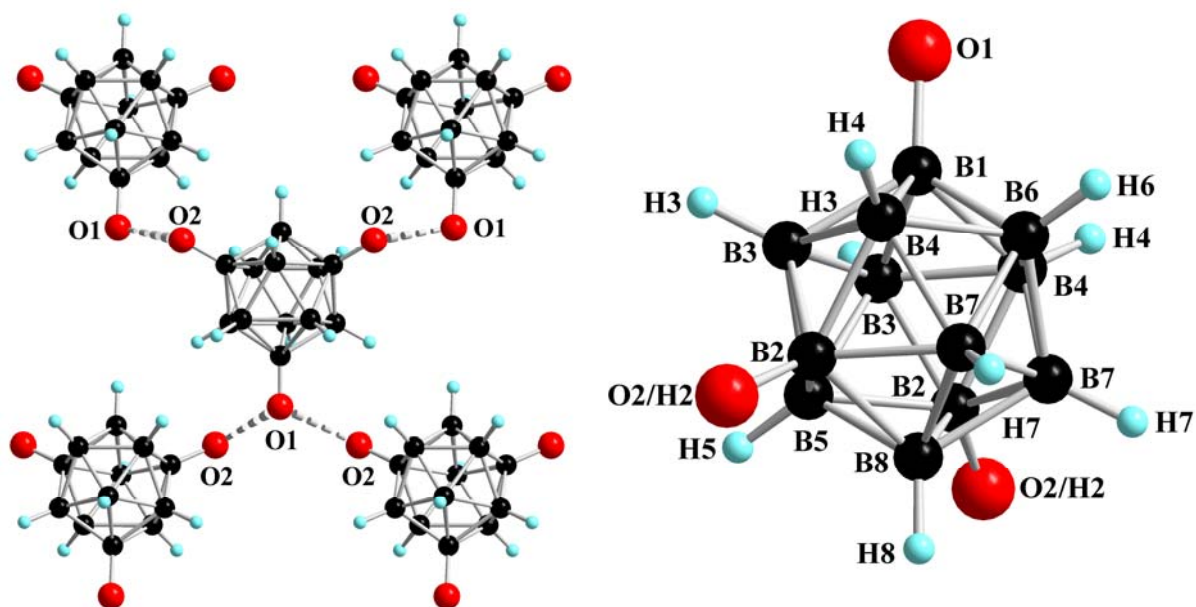


Fig. 70: Sketch of the strong $\text{O}-\text{H}^{\delta+}\cdots\delta^-\text{O}$ hydrogen bridging bonds (*left*) and the *quasi*-icosahedral $[1,7-\text{B}_{12}\text{H}_{10}(\text{OH})_2]^{2-}$ -cluster anion (*right*) in the crystal structure of $\text{Cs}_2[1,7-\text{B}_{12}\text{H}_{10}(\text{OH})_2]$

Table 69: Crystallographic data for Cs₂[1,7-B₁₂H₁₀(OH)₂] and their determination

Crystal system	orthorhombic
Space group	Pnma (no. 62)
Unit cell parameters:	
a (pm)	1429.60(9)
b (pm)	929.38(6)
c (pm)	1030.70(7)
Number of formula units per unit cell	Z = 4
Calculated density (D _x /g cm ⁻³)	2.132
Molar volume (V _m /cm ³ mol ⁻¹)	206.2
Diffractometer	κ-CCD (Bruker-Nonius)
Radiation	Mo-Kα: λ = 71.07 pm, graphite monochromator
Index range	±h _{max} = 18, ±k _{max} = 12, ±l _{max} = 13
θ _{max} (deg)	27.5
F(000)	792
Absorption coefficient (μ/mm ⁻¹)	5.29
Absorption correction	numerical, Program X-SHAPE [64]
Other data corrections	background, polarization and <i>Lorentz</i> factors
Collected reflections	21162
Unique reflections	1665
R _{int} , R _σ	0.047, 0.018
Structure solution and refinement	Program SHELXS-97 and SHELXL-97 [68]
Scattering factors	International Tables for Crystallography, Vol. C [87]
R ₁ , R ₁ with F _o ≥ 4σ(F _o)	0.087, 0.085
Reflections with F _o ≥ 4σ(F _o)	1568
wR ₂ , Goodness of fit (GooF)	0.268, 1.151
Extinction (g)	0.011(2)
Residual electron density (<i>max.</i> , <i>min.</i> in ρ/e ⁻¹ 10 ⁶ pm)	3.66, -1.50

Table 70: Atomic coordinates for Cs₂[1,7-B₁₂H₁₀(OH)₂]

Atom	Wyckoff position	x/a	y/b	z/c
Cs1	4 <i>c</i>	0.3828(1)	¹ / ₄	0.0279(1)
Cs2 ^{a)}	8 <i>d</i>	0.5117(2)	0.0260(3)	0.4578(3)
O1	4 <i>c</i>	0.2283(13)	¹ / ₄	0.3311(18)
O2 ^{b)} /H2	8 <i>d</i>	0.3690(10)	0.0359(16)	0.2615(15)
B1	4 <i>c</i>	0.2147(15)	¹ / ₄	0.4685(19)
B2	8 <i>d</i>	0.3365(10)	0.9088(15)	0.2012(14)
B3	8 <i>d</i>	0.1258(11)	0.1478(15)	0.5454(16)
B4	8 <i>d</i>	0.2417(10)	0.0931(14)	0.5624(13)
B5	4 <i>c</i>	0.0908(14)	¹ / ₄	0.6913(22)
B6	4 <i>c</i>	0.3118(15)	¹ / ₄	0.5792(22)
B7	8 <i>d</i>	0.2812(9)	0.1532(15)	0.7205(15)
B8	4 <i>c</i>	0.1921(16)	¹ / ₄	0.7993(21)
H3 ^{c)}	8 <i>d</i>	0.076	0.082	0.490
H4 ^{c)}	8 <i>d</i>	0.268	-0.006	0.518
H5 ^{c)}	4 <i>c</i>	0.018	¹ / ₄	0.728
H6 ^{c)}	4 <i>c</i>	0.385	¹ / ₄	0.544
H7 ^{c)}	8 <i>d</i>	0.332	0.090	0.777
H8 ^{c)}	4 <i>c</i>	0.183	¹ / ₄	0.906

^{a)} s.o.f. of Cs2: 0.43(1), ^{b)} s.o.f. of O2: 0.58(3);

^{c)} refinement with DFIX constraint ($d(\text{B-H}) = 110 \text{ pm}$); $U_{\text{iso}}(\text{H}) = 1.2 \cdot U_{\text{iso}}(\text{B})$.

Table 71: Anisotropic thermal displacement coefficients^{a)} (U_{ij}/pm^2) for $\text{Cs}_2[1,7\text{-B}_{12}\text{H}_{10}(\text{OH})_2]$

Atom	U_{11}	U_{22}	U_{33}	U_{23}	U_{13}	U_{12}
Cs1	436(7)	342(7)	519(8)	0	-7(5)	0
Cs2	668(18)	594(19)	827(20)	-53(13)	-132(14)	292(13)
O1	687(105)	765(124)	634(104)	0	84(88)	0
O2/H2	1064(118)	736(96)	942(106)	14(88)	96(91)	-240(87)
B1	391(100)	356(100)	343(94)	0	1(79)	0
B2	376(67)	282(62)	452(72)	4(57)	-15(58)	-27(55)
B3	518(85)	215(57)	537(84)	-21(59)	66(67)	-36(60)
B4	418(69)	231(59)	388(67)	27(52)	22(55)	-25(53)
B5	334(92)	293(86)	506(114)	0	45(84)	0
B6	365(101)	463(118)	506(120)	0	-64(94)	0
B7	324(60)	337(62)	478(75)	52(60)	-30(56)	52(55)
B8	504(121)	429(108)	366(100)	0	55(88)	0
H3	52					
H4	41					
H5	45					
H6	51					
H7	46					
H8	52					

^{a)} For Cs, O and B defined as anisotropic temperature factor according to: $\exp[-2\pi^2 (U_{11}h^2a^{*2} + U_{22}k^2b^{*2} + U_{33}l^2c^{*2} + 2U_{23}klb^{*}c^{*} + 2U_{13}hla^{*}c^{*} + 2U_{13}hka^{*}b^{*})]$; for H isotropically defined as temperature factor in: $\exp[-8\pi^2(U_{\text{iso}}\sin^2\theta/\lambda^2)]$.

Table 72: Selected interatomic distances (d/pm) for Cs₂[1,7-B₁₂H₁₀(OH)₂]

[(Cs1)O ₃ H ₁₀] polyhedron:			[(Cs2)O ₂ H ₁₀] polyhedron:		
Cs1	– O2/H2	312.9 (2×)	Cs2	– O2/H2	287.5 (2×)
	– O1	382.8		– H6	290.5
	– H7	307.0 (2×)		– H6'	296.4
	– H8	312.7		– H4	316.3
	– H4	313.0 (2×)		– H7	346.1
	– H3	316.6 (2×)		– H8	350.6
	– H3'	317.9 (2×)		– H5	352.2
	– H5	326.7		– H4'	355.2
				– H8'	382.1
				– H5'	385.7
				– H7'	421.2
[1,7-B ₁₂ H ₁₀ (OH) ₂] ²⁻ anion:					
B1	– B3	177.4 (2×)	B2	– B3	176.3
	– B6	179.0		– B7	177.4
	– B4	179.8 (2×)		– B4	178.7
	– O1	145.0		– B5	182.2
				– B8	183.8
				– O2	142.5
B4	– B3	173.5	B5	– B2	182.2 (2×)
	– B6	177.6		– B8	183.6
	– B2	178.7		– B3	184.2 (2×)
	– B1	179.8		– H5	110.0
	– B7	180.1			
	– H4	110.0			
B7	– B8	175.2	B8	– B7	175.2 (2×)
	– B6	176.6		– B5	183.6
	– B2	177.4		– B2	183.8 (2×)
	– B7	179.8		– H8	110.0
	– B4	180.1			
	– H7	110.0			

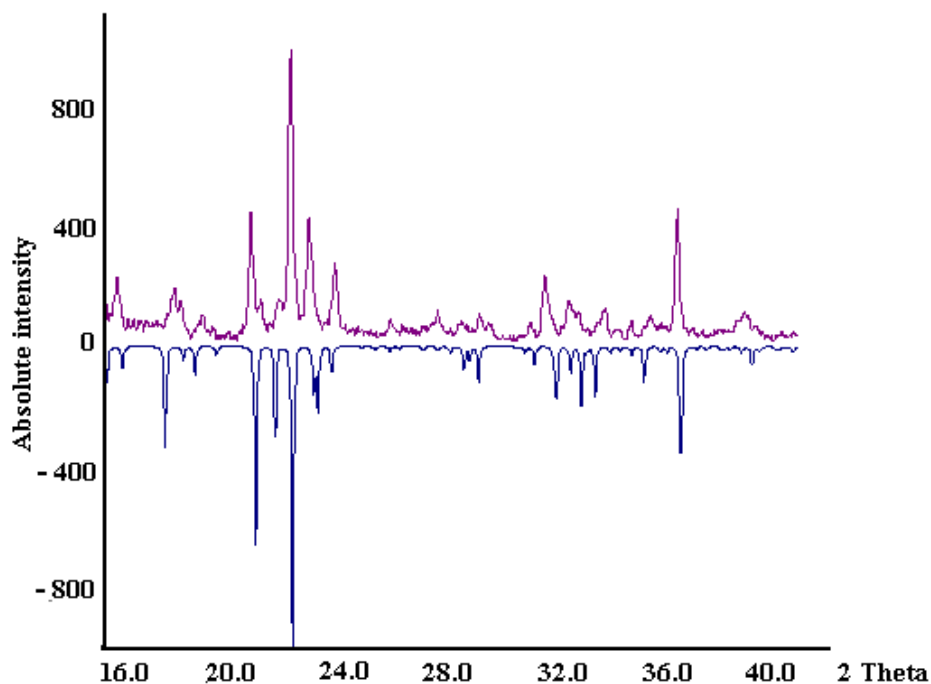


Fig. 71: Comparison of the measured powder X-ray diffractogram of $\text{Cs}_2[1,7\text{-B}_{12}\text{H}_{10}(\text{OH})_2]$ (*above*) and the simulated one (*below*)

4.3.3 Thermal Analysis of $\text{Cs}_2[1,7\text{-B}_{12}\text{H}_{10}(\text{OH})_2]$

The thermal stability of single-phase $\text{Cs}_2[1,7\text{-B}_{12}\text{H}_{10}(\text{OH})_2]$ was investigated by DTA/TG methods in argon atmosphere. Because of the high isomeric and crystalline phase purity of the sample examined by NMR and X-ray powder diffraction measurements (see Fig. 71), respectively, it is reasonable to expect that the thermal behaviour of the sample is really characteristic for $\text{Cs}_2[1,7\text{-B}_{12}\text{H}_{10}(\text{OH})_2]$ only. Although some exothermic and endothermic signals are observed in the DTA curve, there is no thermal decomposition of the investigated sample up to 878 °C in the TG curve (Fig. 72). Thus the signals observed in the DTA experiment can be referred to the occurrence of phase transitions of the investigated compound. Thus $\text{Cs}_2[1,7\text{-B}_{12}\text{H}_{10}(\text{OH})_2]$ is obviously a non-solvent containing thermally very stable compound. The boron cage of $\text{Cs}_2[1,7\text{-B}_{12}\text{H}_{10}(\text{OH})_2]$ is going to be destroyed at 878 °C. This temperature value is comparable to that of $\text{Cs}_2[\text{B}_{12}\text{H}_{11}(\text{OH})] \cdot \text{H}_2\text{O}$ (906 °C) and $\text{Cs}_2[\text{B}_{12}\text{H}_{12}]$ (908 °C) [85]. Thermal analyses of $\text{Cs}_2[\text{B}_{12}\text{H}_{11}(\text{OH})] \cdot \text{H}_2\text{O}$ and $\text{Cs}_2[1,7\text{-B}_{12}\text{H}_{10}(\text{OH})_2]$ show that the thermal stability of the boron cage is not considerably influenced by replacing one or two hydrogen atoms of the parent $[\text{B}_{12}\text{H}_{12}]^{2-}$ by OH groups.

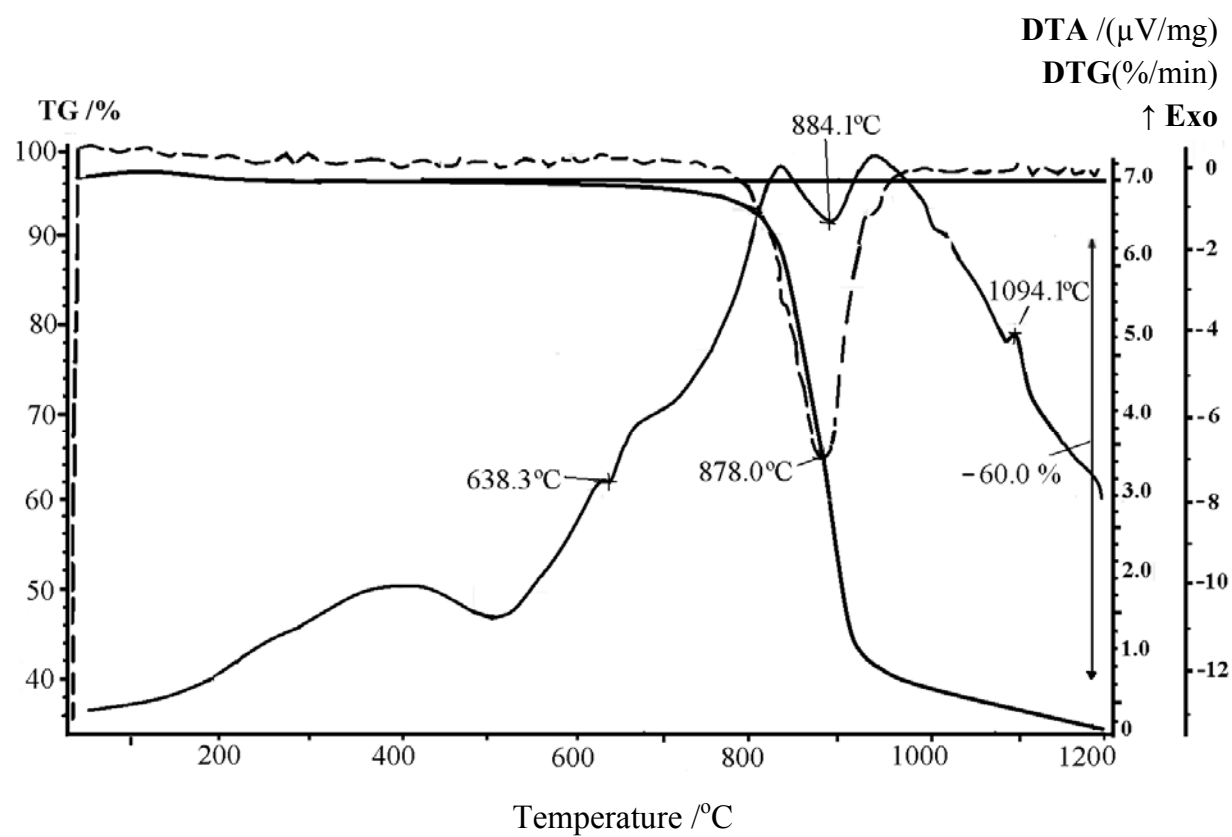


Fig. 72: DTA/TG diagram of $\text{Cs}_2[1,7\text{-B}_{12}\text{H}_{10}(\text{OH})_2]$ from room temperature up to 1200 $^{\circ}\text{C}$

4.4 Dicesium 1,2,3-Trihydroxo-Enneahydro-*closo*-Dodecaborate Monohydrate

4.4.1 Synthesis of $\text{Cs}_2[1,2,3\text{-B}_{12}\text{H}_9(\text{OH})_3] \cdot \text{H}_2\text{O}$

$\text{Cs}_2[\text{B}_{12}\text{H}_9(\text{OH})_3] \cdot \text{H}_2\text{O}$ is synthesized readily by stirring 1 g of $\text{Cs}_2[\text{B}_{12}\text{H}_{12}]$ with 3 ml H_2O_2 (30 %) in aqueous solution at 65 °C for 8 hours. Colourless, polyhedrally shaped single crystals are obtained by isothermal evaporation of resulting solution at room temperature.

4.4.2 Structure Description of $\text{Cs}_2[1,2,3\text{-B}_{12}\text{H}_9(\text{OH})_3] \cdot \text{H}_2\text{O}$

The title compound $\text{Cs}_2[\text{B}_{12}\text{H}_9(\text{OH})_3] \cdot \text{H}_2\text{O}$ crystallizes orthorhombically in space group *Pbcm* (no. 57) with $Z = 4$ (Fig. 73). The cesium cations in this crystal structure occupy three different *Wyckoff* positions ($2 \times 4c + 1 \times 4d$) with both of $4c$ sites half-occupied only. The boron (B1 – B8) and the hydrogen atoms (H3 – H8) of the $[\text{B}_{12}\text{H}_9(\text{OH})_3]^{2-}$ -cluster anions are located at the *Wyckoff* positions $4d$ and $8e$. The centers of gravity of the cage anions reside at the *Wyckoff* site $4d$. The oxygen atoms of the crystal water molecules (Ow) reside at the *Wyckoff* position $4d$ ($x/a, y/b, z/c = 1/4$; site symmetry: $\dots m$), and the two oxygen atoms (O1 and O2) of the three hydroxyl groups of each $[\text{B}_{12}\text{H}_9(\text{OH})_3]^{2-}$ -cluster anion occupy the *Wyckoff* sites $4d$ and $8e$ ($x/a, y/b, z/c$; site symmetry: 1), respectively. So three hydroxyl groups originate from two crystallographically different hydroxyl oxygen atoms of one triangular face of the $[\text{B}_{12}\text{H}_9(\text{OH})_3]^{2-}$ -cluster anion. As a consequence, this $[\text{B}_{12}\text{H}_9(\text{OH})_3]^{2-}$ species is assigned to the 1,2,3-isomer from the crystal structure analysis. Cs1 and Cs2 (both are located at $4c$: $x/a, y/b = 1/4, z/c = 0$; site symmetry: $2\dots$) exhibit coordination numbers of twelve and each one is tetrahedrally surrounded by four $[1,2,3\text{-B}_{12}\text{H}_9(\text{OH})_3]^{2-}$ anions via hydrogen and oxygen atoms of the boron cages as well as oxygen atoms of the crystal water molecules. The $(\text{Cs1})^+$ cation is coordinated by ten hydrogen atoms of the four nearest boron cages ($d(\text{Cs1-H}) = 308 - 338$ pm, $10\times$) and two oxygen atoms of crystal water molecules ($d(\text{Cs1-Ow}) = 328$ pm, $2\times$) (Fig. 74, left). The $(\text{Cs2})^+$ cation has contact to six hydrogen atoms of the boron cages with the Cs2-H distances in the range of $317 - 348$ pm ($6\times$) and to six oxygen atoms ($d(\text{Cs2-Ow}) = 313$ pm, $2\times$; $d(\text{Cs2-O1}) = 283$ pm, $2\times$; $d(\text{Cs2-O2}) = 303$ pm, $2\times$) (Fig. 74, right). The $(\text{Cs3})^+$ cations located at $4d$, however, are surrounded by five boron cages arranged as a trigonal bipyramid grafting via hydrogen ($d(\text{Cs3-H}) = 314 - 350$ pm, $9\times$) and oxygen atoms ($d(\text{Cs3-O}) = 317 - 328$ pm, $4\times$) with $\text{CN} = 13$ (Fig. 75, left). Considering two boron cages as apical positions of this trigonal bipyramid, the central $(\text{Cs3})^+$

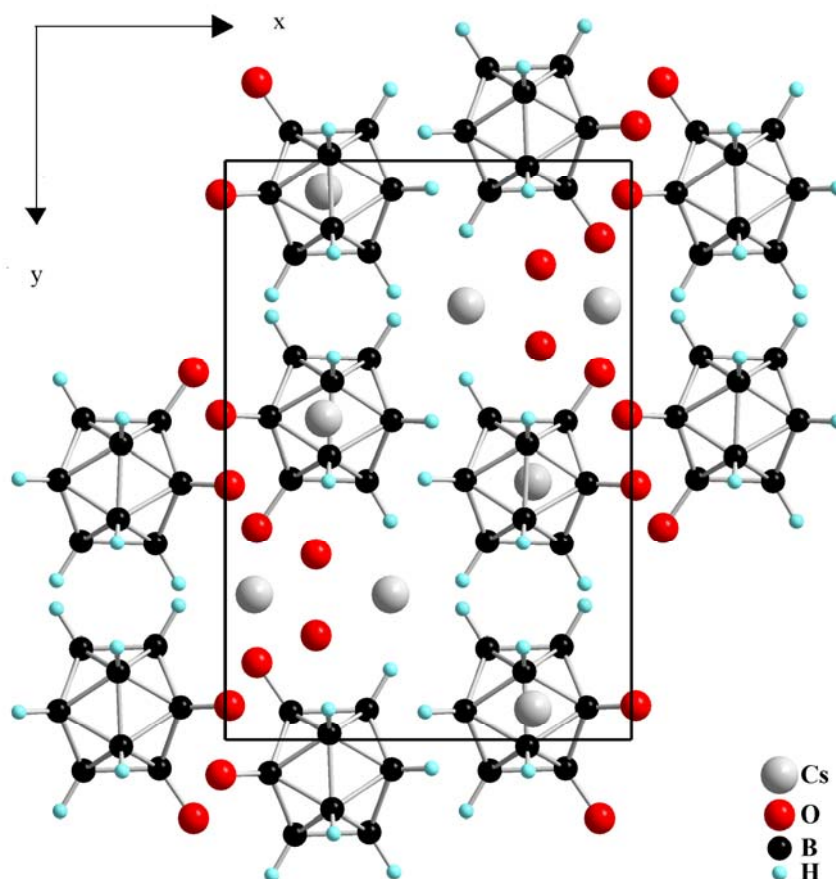


Fig. 73: Perspective view at the unit cell of $\text{Cs}_2[1,2,3\text{-B}_{12}\text{H}_9(\text{OH})_3] \cdot \text{H}_2\text{O}$ along $[001]$

cation coordinates to both cages via three hydrogen atoms originating from one triangular face each. Another one at an equatorial position is attached via three hydroxyl oxygen atoms of a single triangular face. Each of the remaining two boron cages at the equatorial positions coordinates to this cation via two hydrogen atoms as edges of each cage. CN = 13 for the $(\text{Cs}3)^+$ cation is completed by one oxygen atom (O_w) of a crystal water molecule with $d(\text{Cs}3\text{--}\text{O}_w) = 322$ pm. These crystallographically distinct cesium cations in this crystal structure are linked together via hydroxyl oxygen atoms and oxygen atoms of crystal water molecules to form a polymeric network. The *quasi*-icosahedral $[1,2,3\text{-B}_{12}\text{H}_9(\text{OH})_3]^{2-}$ anion is slightly distorted with B–B and B–O bond lengths ranging from 176 to 180 pm and from 136 to 144 pm, respectively (Fig. 75, *right*), while all B–H bond lengths are fixed at 110 pm by constraint. The hydroxyl oxygen atoms of each boron cage are linked to hydroxyl oxygen atoms of other neighbouring boron cages or oxygen atoms of the crystal water molecules via strong $\text{O}\text{--}\text{H}^{\delta+}\cdots\delta^-\text{O}$ hydrogen bridges indicated by $d(\text{O}\cdots\text{O}) = 261 - 307$ pm as donor-acceptor distances. Non-classical “dihydrogen bridges” are also found in the crystal structure of

$\text{Cs}_2[1,2,3\text{-B}_{12}\text{H}_9(\text{OH})_3] \cdot \text{H}_2\text{O}$ between the negatively polarized cage hydrogen atoms and the hydrogen atoms of the crystal water molecules as well as the hydroxyl hydrogen atoms of other neighbouring boron cages ($d(\text{B-H}^{\delta-} \cdots \delta^+\text{H-O}) = 326 - 407 \text{ pm}$) with reversed polarity.

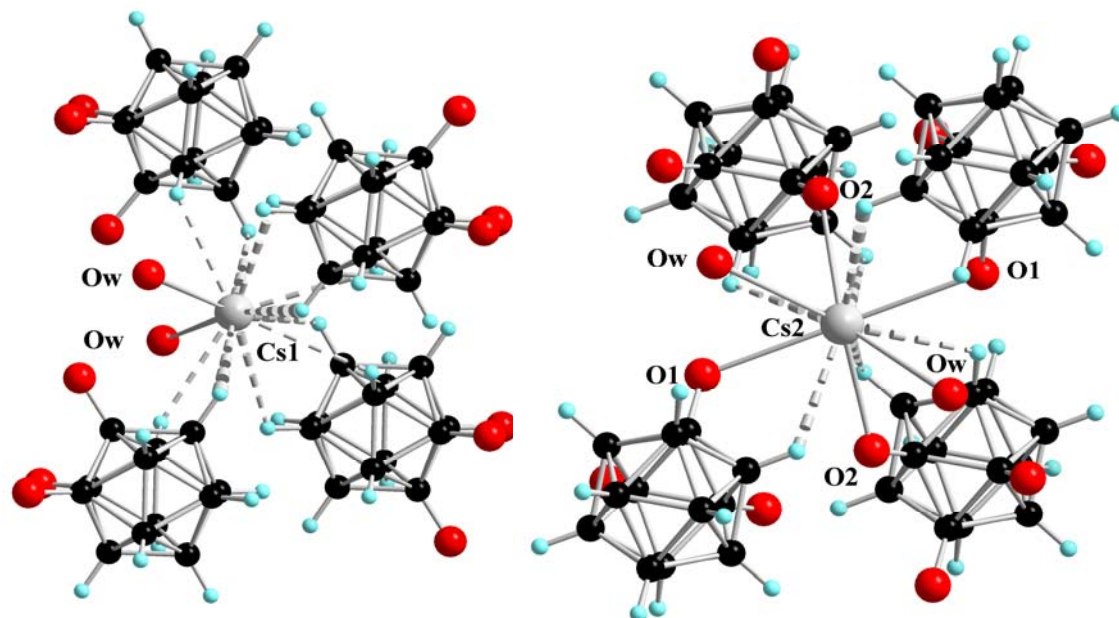


Fig. 74: View at the tetrahedral coordination spheres of the $(\text{Cs1})^+$ (*left*) and the $(\text{Cs2})^+$ (*right*) both with CN = 12

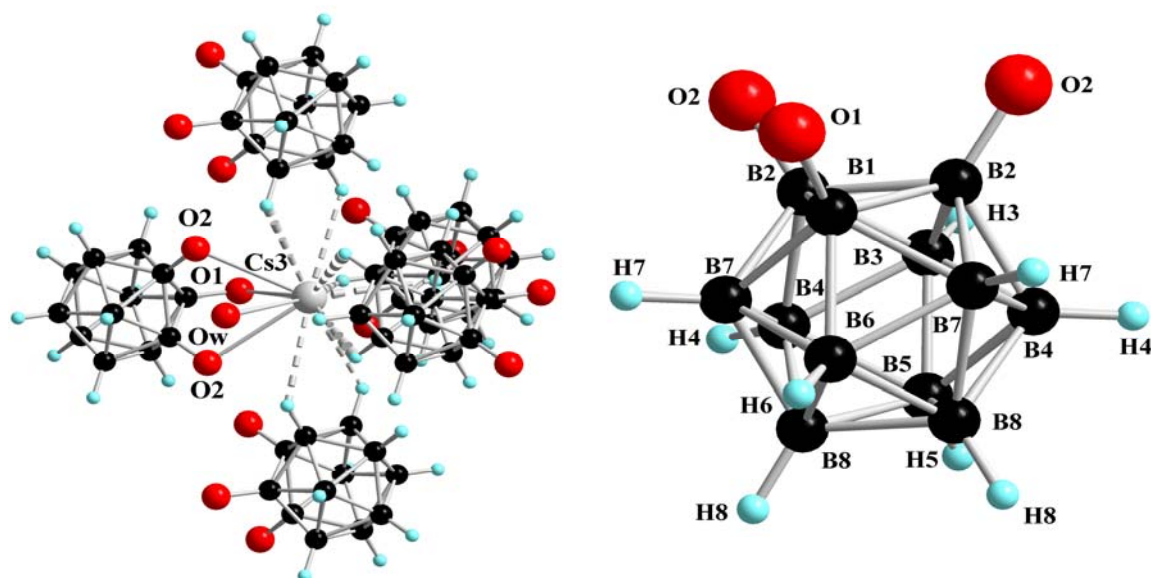


Fig. 75: Trigonal-bipyramidal coordination sphere of the $(\text{Cs3})^+$ cation (*left*) and the *quasi*-icosahedral $[1,2,3\text{-B}_{12}\text{H}_9(\text{OH})_3]^{2-}$ -cluster anion (*right*) in the crystal structure of $\text{Cs}_2[1,2,3\text{-B}_{12}\text{H}_9(\text{OH})_3] \cdot \text{H}_2\text{O}$

Table 73: Crystallographic data for $\text{Cs}_2[1,2,3\text{-B}_{12}\text{H}_9(\text{OH})_3] \cdot \text{H}_2\text{O}$ and their determination

Crystal system	orthorhombic
Space group	Pbcm (no. 57)
Unit cell parameters:	
a (pm)	916.35(6)
b (pm)	1373.10(9)
c (pm)	1039.41(7)
Number of formula units per unit cell	Z = 4
Calculated density ($D_x/\text{g cm}^{-3}$)	2.215
Molar volume ($V_m/\text{cm}^3 \text{ mol}^{-1}$)	206.6
Diffractometer	κ -CCD (Bruker-Nonius)
Radiation	Mo-K α : $\lambda = 71.07$ pm, graphite monochromator
Index range	$\pm h_{\max} = 12, \pm k_{\max} = 17, \pm l_{\max} = 13$
θ_{\max} (deg)	27.5
F(000)	864
Absorption coefficient (μ/mm^{-1})	5.30
Absorption correction	numerical, Program X-SHAPE [64]
Other data corrections	background, polarization and <i>Lorentz</i> factors
Collected reflections	14378
Unique reflections	1654
$R_{\text{int}}, R_{\sigma}$	0.109, 0.046
Structure solution and refinement	Program SHELXS-97 and SHELXL-97 [68]
Scattering factors	International Tables for Crystallography, Vol. C [87]
R_1, R_1 with $ F_o \geq 4\sigma(F_o)$	0.053, 0.050
Reflections with $ F_o \geq 4\sigma(F_o)$	1546
w R_2 , Goodness of fit (GooF)	0.135, 1.094
Extinction (g)	0.005(9)
Residual electron density (<i>max.</i> , <i>min.</i> in $\rho/e^{-1} 10^6$ pm)	2.13, -1.40

Table 74: Atomic coordinates for Cs₂[1,2,3-B₁₂H₉(OH)₃] · H₂O

Atom	Wyckoff position	x/a	y/b	z/c
Cs1 ^{a)}	4c	0.4070(1)	1/4	0
Cs2 ^{a)}	4c	0.0724(3)	1/4	0
Cs3	4d	0.7576(1)	0.4458(1)	1/4
O1	4d	0.0761(9)	0.3675(9)	1/4
O2	8e	0.0116(9)	0.0595(9)	0.0934(9)
Ow	4d	0.2236(8)	0.1812(5)	1/4
B1	4d	0.1620(8)	0.4500(6)	1/4
B2	8e	0.8900(6)	0.0571(4)	0.1651(8)
B3	4d	0.8281(8)	0.1612(6)	1/4
B4	8e	0.7365(6)	0.1193(4)	0.1101(8)
B5	4d	0.6453(8)	0.1581(6)	1/4
B6	4d	0.3486(8)	0.4475(5)	1/4
B7	8e	0.7436(5)	0.9887(4)	0.1122(7)
B8	8e	0.5901(6)	0.0512(4)	0.1644(7)
H3 ^{b)}	4d	0.885	0.231	1/4
H4 ^{b)}	8e	0.734	0.161	0.020
H5 ^{b)}	4d	0.584	0.226	1/4
H6 ^{b)}	4d	0.407	0.379	1/4
H7 ^{b)}	8e	0.746	0.946	0.023
H8 ^{b)}	8e	0.493	0.049	0.109

^{a)} s.o.f. of Cs1: 0.87(1), s.o.f. of Cs2: 0.26(1);

^{b)} refinement with DFIX constraint ($d(\text{B-H}) = 110 \text{ pm}$); $U_{\text{iso}}(\text{H}) = 1.2 \cdot U_{\text{iso}}(\text{B})$.

Table 75: Anisotropic thermal displacement coefficients^{a)} (U_{ij}/pm^2) for $\text{Cs}_2[1,2,3\text{-B}_{12}\text{H}_9(\text{OH})_3] \cdot \text{H}_2\text{O}$

Atom	U_{11}	U_{22}	U_{33}	U_{23}	U_{13}	U_{12}
Cs1	272(4)	178(3)	259(5)	4(2)	0	0
Cs2	434(15)	304(13)	457(22)	51(11)	0	0
Cs3	220(3)	272(4)	261(5)	0	0	15(2)
O1	1035(122)	1443(169)	2198(207)	0	0	-313(103)
O2	1277(109)	1897(126)	2276(226)	232(144)	-110(118)	69(63)
Ow	597(43)	377(37)	483(61)	0	0	-66(28)
B1	200(37)	163(36)	215(56)	0	0	34(24)
B2	178(24)	175(26)	258(40)	35(26)	-21(25)	-44(17)
B3	228(39)	232(41)	248(58)	0	0	-35(27)
B4	241(28)	175(26)	232(42)	4(25)	-1(25)	1(18)
B5	274(39)	142(37)	238(59)	0	0	58(27)
B6	200(27)	98(34)	293(60)	0	0	26(24)
B7	228(27)	186(26)	169(39)	-3(24)	-22(23)	-7(17)
B8	200(26)	206(27)	186(27)	26(26)	-8(24)	-5(17)
H3	283					
H4	259					
H5	262					
H6	233					
H7	233					
H8	236					

^{a)} For Cs, O and B defined as anisotropic temperature factor according to: $\exp[-2\pi^2(U_{11}h^2a^{*2} + U_{22}k^2b^{*2} + U_{33}l^2c^{*2} + 2U_{23}klb^*c^* + 2U_{13}hla^*c^* + 2U_{13}hka^*b^*)]$; for H isotropically defined as temperature factor in: $\exp[-8\pi^2(U_{\text{iso}}\sin^2\theta/\lambda^2)]$.

Table 76: Selected interatomic distances (d/pm) for Cs₂[1,2,3-B₁₂H₉(OH)₃] · H₂O

[(Cs1)O ₂ H ₁₀] polyhedron:			[(Cs2)O ₆ H ₆] polyhedron:			[(Cs3)O ₄ H ₉] polyhedron:		
Cs1	– Ow	327.9 (2×)	Cs2	– O2	284.8 (2×)	Cs3	– O2	316.5 (2×)
	– H3	307.8 (2×)		– O1	304.7 (2×)		– Ow	322.3
	– H8	309.5 (2×)		– Ow	313.0 (2×)		– O2	327.0
	– H6	312.7 (2×)		– H4	316.8 (2×)		– H8	314.4 (2×)
	– H7	313.6 (2×)		– H3	322.2 (2×)		– H5	316.7 (2×)
	– H5	337.8 (2×)		– H5	348.4 (2×)		– H3	319.1 (2×)
							– H4	319.3
							– H6	345.1
							– H7	350.2
[1,2,3-B ₁₂ H ₉ (OH) ₃] ²⁻ anion:								
B1	– B7	177.7 (2×)	B2	– B2	176.5	B3	– B5	175.8
	– B2	178.7 (2×)		– B7	177.9		– B2	178.2 (2×)
	– B6	179.4		– B3	178.2		– B4	179.5 (2×)
	– O1	140.1		– B1	178.7		– H3	110.0
				– B4	179.9			
				– O2	138.7			
B4	– B5	178.0	B5	– B3	175.8	B6	– B7	177.7 (2×)
	– B8	178.2		– B4	178.0 (2×)		– B8	177.9 (2×)
	– B7	179.5		– B8	179.6 (2×)		– B1	179.4
	– B3	179.5		– H5	110.0		– H6	110.0
	– B2	179.9						
	– H4	110.0						
B7	– B1	177.7				B8	– B8	177.9
	– B6	177.7					– B6	177.9
	– B2	177.9					– B4	178.2
	– B8	179.1					– B7	179.1
	– B4	179.4					– B5	179.6
	– H7	110.0					– H8	110.0

4.5 Dicesium 1,2,3,5-Tetrahydroxo-Octahydro-*closo*-Dodecaborate Dihydrate

The synthesis of the $[\text{B}_{12}\text{H}_8(\text{OH})_4]^{2-}$ anion and its functionalized derivatives has been reported in literature already [48]. However, due to difficulties in crystal growth, there is no crystal structure of any tetrahydroxo-octahydro-*closo*-dodecaborate salt available so far.

4.5.1 Synthesis of $\text{Cs}_2[1,2,3,5\text{-B}_{12}\text{H}_8(\text{OH})_4] \cdot 2 \text{H}_2\text{O}$

Similar to the synthesis procedure of other partially hydroxylated derivatives of the $[\text{B}_{12}\text{H}_{12}]^{2-}$ anion, $\text{Cs}_2[\text{B}_{12}\text{H}_8(\text{OH})_4] \cdot 2 \text{H}_2\text{O}$ is prepared by stirring 1 g $\text{Cs}_2[\text{B}_{12}\text{H}_{12}]$ (Strem: 98%) with 4 ml hydrogen peroxide H_2O_2 (30 %) at 90 °C for 8 hours. Colourless, polyhedrally shaped single crystals are obtained by isothermal evaporation of the resulting solution at room temperature.

4.5.2 Structural Description of $\text{Cs}_2[1,2,3,5\text{-B}_{12}\text{H}_8(\text{OH})_4] \cdot 2 \text{H}_2\text{O}$

The title compound crystallizes in the orthorhombic space group *Pbcm* (no. 57) with four formula units per unit cell (Fig. 76). The cesium cations occupy two crystallographically different *Wyckoff* positions, *4c* ($x/a, y/b = 1/4, z/c = 0$; site symmetry: $2..$) and *4d* ($x/a, y/b, z/c = 1/4$; site symmetry: $..m$) namely. The oxygen atoms of the crystal water molecules are located at the two distinct *Wyckoff* positions *4c* and *4d* as well. Two of three hydroxyl oxygen atoms (O1 and O2) reside at the two fully occupied *Wyckoff* positions *4d* and *8e* ($x/a, y/b, z/c$; site symmetry: 1), the third one (O3) is found at a mix occupied *8e* site (site occupancy: 0.63) and, as a result, $[\text{B}_{12}\text{H}_8(\text{OH})_4]^{2-}$ species is a 1,2,3,5-isomer (Fig. 77). The boron and hydrogen atoms of the boron cage occupy the *Wyckoff* sites *4d* and *8e*. The centers of gravity of the $[1,2,3,5\text{-B}_{12}\text{H}_8(\text{OH})_4]^{2-}$ -cluster anions are found at the *Wyckoff* position *4d*. The $(\text{Cs}1)^+$ cation is tetrahedrally surrounded by four neighbouring *quasi*-icosahedral boron cages and coordinated via eight hydrogen atoms ($d(\text{Cs}1\text{-H}) = 309 - 322$ pm, $8\times$), two hydroxyl oxygen atoms ($d(\text{Cs}1\text{-O}3) = 283$ pm, $2\times$) and three oxygen atoms of crystal water molecules ($d(\text{Cs}1\text{-Ow}) = 324 - 329$ pm, $3\times$) (Fig. 78, *left*). Thus all $(\text{Cs}1)^+$ cations have the coordination number thirteen. The $(\text{Cs}2)^+$ cations, on the other hand, are surrounded by five boron cages arranged as a trigonal pyramid with contacts to seven hydrogen and five hydroxyl oxygen atoms ($d(\text{Cs}$ -

H) = 311 – 355 pm, 7×; d(Cs2–O) = 311 – 329 pm, 5×) (Fig. 78, *right*). But all (Cs2)⁺ cations are linked to another oxygen atom of a crystal water molecule with d(Cs2–Ow) = 332 pm, so their coordination numbers also amount to thirteen. In this crystal structure, as the same as in all other known partially hydroxylated dodecahydro-*closo*-dodecaborate salts of cesium, the central Cs⁺ cations have a mixed coordination sphere consisting of both oxygen and hydrogen atoms. Similar to all the other partially hydroxylated derivatives of the dodecahydro-*closo*-dodecaborate of cesium, the Cs⁺ cations are linked together via oxygen atoms of both hydroxyl groups and crystal water molecules to form a polymeric network in the crystal structure of Cs₂[1,2,3,5-B₁₂H₈(OH)₄] · 2 H₂O. The B–O and B–B bond lengths of the [1,2,3,5-B₁₂H₈(OH)₄]²⁻-cluster anion range from 140 to 141 pm and from 175 to 180 pm, respectively, while the B–H distances were fixed at 110 pm. This reveals that in Cs₂[1,2,3,5-B₁₂H₈(OH)₄] · 2 H₂O, the *quasi*-icosahedral [1,2,3,5-B₁₂H₈(OH)₄]²⁻ anion is only slightly distorted from its parent [B₁₂H₁₂]²⁻. The crystal structure of Cs₂[1,2,3,5-B₁₂H₈(OH)₄] · 2 H₂O is stabilized by both classical and non-classical hydrogen bridging bonds. The hydroxyl oxygen atoms of the [1,2,3,5-B₁₂H₈(OH)₄]²⁻ cluster are linked to those of crystal water molecules and hydroxyl groups of other boron cages via strong classical O–H^{δ+}...^{δ-}O hydrogen bridges (d(O...O) = 231 – 315 pm). Thereby the linkage between [1,2,3,5-B₁₂H₈(OH)₄]²⁻-cluster anions forms layers that spread out perpendicular to the *a* axis. In addition, the weak non-classical B–H^{δ-}...^{δ+}H–O hydrogen bridging bonds found between hydrogen atoms of the boron cage and the hydrogen atoms from crystal water or hydroxyl groups of other boron cages (d(Ow...H) = 331 – 350 pm) also add some stabilization to this whole coordination-polymeric scaffold. Surprisingly enough, the water solubility of Cs₂[1,2,3,5-B₁₂H₈(OH)₄] · 2 H₂O is considerably higher than that of perhydroxylated species having less hydroxylated vertices involved in strong hydrogen bridging bonds and less dense packing for the linkage between the Cs⁺ cations.

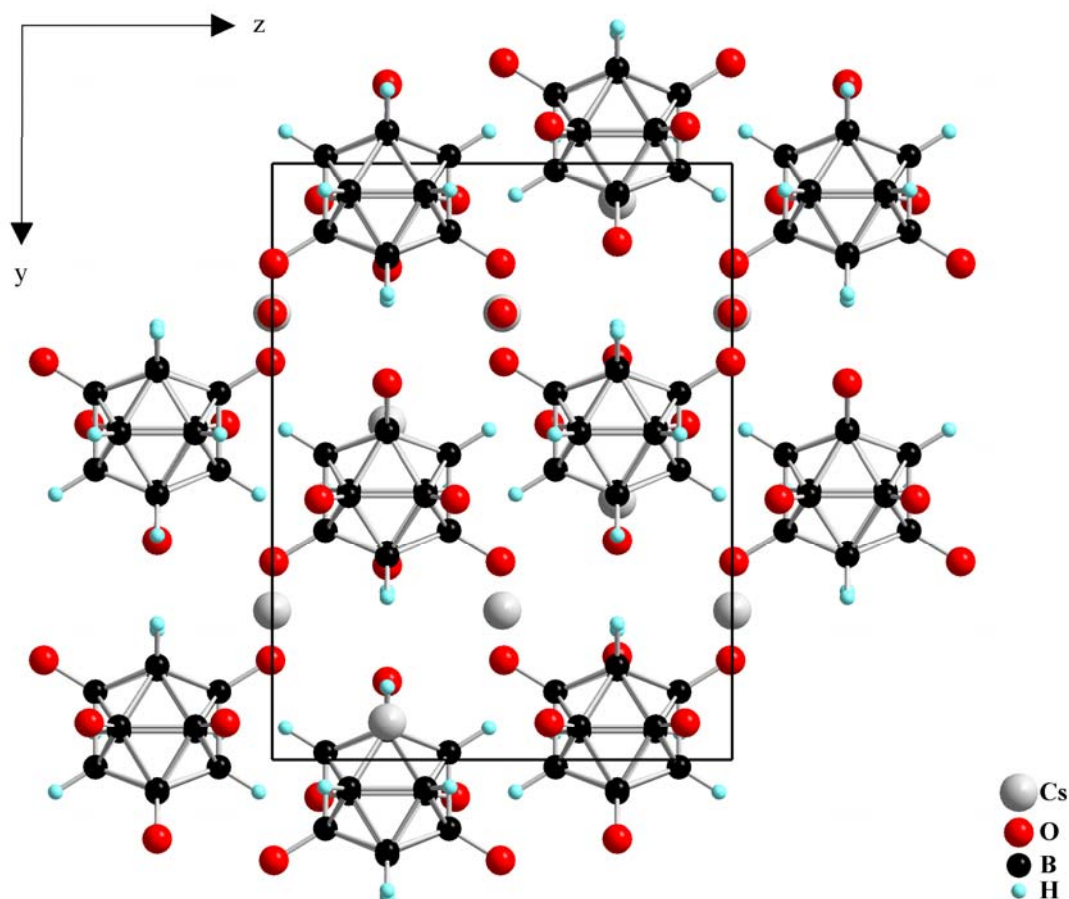


Fig. 76: (100) projection of the crystal structure of $\text{Cs}_2[1,2,3,5\text{-B}_{12}\text{H}_8(\text{OH})_4] \cdot 2 \text{H}_2\text{O}$

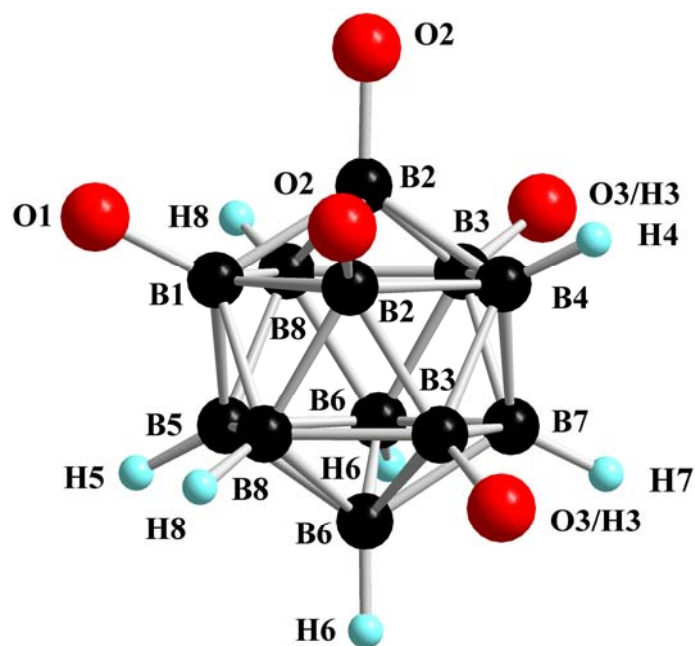


Fig. 77: View at the *quasi*-icosahedral $[1,2,3,5\text{-B}_{12}\text{H}_8(\text{OH})_4]^{2-}$ -cluster anion in the crystal structure of $\text{Cs}_2[1,2,3,5\text{-B}_{12}\text{H}_8(\text{OH})_4] \cdot 2 \text{H}_2\text{O}$

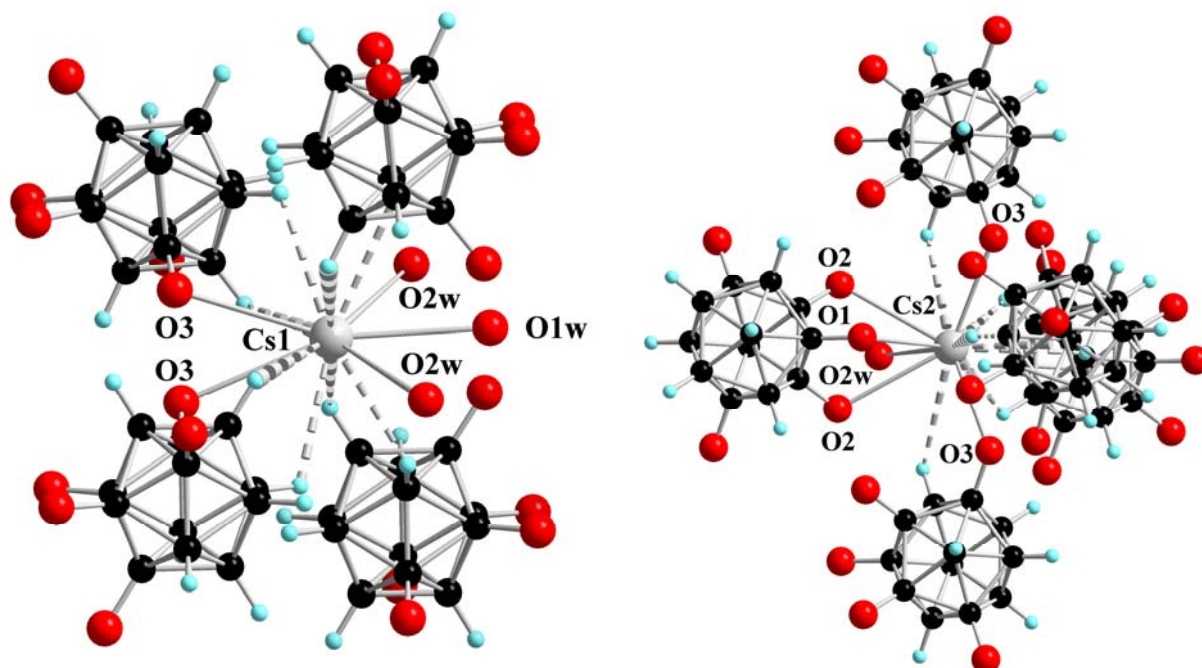


Fig. 78: View at the tetrahedral coordination spheres of the $(\text{Cs1})^+$ cation (CN = 13) (*left*) and at the trigonal-bipyramidal one of the $(\text{Cs2})^+$ cation (CN = 13) (*right*) in the crystal structure of $\text{Cs}_2[1,2,3,5\text{-B}_{12}\text{H}_8(\text{OH})_4] \cdot 2 \text{H}_2\text{O}$

Table 77: Crystallographic data of Cs₂[1,2,3,5-B₁₂H₈(OH)₄] · 2 H₂O and their determination

Crystal system	orthorhombic
Space group	Pbcm (no. 57)
Unit cell parameters:	
a (pm)	972.16(6)
b (pm)	1396.69(9)
c (pm)	1074.71(7)
Number of formula units per unit cell	Z = 4
Calculated density (D _x /g cm ⁻³)	2.311
Molar volume (V _m /cm ³ mol ⁻¹)	219.7
Diffractometer	κ-CCD (Bruker-Nonius)
Radiation	Mo-Kα: λ = 71.07 pm, graphite monochromator
Index range	±h _{max} = 12, ±k _{max} = 18, ±l _{max} = 14
θ _{max} (deg)	28.3
F(000)	936
Absorption coefficient (μ/mm ⁻¹)	5.00
Absorption correction	numerical, Program X-SHAPE [64]
Other data corrections	background, polarization and Lorentz factors
Collected reflections	24063
Unique reflections	1904
R _{int} , R _σ	0.075, 0.030
Structure solution and refinement	Program SHELXS-97 and SHELXL-97 [68]
Scattering factors	International Tables for Crystallography, Vol. C [87]
R ₁ , R ₁ with F _o ≥ 4σ(F _o)	0.087, 0.070
Reflections with F _o ≥ 4σ(F _o)	1567
wR ₂ , Goodness of fit (GooF)	0.195, 1.150
Extinction (g)	0.0003(1)
Residual electron density (max., min. in ρ/e ⁻¹ 10 ⁶ pm)	2.60, -0.82

Table 78: Atomic coordinates for Cs₂[1,2,3,5-B₁₂H₈(OH)₄] · 2 H₂O

Atom	Wyckoff position	x/a	y/b	z/c
Cs1	4 <i>c</i>	0.5968(1)	¹ / ₄	0
Cs2	4 <i>d</i>	0.2405(1)	0.4367(1)	¹ / ₄
O1	4 <i>d</i>	0.0829(8)	0.8680(7)	¹ / ₄
O2	8 <i>e</i>	0.9927(8)	0.0623(6)	0.1025(9)
O3 ^{a)}	8 <i>e</i>	0.2769(30)	0.3328(21)	0.9964(29)
O1w	4 <i>c</i>	0.9259(9)	¹ / ₄	0
O2w	4 <i>d</i>	0.7800(15)	0.1740(12)	¹ / ₄
B1	4 <i>d</i>	0.1673(12)	0.9502(8)	¹ / ₄
B2	8 <i>e</i>	0.1182(8)	0.0562(6)	0.1665(9)
B3	8 <i>e</i>	0.2688(9)	0.3851(6)	0.8844(9)
B4	4 <i>d</i>	0.1836(15)	0.3417(9)	³ / ₄
B5	4 <i>d</i>	0.3516(12)	0.9456(9)	¹ / ₄
B6	8 <i>e</i>	0.4141(9)	0.4520(6)	0.8327(9)
B7	4 <i>d</i>	0.3636(14)	0.3474(9)	³ / ₄
B8	8 <i>e</i>	0.2613(8)	0.9878(6)	0.1160(9)
H4 ^{b)}	4 <i>d</i>	0.130	0.272	³ / ₄
H5 ^{b)}	4 <i>d</i>	0.407	0.877	¹ / ₄
H6 ^{b)}	8 <i>e</i>	0.510	0.454	0.886
H7 ^{b)}	4 <i>d</i>	0.427	0.282	³ / ₄
H8 ^{b)}	8 <i>e</i>	0.259	0.946	0.029

^{a)} s.o.f. of O3: 0.61(3);

^{b)} refinement with DFIX constraint ($d(\text{B-H}) = 110 \text{ pm}$); $U_{\text{iso}}(\text{H}) = 1.2 \cdot U_{\text{iso}}(\text{B})$.

Table 79: Anisotropic thermal displacement coefficients^{a)} (U_{ij}/pm^2) for $\text{Cs}_2[1,2,3,5\text{-B}_{12}\text{H}_8(\text{OH})_4] \cdot 2 \text{H}_2\text{O}$

Atom	U_{11}	U_{22}	U_{33}	U_{23}	U_{13}	U_{12}
Cs1	565(5)	389(4)	502(5)	-7(4)	0	0
Cs2	418(5)	550(55)	704(7)	0	0	-27(4)
O1	754(74)	958(87)	1158(95)	0	0	-114(76)
O2	626(45)	787(52)	796(56)	2(47)	-223(43)	45(39)
O3	1897(278)	1301(212)	1536(255)	218(174)	185(168)	43(189)
Ow1	467(43)	235(32)	471(46)	286(34)	0	0
Ow2	901(95)	854(100)	1159(125)	0	0	185(79)
B1	227(48)	274(54)	454(70)	0	0	-37(42)
B2	285(36)	304(39)	383(45)	18(35)	-25(34)	31(30)
B3	404(44)	309(39)	347(43)	35(34)	30(36)	-18(35)
B4	511(75)	253(53)	325(63)	0	0	-56(51)
B5	280(53)	348(59)	273(56)	0	0	13(46)
B6	275(37)	353(42)	380(46)	-1(36)	-52(33)	12(31)
B7	394(64)	254(54)	448(72)	0	0	90(47)
B8	281(37)	297(38)	394(45)	-15(33)	-12(34)	14(31)
H4	436					
H5	361					
H6	403					
H7	439					
H8	389					

^{a)} For Cs, O and B defined as anisotropic temperature factor according to: $\exp[-2\pi^2(U_{11}h^2a^{*2} + U_{22}k^2b^{*2} + U_{33}l^2c^{*2} + 2U_{23}klb^{*}c^{*} + 2U_{13}hla^{*}c^{*} + 2U_{12}hka^{*}b^{*})]$; for H isotropically defined as temperature factor in: $\exp[-8\pi^2(U_{\text{iso}}\sin^2\theta/\lambda^2)]$.

Table 80: Selected interatomic distances (d/pm) for Cs₂[1,2,3,5-B₁₂H₈(OH)₄] · 2 H₂O

[(Cs1)O ₅ H ₈] polyhedron:		[(Cs2)O ₆ H ₇] polyhedron:			
Cs1 – O1w	323.5	Cs2 – O3/H3	310.0 (2×)		
– O3/H3	332.2 (2×)	– O1	327.8 (2×)		
– O2w	339.3 (2×)	– O2	328.8		
– H8	309.5 (2×)	– O2w	332.0		
– H7	318.5 (2×)	– H4	310.6		
– H6	321.7 (2×)	– H6	321.3 (2×)		
– H5	322.0 (2×)	– H8	342.1 (2×)		
		– H5	353.4		
		– H7	355.5		
[1,2,3,5-B ₁₂ H ₈ (OH) ₄] ²⁻ anion:					
B1 – B3	176.6	B2 – B8	178.5 (2×)	B3 – B1	176.6
– B8	177.3	– B5	179.2	– B4	177.1
– B1	179.4	– B1	179.6 (2×)	– B8	177.7
– B2	179.6	– O2	141.1	– B6	178.3
– B4	180.1			– B7	179.2
– O1	140.5			– O3	140.5
B4 – B7	175.2	B5 – B8	178.7 (2×)	B6 – B6	177.6
– B3	177.2 (2×)	– B6	179.0 (2×)	– B7	177.9
– B1	180.1 (2×)	– B2	179.2	– B3	178.3
– H4	110.0	– H5	110.0	– B5	179.0
				– B8	179.4
				– H6	110.0
B7 – B4	175.2			B8 – B1	177.3
– B6	177.9 (2×)			– B3	177.7
– B3	179.2 (2×)			– B2	178.5
– H7	110.0			– B5	178.7
				– B6	179.4
				– H8	110.0

5 Dodecahydroxo-*closo*-Dodecaborates

5.1 Dirubidium Dodecahydroxo-*closo*-Dodecaborate Dihydrates

By total substitution of all available hydrogen vertices the essentially spherical structures of the *quasi*-icosahedral $[\text{B}_{12}\text{H}_{12}]^{2-}$ -cluster modules can be used to orient exopolyhedral organic or inorganic substituents located on the cluster surface. Perhydroxylation of $[\text{B}_{12}\text{H}_{12}]^{2-}$ -cluster anion is the usual intermediate step of this functionalization. The syntheses and crystal structure determination of dodecahydroxo-*closo*-dodecaborate salts were first reported by Hawthorne *et al.* in 1999 [49]. The $[\text{B}_{12}(\text{OH})_{12}]^{2-}$ -cluster anion is the only anion known to date that forms almost water insoluble salts even with alkali metal cations [104]. Crystallographic data of dodecahydroxo-*closo*-dodecaborate salts with other inorganic cations have not been published yet, however. Crystal growth of dodecahydroxo-*closo*-dodecaborates is thus much more difficult than that of dodecahydro-*closo*-dodecaborates and dodecahalo-*closo*-dodecaborates, because of their very low solubility even in water, the most suitable solvent for the crystallization of these salts. Recently, the synthesis and crystal structure not only of $\text{Cs}_2[\text{B}_{12}(\text{OH})_{12}] \cdot 2 \text{H}_2\text{O}$ (monoclinic, $P2_1/c$), but also of $\text{Rb}_2[\text{B}_{12}(\text{OH})_{12}] \cdot 2 \text{H}_2\text{O}$ (monoclinic, $C2/c$) have been published in literature [104]. This monoclinic form of $\text{Rb}_2[\text{B}_{12}(\text{OH})_{12}] \cdot 2 \text{H}_2\text{O}$ is obtained by adding rubidium chloride RbCl to an aqueous solution of $\text{Cs}_2[\text{B}_{12}(\text{OH})_{12}]$ and recrystallization of the resulting precipitate from water. In this crystal structure, the rubidium cations exhibit CN = 10 with oxygen atoms, one of crystal water and nine of hydroxyl groups of the $[\text{B}_{12}(\text{OH})_{12}]^{2-}$ -cluster anion ($d(\text{Rb}-\text{O}) = 289 - 329 \text{ pm}$; $d(\text{Rb}-\text{Ow}) = 296 \text{ pm}$). The $\text{Rb}\cdots\text{Rb}$ distance of 363 pm is unusually short and just about twice the ionic radius (199 pm) of a tenfold coordinate rubidium cation. Up to date, other polymorphs of $\text{Rb}_2[\text{B}_{12}(\text{OH})_{12}] \cdot 2 \text{H}_2\text{O}$ have not been reported. In our work, $\text{Rb}_2[\text{B}_{12}(\text{OH})_{12}] \cdot 2 \text{H}_2\text{O}$ was directly prepared by the reaction between $\text{Rb}_2[\text{B}_{12}\text{H}_{12}]$ and hydrogen peroxide H_2O_2 . Depending upon the actual reacting conditions, three other polymorphs of $\text{Rb}_2[\text{B}_{12}(\text{OH})_{12}] \cdot 2 \text{H}_2\text{O}$, namely a P-monoclinic, a P-orthorhombic and a C-orthorhombic one can be obtained.

5.1.1 Synthesis and Crystal Structure of P-orthorhombic $\text{Rb}_2[\text{B}_{12}(\text{OH})_{12}] \cdot 2 \text{H}_2\text{O}$

5.1.1.1 Synthesis of P-orthorhombic $\text{Rb}_2[\text{B}_{12}(\text{OH})_{12}] \cdot 2 \text{H}_2\text{O}$

The title compound is synthesized by using $\text{Rb}_2[\text{B}_{12}\text{H}_{12}]$ as starting material, which is obtained by neutralizing the free acid $(\text{H}_3\text{O})_2[\text{B}_{12}\text{H}_{12}]$ with rubidium hydroxide RbOH . A

suspension of $\text{Rb}_2[\text{B}_{12}\text{H}_{12}]$ (1 g, 0.00317 mmol) in 18 ml of 30% hydrogen peroxide H_2O_2 was reacted at 60 °C for 5 days and the resulting solution was then cooled down for 12 h in a refrigerator to precipitate the crude solid. The precipitation was collected by filtration and washed with cold water to remove the excess amount of hydrogen peroxide. The $^{11}\text{B}\{^1\text{H}\}$ -NMR spectrum of $\text{Rb}_2[\text{B}_{12}(\text{OH})_{12}] \cdot 2 \text{H}_2\text{O}$ in D_2O showed a symmetrical singlet at $\delta = -17$ ppm and thus the total perhydroxylation of the $[\text{B}_{12}\text{H}_{12}]^{2-}$ -cluster anion was achieved. Colourless, lath-shaped single crystals were obtained by recrystallizing this precipitate from hot water. Suitable single crystals were selected for X-ray diffraction measurements. The coincidence of the powder X-ray diffraction pattern of P-orthorhombic $\text{Rb}_2[\text{B}_{12}(\text{OH})_{12}] \cdot 2 \text{H}_2\text{O}$ with the simulated one from single crystal data showed that at the selected reacting conditions, only this polymorphic type of $\text{Rb}_2[\text{B}_{12}(\text{OH})_{12}] \cdot 2 \text{H}_2\text{O}$ can be obtained readily as the main product (Fig. 79).

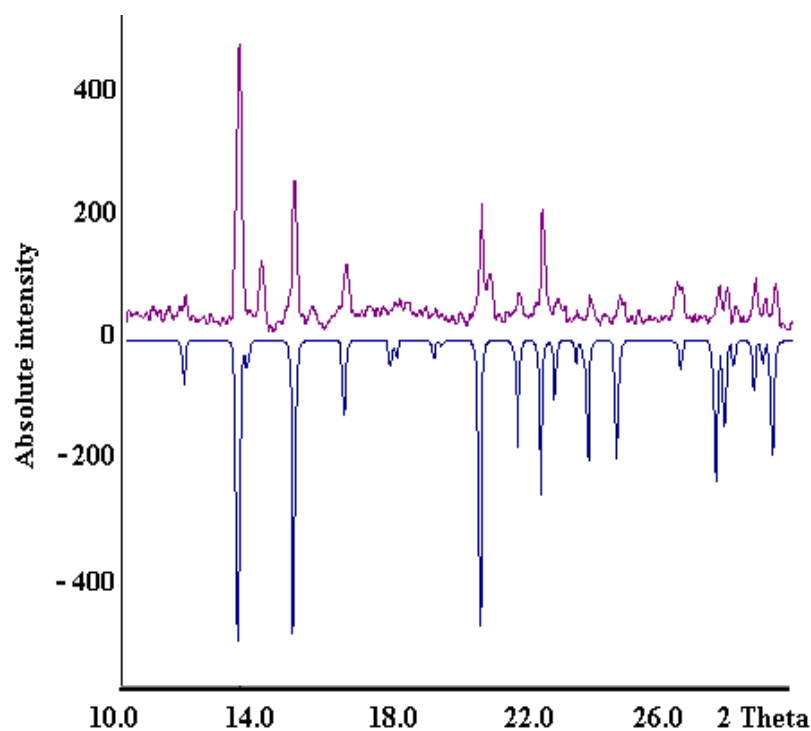


Fig. 79: Comparison of the measured powder X-ray diffraction diagram of P-orthorhombic $\text{Rb}_2[\text{B}_{12}(\text{OH})_{12}] \cdot 2 \text{H}_2\text{O}$ (*above*) and the simulated one (*below*)

5.1.1.2 Structure Description of P-orthorhombic $\text{Rb}_2[\text{B}_{12}(\text{OH})_{12}] \cdot 2 \text{H}_2\text{O}$

The P-orthorhombic polymorph of $\text{Rb}_2[\text{B}_{12}(\text{OH})_{12}] \cdot 2 \text{H}_2\text{O}$ crystallizes in space group Pnma (no. 62) with four formula units per unit cell (Fig. 80). In this crystal structure the rubidium cations occupy the general crystallographic *Wyckoff* position $8d$ ($x/a, y/b, z/c$; site symmetry: 1). The boron and the hydroxyl oxygen atoms of the $[\text{B}_{12}(\text{OH})_{12}]^{2-}$ -cluster anion reside at two crystallographically distinct *Wyckoff* positions $4c$ ($x/a, y/b = 1/4, z/c$; site symmetry: .m.) and $8d$, while the oxygen atoms belonging to crystal water molecules are located at the general *Wyckoff* site $8d$. The centers of gravity of the *quasi*-icosahedral $[\text{B}_{12}(\text{OH})_{12}]^{2-}$ -cluster anions are found at the *Wyckoff* position $4c$. Each Rb^+ cation is coordinated with ten oxygen atoms, nine from hydroxyl groups of boron cages and one from a crystal water molecule O9w ($d(\text{Rb}-\text{O}) = 291 - 340 \text{ pm}$). Via these nine hydroxyl oxygen atoms belonging to three triangular faces of three boron cages, each rubidium cation is coordinated with three nearest *quasi*-icosahedral $[\text{B}_{12}(\text{OH})_{12}]^{2-}$ -cluster anions forming a tetrahedron together with the crystal water molecule (Fig. 81, *left*). Each rubidium cation also forms an empty tetrahedron with other three neighbouring rubidium cations via two hydroxyl oxygen atoms of boron cages per each (Fig. 81, *right*). As a result, each Rb^+ cation is surrounded by three *quasi*-icosahedral $[\text{B}_{12}(\text{OH})_{12}]^{2-}$ -cluster anions and three other Rb^+ cations via hydroxyl oxygen atoms, forming sort of a hexagonal pyramid (Fig. 82). The B–B and B–O bond lengths of the *quasi*-icosahedral $[\text{B}_{12}(\text{OH})_{12}]^{2-}$ -cluster anions are in the common interval ($d(\text{B}-\text{B}) = 178 - 181 \text{ pm}$, $d(\text{B}-\text{O}) = 143 - 146 \text{ pm}$) (Fig. 83, *left*). The distances from each center of gravity to the twelve boron atoms of any cluster anion range from 168 to 177 pm providing an inner diameter of the cage ranging from 336 to 354 pm. Each *quasi*-icosahedral $[\text{B}_{12}(\text{OH})_{12}]^{2-}$ -cluster anion is nearly coplanar surrounded with six nearest Rb^+ cations via hydroxyl oxygen atoms (Fig. 83, *right*). There are strong hydrogen bridging bonds connecting the hydroxyl oxygen atoms of each *quasi*-icosahedral $[\text{B}_{12}(\text{OH})_{12}]^{2-}$ -cluster anion to hydroxyl oxygen atoms of other neighbouring boron cages and also to oxygen atoms of crystal water molecules ($d(\text{O}\cdots\text{O}) = 272 - 327 \text{ pm}$; $d(\text{O}\cdots\text{Ow}) = 268 - 330 \text{ pm}$).

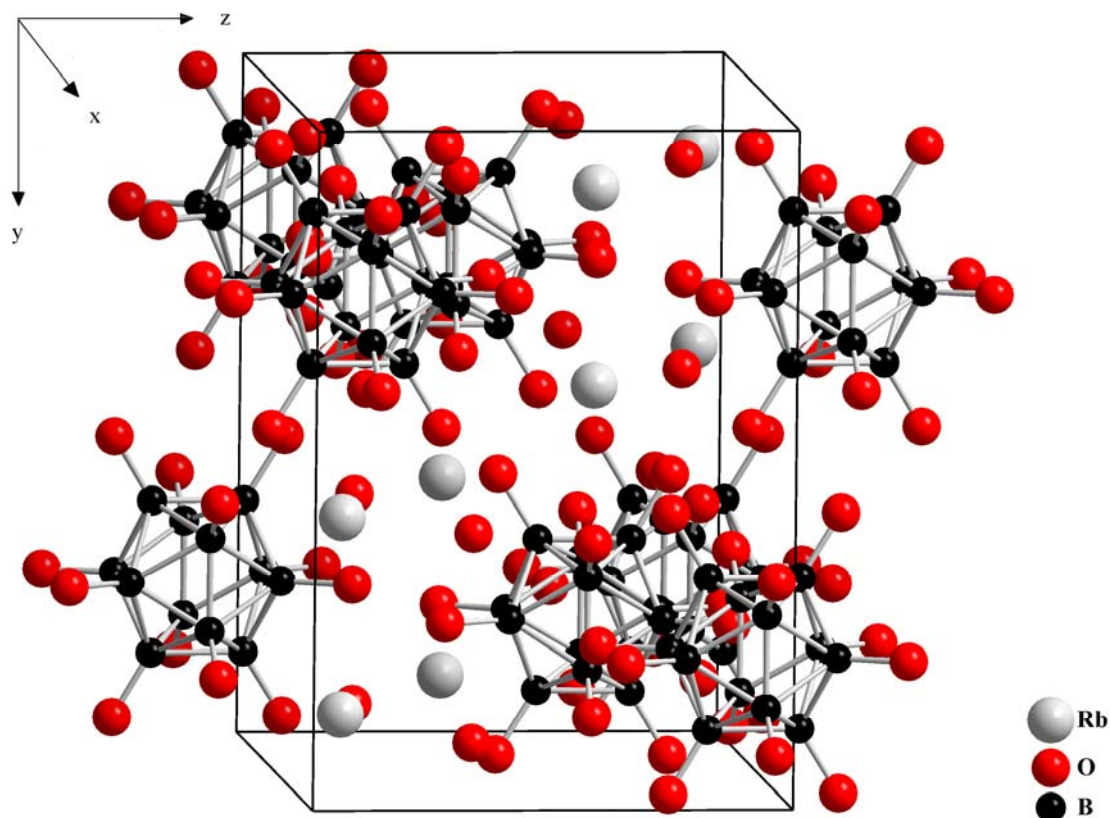


Fig. 80: Perspective view at the unit cell of P-orthorhombic $\text{Rb}_2[\text{B}_{12}(\text{OH})_{12}] \cdot 2 \text{H}_2\text{O}$ along $[100]$

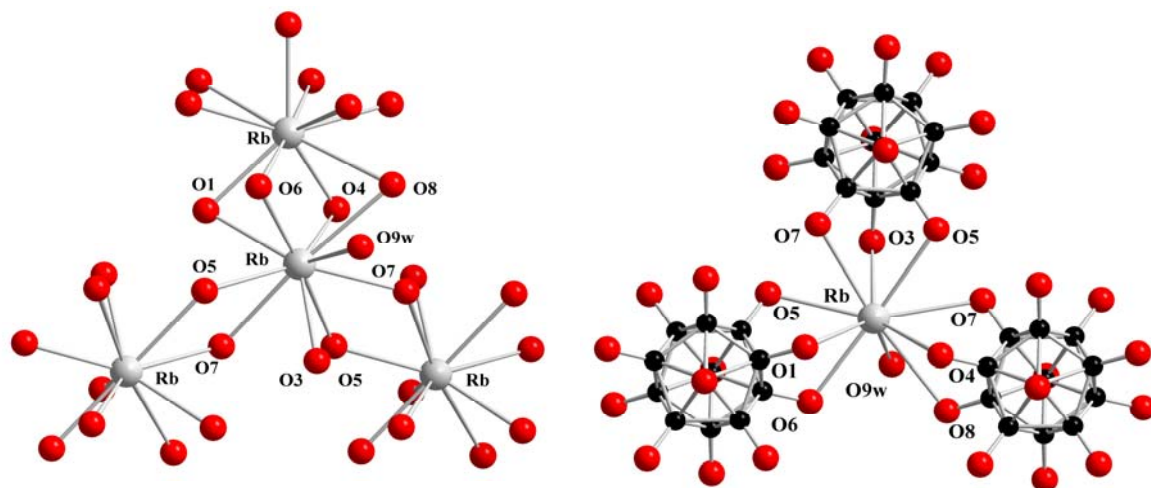


Fig. 81: View of the polymeric structure formed by the coordination spheres of the Rb^+ cations (*left*) and the arrangement of the three nearest *quasi*-icosahedral $[\text{B}_{12}(\text{OH})_{12}]^{2-}$ -cluster anions (plus O9w for the crystal water molecule) around Rb^+ (*right*)

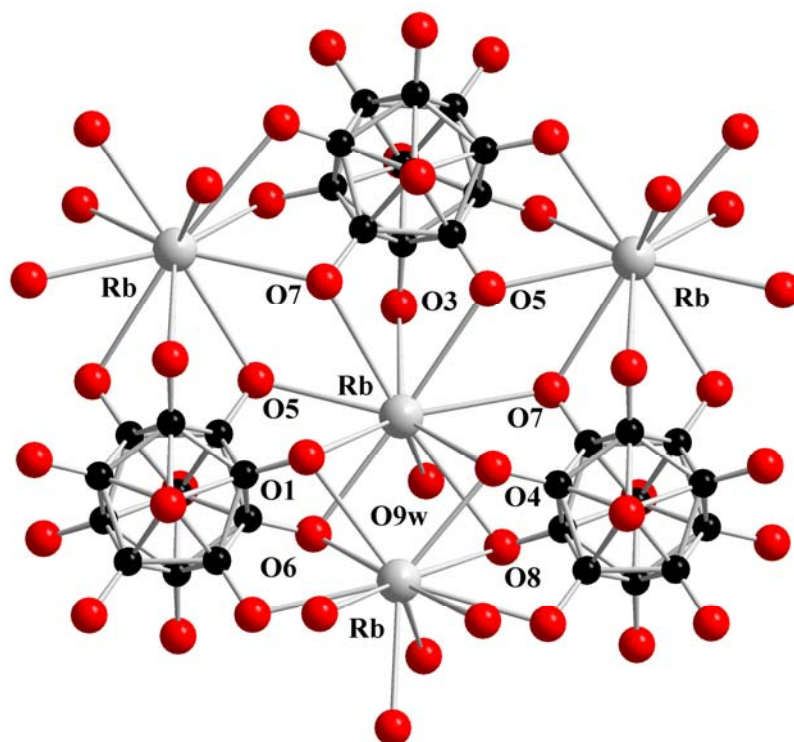


Fig. 82: Coordination environment of Rb^+ with three *quasi*-icosahedral $[\text{B}_{12}(\text{OH})_{12}]^{2-}$ -cluster anions and three neighbouring other Rb^+ cations

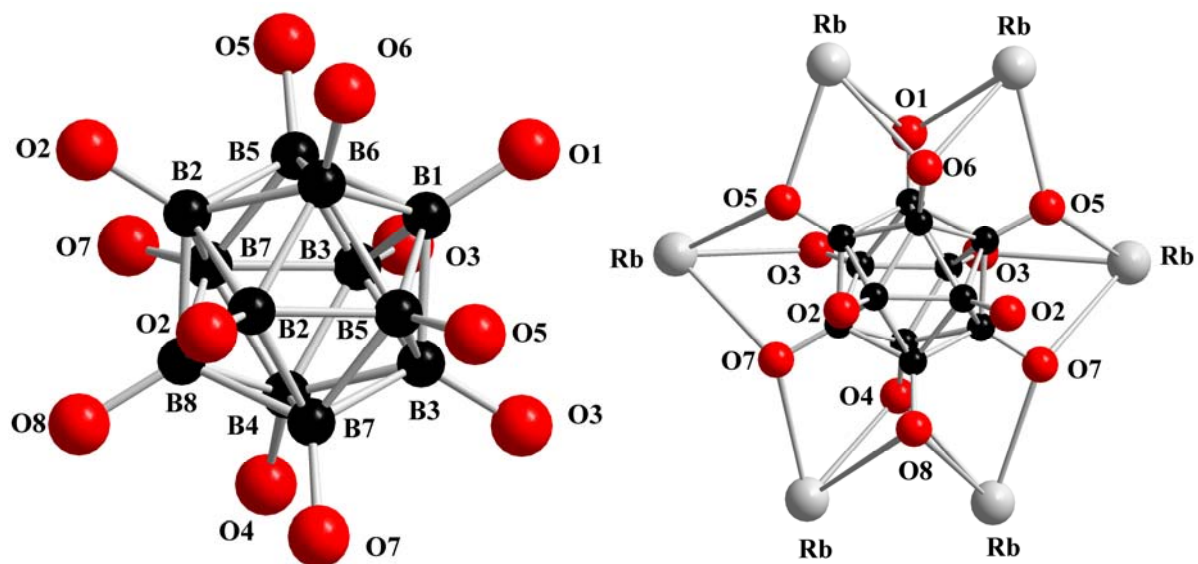


Fig. 83: View at the *quasi*-icosahedral $[\text{B}_{12}(\text{OH})_{12}]^{2-}$ -cluster anion (*left*) and its coordination environment with six nearest Rb^+ cations (*right*) in P-orthorhombic $\text{Rb}_2[\text{B}_{12}(\text{OH})_{12}] \cdot 2 \text{H}_2\text{O}$

Table 81: Crystallographic data for P-orthorhombic $\text{Rb}_2[\text{B}_{12}(\text{OH})_{12}] \cdot 2 \text{H}_2\text{O}$ and their determination

Crystal system	orthorhombic
Space group	Pnma (no. 62)
Unit cell parameters:	
a (pm)	1330.27(9)
b (pm)	1300.94(9)
c (pm)	918.59(6)
Number of formula units per unit cell	Z = 4
Calculated density ($D_x/\text{g cm}^{-3}$)	2.260
Molar volume ($V_m/\text{cm}^3 \text{mol}^{-1}$)	239.3
Diffractometer	κ -CCD (Bruker-Nonius)
Radiation	Mo-K α : $\lambda = 71.07 \text{ pm}$, graphite monochromator
Index range	$\pm h_{\text{max}} = 18, \pm k_{\text{max}} = 12, \pm l_{\text{max}} = 13$
θ_{max} (deg)	27.4
F(000)	1048
Absorption coefficient (μ/mm^{-1})	3.11
Absorption correction	numerical, Program X-SHAPE [64]
Other data corrections	background, polarization and Lorentz factors
Collected reflections	18074
Unique reflections	1884
$R_{\text{int}}, R_{\sigma}$	0.047, 0.021
Structure solution and refinement	Program SHELXS-97 and SHELXL-97 [68]
Scattering factors	International Tables for Crystallography, Vol. C [87]
R_1, R_w with $ F_o \geq 4\sigma(F_o)$	0.039, 0.042
Reflections with $ F_o \geq 4\sigma(F_o)$	1721
wR_2 , Goodness of fit (GooF)	0.117, 1.088
Extinction (g)	0.0012(8)
Residual electron density (<i>max.</i> , <i>min.</i> in $\rho/e^{-1} 10^6 \text{ pm}$)	1.26, -0.73

Table 82: Atomic coordinates for P-orthorhombic $\text{Rb}_2[\text{B}_{12}(\text{OH})_{12}] \cdot 2 \text{H}_2\text{O}$

Atom	Wyckoff position	x/a	y/b	z/c
Rb	8 <i>d</i>	0.6829(1)	0.6047(1)	0.1063(1)
O1	4 <i>c</i>	0.8041(2)	$\frac{3}{4}$	0.8996(3)
O2	8 <i>d</i>	0.9727(2)	0.6201(2)	0.8703(2)
O3	8 <i>d</i>	0.8737(2)	0.6214(2)	0.5986(2)
O4	4 <i>c</i>	0.7802(2)	$\frac{3}{4}$	0.3069(3)
O5	8 <i>d</i>	0.6775(1)	0.5432(2)	0.7885(2)
O6	4 <i>c</i>	0.5689(2)	$\frac{3}{4}$	0.9200(3)
O7	8 <i>d</i>	0.8346(1)	0.4566(2)	0.9326(2)
O8	4 <i>c</i>	0.5393(2)	$\frac{3}{4}$	0.3324(3)
O9w	8 <i>d</i>	0.4683(2)	0.5954(2)	0.1655(3)
B1	4 <i>c</i>	0.7463(3)	$\frac{3}{4}$	0.7651(4)
B2	8 <i>d</i>	0.0645(2)	0.6805(2)	0.8763(3)
B3	8 <i>d</i>	0.7819(2)	0.6810(2)	0.6034(3)
B4	4 <i>c</i>	0.7339(3)	$\frac{3}{4}$	0.4490(4)
B5	8 <i>d</i>	0.6770(2)	0.6379(2)	0.7092(3)
B6	4 <i>c</i>	0.6129(3)	$\frac{3}{4}$	0.7763(4)
B7	8 <i>d</i>	0.8319(2)	0.3615(2)	0.0156(3)
B8	4 <i>c</i>	0.5993(3)	$\frac{3}{4}$	0.4622(4)

Table 83: Anisotropic thermal displacement coefficients^{a)} (U_{ij}/pm^2) for P-orthorhombic $\text{Rb}_2[\text{B}_{12}(\text{OH})_{12}] \cdot 2 \text{H}_2\text{O}$

Atom	U_{11}	U_{22}	U_{33}	U_{23}	U_{13}	U_{12}
Rb	429(3)	331(2)	248(2)	13(1)	-18(1)	6(1)
O1	223(13)	284(13)	172(15)	0	-44(10)	0
O2	204(9)	290(16)	267(10)	-1(8)	-13(8)	-43(7)
O3	209(10)	226(9)	268(11)	-17(8)	-11(7)	86(8)
O4	274(14)	299(10)	188(14)	0	58(11)	0
O5	255(9)	331(15)	287(11)	68(8)	-5(7)	-9(7)
O6	253(14)	319(15)	147(12)	0	46(10)	0
O7	245(9)	200(10)	260(10)	80(8)	-16(8)	-7(7)
O8	327(15)	378(16)	197(14)	0	-109(12)	0
O9w	531(15)	486(14)	360(14)	58(11)	-101(12)	-204(12)
B1	177(16)	172(16)	157(18)	0	4(14)	0
B2	171(12)	183(11)	168(12)	10(10)	15(10)	-1(10)
B3	157(12)	193(12)	193(14)	-2(10)	8(9)	6(11)
B4	196(18)	195(17)	169(19)	0	18(15)	0
B5	162(12)	196(13)	156(13)	28(11)	-6(9)	2(10)
B6	171(17)	183(16)	134(17)	0	16(14)	0
B7	190(12)	189(13)	174(13)	14(11)	-5(10)	29(10)
B8	204(18)	184(17)	153(18)	0	-16(14)	0

^{a)} For Rb, O and B defined as anisotropic temperature factor according to: $\exp[-2\pi^2(U_{11}h^2a^{*2} + U_{22}k^2b^{*2} + U_{33}l^2c^{*2} + 2U_{23}klb^{*}c^{*} + 2U_{13}hla^{*}c^{*} + 2U_{13}hka^{*}b^{*})]$.

Table 84: Selected interatomic distances (d/pm) for P-orthorhombic $\text{Rb}_2[\text{B}_{12}(\text{OH})_{12}] \cdot 2 \text{H}_2\text{O}$

[RbO ₁₀] polyhedron:					
Rb – O9w	290.6	Rb – O7	311.0		
– O4	294.0	– O1	312.7		
– O6	296.7	– O5'	315.5		
– O5	302.8	– O7'	321.5		
– O3	303.7	– O8	339.7		
[B ₁₂ (OH) ₁₂] ²⁻ anion:					
B1 – B6	177.8	B2 – B5	177.8	B3 – B5	179.0
– B3	179.9 (2×)	– B7	178.5	– B4	179.6
– B5	180.0 (2×)	– B6	178.8	– B3	179.7
– O1	145.5	– B8	179.8	– B1	179.9
		– B2	180.9	– B7	180.2
		– O2	145.2	– O3	144.7
B4 – B8	179.5	B5 – B2	177.9	B6 – B1	177.8
– B3	179.6 (2×)	– B7	178.2	– B2	178.8 (2×)
– B7	180.2 (2×)	– B3	179.0	– B5	179.8 (2×)
– O4	144.4	– B6	179.8	– O6	144.4
		– B1	180.0		
		– O5	143.2		
B7 – B5	178.2	B8 – B7	178.4 (2×)		
– B8	178.4	– B4	179.5		
– B2	178.5	– B2	179.8 (2×)		
– B4	180.2	– O8	143.5		
– B3	180.2				
– O7	145.3				

5.1.2 Synthesis and Crystal Structure of C-orthorhombic $\text{Rb}_2[\text{B}_{12}(\text{OH})_{12}] \cdot 2 \text{H}_2\text{O}$

5.1.2.1 Synthesis of C-orthorhombic $\text{Rb}_2[\text{B}_{12}(\text{OH})_{12}] \cdot 2 \text{H}_2\text{O}$

C-orthorhombic $\text{Rb}_2[\text{B}_{12}(\text{OH})_{12}] \cdot 2 \text{H}_2\text{O}$ can be prepared by heating a suspension of $\text{Rb}_2[\text{B}_{12}\text{H}_{12}]$ with hydrogen peroxide H_2O_2 (30%) at 90 °C for 5 days. The precipitate is then washed and recrystallized from hot water. The end point of the reaction, at which the total hydroxylation of the $[\text{B}_{12}\text{H}_{12}]^{2-}$ -cluster anion is achieved, can be determined by $^{11}\text{B}\{^1\text{H}\}$ -NMR measurements of precipitated solid in D_2O . Colourless, bead-shaped single crystals were collected for X-ray diffraction investigations.

5.1.2.2 Structure Description of C-orthorhombic $\text{Rb}_2[\text{B}_{12}(\text{OH})_{12}] \cdot 2 \text{H}_2\text{O}$

The title compound crystallizes orthorhombically in space group Cmce (no. 64) with four formula units per unit cell (Fig. 84). The rubidium cations in this crystal structure occupy the special *Wyckoff* position $8d$ ($x/a, y/b = 1/2, z/c = 1/2$; site symmetry: $2..$). Every Rb^+ cation is coordinated with ten nearest oxygen atoms, eight from hydroxyl groups of boron cages and two belonging to crystal water molecules ($d(\text{Rb}-\text{O}) = 289 - 317$ pm; $d(\text{Rb}-\text{Ow}) = 338$ pm) (Fig. 85, *left*). Via these eight hydroxyl oxygen atoms, each rubidium cation is coplanar coordinated with three nearest *quasi*-icosahedral $[\text{B}_{12}(\text{OH})_{12}]^{2-}$ -cluster anions. The Rb^+ cations connect to two $[\text{B}_{12}(\text{OH})_{12}]^{2-}$ -cluster anions via three hydroxyl oxygen atoms originating from a triangular face per each and to the third boron-cage anion via only two hydroxyl oxygen atoms. Consequently, the distance of 505 pm from the center of gravity of the third $[\text{B}_{12}(\text{OH})_{12}]^{2-}$ -cluster anion to Rb^+ is longer than that of the other two (495 pm). The rubidium cation is linked to three other cations via two oxygen atoms of hydroxyl groups (Fig. 85, *right*). Moreover, two other rubidium cations link to a central Rb^+ via only one oxygen atom of a crystal water molecule per each. As a result, each rubidium cation is linked to five nearest rubidium cations located at the corners of a trigonal pyramid with $\text{Rb}\cdots\text{Rb}$ distances in the range of 462 – 660 pm. All oxygen atoms of hydroxyl groups are linked to other hydroxyl and crystal water oxygen atoms via strong hydrogen bridging bonds ($d(\text{O}\cdots\text{O}) = 272$ pm; $d(\text{O}\cdots\text{Ow}) = 286 - 318$ pm). This linkage between Rb^+ cations and hydrogen bridging bonds forms a polymeric network throughout the crystal structure of C-orthorhombic $\text{Rb}_2[\text{B}_{12}(\text{OH})_{12}] \cdot 2 \text{H}_2\text{O}$. The centers of gravity of the $[\text{B}_{12}(\text{OH})_{12}]^{2-}$ -cluster anions are found

at the crystallographic *Wyckoff* position $4b$ ($x/a = y/b = z/c = 0$; site symmetry: $2/m..$). The B–O and B–B bond lengths of the boron cages are within the common interval ($d(\text{B–O}) = 144 - 145$ pm, $d(\text{B–B}) = 178 - 181$ pm) (Fig. 86, *left*). These values show that the boron cage in C-orthorhombic $\text{Rb}_2[\text{B}_{12}(\text{OH})_{12}] \cdot 2 \text{H}_2\text{O}$ is less distorted than that one in partially hydroxylated derivatives. Each *quasi*-icosahedral $[\text{B}_{12}(\text{OH})_{12}]^{2-}$ -cluster anion is coplanar surrounded with six nearest Rb^+ cations via hydroxyl oxygen atoms (Fig. 86, *right*).

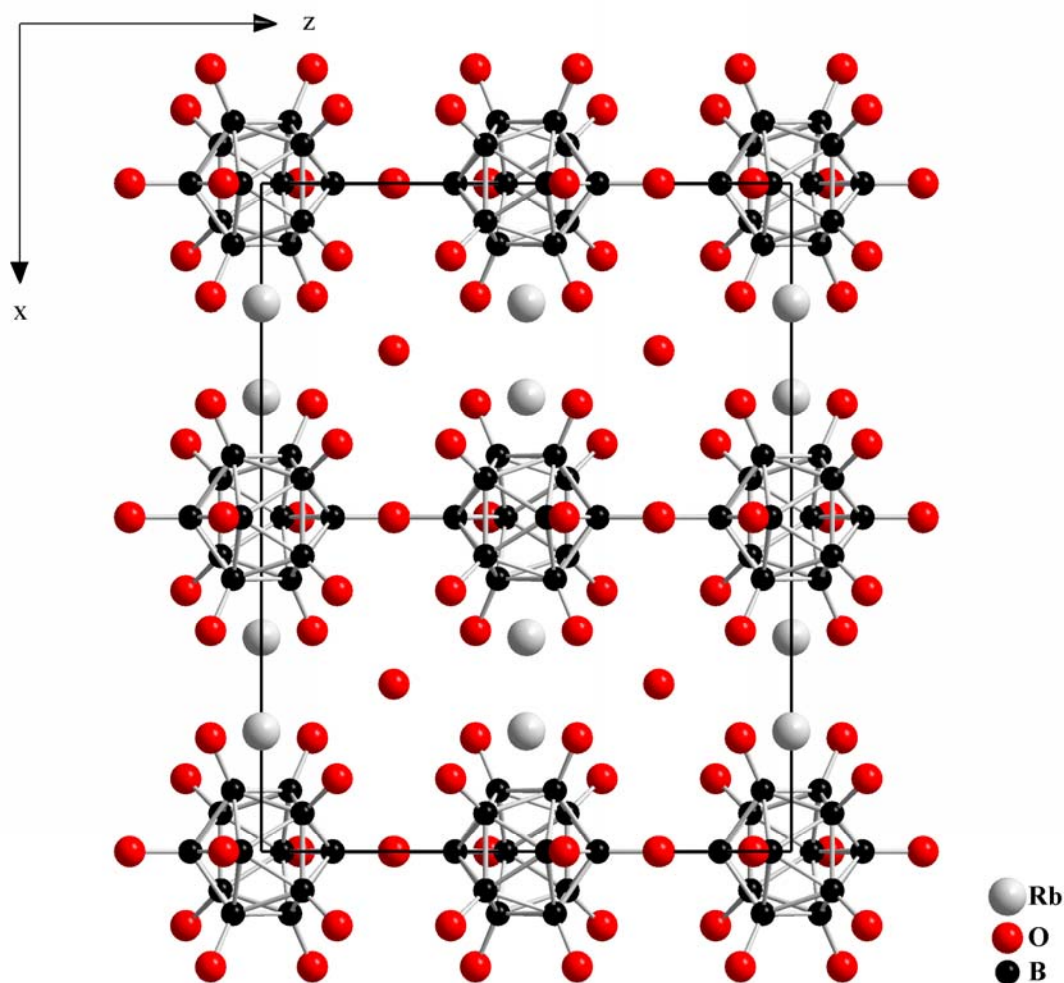


Fig. 84: Perspective view at the unit cell of C-orthorhombic $\text{Rb}_2[\text{B}_{12}(\text{OH})_{12}] \cdot 2 \text{H}_2\text{O}$ along $[010]$

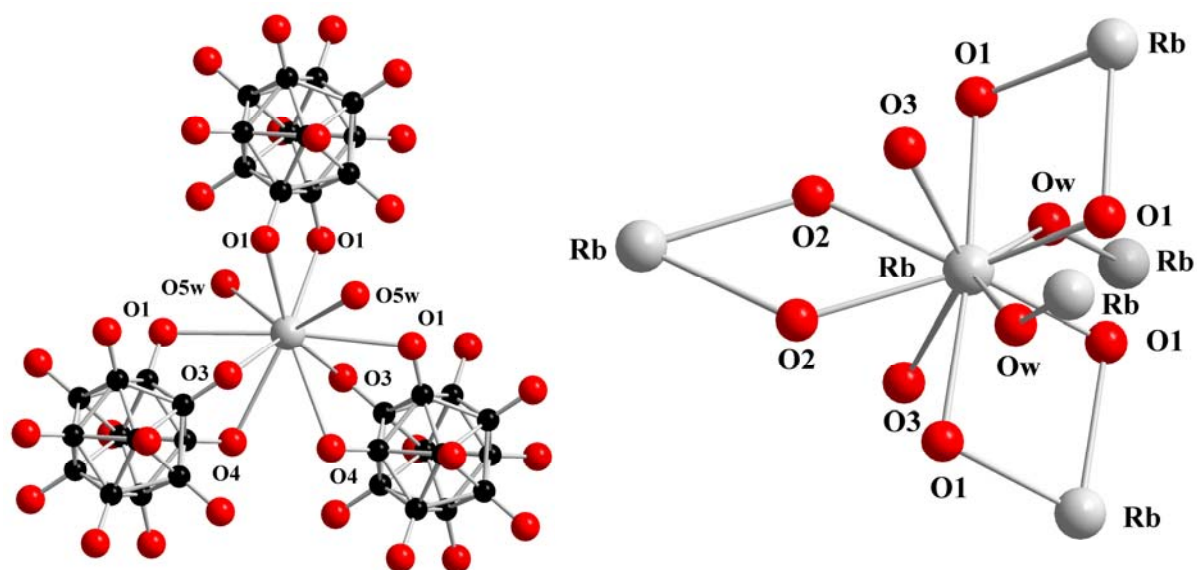


Fig. 85: Coordination environment of the Rb^+ cations with three nearest *quasi*-icosahedral $[\text{B}_{12}(\text{OH})_{12}]^{2-}$ -cluster anions and two crystal water molecules (O5w) (*left*) as well as five neighbouring Rb^+ cations (*right*) in C-orthorhombic $\text{Rb}_2[\text{B}_{12}(\text{OH})_{12}] \cdot 2 \text{H}_2\text{O}$

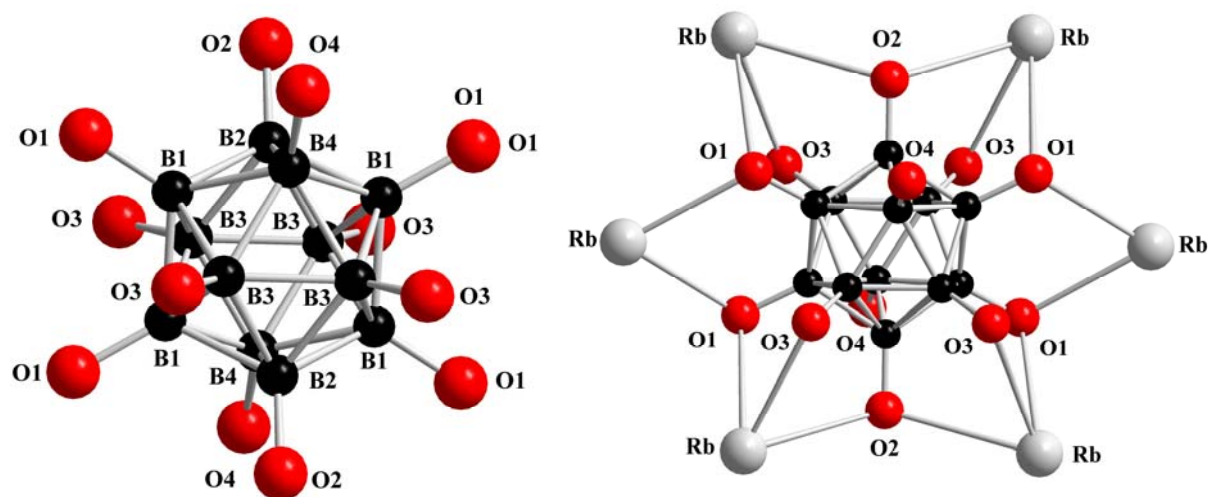


Fig. 86: *Quasi*-icosahedral $[\text{B}_{12}(\text{OH})_{12}]^{2-}$ -cluster anion (*left*) and its coordination environment with six neighbouring Rb^+ cations (*right*) in C-orthorhombic $\text{Rb}_2[\text{B}_{12}(\text{OH})_{12}] \cdot 2 \text{H}_2\text{O}$

Table 85: Crystallographic data for C-orthorhombic $\text{Rb}_2[\text{B}_{12}(\text{OH})_{12}] \cdot 2 \text{H}_2\text{O}$ and their determination

Crystal system	orthorhombic
Space group	Cmce (no. 64)
Unit cell parameters:	
a (pm)	1577.73(9)
b (pm)	812.18(5)
c (pm)	1243.56(7)
Number of formula units per unit cell	Z = 4
Calculated density ($D_x/\text{g cm}^{-3}$)	2.254
Molar volume ($V_m/\text{cm}^3 \text{mol}^{-1}$)	239.9
Diffractometer	κ -CCD (Bruker-Nonius)
Radiation	Mo-K α : $\lambda = 71.07$ pm, graphite monochromator
Index range	$\pm h_{\text{max}} = 20, \pm k_{\text{max}} = 10, \pm l_{\text{max}} = 16$
θ_{max} (deg)	28.3
F(000)	1048
Absorption coefficient (μ/mm^{-1})	6.21
Absorption correction	numerical, Program X-SHAPE [64]
Other data corrections	background, polarization and Lorentz factors
Collected reflections	12127
Unique reflections	1027
$R_{\text{int}}, R_{\sigma}$	0.073, 0.028
Structure solution and refinement	Program SHELXS-97 and SHELXL-97 [68]
Scattering factors	International Tables for Crystallography, Vol. C [87]
R_1, R_w with $ F_o \geq 4\sigma(F_o)$	0.074, 0.069
Reflections with $ F_o \geq 4\sigma(F_o)$	496
w R_2 , Goodness of fit (GooF)	0.158, 1.131
Extinction (g)	0.0015(8)
Residual electron density (<i>max.</i> , <i>min.</i> in $\rho/e^{-1} 10^6$ pm)	1.34, -2.72

Table 86: Atomic parameters for C-orthorhombic $\text{Rb}_2[\text{B}_{12}(\text{OH})_{12}] \cdot 2 \text{H}_2\text{O}$

Atom	Wyckoff position	x/a	y/b	z/c
Rb	8 <i>d</i>	0.1798(1)	0	0
O1	16 <i>g</i>	0.3302(2)	0.1391(5)	0.0961(3)
O2	8 <i>f</i>	$\frac{1}{2}$	0.3734(6)	0.0713(4)
O3	16 <i>g</i>	0.3907(2)	0.2592(4)	0.3572(3)
O4	8 <i>f</i>	$\frac{1}{2}$	0.0648(6)	0.2487(4)
O5w	8 <i>e</i>	$\frac{1}{4}$	0.4100(9)	$\frac{1}{4}$
B1	16 <i>g</i>	0.4085(3)	0.0771(6)	0.0536(4)
B2	8 <i>f</i>	$\frac{1}{2}$	0.2028(8)	0.0390(6)
B3	16 <i>g</i>	0.4426(3)	0.3678(6)	0.4228(4)
B4	8 <i>f</i>	$\frac{1}{2}$	0.4623(8)	0.1342(6)

Table 87: Anisotropic thermal displacement coefficients^{a)} (U_{ij}/pm^2) for C-orthorhombic $\text{Rb}_2[\text{B}_{12}(\text{OH})_{12}] \cdot 2 \text{H}_2\text{O}$

Atom	U_{11}	U_{22}	U_{33}	U_{23}	U_{13}	U_{12}
Rb	105(4)	434(6)	800(8)	-431(5)	0	0
O1	148(17)	238(18)	159(17)	-26(14)	5(13)	53(14)
O2	155(21)	135(21)	55(19)	8(17)	0	0
O3	140(16)	153(16)	127(15)	36(13)	-10(12)	55(14)
O4	260(27)	82(21)	164(24)	-26(18)	0	0
O5w	1558(107)	324(40)	720(59)	0	-825(71)	0
B1	131(23)	83(20)	50(20)	8(16)	3(17)	5(18)
B2	104(30)	71(29)	60(28)	20(23)	0	0
B3	130(22)	62(20)	57(19)	25(16)	3(17)	-11(17)
B4	134(32)	85(30)	70(28)	-11(25)	0	0

^{a)} For Rb, O and B defined as anisotropic temperature factor according to: $\exp[-2\pi^2(U_{11}h^2a^{*2} + U_{22}k^2b^{*2} + U_{33}l^2c^{*2} + 2U_{23}klb^{*}c^{*} + 2U_{13}hla^{*}c^{*} + 2U_{13}hka^{*}b^{*})]$.

Table 88: Selected interatomic distances (d/pm) and angles (\angle /deg) for C-orthorhombic $\text{Rb}_2[\text{B}_{12}(\text{OH})_{12}] \cdot 2 \text{H}_2\text{O}$

[RbO ₁₀] polyhedron:					
				Rb – O1 (2×)	288.6
				– O3 (2×)	297.1
				– O4 (2×)	314.5
				– O1' (2×)	316.9
				– O5w (2×)	338.0
O1–Rb–O1'	69.4	O1–Rb–O5w	55.6	O3–Rb–O5w	121.3
O1–Rb–O3	146.4	O1–Rb–O5w'	91.5	O3–Rb–O5w'	74.1
O1–Rb–O3'	77.5	O3–Rb–O3'	136.0	O4–Rb–O4'	51.2
O1–Rb–O4	138.8	O3–Rb–O4	66.4	O4–Rb–O1''	63.1
O1–Rb–O4'	138.9	O3–Rb–O4'	74.1	O4–Rb–O1'''	111.4
O1–Rb–O1''	104.3	O3–Rb–O1''	63.3	O4–Rb–O5w	88.0
O1–Rb–O1'''	184.5	O3–Rb–O1'''	114.3	O4–Rb–O5w'	128.8
[B ₁₂ (OH) ₁₂] ²⁻ anion:					
B1 – B3	177.6	B3 – B1		176.6	
– B2	178.6	– B1'		179.3	
– B4	178.8	– B2		179.7	
– B3'	179.3	– B4		180.0	
– B1	180.8	– B3		181.2	
– O1	144.0	– O3		145.4	
B2 – B1	178.6 (2×)	B4 – B1		178.8 (2×)	
– B4	179.0	– B2		179.0	
– B3	179.7 (2×)	– B3		180.0 (2×)	
– O2	144.0	– O4		144.3	

5.1.3 Synthesis and Crystal Structure of P-monoclinic $\text{Rb}_2[\text{B}_{12}(\text{OH})_{12}] \cdot 2 \text{H}_2\text{O}$

Both of P- and C-orthorhombic $\text{Rb}_2[\text{B}_{12}(\text{OH})_{12}] \cdot 2 \text{H}_2\text{O}$ were prepared at relatively low temperatures (65 °C and 90 °C, respectively) with respect to the maximum reflux temperature (145 °C) for reactions between $\text{Rb}_2[\text{B}_{12}\text{H}_{12}]$ and hydrogen peroxide H_2O_2 (30 %). At higher temperatures (110 °C), P-monoclinic $\text{Rb}_2[\text{B}_{12}(\text{OH})_{12}] \cdot 2 \text{H}_2\text{O}$ is obtained.

5.1.3.1 Synthesis of P-monoclinic $\text{Rb}_2[\text{B}_{12}(\text{OH})_{12}] \cdot 2 \text{H}_2\text{O}$

The title compound can be synthesized by heating a suspension of 1 g $\text{Rb}_2[\text{B}_{12}\text{H}_{12}]$ with 18 ml of hydrogen peroxide H_2O_2 (30 %) in aqueous solution at 110 °C for 5 days. The precipitate is then collected and recrystallized twice from water. The completeness of the hydroxylation of the product is again confirmed by $^{11}\text{B}\{^1\text{H}\}$ -NMR measurements with their characteristic singlet ($\delta = -17$ ppm) for the perhydroxylated cage $[\text{B}_{12}(\text{OH})_{12}]^{2-}$.

5.1.3.2 Structure Description of P-monoclinic $\text{Rb}_2[\text{B}_{12}(\text{OH})_{12}] \cdot 2 \text{H}_2\text{O}$

The P-monoclinic form of $\text{Rb}_2[\text{B}_{12}(\text{OH})_{12}] \cdot 2 \text{H}_2\text{O}$ crystallizes in space group $\text{P}2_1/\text{c}$ (no.14) with two formula units per unit cell (Fig. 87). This crystal structure is finally isostructural to that one of $\text{Cs}_2[\text{B}_{12}(\text{OH})_{12}] \cdot 2 \text{H}_2\text{O}$ reported by Hawthorne *et al.* [49] and therefore characterized as a layer-like structure with an alternative arrangement of Rb^+ cations and $[\text{B}_{12}(\text{OH})_{12}]^{2-}$ -cluster anions. In this crystal structure the rubidium cations, all boron atoms and all of the oxygen atoms occupy the general crystallographic *Wyckoff* position 4e (x/a, y/b, z/c; site symmetry: 1). The centers of gravity of $[\text{B}_{12}(\text{OH})_{12}]^{2-}$ -cluster anions are located at the *Wyckoff* position 2a (x/a = 0, y/b = 1/2, z/c = 1/2; site symmetry: $\bar{1}$). The Rb^+ cation now exhibits CN = 10 with ten oxygen atoms, two from crystal water molecules and eight from hydroxyl groups of boron cages ($d(\text{Rb}-\text{O}) = 291 - 347$ pm; $d(\text{Rb}-\text{Ow}) = 294 - 303$ pm). Each Rb^+ cation, similar to that one found in C-monoclinic $\text{Rb}_2[\text{B}_{12}(\text{OH})_{12}] \cdot 2 \text{H}_2\text{O}$, is linked to only two other rubidium cations via four oxygen atoms per each, three of these belonging to hydroxyl groups and the fourth one to a water molecule. As a result, the coordination spheres of the rubidium cations are connected into a polymeric structure forming a zigzag chain along [010] via oxygen atoms (Fig. 88). This linkage of cations is one-dimensional, whereas that one of C-monoclinic, C- and P-orthorhombic $\text{Rb}_2[\text{B}_{12}(\text{OH})_{12}] \cdot 2 \text{H}_2\text{O}$ appears three-

dimensional. Two adjacent chains are separated by a layer of *quasi*-icosahedral $[\text{B}_{12}(\text{OH})_{12}]^{2-}$ -cluster anions and these cages can link to the coordination spheres of the rubidium cations either directly via hydroxyl oxygen atoms or indirectly via hydrogen bridging bonds. Among the four known polymorphic structures of $\text{Rb}_2[\text{B}_{12}(\text{OH})_{12}] \cdot 2 \text{H}_2\text{O}$, the $\text{Rb}\cdots\text{Rb}$ distance of 395 pm is here considerably longer than the values found in the C-monoclinic (363 pm) [104] and the P-orthorhombic crystal structures (378 pm), but distinctly shorter than that one found in C-orthorhombic one (462 pm). Each cation is slightly shifted off the plane of four nearest centers of gravity of the boron cages forming a distorted square pyramid (Fig. 89, *left*). The distances from each rubidium cation to these centers of gravity range from 508 to 655 pm. Totally, each Rb^+ cation is surrounded by two other rubidium cations and four *quasi*-icosahedral $[\text{B}_{12}(\text{OH})_{12}]^{2-}$ -cluster anions nearby (Fig. 89, *right*). The existence of strong hydrogen bridging bonds are found with $\text{O}\cdots\text{O}$ distances in the range of 268 to 322 pm between all hydroxyl oxygen atoms and other hydroxyl or crystal water oxygen atoms. The B–B and B–O distances of the $[\text{B}_{12}(\text{OH})_{12}]^{2-}$ -cluster anions are in the common interval ($d(\text{B}–\text{B}) = 177 – 181$ pm, $d(\text{B}–\text{O}) = 144 – 145$ pm) (Fig. 90, *left*). These values reflect nicely the fact

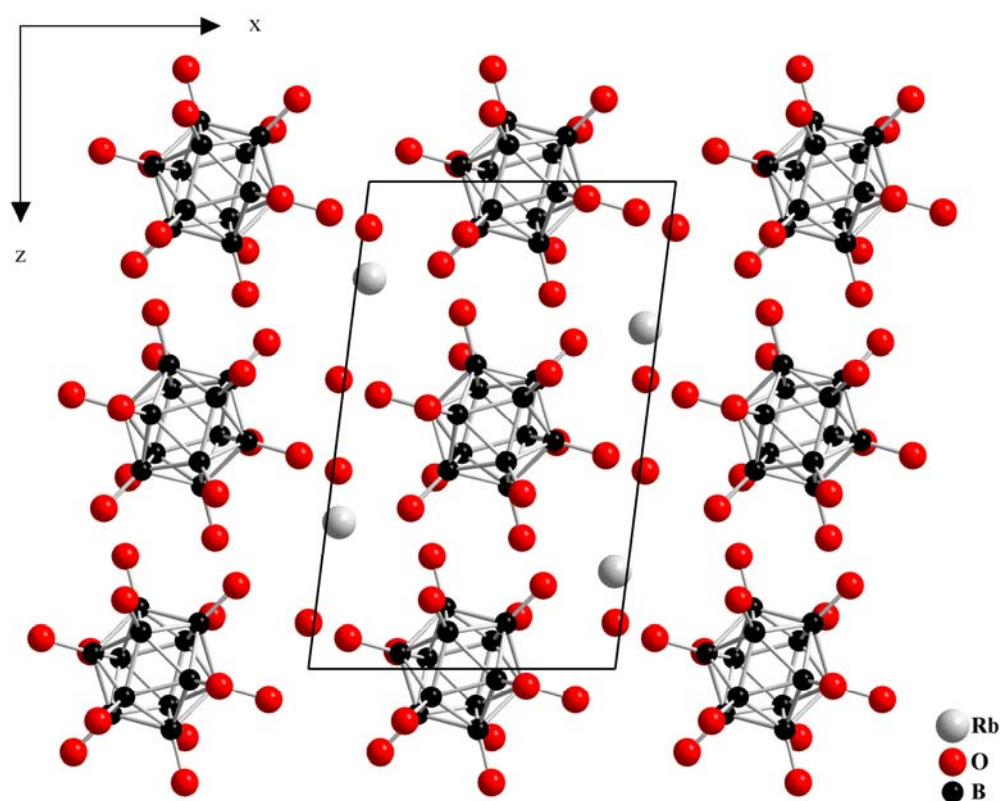


Fig. 87: Perspective view at a unit cell of the crystal structure of P-monoclinic $\text{Rb}_2[\text{B}_{12}(\text{OH})_{12}] \cdot 2 \text{H}_2\text{O}$ as viewed along $[010]$

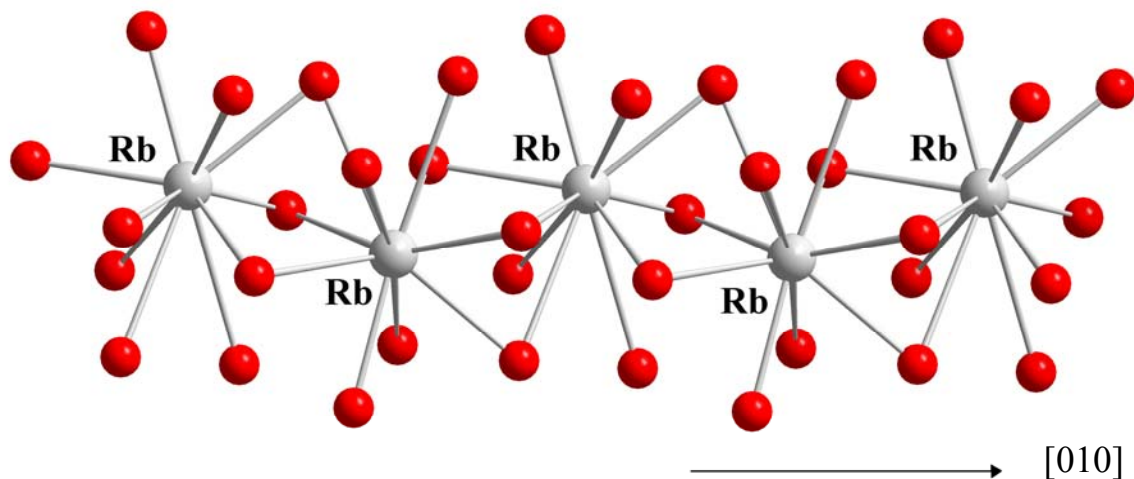


Fig. 88: View of a zigzag chain of interconnected $[\text{RbO}_{10}]$ coordination spheres along $[010]$

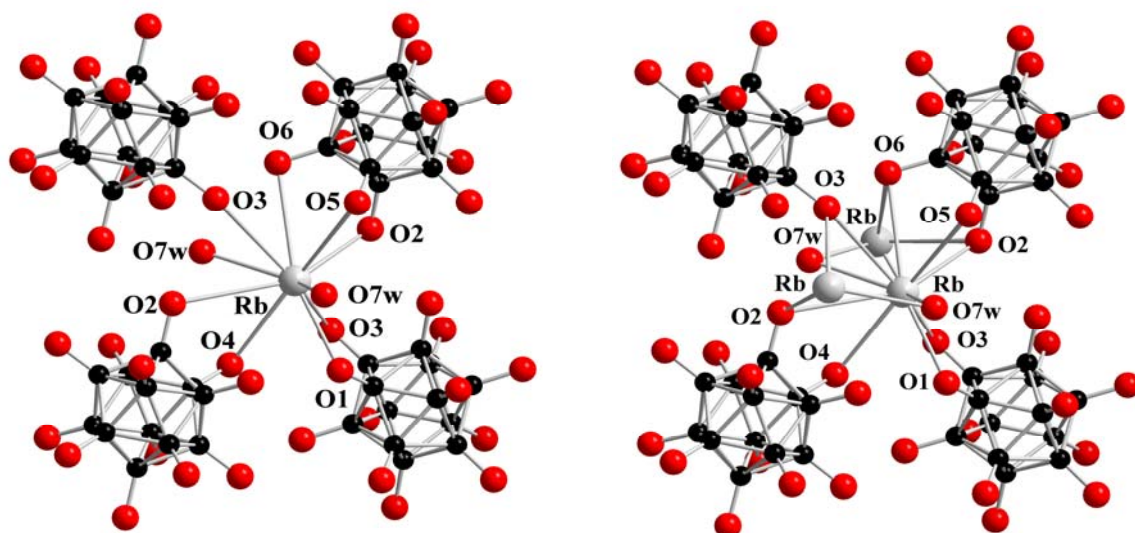


Fig. 89: View of the coordination environment of the Rb^+ cations with four nearest *quasi*-icosahedral $[\text{B}_{12}(\text{OH})_{12}]^{2-}$ -cluster anions along with two crystal water molecules (*left*) and with four *quasi*-icosahedral $[\text{B}_{12}(\text{OH})_{12}]^{2-}$ -cluster anions *plus* two neighbouring Rb^+ cations (*right*) in P-monoclinic $\text{Rb}_2[\text{B}_{12}(\text{OH})_{12}] \cdot 2 \text{H}_2\text{O}$

that the $[\text{B}_{12}(\text{OH})_{12}]^{2-}$ -cluster anions in P-monoclinic $\text{Rb}_2[\text{B}_{12}(\text{OH})_{12}] \cdot 2 \text{H}_2\text{O}$ are not much distorted from the parent $[\text{B}_{12}\text{H}_{12}]^{2-}$ -cluster anion. Each boron cage is surrounded by eight Rb^+ cations, instead of only six in the crystal structures of P- and C-orthorhombic $\text{Rb}_2[\text{B}_{12}(\text{OH})_{12}] \cdot 2 \text{H}_2\text{O}$, arranged as a parallelepiped-shaped brick (Fig. 90, *right*). The one-dimensional chains between the rubidium cations and the hydrogen bridging bonds form a

polymeric structure throughout the crystal structure. This polymeric network apparently causes the high water insolubility of P-monoclinic $\text{Rb}_2[\text{B}_{12}(\text{OH})_{12}] \cdot 2 \text{H}_2\text{O}$. Thus beside the reported C-monoclinic $\text{Rb}_2[\text{B}_{12}(\text{OH})_{12}] \cdot 2 \text{H}_2\text{O}$, three polymorphs of $\text{Rb}_2[\text{B}_{12}(\text{OH})_{12}] \cdot 2 \text{H}_2\text{O}$, namely a P-monoclinic, a P-orthorhombic and a C-orthorhombic one are added to literature (see Table 89).

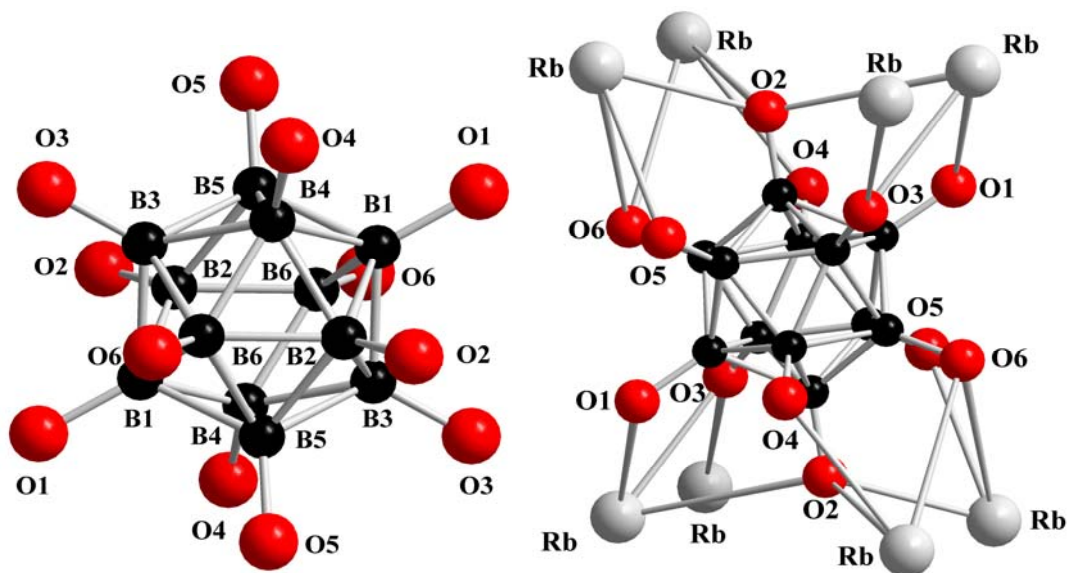


Fig. 90: View of the *quasi*-icosahedral $[\text{B}_{12}(\text{OH})_{12}]^{2-}$ -cluster anion (*left*) and its coordination environment with eight nearest Rb^+ cations in the crystal structure of P-monoclinic $\text{Rb}_2[\text{B}_{12}(\text{OH})_{12}] \cdot 2 \text{H}_2\text{O}$ (*right*)

Table 89: Lattice parameters of the polymorphs of $\text{A}_2[\text{B}_{12}(\text{OH})_{12}] \cdot 2 \text{H}_2\text{O}$ (A = Rb, Cs)

$\text{A}_2[\text{B}_{12}(\text{OH})_{12}] \cdot 2 \text{H}_2\text{O}$		a(pm)	b (pm)	c(pm)	$\beta(^{\circ})$	V_m ($\text{cm}^3 \text{mol}^{-1}$)
A	Polymorphs					
Rb	orthorhombic, Pnma (no. 62), Z = 4	1330.27(9)	1300.94(9)	918.59(6)	90	239.3
Rb	orthorhombic, Cmce (no. 64), Z = 4	1577.73(9)	812.18(5)	1243.56(7)	90	239.9
Rb [104]	monoclinic, C2/c (no. 15), Z = 4	1339.78(8)	918.62(5)	1333.31(8)	106.418(1)	237.0
Rb	monoclinic, P2 ₁ /c (no. 14), Z = 2	812.30(6)	728.19(5)	1303.51(9)	97.096(3)	230.4
Cs [49]		832.62(5)	736.57(4)	1314.80(8)	97.411(2)	239.1

Table 90: Crystallographic data for P-monoclinic $\text{Rb}_2[\text{B}_{12}(\text{OH})_{12}] \cdot 2 \text{H}_2\text{O}$

Crystal system	monoclinic
Space group	$\text{P}2_1/\text{c}$ (no. 14)
Unit cell parameters:	
a (pm)	812.30(6)
b (pm)	728.19(5)
c (pm)	1303.51(9)
β (deg)	97.096(3)
Number of formula units per unit cell	$Z = 2$
Calculated density ($D_x/\text{g cm}^{-3}$)	2.348
Molar volume ($V_m/\text{cm}^3 \text{mol}^{-1}$)	230.4
Diffractometer	κ -CCD (Bruker-Nonius)
Radiation	Mo-K α : $\lambda = 71.07$ pm, graphite monochromator
Index range	$\pm h_{\text{max}} = 10, \pm k_{\text{max}} = 9, \pm l_{\text{max}} = 17$
θ_{max} (deg)	28.3
F(000)	524
Absorption coefficient (μ/mm^{-1})	6.47
Absorption correction	numerical, Program X-SHAPE [64]
Other data corrections	background, polarization and Lorentz factors
Collected reflections	15380
Unique reflections	1897
$R_{\text{int}}, R_{\sigma}$	0.072, 0.031
Structure solution and refinement	Program SHELXS-97 and SHELXL-97 [68]
Scattering factors	International Tables for Crystallography, Vol. C [87]
R_1, R_w with $ F_o \geq 4\sigma(F_o)$	0.039, 0.030
Reflections with $ F_o \geq 4\sigma(F_o)$	3015
wR_2 , Goodness of fit (GooF)	0.072, 1.039
Extinction (g)	0.0081(4)
Residual electron density (<i>max.</i> , <i>min.</i> in $\rho/e^{-1} 10^6$ pm)	1.47, -1.31

Table 91: Atomic parameters for P-monoclinic $\text{Rb}_2[\text{B}_{12}(\text{OH})_{12}] \cdot 2 \text{H}_2\text{O}$

Atom	<i>Wyckoff</i> position	x/a	y/b	z/c
Rb	4e	0.5405(1)	0.2283(1)	0.1990(1)
O1	4e	0.8746(6)	0.1664(6)	0.3594(3)
O2	4e	0.8358(6)	0.3300(6)	0.1072(3)
O3	4e	0.7832(6)	0.8601(6)	0.4644(3)
O4	4e	0.7682(6)	0.9060(6)	0.1701(3)
O5	4e	0.8574(6)	0.5829(6)	0.2692(3)
O6	4e	0.3832(6)	0.9443(6)	0.0630(3)
O7w	4e	0.5182(7)	0.6007(7)	0.0945(4)
B1	4e	0.9392(8)	0.3187(9)	0.4243(6)
B2	4e	0.9121(8)	0.1787(9)	0.0579(5)
B3	4e	0.8827(8)	0.6960(9)	0.4778(5)
B4	4e	0.8754(8)	0.9444(9)	0.0931(5)
B5	4e	0.9221(8)	0.5471(9)	0.3755(5)
B6	4e	0.2078(8)	0.9718(9)	0.0326(5)

Table 92: Anisotropic thermal displacement coefficients^{a)} (U_{ij}/pm^2) for P-monoclinic $\text{Rb}_2[\text{B}_{12}(\text{OH})_{12}] \cdot 2 \text{H}_2\text{O}$

Atom	U_{11}	U_{22}	U_{33}	U_{23}	U_{13}	U_{12}
Rb	408(5)	241(4)	431(5)	-14(3)	103(31)	-45(3)
O1	260(22)	125(20)	184(21)	-72(16)	29(17)	-39(17)
O2	294(23)	106(19)	103(18)	-2(15)	41(16)	46(17)
O3	231(22)	127(20)	240(23)	25(17)	43(18)	59(17)
O4	262(23)	188(21)	143(29)	58(17)	96(17)	54(18)
O5	319(24)	151(20)	86(19)	15(16)	-42(17)	10(18)
O6	165(20)	222(22)	185(21)	30(18)	-1(13)	10(17)
O7w	363(30)	276(27)	477(34)	52(25)	111(26)	33(23)
B1	143(29)	92(28)	194(31)	-12(23)	49(24)	5(22)
B2	201(30)	80(27)	118(28)	10(22)	21(23)	1(23)
B3	165(29)	98(28)	145(28)	30(23)	20(23)	10(23)
B4	217(31)	96(27)	131(28)	18(23)	65(24)	-6(24)
B5	206(30)	92(27)	75(21)	-16(21)	2(23)	-10(23)
B6	196(30)	99(27)	112(28)	32(22)	7(23)	10(24)

^{a)} For Rb, O and B defined as anisotropic temperature factor according to: $\exp[-2\pi^2 (U_{11}h^2a^{*2} + U_{22}k^2b^{*2} + U_{33}l^2c^{*2} + 2U_{23}klb^{*}c^{*} + 2U_{13}hla^{*}c^{*} + 2U_{13}hka^{*}b^{*})]$.

Table 93: Selected interatomic distances (d/pm) and angles (\angle /deg) for P-monoclinic $\text{Rb}_2[\text{B}_{12}(\text{OH})_{12}] \cdot 2 \text{H}_2\text{O}$

[RbO ₁₀] polyhedron:					
	Rb – O1	290.6		Rb – O4	324.5
	– O2	291.4		– O5	331.5
	– O2'	346.5		– O6	347.5
	– O3	304.1		– O7w	329.2
	– O3'	345.4		– O7w'	303.0
O1–Rb–O2	104.7	O2–Rb–O7w'	102.9	O3–Rb–O5	126.2
O1–Rb–O7w'	133.8	O2–Rb–O7w	111.4	O3–Rb–O3'	147.2
O1–Rb–O7w	66.0	O2–Rb–O3	66.7	O3–Rb–O2'	114.7
O1–Rb–O3	66.4	O2–Rb–O4	124.2	O3–Rb–O6	111.6
O1–Rb–O4	68.5	O2–Rb–O5	64.0	O4–Rb–O5	171.0
O1–Rb–O5	106.9	O2–Rb–O3'	160.0	O4–Rb–O3'	109.5
O1–Rb–O3'	142.6	O2–Rb–O2'	152.0	O4–Rb–O2'	56.2
O1–Rb–O2'	100.8	O2–Rb–O6	60.8	O4–Rb–O6	126.6
O1–Rb–O6	162.6	O3–Rb–O4	60.0	O5–Rb–O3'	69.1
[B ₁₂ (OH) ₁₂] ²⁻ anion:					
B1 – B4	178.3	B2 – B4	177.4	B3 – B4	180.0
– B6	178.8	– B6	177.7	– B2	180.1
– B5	179.0	– B5	178.9	– B1	180.1
– B3	180.1	– B3	180.1	– B6	180.7
– B2	180.5	– B1	180.5	– B5	182.4
– O1	145.2	– O2	144.4	– O3	143.5
B4 – B2	177.4	B5 – B6	177.8	B6 – B2	177.7
– B6	178.0	– B2	178.9	– B5	177.8
– B1	178.3	– B1	179.0	– B4	178.0
– B3	180.0	– B4	181.0	– B1	178.8
– B5	181.1	– B3	182.4	– B8	180.7
– O4	145.4	– O5	144.1	– O6	144.5

5.2 Synthesis, Characterization and Crystal Structure of Cs[B₁₂(OH)₁₂]

The icosahedral dodecahydro-*closo*-dodecaborate anion, [B₁₂H₁₂]²⁻, is the most prominent member of the hydroborate cluster family. Its stability as explained by Wade's rules was frequently compared with that of planar "aromatic" compounds in hydrocarbon chemistry [7, 105]. In contrast to such quintessential organic systems, the [B₁₂X₁₂]²⁻ clusters exhibit three-dimensional electron delocalization, and they normally lack two well established kinds of features, which characterize the chemistry of organic aromatic compounds: they are less easily functionalized, and they usually do not undergo facile reversible electron transfer [8, 41, 106]. However, recent studies to functionalize and substitute [B₁₂H₁₂]²⁻ have provided a variety of closomers [48 – 50]. With respect to the parent anion, [B₁₂H₁₂]²⁻, these closomers retain the icosahedral cage, but incorporate variable additional properties relating to geometrical and electronic structure, ionic charge, redox capability, paramagnetism, chromophoric features or hydrophobicity. In terms of charge, the boron cage of most known closomers is isoelectronic to that of [B₁₂H₁₂]²⁻. However, some closomers can exist with less than the standard number of cage-bonding electrons and are thus described as *hypocloso*-[B₁₂X₁₂]ⁿ⁻ (n = 1 for radical and n = 0 for neutral forms). Only two neutral species, *hypocloso*-B₁₂Cl₁₂ and *hypocloso*-B₁₂(OCH₂Ph)₁₂, along with many radical anions, such as *hypocloso*-[B₁₂Me₁₂]^{•-} and *hypocloso*-[B₁₂(OCH₂Ph)₁₂]^{•-} have been reported in literature up to date [107, 108]. With one or two electrons removed, the point symmetry of the boron cage is lower than I_h with its quadruply degenerate HOMO, resulting from a Jahn-Teller distortion. The lower electron density in the boron cage may be compensated by external donor substituents, involving steric crowding, π back-donation, inductive and electronegativity effects [107]. In the known persubstituted 12-vertex boron radicals, the stabilization of *hypocloso*-[B₁₂Me₁₂]^{•-} may be attributed to steric crowding and the combined inductive effect, while π back-donation from the oxygen non-bonding electron pairs into the electron-deficient cage is the main reason for the persistence of *hypocloso*-[B₁₂(OR)₁₂]^{•-} (R = CH₂Ph). Both of these air-stable radical compounds contain organic substituents and are obtained by one-electron oxidation reactions of the corresponding closomer anions with oxidants such as Fe³⁺ for [B₁₂(OCH₂Ph)₁₂]^{•-} and Ce⁴⁺ for [B₁₂Me₁₂]^{•-}. Neither inorganic derivatives nor alternative methods of synthesis have been published to date. All reported closomers resulting from functionalization reactions of *closo*-[B₁₂H₁₂]²⁻ were obtained in the -2 state [48 – 50, 53, 109]. The perhydroxylation of

closo-[B₁₂H₁₂]²⁻, for example, has been carried out by the oxidation reaction between the cesium salt of *closo*-[B₁₂H₁₂]²⁻ and hydrogen peroxide, H₂O₂ (30 %). With modifications in the amount of hydrogen peroxide and temperatures ranging from 105 °C up to reflux, this reaction led only to Cs₂[B₁₂(OH)₁₂] · 2 H₂O as the reaction product despite of the donor capability of OH⁻ and the oxidizing power of H₂O₂ [104, 110]. Efforts to obtain the perhydroxylated radical by one-electron oxidation of *closo*-[B₁₂(OH)₁₂]²⁻ with strong oxidants such as MnO₄⁻, Fe³⁺ and Ce⁴⁺ did not succeed.

In this work we describe how a simple reaction using hydrogen peroxide leads to the cesium salts of both the diamagnetic *closo*-[B₁₂(OH)₁₂]²⁻ and the paramagnetic *hypocloso*-[B₁₂(OH)₁₂]⁻, thus producing a B₁₂ cluster redox system with potential for functionalization at the OH groups. Both the electron transfer potential and the possible functionalization via OH would be of interest for areas such as material science (spin-bearing oligoboranes) or medicine (boron neutron capture therapy, BNCT).

5.2.1 Synthesis of Cs[B₁₂(OH)₁₂]

To an aqueous solution of Cs₂[B₁₂H₁₂] (6.0 g, 14.7 mmol) 12 ml of 30 % hydrogen peroxide H₂O₂ were added, and the mixture was heated to 65 °C with vigorous stirring. Additional H₂O₂ was added slowly in 4-ml portions until all Cs₂[B₁₂H₁₂] was dissolved. The precipitation of the greenish yellow anhydrous radical compound begins after 4 days. Total hydroxylation of the [B₁₂H₁₂]²⁻-cluster anion with high purity is obtained after 6 days. Further increasing reaction temperature over 100 °C led to the formation of diamagnetic Cs₂[B₁₂(OH)₁₂] · 2 H₂O, the crystal structure of which was already characterized by Hawthorne *et al.* [49, 104]. With this preparation process not only the hydroxylation, but also a one-electron oxidation of the boron cage took place. Due to its low solubility in water, the radical compound is easily separated from the reaction mixture. X-ray powder diffraction measurements show only the single crystalline phase of Cs[B₁₂(OH)₁₂] (Fig. 91). The coincidence of the powder diffraction pattern to the calculated one based on the result of the X-ray single crystal structure determination confirms that Cs[B₁₂(OH)₁₂] is the main product with high purity of the hydroxylation of Cs₂[B₁₂H₁₂] by H₂O₂ at relative low temperature of around 65 °C. If this hydroxylation is carried out at higher temperatures ranging from 105 °C up to 145 °C the paramagnetic Cs[B₁₂(OH)₁₂] appeared only as a yellow by-product together with diamagnetic

$\text{Cs}_2[\text{B}_{12}(\text{OH})_{12}] \cdot 2 \text{H}_2\text{O}$ as main product, the situation is opposite with no peaks of the crystalline diamagnetic species observed in the X-ray powder diagram when this reaction is controlled at low temperature.

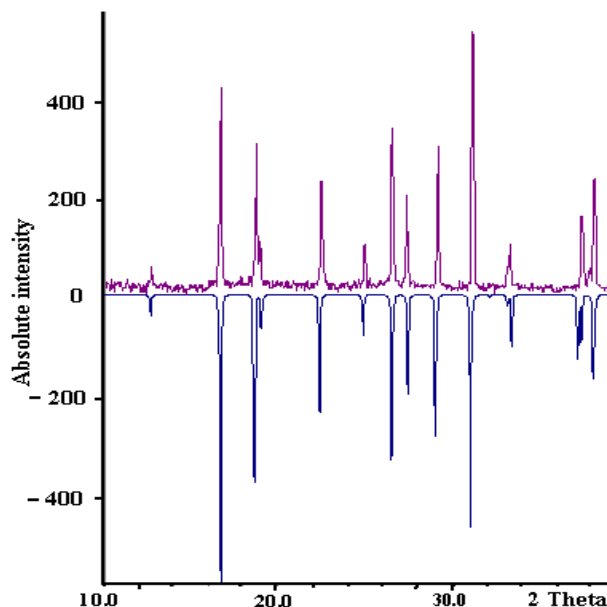


Fig. 91: Comparison of the measured powder X-ray diffraction diagram of $\text{Cs}[\text{B}_{12}(\text{OH})_{12}]$ (*above*) and the simulated one (*below*)

5.2.2 Electron Paramagnetic Resonance (EPR) and UV-VIS Investigations

The dodecahydroxo-*hypocloso*-dodecaborate radical anion exhibits an unresolved EPR signal at $g = 2.0042$ (2.5 mT peak-to-peak distance) in the solid state, which is close to the free electron value of 2.0023 and not much different from 2.0076 for *hypocloso*- $[\text{B}_{12}\text{Me}_{12}]^{\cdot -}$ [50, 111] (Fig. 92). In the absence of elements with significant spin-orbit coupling the higher $g = 2.1997$ reported for the ester *hypocloso*- $[\text{B}_{12}(\text{OCH}_2\text{Ph})_{12}]^{\cdot -}$ may be caused by different symmetry properties [108]. The lack of EPR spectral resolution reflects the large number of theoretical lines calculated for the interaction of one unpaired electron with 12 ^1H and 12 ^{11}B nuclei and the presence of a vast number of different isotopomers (^{11}B : 80.2 %, $I = 3/2$; ^{10}B : 19.8 %, $I = 3$). Considering only the all-(^{11}B) combinations one arrives at 481 lines, the other, partially more abundant $^{10}\text{B}/^{11}\text{B}$ combinations yield even more hyperfine lines. EPR measurement at high frequencies (95, 190, 285 GHz) showed no g factor anisotropy $\Delta g = g_1 - g_3$ for the solid radical at 5 K. At 285 GHz a very slight signal asymmetry could be associated

with a Δg value of about 0.01. This result supports the notion of the spin being delocalized mainly over the light boron atoms with their small spin-orbit coupling constants. The UV-VIS spectrum of greenish yellow $\text{Cs}[\text{B}_{12}(\text{OH})_{12}]$ in acetonitrile shows an absorption maximum at $\lambda = 477 \text{ nm}$ (Fig. 93).

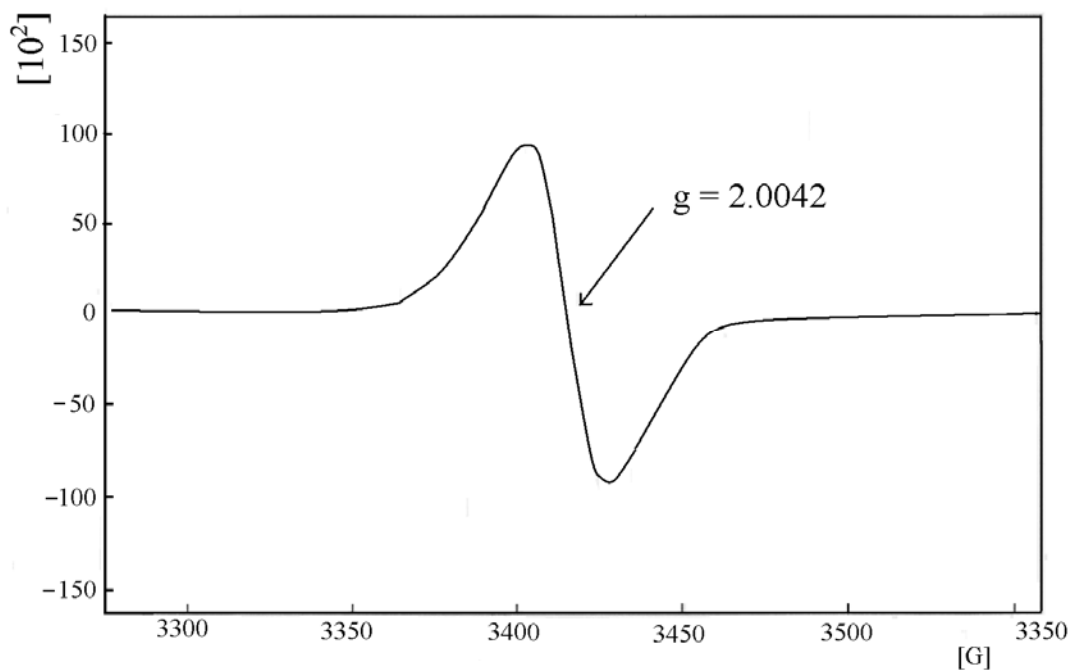


Fig. 92: EPR spectrum of solid $\text{Cs}[\text{B}_{12}(\text{OH})_{12}]$

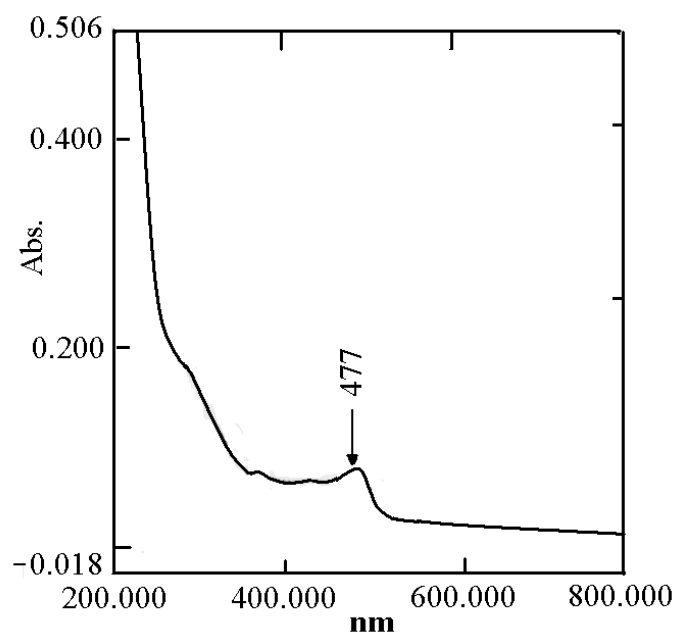


Fig. 93: UV-VIS absorption spectrum of $\text{Cs}[\text{B}_{12}(\text{OH})_{12}]$ in acetonitrile

5.2.3 Results of Cyclic Voltammetry Measurements

Electrochemical studies of the interconversion $[\text{B}_{12}(\text{OH})_{12}]^{2-/-}$ were hampered by the poor solubility of $\text{Cs}[\text{B}_{12}(\text{OH})_{12}]$. The best, reproducible results were obtained using cyclic voltammetry with either a Pt electrode after reacting the solid with 0.2 M $\text{Bu}_4\text{NPF}_6/\text{CH}_3\text{CN}$ solution for several hours at room temperature, or with a gold electrode at 75 °C in 0.1 M $\text{KNO}_3/\text{H}_2\text{O}$ (Fig. 94). Under these conditions, the anodic oxidation of *closo*- $[\text{B}_{12}(\text{OH})_{12}]^{2-}$ is irreversible at slow scan rates, but increasingly reversible above 1 V/s. Against ferrocenium/ferrocene as internal standard the half-wave potentials were determined as +0.45 V in CH_3CN and +0.75 V in water, reflecting the expected large difference for a polyhydroxo-species in aprotic and aqueous systems. Nevertheless, the twelvefold substitution of H in $[\text{B}_{12}\text{H}_{12}]^{2-}$ by OH in $[\text{B}_{12}(\text{OH})_{12}]^{2-}$ lowers the oxidation

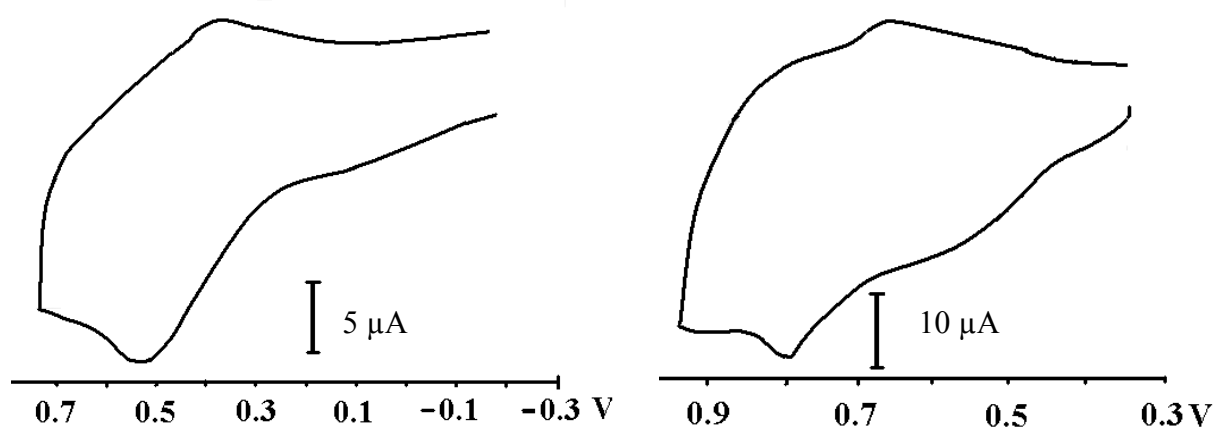


Fig. 94: Cyclovoltammogram of $\text{NBu}_4[\text{B}_{12}(\text{OH})_{12}]$ in 0.2 M $\text{Bu}_4\text{NPF}_6/\text{CH}_3\text{CN}$ solution at room temperature (*left*) and in 0.1 M $\text{KNO}_3/\text{H}_2\text{O}$ at 75 °C (*right*)

potential through π back-donation sufficiently to allow for the generation of the one-electron oxidized *hypocloso*- $[\text{B}_{12}(\text{OH})_{12}]^{\cdot-}$ as a stable radical anion and its isolation in the form of the cesium salt.

5.2.4 Structure Description of $\text{Cs}[\text{B}_{12}(\text{OH})_{12}]$

The crystal structure of $\text{Cs}[\text{B}_{12}(\text{OH})_{12}]$ was determined from X-ray single crystal diffraction data. The title compound crystallizes trigonally in space group $R\bar{3}m$ (no. 166) with three

formula units per unit cell (Fig. 95). In this crystal structure the cesium cations are located at the *Wyckoff* position $3a$ ($x/a = y/b = z/c = 0$; site symmetry: $\bar{3}m$). Both the boron (B1 – B2) and the hydroxyl oxygen atoms (O1 – O2) of the *hypocloso*- $[B_{12}(OH)_{12}]^{-}$ -cluster anion occupy two crystallographically distinct *Wyckoff* sites $18h$ ($x/a, y/b, z/c$; site symmetry: 1). In contrast to the unusually short Cs...Cs separation of 397 pm in $Cs_2[B_{12}(OH)_{12}] \cdot 2 H_2O$, there are no such interactions in $Cs[B_{12}(OH)_{12}]$ with the Cs...Cs separations of 704 pm. As a result, the interaction between the cations via the hydroxyl oxygen atoms found in all other known dodecahydroxo-*closo*-dodecaborate salts with alkali metal cations is diminished in the crystal structure of $Cs[B_{12}(OH)_{12}]$. Each Cs^{+} cation is surrounded by six nearest radical monoanionic

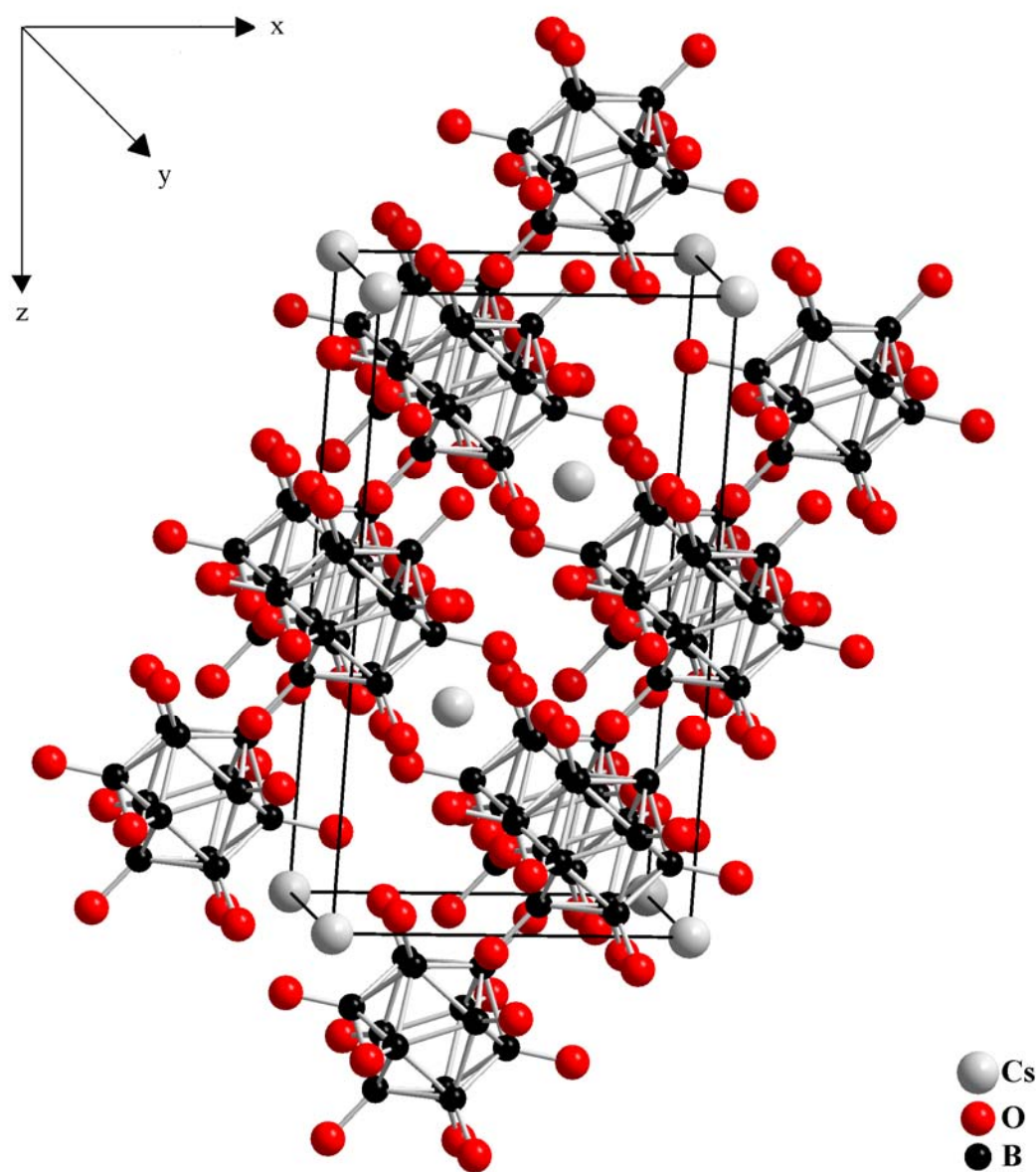


Fig. 95: Perspective view of the crystal structure of $Cs[B_{12}(OH)_{12}]$ along $[010]$

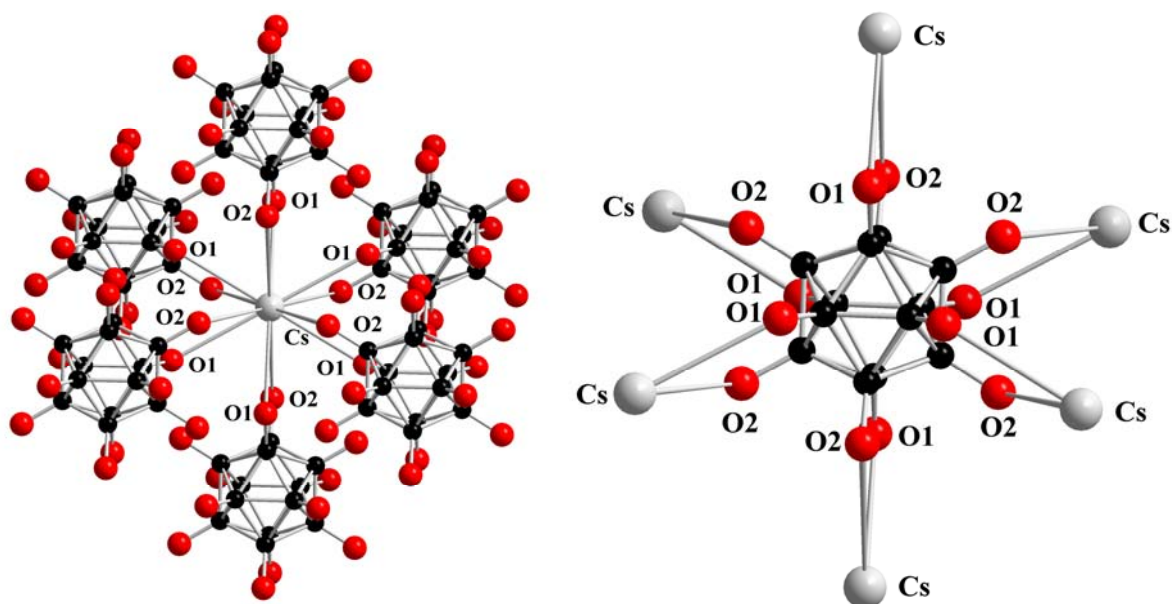


Fig. 96: Coordination sphere of the Cs^+ cations (*left*) and coordination environment of the *hypocloso*- $[\text{B}_{12}(\text{OH})_{12}]^-$ -cluster anions (*right*) in the crystal structure of $\text{Cs}[\text{B}_{12}(\text{OH})_{12}]$

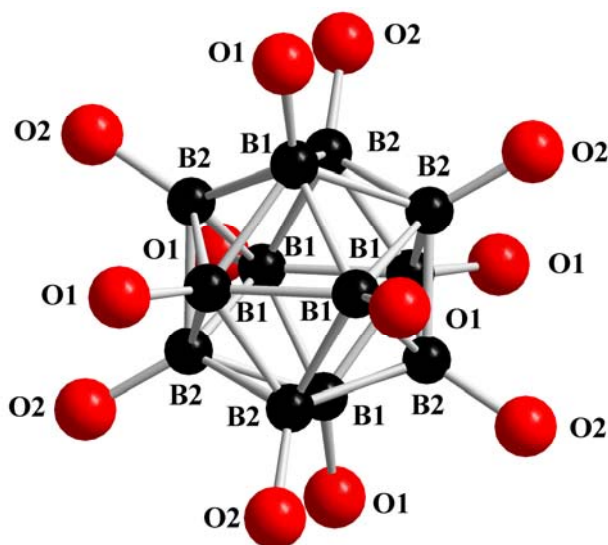


Fig. 97: The *hypocloso*- $[\text{B}_{12}(\text{OH})_{12}]^-$ -cluster anion in the crystal structure of $\text{Cs}[\text{B}_{12}(\text{OH})_{12}]$

boron cages via twelve hydroxyl oxygen atoms forming a distorted octahedron ($d(\text{Cs}-\text{O}) = 340 - 360 \text{ pm}$) (Fig. 96, *left*). This fact reveals that the $\text{Cs}-\text{O}$ distances are longer than those in the diamagnetic compound $\text{Cs}_2[\text{B}_{12}(\text{OH})_{12}] \cdot 2 \text{ H}_2\text{O}$ ($307 - 352 \text{ pm}$) and the Cs^+ cations in $\text{Cs}[\text{B}_{12}(\text{OH})_{12}]$ exhibits a coordination number of 12 instead of only 10 in $\text{Cs}_2[\text{B}_{12}(\text{OH})_{12}] \cdot 2 \text{ H}_2\text{O}$. The B–B bond lengths of the *hypocloso*- $[\text{B}_{12}(\text{OH})_{12}]^-$ -cluster anion fall in a small range

from 179 to 180 pm, whereas the B–O bond lengths range between 143 and 144 pm. This result confirms the completeness of the hydroxylation of all B–H vertices of the $[\text{B}_{12}\text{H}_{12}]^{2-}$ -cluster anion although the radical preparation reaction was carried out at rather low temperature. These bond lengths are in the common intervals for B–B and B–O single bonds (177 and 144 pm, respectively) and almost the same as those of the $[\text{B}_{12}(\text{OH})_{12}]^{2-}$ -cluster anion ($d(\text{B–O}) = 143 - 146$ pm; $d(\text{B–B}) = 178 - 181$ pm). Thus in $\text{Cs}[\text{B}_{12}(\text{OH})_{12}]$, the boron cluster is not distorted while one electron is removed. Among *hypocloso*- $[\text{B}_{12}\text{X}_{12}]^{\cdot-}$ radicals (X: OH, Me, OCH_2Ph), the lengthening of B–B bonds and the shortening of B–O bonds in *hypocloso*- $[\text{B}_{12}(\text{OH})_{12}]^{\cdot-}$ is less pronounced than those in *hypocloso*- $[\text{B}_{12}\text{Me}_{12}]^{\cdot-}$ ($d(\text{B–B}) = 179 - 181$ pm; $d(\text{B–C}) = 140 - 146$ pm) and *hypocloso*- $[\text{B}_{12}(\text{OCH}_2\text{Ph})_{12}]^{\cdot-}$ ($d(\text{B–B}) = 177 - 184$ pm; $d(\text{B–O}) = 140 - 142$ pm). The centers of gravity of the *hypocloso*- $[\text{B}_{12}(\text{OH})_{12}]^{\cdot-}$ -cluster anions are found at the *Wyckoff* site $3b$ ($x/a = y/b = 0$, $z/c = 1/2$; site symmetry: $\bar{3}m$). Each *hypocloso*- $[\text{B}_{12}(\text{OH})_{12}]^{\cdot-}$ -cluster anion is octahedrally surrounded by six cesium cations (Fig. 96, right). The distances from this center of gravity to the twelve boron atoms of the *hypocloso*- $[\text{B}_{12}(\text{OH})_{12}]^{\cdot-}$ -boron cage range from 170 to 172 pm providing an inner diameter of 340 – 344 pm for the *hypocloso*- $[\text{B}_{12}(\text{OH})_{12}]^{\cdot-}$ monoanion (Fig. 97). There are strong hydrogen bridging bonds in this compound between hydroxyl hydrogen atoms of one boron cage to oxygen atoms of the six nearest others arranged as an octahedron as judged from the short donor-acceptor distances $d(\text{O}\cdots\text{O}) = 264$ pm (Fig. 98). These six boron cages, in their turns, also link to six nearest others via strong hydrogen bridging bonds. Thus each boron cage is cuboctahedrally surrounded by twelve others. Compared to $\text{Cs}_2[\text{B}_{12}(\text{OH})_{12}] \cdot 2 \text{H}_2\text{O}$ no hydrogen bridging bonds between hydroxyl hydrogen atoms and oxygen atoms of free water molecules are found in $\text{Cs}[\text{B}_{12}(\text{OH})_{12}]$ due to the absence of any crystal water. Further detailed studies will be required to explain the existence of air-stable, paramagnetic $\text{Cs}[\text{B}_{12}(\text{OH})_{12}]$, in which the external donor substituent OH^- of *hypocloso*- $[\text{B}_{12}(\text{OH})_{12}]^{\cdot-}$ has no property of steric crowding, but only π back-donation to compensate the lower electron density in the boron cage. However, we presume that the hydroxylation of $[\text{B}_{12}\text{H}_{12}]^{2-}$ by H_2O_2 consists of two stages. Both total hydroxylation and one-electron oxidation of the boron cage take place to form the *hypocloso*- $[\text{B}_{12}(\text{OH})_{12}]^{\cdot-}$ radical in the first stage at a relatively low temperature. Increasing reacting times or temperatures, the second stage begins with the conversion of the *hypocloso*- $[\text{B}_{12}(\text{OH})_{12}]^{\cdot-}$ -cluster radical into $[\text{B}_{12}(\text{OH})_{12}]^{2-}$ in the presence of H_2O_2 . For the hydroxylation of $\text{Cs}_2[\text{B}_{12}\text{H}_{12}]$, $\text{Cs}[\text{B}_{12}(\text{OH})_{12}]$ having a significantly lower water solubility than $\text{Cs}_2[\text{B}_{12}(\text{OH})_{12}] \cdot 2 \text{H}_2\text{O}$ precipitates separately from the reaction mixture in the

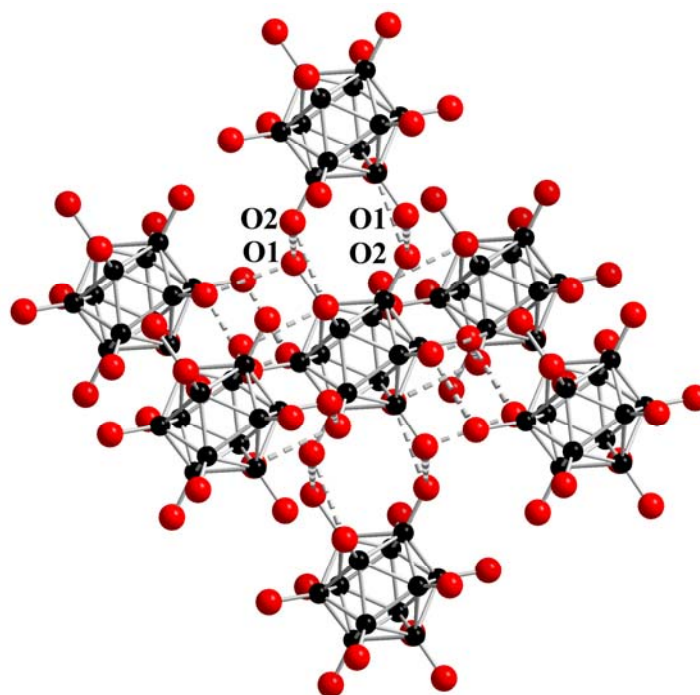


Fig. 98: The strong $\text{O}-\text{H}^{\delta+}\cdots\delta^-\text{O}$ hydrogen bond bridges between hydroxyl oxygen atoms of the *hypocloso*- $[\text{B}_{12}(\text{OH})_{12}]^{-}$ -cluster anion to those of the six nearest *hypocloso*- $[\text{B}_{12}(\text{OH})_{12}]^{-}$ -cluster anions arranged as an octahedron

first stage and does not further react with H_2O_2 to form $[\text{B}_{12}(\text{OH})_{12}]^{2-}$ in the second stage. The difference in water insolubility between the diamagnetic $\text{Cs}_2[\text{B}_{12}(\text{OH})_{12}] \cdot 2 \text{H}_2\text{O}$ and the paramagnetic $\text{Cs}[\text{B}_{12}(\text{OH})_{12}]$ depends on a number of factors including the nature of the counter-cation. The paramagnetic species could not be obtained from the hydroxylation of the dodecahydro-*closo*-dodecaborate salts of other alkali metals ($A = \text{Li}, \text{Na}, \text{K}$ and Rb). For example, although the synthesis conditions for the hydroxylation of $\text{Rb}_2[\text{B}_{12}\text{H}_{12}]$ are similar to that of $\text{Cs}_2[\text{B}_{12}\text{H}_{12}]$, the P-orthorhombic $\text{Rb}_2[\text{B}_{12}(\text{OH})_{12}] \cdot 2 \text{H}_2\text{O}$ is obtained instead of the paramagnetic species. Thus $\text{Cs}[\text{B}_{12}(\text{OH})_{12}]$ with its rocksalt-kind of crystal structure is the only air-stable radical species in a salt of an inorganic cation in the cluster-chemistry of boron and also the only paramagnetic derivative of *hypocloso*- $[\text{B}_{12}\text{H}_{12}]^{-}$ obtained without using the corresponding diamagnetic species as starting material to date.

From all above experimental results, it can be concluded that a surprisingly straightforward reaction between $\text{Cs}_2[\text{B}_{12}\text{H}_{12}]$ and H_2O_2 (30 %) yields both diamagnetic $\text{Cs}_2[\text{B}_{12}(\text{OH})_{12}] \cdot 2 \text{H}_2\text{O}$ and paramagnetic $\text{Cs}[\text{B}_{12}(\text{OH})_{12}]$ as parts of a new structurally characterized oligoborane cluster redox system with potential for further functionalization through the OH groups.

Table 94: Crystallographic data for Cs[B₁₂(OH)₁₂] and their determination

Crystal system	trigonal
Space group	R $\bar{3}$ m (no. 166)
Unit cell parameters:	
a (pm)	929.85(6)
c (pm)	1364.78(9)
Number of formula units per unit cell	Z = 3
Calculated density (D _x /g cm ⁻³)	2.276
Molar volume (V _m /cm ³ mol ⁻¹)	205.1
Diffractometer	κ-CCD (Bruker-Nonius)
Radiation	Mo-Kα: λ = 71.07 pm, graphite monochromator
Index range	±h _{max} = 12, ±k _{max} = 12, ±l _{max} = 18
θ _{max} (deg)	28.2
F(000)	669
Absorption coefficient (μ/mm ⁻¹)	2.78
Absorption correction	numerical, Program X-SHAPE [64]
Other data corrections	background, polarization and Lorentz factors
Collected reflections	2877
Unique reflections	338
R _{int} , R _σ	0.112, 0.042
Structure solution and refinement	Program SHELXS-97 and SHELXL-97 [68]
Scattering factors	International Tables for Crystallography, Vol. C [87]
R ₁ , R _w with F _o ≥ 4σ(F _o)	0.056, 0.036
Reflections with F _o ≥ 4σ(F _o)	251
wR ₂ , Goodness of fit (GooF)	0.075, 1.057
Extinction (g)	0.0031(4)
Residual electron density	
(max., min. in ρ/e ⁻¹ 10 ⁶ pm)	0.55, -0.27

Table 95: Atomic coordinates for Cs[B₁₂(OH)₁₂]

Atom	Wyckoff position	x/a	y/b	z/c
Cs	3a	0	0	0
O1	18h	0.1221(1)	0.8779(1)	0.6809(2)
O2	18h	0.1915(1)	0.8086(1)	0.4609(2)
B1	18h	0.7312(3)	0.4624(3)	0.9336(3)
B2	18h	0.4370(3)	0.5630(3)	0.1432(3)

Table 96: Anisotropic thermal displacement coefficients^{a)} (U_{ij}/pm²) for Cs[B₁₂(OH)₁₂]

Atom	U ₁₁	U ₂₂	U ₃₃	U ₂₃	U ₁₃	U ₁₂
Cs	765(8)	= U ₁₁	1039(19)	0	0	= 1/2 U ₁₁
O1	247(16)	= U ₁₁	230(31)	40(9)	= -U ₂₃	114(18)
O2	290(19)	= U ₁₁	300(24)	-15(9)	= -U ₂₃	259(14)
B1	187(21)	= U ₁₁	197(28)	-13(16)	= -U ₂₃	88(24)
B2	212(21)	= U ₁₁	191(28)	-17(12)	= -U ₂₃	139(24)

^{a)} For Cs, O and B defined as anisotropic temperature factor according to: $\exp[-2\pi^2(U_{11}h^2a^{*2} + U_{22}k^2b^{*2} + U_{33}l^2c^{*2} + 2U_{23}klb^*c^* + 2U_{13}hla^*c^* + 2U_{13}hka^*b^*)]$.

Table 97: Selected interatomic distances (d/pm) for Cs[B₁₂(OH)₁₂]

[CsO₁₂] polyhedron:

Cs – O1	340.7 (6×)
– O2	362.1 (6×)

[B₁₂(OH)₁₂]⁻ radical anion:

B1 – B2	179.6	B2 – B2	178.9 (2×)
– B2'	179.7 (2×)	– B1	179.6
– B1	179.8 (2×)	– B1'	179.7 (2×)
– O1	144.4	– O2	142.8

6. Summary and Outlook

Ionic salts of dodecahydro-*closo*-dodecaborates and hydroxylated derivatives were synthesized in this thesis. The main studying object was the structure determination of these salts by X-ray single crystal diffraction and NMR spectroscopic methods.

6.1 Results

6.1.1 Dodecahydro-*closo*-Dodecaborates

6.1.1.1 Dithallium(I) Dodecahydro-*closo*-Dodecaborate

The crystal structure of $\text{Tl}_2[\text{B}_{12}\text{H}_{12}]$ (cubic, $\text{Fm}\bar{3}$ (no. 202), $a = 1075.51(6)$ pm, $Z = 4$) can be described as an *anti*- CaF_2 -type arrangement, in which the Tl^+ cations occupy all the tetrahedral interstices within a cubic closest packed host lattice of the *quasi*-icosahedral $[\text{B}_{12}\text{H}_{12}]^{2-}$ -cluster anions. Tl^+ is thus tetrahedrally coordinated by four nearest neighbour $[\text{B}_{12}\text{H}_{12}]^{2-}$ units and twelve hydrogen atoms belonging to triangular faces of these four clusters provide an almost perfect cuboctahedral coordination sphere for each Tl^+ cation (CN = 12). The aqueous $^{11}\text{B}\{^1\text{H}\}$ -NMR measurements showed that the *closo*- $[\text{B}_{12}\text{H}_{12}]^{2-}$ anion in solution indeed exhibits the highest possible point symmetry ($\bar{5}\bar{3}2/m$). The crystal structure analysis revealed that *closo*- $[\text{B}_{12}\text{H}_{12}]^{2-}$ anions always possess a point symmetry lower than I_h as a consequence of the lack of a fivefold rotation axis in the three-dimensional periodic crystalline state. The lone-pair electrons at the Tl^+ cations in $\text{Tl}_2[\text{B}_{12}\text{H}_{12}]$ have real $6s^2$ character and are therefore stereochemically inactive.

6.1.1.2 Mercury(II) Dodecahydro-*closo*-Dodecaborate

In crystal structure of $\text{Hg}[\text{B}_{12}\text{H}_{12}]$ (triclinic, $\text{P}\bar{1}$ (no. 2), $a = 798.69(4)$, $b = 978.21(5)$, $c = 1694.12(9)$ pm, $\alpha = 101.105(3)$, $\beta = 103.630(3)$, $\gamma = 90.027(3)^\circ$, $Z = 7$) the *quasi*-icosahedral $[\text{B}_{12}\text{H}_{12}]^{2-}$ -cluster anions are strongly distorted from an ideal icosahedron. Each Hg^{2+} cation is cubically surrounded by eight $[\text{B}_{12}\text{H}_{12}]^{2-}$ anions and each *quasi*-icosahedral $[\text{B}_{12}\text{H}_{12}]^{2-}$ -cluster anion is also coordinated by eight nearest Hg^{2+} cations arranged as a almost perfect cubic fashion. In this CsCl-type of structure no covalent bonds between Hg^{2+} cations and hydrogen atoms of the boron cages are found.

6.1.1.3 Dodecahydro-*closo*-Dodecaborates with Divalent Transition Metals

The crystal structure of $\text{Ni}(\text{H}_2\text{O})_6[\text{B}_{12}\text{H}_{12}] \cdot 6 \text{H}_2\text{O}$ (cubic, $\text{F4}32$ (no. 210), $a = 1633.47(8)$ pm, $Z = 8$) can be described as a NaTl-type arrangement, in which the centers of gravity of

the *quasi*-icosahedral $[B_{12}H_{12}]^{2-}$ -cluster anions occupy the positions of Tl^- , whereas the Ni^{2+} cations replace Na^+ . There are both strong $O-H^{\delta+} \cdots \delta^-O$ and weak $B-H^{\delta-} \cdots \delta^+H-O$ hydrogen bridging bonds in crystal structure of $Ni(H_2O)_6[B_{12}H_{12}] \cdot 6 H_2O$. Via $O-H^{\delta+} \cdots \delta^-O$ hydrogen bonds the $[Ni(H_2O)_6]^{2+}$ octahedra are icosahedrally connected to “zeolitic” crystal water molecules to form a second coordination sphere. On the other hand, $Fe(H_2O)_6[B_{12}H_{12}]$ (monoclinic, $C2/m$ (no. 12), $a = 1393.45(9)$, $b = 1449.78(9)$, $c = 732.00(5)$ pm, $\beta = 95.879(3)^\circ$, $Z = 4$) crystallizes in a distortion variant of the CsCl-type structure. As no “zeolitic” crystal water molecules are present, its crystal structure is stabilized by only weak $B-H^{\delta-} \cdots \delta^+H-O$ hydrogen bridging bonds.

6.1.1.4 Dioxonium Dodecahydro-*closo*-Dodecaborates with Divalent Transition Metals

The crystal structure of the double salts $[M(H_2O)_6](H_3O)_2[B_{12}H_{12}]_2 \cdot 6 H_2O$ ($M = Mn, Fe, Co, Ni, Cu, Zn$ and Cd) is characterized as a layer-like structure with $[M(H_2O)_6]^{2+}$, $[B_{12}H_{12}]^{2-}$ and H_3O^+ sheets alternatively arranged along $[001]$. Each M^{2+} cation is octahedrally coordinated by six water molecules. The crystal structure is stabilized by both strong $O-H^{\delta+} \cdots \delta^-O$ and weak $B-H^{\delta-} \cdots \delta^+H-O$ hydrogen bridging bonds.

orthorhombic, Pnmm (no. 58), $Z = 2$	lattice constants		
	a / pm	b / pm	c / pm
$[Mn(H_2O)_6](H_3O)_2[B_{12}H_{12}]_2 \cdot 6 H_2O$	1160.56(7)	1512.86(9)	925.55(6)
$[Fe(H_2O)_6](H_3O)_2[B_{12}H_{12}]_2 \cdot 6 H_2O$	1160.38(7)	1504.89(9)	923.30(6)
$[Co(H_2O)_6](H_3O)_2[B_{12}H_{12}]_2 \cdot 6 H_2O$	1157.45(7)	1495.14(9)	924.68(6)
$[Ni(H_2O)_6](H_3O)_2[B_{12}H_{12}]_2 \cdot 6 H_2O$	1156.25(7)	1488.47(9)	924.98(6)
$[Cu(H_2O)_6](H_3O)_2[B_{12}H_{12}]_2 \cdot 6 H_2O$	1162.81(7)	1493.21(9)	921.60(6)
$[Zn(H_2O)_6](H_3O)_2[B_{12}H_{12}]_2 \cdot 6 H_2O$	1157.57(7)	1493.03(9)	924.93(6)
$[Cd(H_2O)_6](H_3O)_2[B_{12}H_{12}]_2 \cdot 6 H_2O$	1159.02(7)	1532.90(9)	923.90(6)

6.1.1.5 Triqua-Lead(II) Dodecahydro-*closo*-Dodecaborate Trihydrate

The crystal structure of $Pb(H_2O)_3[B_{12}H_{12}] \cdot 3 H_2O$ (orthorhombic, $Pna2_1$ (no. 33), $a = 1839.08(9)$, $b = 1166.52(6)$, $c = 717.27(4)$ pm, $Z = 4$) is characterized as a layer-like structure, in which Pb^{2+} and $[B_{12}H_{12}]^{2-}$ are alternatively arranged. The Pb^{2+} cations are coordinated in first sphere excentrically with only three oxygen atoms of water molecules. Furthermore, Pb^{2+} is connected to three hydrogen atoms of $[B_{12}H_{12}]^{2-}$ anions to form a second coordination sphere, in which each Pb^{2+} cation has a total coordination number of six and is surrounded by

both hydrogen and oxygen atoms. This relatively strange coordination environment of Pb^{2+} is a consequence of the stereochemical activity of its $6s^2$ lone-pair electrons.

6.1.1.6 Diaqua-Monohydroxo-Bismuth(III) Dodecahydro-*closo*-Dodecaborate

The series of crystal structures of dodecahydro-*closo*-dodecaborate salts of Tl^+ , Pb^{2+} and Bi^{3+} cations that possess $6s^2$ lone-pair electrons is completed by that one of $\text{Bi}(\text{H}_2\text{O})_2(\text{OH})[\text{B}_{12}\text{H}_{12}]$ (orthorhombic, Pnma (no. 62), $a = 1382.29(9)$, $b = 892.78(6)$, $c = 982.47(7)$ pm, $Z = 4$). In this structure each Bi^{3+} cation is nearly coplanar coordinated by three neighbouring oxygen atoms with two of coordinated crystal water and one of the OH^- group. Moreover, the Bi^{3+} cations are surrounded by three nearest *quasi*-icosahedral $[\text{B}_{12}\text{H}_{12}]^{2-}$ -cluster anions via hydrogen atoms of the boron cages. The excentric coordination environment of Bi^{3+} shows that the $6s^2$ lone-pair electrons are stereochemically active.

6.1.1.7 Bis-Hexaaqua-Chromium(III) and Bis-Hexaaqua-Indium(III) Tris-Dodecahydro-*closo*-Dodecaborate Pentadecahydrate

The crystal structure of the salts $[\text{M}(\text{H}_2\text{O})_6]_2[\text{B}_{12}\text{H}_{12}]_3 \cdot 15 \text{H}_2\text{O}$ ($\text{M} = \text{Cr}$ and In) can be described as two independent interpenetrating layered motives, namely one of the $[\text{M}(\text{H}_2\text{O})_6]^{3+}$ cations and one of the $[\text{B}_{12}\text{H}_{12}]^{2-}$ -cluster anions, as lattice components. The chromium(III) and indium(III) cations arrange in a cubic closest packed fashion with the stacking sequence *abc* just like the Cu-type structure and the $[\text{B}_{12}\text{H}_{12}]^{2-}$ anions form 9-layer stacking sequence such as *ABCCABBCA*. Both strong $\text{O}-\text{H}^{\delta+}\cdots\delta^-\text{O}$ and weak $\text{B}-\text{H}^{\delta-}\cdots\delta^+\text{H}-\text{O}$ hydrogen bridging bonds are found in the isotypic structures of the salt hydrates $[\text{M}(\text{H}_2\text{O})_6]_2[\text{B}_{12}\text{H}_{12}]_3 \cdot 15 \text{H}_2\text{O}$ ($\text{M} = \text{Cr}$ and In).

trigonal, $\text{R}\bar{3}\text{c}$ (no. 167), $Z = 6$	lattice constants	
	a / pm	c / pm
$[\text{Cr}(\text{H}_2\text{O})_6]_2[\text{B}_{12}\text{H}_{12}]_3 \cdot 15 \text{H}_2\text{O}$	1157.62(3)	6730.48(9)
$[\text{In}(\text{H}_2\text{O})_6]_2[\text{B}_{12}\text{H}_{12}]_3 \cdot 15 \text{H}_2\text{O}$	1171.71(3)	6740.05(9)

6.1.1.8 Hexaaqua-Chromium Aqua-Oxonium Dodecahydro-*closo*-Dodecaborate Hexahydrate

The crystal structure of $[\text{Cr}(\text{H}_2\text{O})_6](\text{H}_5\text{O}_2)[\text{B}_{12}\text{H}_{12}]_2 \cdot 6 \text{H}_2\text{O}$ (orthorhombic, Pnmm (no. 58), $a = 1086.55(7)$, $b = 1483.17(9)$, $c = 949.24(6)$ pm, $Z = 2$) is characterized as a layer-like structure with $[\text{Cr}(\text{H}_2\text{O})_6]^{3+}$, $[\text{B}_{12}\text{H}_{12}]^{2-}$ and H_5O_2^+ layers alternatively arranged along $[001]$.

The Zundel-type aqua-oxonium cation (H_5O_2^+) with two symmetry-related oxygen atom possesses a strong centered $\text{O}-\text{H}\cdots\text{O}$ hydrogen bond. Each Cr^{3+} cation ($\text{CN} = 6$) is coordinated by six nearest water molecules forming an almost perfect octahedron.

6.1.1.9 Bis-Hexaqua-Aluminium(III) Oxosulfate Tris-Dodecahydro-*closo*-Dodecaborate Pentadecahydrate

In the crystal structure of $[\text{Al}(\text{H}_2\text{O})_6]_2(\text{SO}_4)[\text{B}_{12}\text{H}_{12}]_2 \cdot 15 \text{H}_2\text{O}$ (trigonal, $R\bar{3}c$ (no. 167), $a = 1083.82(2)$, $c = 6776.56(9)$ pm, $Z = 6$) the arrangement of both the $[\text{B}_{12}\text{H}_{12}]^{2-}$ and the SO_4^{2-} anions follows the cubic closest packed fashion with stacking sequences such as $abc\ a'b'c'$. The stacking sequence of the hexahydrated Al^{3+} cations is $aa\ bb\ cc$, a double-layer feature of the copper structure type. The shape of the SO_4^{2-} anion, with sulfur-coordinated oxygen atoms located at two half-occupied *Wyckoff* sites, is a distorted hexagonal scalenohedron rather than a common tetrahedron due to structural disorder, whereas the Al^{3+} cation is octahedrally bonded to six nearest oxygen atoms of crystal water molecules.

6.1.1.10 Dodecahydro-*closo*-Dodecaborate Hydrates of Trivalent Rare-Earth Metals

The water-rich salts $[\text{M}(\text{H}_2\text{O})_9]_2[\text{B}_{12}\text{H}_{12}]_3 \cdot 15 \text{H}_2\text{O}$ ($\text{M} = \text{Pr}$ and Ho) crystallize with structures that can be described as two independent interpenetrating layered motifs, namely the $[\text{M}(\text{H}_2\text{O})_9]^{3+}$ cations and the $[\text{B}_{12}\text{H}_{12}]^{2-}$ anions, as lattice components. The $[\text{B}_{12}\text{H}_{12}]^{2-}$ cluster anions are arranged according the α -Sm-type structure, whereas the hydrated trications are stacked according to the Cu-type structure.

trigonal, $R\bar{3}c$ (no. 167), $Z = 6$	lattice constants	
	a / pm	c / pm
$[\text{Pr}(\text{H}_2\text{O})_9]_2[\text{B}_{12}\text{H}_{12}]_3 \cdot 15 \text{H}_2\text{O}$	1187.80(2)	7290.76(9)
$[\text{Ho}(\text{H}_2\text{O})_9]_2[\text{B}_{12}\text{H}_{12}]_3 \cdot 15 \text{H}_2\text{O}$	1172.65(2)	7204.12(9)

By the reaction of lanthanum nitrate hexahydrate $\text{La}(\text{NO}_3)_3 \cdot 6 \text{H}_2\text{O}$ with the free acid $(\text{H}_3\text{O})_2[\text{B}_{12}\text{H}_{12}]$, $[\text{La}(\text{H}_2\text{O})_9]_2[\text{B}_{12}\text{H}_{12}]_3 \cdot 7 \text{H}_2\text{O}$ (triclinic, $P\bar{1}$ (no. 2), $a = 1186.54(6)$, $b = 1277.09(7)$, $c = 1789.15(9)$ pm, $\alpha = 70.492(3)$, $\beta = 85.201(3)$, $\gamma = 87.633(3)^\circ$, $Z = 2$) with only 25 water molecules is obtained. In the crystal structure the La^{3+} cations are also coordinated by nine oxygen atoms of the water molecules forming a distorted monocapped square antiprism ($\text{CN} = 9$). Both the crystal structures of $[\text{M}(\text{H}_2\text{O})_9]_2[\text{B}_{12}\text{H}_{12}]_3 \cdot 15 \text{H}_2\text{O}$ ($\text{M} = \text{Pr}$ and Ho) and $[\text{La}(\text{H}_2\text{O})_9]_2[\text{B}_{12}\text{H}_{12}]_3 \cdot 7 \text{H}_2\text{O}$ are stabilized by strong $\text{O}-\text{H}^{\delta+}\cdots\delta^-\text{O}$ and weak $\text{B}-\text{H}^{\delta-}\cdots\delta^+\text{H}-\text{O}$ hydrogen bridging bonds. The strong $\text{O}-\text{H}^{\delta+}\cdots\delta^-\text{O}$ hydrogen bonds in

$[\text{La}(\text{H}_2\text{O})_9]_2[\text{B}_{12}\text{H}_{12}]_3 \cdot 7 \text{H}_2\text{O}$, however, are found between oxygen atoms of $[\text{La}(\text{H}_2\text{O})_9]^{3+}$ cations and those of both crystal water molecules and coordinated oxygen atoms of other La^{3+} cations, while the oxygen atoms of the tricapped trigonal prismatic $[\text{M}(\text{H}_2\text{O})_9]^{3+}$ cations ($\text{M} = \text{Pr}$ and Ho) connect only to those of “zeolitic” crystal water molecules.

6.1.1.11 A Mixed Cationic Holmium(III) Oxonium Dodecahydro-*closo*-Dodecaborate Hydrate

$[\text{Ho}(\text{H}_2\text{O})_9](\text{H}_3\text{O})_3[\text{B}_{12}\text{H}_{12}]_3 \cdot 9 \text{H}_2\text{O}$ (trigonal, $R3c$ (no. 161), $a = 2351.04(9)$, $c = 1472.73(6)$ pm, $Z = 6$) is synthesized by the reaction of $[\text{Ho}(\text{H}_2\text{O})_9]_2[\text{B}_{12}\text{H}_{12}]_3 \cdot 15 \text{H}_2\text{O}$ and the free acid $(\text{H}_3\text{O})_2[\text{B}_{12}\text{H}_{12}]$ from aqueous solution. The crystal structure can be described as three independent interpenetrating layered motifs, namely the $[\text{Ho}(\text{H}_2\text{O})_9]^{3+}$ and H_3O^+ cations and the $[\text{B}_{12}\text{H}_{12}]^{2-}$ anions, as lattice components. All these building blocks alternatively arrange in a cubic closest packed fashion with the same stacking sequence *abc*. The holmium(III) cations are always coordinated by nine nearest oxygen atoms of crystal water molecules forming a distorted tricapped trigonal prism for each.

6.1.2 Partially Hydroxylated Dodecahydro-*closo*-Dodecaborates

6.1.2.1 Undeca-*hydro*-Monohydroxo-*closo*-Dodecaborate Monohydrates

In the crystal structure of $(\text{H}_3\text{O})_2[\text{B}_{12}\text{H}_{11}(\text{OH})] \cdot \text{H}_2\text{O}$, the oxonium cations occupy two crystallographically distinct positions. Each oxonium cation $(\text{H}_3\text{O}1)^+$ is tetrahedrally coordinated by four nearest $[\text{B}_{12}\text{H}_{11}(\text{OH})]^{2-}$ -cluster anions via ten hydrogen and two oxygen atoms of the boron cages. Each oxonium cation $(\text{H}_3\text{O}2)^+$ is also tetrahedrally coordinated with four nearest $[\text{B}_{12}\text{H}_{11}(\text{OH})]^{2-}$ -cluster anions, but now via three hydrogen atoms originating from one triangular face per each. Monohydroxylation of the boron cage causes a pronounced distortion from an ideal icosahedron. The crystal structure of $\text{Cs}_2[\text{B}_{12}\text{H}_{11}(\text{OH})] \cdot \text{H}_2\text{O}$ is basically isostructural to that of $(\text{H}_3\text{O})_2[\text{B}_{12}\text{H}_{11}(\text{OH})] \cdot \text{H}_2\text{O}$, but the cesium cations occupy three crystallographically different *Wyckoff* positions, whereas the oxygen atoms of the oxonium cations $(\text{H}_3\text{O}1)^+$ and $(\text{H}_3\text{O}2)^+$ in $(\text{H}_3\text{O})_2[\text{B}_{12}\text{H}_{11}(\text{OH})] \cdot \text{H}_2\text{O}$ were only distributed over two. In both crystal structures, however, there exist both of classical $\text{O}-\text{H}^{\delta+} \cdots \delta^- \text{O}$ and non-classical $\text{B}-\text{H}^{\delta-} \cdots \delta^+ \text{H}-\text{O}$ hydrogen bonds.

orthorhombic, Ama2 (no. 40), $Z = 4$	lattice constants		
	a / pm	b / pm	c / pm
$(\text{H}_3\text{O})_2[\text{B}_{12}\text{H}_{11}(\text{OH})] \cdot \text{H}_2\text{O}$	868.60(6)	1252.16(9)	1149.29(8)
$\text{Cs}_2[\text{B}_{12}\text{H}_{11}(\text{OH})] \cdot \text{H}_2\text{O}$	1039.54(7)	1365.67(9)	958.16(6)

6.1.2.2 Dicesium 1,7-Dihydroxo-Decahydro-*closo*-Dodecaborate

The isomeric assignment of $\text{Cs}_2[1,7\text{-B}_{12}\text{H}_{10}(\text{OH})_2]$ was achieved by both crystal structure analysis and one-dimensional NMR measurements. In the crystal structure of $\text{Cs}_2[1,7\text{-B}_{12}\text{H}_{10}(\text{OH})_2]$ (orthorhombic, *Pnma* (no. 62), $a = 1429.60(9)$, $b = 929.38(6)$, $c = 1030.70(7)$ pm, $Z = 4$) both cesium cations and the hydroxyl oxygen atoms of the boron cage occupy two different crystallographic positions with one half-occupied in each case. The cesium cation at the fully occupied site is surrounded by five boron cages arranged as a trigonal pyramid and coordinated via ten hydrogen and three hydroxyl oxygen atoms (CN = 13). The cesium cation at the half-occupied site is nearly coplanar surrounded with four nearest boron cages, which are attached via ten hydrogen and two hydroxyl oxygen atoms (CN = 12). The *quasi*-icosahedral $[1,7\text{-B}_{12}\text{H}_{10}(\text{OH})_2]^{2-}$ -cluster anion is more distorted as compared to the parent $[\text{B}_{12}\text{H}_{12}]^{2-}$ unit. Each boron cage connects to four neighbouring ones via strong $\text{O-H}^{\delta+}\cdots\delta-\text{O}$ hydrogen bridges between their hydroxyl oxygen atoms to form a pyramid. Thermal analysis of $\text{Cs}_2[1,7\text{-B}_{12}\text{H}_{10}(\text{OH})_2]$ shows that the thermal stability of the boron cage is not considerably diminished by introducing two OH groups.

6.1.2.3 Dicesium 1,2,3-Trihydroxo-Enneahydro-*closo*-Dodecaborate Monohydrate

In the crystal structure of $\text{Cs}_2[1,2,3\text{-B}_{12}\text{H}_9(\text{OH})_3] \cdot \text{H}_2\text{O}$ (orthorhombic, *Pbcm* (no. 57), $a = 916.35(6)$, $b = 1373.10(9)$, $c = 1039.41(7)$ pm, $Z = 4$) three hydroxyl groups originating from one triangular face of a $[\text{B}_{12}\text{H}_9(\text{OH})_3]^{2-}$ -cluster anion assign it as the 1,2,3-isomer species from crystal structure analysis. The cesium cations occupy three crystallographically distinct sites, of which two are only half-occupied. Each of the two Cs^+ cations at the half-occupied sites is tetrahedrally surrounded by four $[1,2,3\text{-B}_{12}\text{H}_9(\text{OH})_3]^{2-}$ -cluster anions (CN = 12), while the cations at the fully occupied site are coordinated by five boron cages arranged as a trigonal bipyramid (CN = 13) attached via hydrogen and hydroxyl oxygen atoms of the boron cages and oxygen atoms of crystal water molecules. The trihydroxylation of the boron cage causes a pronounced distortion of the *quasi*-icosahedral $[1,2,3\text{-B}_{12}\text{H}_9(\text{OH})_3]^{2-}$ -cluster anion.

6.1.2.4 Dicesium 1,2,3,5-Tetrahydroxo-Octahydro-*closo*-Dodecaborate Dihydrate

In the crystal structure of $\text{Cs}_2[1,2,3,5\text{-B}_{12}\text{H}_8(\text{OH})_4] \cdot 2 \text{H}_2\text{O}$ (orthorhombic, *Pbcm* (no. 57), $a = 972.16(6)$, $b = 1396.69(9)$, $c = 1074.71(7)$ pm, $Z = 4$) the four hydroxyl oxygen atoms per cage reside at two fully occupied and one half-occupied *Wyckoff* positions. One of two crystallographically distinct cesium cations is tetrahedrally surrounded by four neighbouring

quasi-icosahedral $[1,2,3,5\text{-B}_{12}\text{H}_8(\text{OH})_4]^{2-}$ -cluster anions and coordinated via eight hydrogen atoms, two hydroxyl oxygen atoms and three oxygen atoms of crystal water molecules (CN = 13), whereas the other one is surrounded by five boron cages arranged as a trigonal pyramid grafted via seven hydrogen atoms, five hydroxyl oxygen atoms and one oxygen atom of a crystal water molecule (CN = 13). The *quasi*-icosahedral $[1,2,3,5\text{-B}_{12}\text{H}_8(\text{OH})_4]^{2-}$ -cluster anion is slightly distorted from the parent $[\text{B}_{12}\text{H}_{12}]^{2-}$ species and can not be assigned easily to just one (e. g. 1,2,3,5-) isomer.

6.1.3 Dodecahydroxo-*closo*-Dodecaborates

6.1.3.1 Dirubidium Dodecahydroxo-*closo*-Dodecaborate Dihydrates

By carrying out the reaction between $\text{Rb}_2[\text{B}_{12}\text{H}_{12}]$ and hydrogen peroxide H_2O_2 at either 65, or 90 or 110 °C, three crystallographically different polymorphs (P- and C-orthorhombic, P-monoclinic) of $\text{Rb}_2[\text{B}_{12}(\text{OH})_{12}] \cdot 2 \text{H}_2\text{O}$ can be obtained, respectively. $^{11}\text{B}\{^1\text{H}\}$ -NMR and X-ray powder diffraction measurements show that total hydroxylation was achieved and the single crystalline phase of each polymorph at the corresponding reaction temperature emerged phase-pure. The Rb^+ cations in all three forms exhibit a coordination number of ten with both nearest oxygen atoms of water molecules and hydroxyl groups of the boron cages. Via these oxygen atoms, the rubidium cations are linked to form one-dimensional (in P-monoclinic $\text{Rb}_2[\text{B}_{12}(\text{OH})_{12}] \cdot 2 \text{H}_2\text{O}$) or three-dimensional (P- and C-orthorhombic $\text{Rb}_2[\text{B}_{12}(\text{OH})_{12}] \cdot 2 \text{H}_2\text{O}$) polymeric networks. In P- and C-orthorhombic $\text{Rb}_2[\text{B}_{12}(\text{OH})_{12}] \cdot 2 \text{H}_2\text{O}$ each *quasi*-icosahedral $[\text{B}_{12}(\text{OH})_{12}]^{2-}$ -cluster anion is nearly or exactly coplanar surrounded by six Rb^+ cations, respectively. In P-monoclinic $\text{Rb}_2[\text{B}_{12}(\text{OH})_{12}] \cdot 2 \text{H}_2\text{O}$ each $[\text{B}_{12}(\text{OH})_{12}]^{2-}$ anion is surrounded by eight Rb^+ cations arranged in a parallelepipedal shape. All three polymorphs are stabilized by strong $\text{O}-\text{H}^{\delta+} \cdots \delta^-\text{O}$ hydrogen bridging bonds. In literature, there is even a fourth form of $\text{Rb}_2[\text{B}_{12}(\text{OH})_{12}] \cdot 2 \text{H}_2\text{O}$ described as C-monoclinic and accessible from RbCl and $\text{Cs}_2[\text{B}_{12}(\text{OH})_{12}]$ in aqueous solution.

$\text{Rb}_2[\text{B}_{12}(\text{OH})_{12}] \cdot 2 \text{H}_2\text{O}$	lattice constants				
	a / pm	b / pm	c / pm	$\beta / ^\circ$	$V_m / \text{cm}^3 \text{mol}^{-1}$
orthorhombic, Pnma (no. 62), Z = 4	1330.27(9)	1300.94(9)	918.59(6)	90	239.3
orthorhombic, Cmce (no. 64), Z = 4	1577.73(9)	812.18(5)	1243.56(7)	90	239.9
monoclinic, P2 ₁ /c (no. 14), Z = 2	812.30(6)	728.19(5)	1303.51(9)	97.096(3)	230.4

6.1.3.2 Cesium Dodecahydroxo-*hypocloso*-Dodecaborate

Paramagnetic, air-stable, dark green $\text{Cs}[\text{B}_{12}(\text{OH})_{12}]$ is prepared by the reaction between $\text{Cs}_2[\text{B}_{12}\text{H}_{12}]$ and hydrogen peroxide, H_2O_2 , at relative low temperatures. Results of single crystal and powder X-ray diffraction analyses, EPR, UV-VIS and cyclic voltammetry measurements show that for the chosen preparation process not only the hydroxylation, but also a one-electron oxidation of the boron cage took place and stable radical [*hypocloso*- $\text{B}_{12}(\text{OH})_{12}]^{\cdot-}$ monoanion is obtained in the form of the cesium salt as a main product with high purity. The *hypocloso*-dodecahydroxo-dodecaborate radical anion exhibits an unresolved EPR signal at $g = 2.0042$ in the solid state, which is close to the free electron value of 2.0023. $\text{Cs}[\text{B}_{12}(\text{OH})_{12}]$ ($a = 929.85(6)$ and $c = 1364.78(9)$ pm) crystallizes trigonally in space group $\bar{R}3m$ (no. 166) with three formula units per unit cell. In the crystal structure of $\text{Cs}[\text{B}_{12}(\text{OH})_{12}]$ the interaction between the cesium cations via the hydroxyl oxygen atoms is diminished. Each cesium cation is surrounded by six nearest radical monoanionic boron cages via twelve hydroxyl oxygen atoms forming a distorted octahedron (CN = 12). There are strong hydrogen bridging bonds in this compound between hydroxyl oxygen atoms of one boron cage to those of six nearest others arranged as an octahedron. The *hypocloso*- $[\text{B}_{12}(\text{OH})_{12}]^{\cdot-}$ -cluster anion is almost not distorted even if the removal of one electron from the boron cage is weakly compensated by only the π back-donation effect. According to a rocksalt-type arrangement, six Cs^+ cations surround each boron cage octahedrally as vice versa.

6.2 Outlook

Synthesis and crystal structure determination of dodecahydro-*closo*-dodecaborate salts with inorganic cations have been systematically investigated by recent works as well as in this thesis. However, the crystal structures of some monovalent (e. g. Ag^+ , Cu^+), divalent (e. g. Be^{2+} , Cr^{2+} , Sn^{2+}), and trivalent cations (e. g. Co^{3+} , Fe^{3+}) are still unknown and require further investigation.

With the exception of the cesium cation, the syntheses, crystallizations, thermal stability and crystal structure determinations of partially hydroxylated dodecahydro-*closo*-dodecaborates with $[\text{B}_{12}\text{H}_{12-n}(\text{OH})_n]^{2-}$ anions ($n = 1 - 4$) are not accomplished with other inorganic counter-cations. Furthermore, crystallographic data of partially hydroxylated dodecahydro-*closo*-

dodecaborate anions $[\text{B}_{12}\text{H}_{12-n}(\text{OH})_n]^{2-}$ with $n > 4$ and a stepwise synthesis method for these derivatives are still not available.

Perhydroxylation of the $[\text{B}_{12}\text{H}_{12}]^{2-}$ -cluster anion is the usual intermediate step of functionalization, but only the syntheses and crystal structure determination of dodecahydroxo-*closo*-dodecaborate salts with heavy alkali metal cations and cesium dodecahydroxo-*hypocloso*-dodecaborate have been successfully achieved to date. It is, however, difficult to obtain single crystals of dodecahydroxo-*closo*-dodecaborate and dodecahydroxo-*hypocloso*-dodecaborate salts with other inorganic cations by conventional crystallization from solution due to their extremely low water solubility. Therefore, to elucidate the crystal structures of these salts by single crystal diffraction methods, seeking for a new crystal growth method is desirable. In addition, to explain the existence of the air-stable, paramagnetic salt $\text{Cs}[\text{B}_{12}(\text{OH})_{12}]$, in which the external donor substituent OH^- of the $[\text{B}_{12}(\text{OH})_{12}]^-$ monoanion has no property of sterical crowding, only π back-donation has to compensate the lower electron density in the boron cage, further detailed studies are necessary.

Functionalization of the three-dimensional aromatic $[\text{B}_{12}\text{H}_{12-n}(\text{OH})_n]^{2-}$ -cluster anions is a new trend in the chemistry of boranes. Although the synthesis, crystallization, crystal structure of functionalized dodecahydro-*closo*-dodecaborate salts of many organic cations have been published, those of inorganic cations are still not available in literature at all. The twelvefold functionalization of an icosahedral surface by total esterification of $[\text{B}_{12}(\text{OH})_{12}]^{2-}$ with oxalyl chloride, sulfonyl chloride or benzoyl chloride, namely, is a prospective research subject not only in sense of basic research but also for application such as drug delivery, BNCT.

7 Zusammenfassung und Ausblick

Ionische Salze der Dodekahydro-*closo*-Dodekaborate und hydroxilierte Derivate wurden synthetisiert und in dieser Arbeit vorgestellt. Die Strukturbestimmung dieser Salze mittels Röntgenbeugungsmethoden und NMR-Spektroskopie waren die Hauptziele dieser Arbeit.

7.1 Ergebnisse

7.1.1 Dodekahydro-*closo*-Dodekaborate

7.1.1.1 Dithallium(I)-Dodekahydro-*closo*-Dodekaborat

Die Kristallstruktur von $\text{Tl}_2[\text{B}_{12}\text{H}_{12}]$ (kubisch, $\text{Fm}\bar{3}$ (Nr. 202), $a = 1075,51(6)$ pm, $Z = 4$) kann als *anti*- CaF_2 -Typ beschrieben werden, in dem die Tl^+ -Kationen alle tetraedrischen Lücken einer kubisch dichtesten Kugelpackung der *quasi*-ikosaedrischen $[\text{B}_{12}\text{H}_{12}]^{2-}$ -Clusteranionen besetzen. Tl^+ ist also tetraedrisch von vier $[\text{B}_{12}\text{H}_{12}]^{2-}$ -Nachbareinheiten koordiniert. Dadurch schaffen zwölf Wasserstoffatome, jeweils drei einer Dreiecksfläche eines $[\text{B}_{12}\text{H}_{12}]^{2-}$ -Anions, eine fast perfekte kuboktaedrische Koordinationssphäre für jedes Tl^+ -Kation (CN = 12). Die in wässriger Lösung durchgeführten $^{11}\text{B}\{^1\text{H}\}$ -NMR-Messungen zeigten, dass die *closo*- $[\text{B}_{12}\text{H}_{12}]^{2-}$ -Anionen in Lösung tatsächlich die höchst mögliche Punktsymmetrie ($\bar{5}\bar{3}2/m$) aufweisen. Die Kristallstrukturanalyse gab zu erkennen, dass *closo*- $[\text{B}_{12}\text{H}_{12}]^{2-}$ -Anionen im Festkörper immer eine niedrigere Punktsymmetrie als I_h besitzen als Folge der fehlenden fünfzähligen Drehachse im dreidimensional periodischen Kristallverband. Die "lone-pair" Elektronen der Tl^+ -Kationen im $\text{Tl}_2[\text{B}_{12}\text{H}_{12}]$ besitzen echten $6s^2$ Charakter und sind deshalb stereochemisch inaktiv.

7.1.1.2 Quecksilber(II)-Dodekahydro-*closo*-Dodekaborat

Das *quasi*-ikosaedrische $[\text{B}_{12}\text{H}_{12}]^{2-}$ -Clusteranion in dieser Kristallstruktur (triklin, $\text{P}\bar{1}$ (Nr. 2), $a = 798,69(4)$, $b = 978,21(5)$, $c = 1694,12(9)$ pm, $\alpha = 101,105(3)$, $\beta = 103,630(3)$, $\gamma = 90,027(3)^\circ$, $Z = 7$) ist stark verzerrt gegenüber einem idealen Ikosaeder. Jedes Hg^{2+} -Kation ist kubisch von acht *quasi*-ikosaedrischen $[\text{B}_{12}\text{H}_{12}]^{2-}$ -Clusteranionen umgeben, und jedes der $[\text{B}_{12}\text{H}_{12}]^{2-}$ -Clusteranionen ist ebenfalls von acht Hg^{2+} -Kationen koordiniert, die ebenfalls fast perfekt kubisch angeordnet sind. Die Existenz einer kovalenten Bindung zwischen Hg^{2+} und Wasserstoffatomen des Borkäfigs wurde in dieser Verbindung nicht festgestellt.

7.1.1.3 Dodekahydro-*closo*-Dodekaborate mit zweiwertigen Übergangsmetallen

Die Kristallstruktur des $\text{Ni}(\text{H}_2\text{O})_6[\text{B}_{12}\text{H}_{12}] \cdot 6 \text{H}_2\text{O}$ (kubisch, $F4_132$ (Nr. 210), $a = 1633,47(8)$ pm, $Z = 8$) kann als eine Anordnung vom NaTl-Typ beschrieben werden, wobei die Schwerpunkte der *quasi*-ikosaedrischen $[\text{B}_{12}\text{H}_{12}]^{2-}$ -Clusteranionen die Tl-Positionen einnehmen, und die Ni^{2+} -Kationen die Na^+ -Positionen besetzen. Die Kristallstruktur von $\text{Ni}(\text{H}_2\text{O})_6[\text{B}_{12}\text{H}_{12}] \cdot 6 \text{H}_2\text{O}$ weist sowohl starke $\text{O}-\text{H}^{\delta+} \cdots \delta^-\text{O}$ - als auch schwache $\text{B}-\text{H}^{\delta-} \cdots \delta^+\text{H}-\text{O}$ -Wasserstoffbrückenbindungen auf. Das $[\text{Ni}(\text{H}_2\text{O})_6]^{2+}$ Oktaeder ist ikosaedrisch mit den "zeolithischen" Kristallwassermolekülen, die eine zweite Koordinationssphäre bilden, durch $\text{O}-\text{H}^{\delta+} \cdots \delta^-\text{O}$ -Wasserstoffbrückenbindungen verbunden. $\text{Fe}(\text{H}_2\text{O})_6[\text{B}_{12}\text{H}_{12}]$ (monoklin, $C2/m$ (Nr. 12), $a = 1393,45(9)$, $b = 1449,78(9)$, $c = 732,00(5)$ pm, $\beta = 95,879(3)^\circ$, $Z = 4$) hingegen kristallisiert als eine monoklin verzerrte Variante des CsCl-Strukturtyps. Da keine "zeolithischen" Kristallwassermoleküle vorhanden sind, wird die Kristallstruktur nur durch schwache $\text{B}-\text{H}^{\delta-} \cdots \delta^+\text{H}-\text{O}$ -Wasserstoffbrückenbindungen stabilisiert.

7.1.1.4 Dioxonium-Dodekahydro-*closo*-Dodekaborate mit zweiwertigen Übergangsmetallkationen

Die Kristallstruktur von $[\text{M}(\text{H}_2\text{O})_6](\text{H}_3\text{O})_2[\text{B}_{12}\text{H}_{12}]_2 \cdot 6 \text{H}_2\text{O}$ ($M = \text{Mn, Fe, Co, Ni, Cu, Zn}$ und Cd) ist schichtartig aufgebaut mit alternierend angeordneten $[\text{M}(\text{H}_2\text{O})_6]^{2+}$, $[\text{B}_{12}\text{H}_{12}]^{2-}$ -Clusteranionen und (H_3O^+) Schichten entlang $[001]$. Jedes der M^{2+} -Kationen ist von sechs Wassermolekülen oktaedrisch koordiniert. Die Kristallstruktur von $[\text{M}(\text{H}_2\text{O})_6](\text{H}_3\text{O})_2[\text{B}_{12}\text{H}_{12}]_2 \cdot 6 \text{H}_2\text{O}$ ($M = \text{Mn, Fe, Co, Ni, Cu, Zn}$ und Cd) wird sowohl durch starke $\text{O}-\text{H}^{\delta+} \cdots \delta^-\text{O}$ - als auch schwache $\text{B}-\text{H}^{\delta-} \cdots \delta^+\text{H}-\text{O}$ -Wasserstoffbrückenbindungen stabilisiert.

orthorhombisch, Pnmm (Nr. 58), $Z = 2$	Gitterkonstanten		
	a / pm	b / pm	c / pm
$[\text{Mn}(\text{H}_2\text{O})_6](\text{H}_3\text{O})_2[\text{B}_{12}\text{H}_{12}]_2 \cdot 6 \text{H}_2\text{O}$	1160,56(7)	1512,86(9)	925,55(6)
$[\text{Fe}(\text{H}_2\text{O})_6](\text{H}_3\text{O})_2[\text{B}_{12}\text{H}_{12}]_2 \cdot 6 \text{H}_2\text{O}$	1160,38(7)	1504,89(9)	923,30(6)
$[\text{Co}(\text{H}_2\text{O})_6](\text{H}_3\text{O})_2[\text{B}_{12}\text{H}_{12}]_2 \cdot 6 \text{H}_2\text{O}$	1157,45(7)	1495,14(9)	924,68(6)
$[\text{Ni}(\text{H}_2\text{O})_6](\text{H}_3\text{O})_2[\text{B}_{12}\text{H}_{12}]_2 \cdot 6 \text{H}_2\text{O}$	1156,25(7)	1488,47(9)	924,98(6)
$[\text{Cu}(\text{H}_2\text{O})_6](\text{H}_3\text{O})_2[\text{B}_{12}\text{H}_{12}]_2 \cdot 6 \text{H}_2\text{O}$	1162,81(7)	1493,21(9)	921,60(6)
$[\text{Zn}(\text{H}_2\text{O})_6](\text{H}_3\text{O})_2[\text{B}_{12}\text{H}_{12}]_2 \cdot 6 \text{H}_2\text{O}$	1157,57(7)	1493,03(9)	924,93(6)
$[\text{Cd}(\text{H}_2\text{O})_6](\text{H}_3\text{O})_2[\text{B}_{12}\text{H}_{12}]_2 \cdot 6 \text{H}_2\text{O}$	1159,02(7)	1532,90(9)	923,90(6)

7.1.1.5 Triaqua-Blei(II)-Dodekahydro-*closo*-Dodekaborat-Trihydrat

Die Kristallstruktur von $\text{Pb}(\text{H}_2\text{O})_3[\text{B}_{12}\text{H}_{12}] \cdot 3 \text{H}_2\text{O}$ (orthorhombisch, $\text{Pna}2_1$ (Nr. 33), $a = 1839,08(9)$, $b = 1166,52(6)$, $c = 717,27(4)$ pm, $Z = 4$) ist schichtartig aufgebaut, wobei die Pb^{2+} und $[\text{B}_{12}\text{H}_{12}]^{2-}$ alternierend angeordnet sind. Das Pb^{2+} -Kation wird in der ersten Sphäre nur von den drei Sauerstoffatomen der Wassermoleküle koordiniert. Darüberhinaus ist das Pb^{2+} -Kation in einer zweiten Koordinationsphäre an drei Wasserstoffatome des $[\text{B}_{12}\text{H}_{12}]^{2-}$ -Clusteranionen gebunden. Das Pb^{2+} -Kation besitzt damit die Koordinationszahl sechs und ist von Wasserstoff- und Sauerstoffatomen umgeben. Die exzentrische Koordinationsumgebung des Pb^{2+} -Kations ist die Folge der stereochemischen Aktivität der $6s^2$ "lone-pair"-Elektronen.

7.1.1.6 Diaqua-Monohydroxo-Bismut(III)-Dodekahydro-*closo*-Dodekaborat

Die gesamte Reihe der Kristallstrukturdaten des Dodekahydro-*closo*-Dodekaborat-Salze der Tl^+ , Pb^{2+} und Bi^{3+} Kationen welche $6s^2$ "lone-pair"-Elektronen wird vervollständigt durch jene von $\text{Bi}(\text{H}_2\text{O})_2(\text{OH})[\text{B}_{12}\text{H}_{12}]$. In dieser Kristallstruktur (orthorhombisch, Pnma (Nr. 62), $a = 1382,29(9)$, $b = 892,78(6)$, $c = 982,47(7)$ pm, $Z = 4$) ist jedes Bi^{3+} Kation fast koplanar durch drei nahe Sauerstoffatome koordiniert zwei Sauerstoffatome von koordiniertem Kristallwasser und eines von der OH^- -Gruppe. Zudem ist das Bi^{3+} -Kation von drei *quasi*-ikosaedrischen $[\text{B}_{12}\text{H}_{12}]^{2-}$ -Clusteranionen umgeben und koordiniert die Wasserstoffatome der Borkäfige. Die exzentrische Koordinationsumgebung des Bi^{3+} -Kations zeigt wieder die stereochemische Aktivität der $6s^2$ "lone-pair"-Elektronen.

7.1.1.7 Bis-Hexaaqua-Chrom(III)- und Bis-Hexaaqua-Indium(III)-Tris-Dodekahydro-*closo*-Dodekaborat-Pentadekahydrat

Die Kristallstruktur von $[\text{M}(\text{H}_2\text{O})_6]_2[\text{B}_{12}\text{H}_{12}]_3 \cdot 15 \text{H}_2\text{O}$ ($\text{M} = \text{Cr}$ und In) kann als zwei voneinander unabhängige, ineinandergreifend geschichtete Motive beschrieben werden, wobei das $[\text{M}(\text{H}_2\text{O})_6]^{3+}$ -Kation und das $[\text{B}_{12}\text{H}_{12}]^{2-}$ -Clusteranion die Komponenten sind. Die Chrom(III)- bzw. Indium(III)-Anionen sind als kubisch dichteste Packung angeordnet und weisen wie im Cu-Strukturtyp die Stapelfolge *abc* auf. Die $[\text{B}_{12}\text{H}_{12}]^{2-}$ -Anionen bilden eine 9-Schicht-Stapelfolge *ABCCABBCA*. Die Kristallstruktur von $[\text{M}(\text{H}_2\text{O})_6]_2[\text{B}_{12}\text{H}_{12}]_3 \cdot 15 \text{H}_2\text{O}$ ($\text{M} = \text{Cr}$ und In) weist sowohl starke $\text{O}-\text{H}^{\delta+} \cdots \delta^- \text{O}$ als auch schwache $\text{B}-\text{H}^{\delta-} \cdots \delta^+ \text{H}-\text{O}$ Wasserstoffbrückenbindungen auf.

trigonal, $R\bar{3}c$ (Nr. 167), $Z = 6$	Gitterkonstanten	
	a / pm	c / pm
$[\text{Cr}(\text{H}_2\text{O})_6]_2[\text{B}_{12}\text{H}_{12}]_3 \cdot 15 \text{H}_2\text{O}$	1157,62(3)	6730,48(9)
$[\text{In}(\text{H}_2\text{O})_6]_2[\text{B}_{12}\text{H}_{12}]_3 \cdot 15 \text{H}_2\text{O}$	1171,71(3)	6740,05(9)

7.1.1.8 Hexaaqua-Chrom(III)-Oxonium Dodekahydro-*closo*-Dodekaborat-Hexahydrat

Die Verbindung $[\text{Cr}(\text{H}_2\text{O})_6](\text{H}_5\text{O}_2)[\text{B}_{12}\text{H}_{12}]_2 \cdot 6 \text{H}_2\text{O}$ (orthorhombisch, Pnmm (Nr. 58), $a = 1086,55(7)$, $b = 1483,17(9)$, $c = 949,24(6)$ pm, $Z = 2$) besitzt eine schichtartige Struktur, in der die $[\text{Cr}(\text{H}_2\text{O})_6]^{3+}$, die $[\text{B}_{12}\text{H}_{12}]^{2-}$ -Clusteranionen und die $(\text{H}_5\text{O}_2)^+$ in Schichten abwechselnd entlang $[001]$ angeordnet sind. Das Dioxoniumion $(\text{H}_5\text{O}_2)^+$ mit zwei Sauerstoffatomen der gleichen kristallographischen Sorte besitzt eine zentrale O–H···O Wasserstoffbindung. Jedes der Cr^{3+} Kationen (CN = 6) ist durch sechs Wassermoleküle koordiniert und bildet ein fast perfektes Oktaeder.

7.1.1.9 Bis-Hexaaqua-Aluminium(III) Oxosulfat Bis-Dodekahydro-*closo*-Dodekaborat-Pentadekahydrat

In der Kristallstruktur von $[\text{Al}(\text{H}_2\text{O})_6]_2(\text{SO}_4)[\text{B}_{12}\text{H}_{12}]_2 \cdot 15 \text{H}_2\text{O}$ (trigonal, $R\bar{3}c$ (Nr. 167), $a = 1083,82(2)$, $c = 6776,56(9)$ pm, $Z = 6$), folgen sowohl die $[\text{B}_{12}\text{H}_{12}]^{2-}$ als auch die SO_4^{2-} Anionen der Anordnung einer kubisch dichtest gepackten Anordnung mit der Stapelfolge abc . Die Stapelfolge der Al^{3+} -Kationen ist wie bei dem Kupferstrukturtyp $aa\ bb\ cc$. Bei dem SO_4^{2-} Anionen sind die Sauerstoffatome auf zwei halbbesetzten *Wyckoff* Positionen untergebracht; insgesamt liegt ein verzerrtes hexagonales Skalenoeder statt eines einfachen Tetraeders vor, wohingegen Al^{3+} oktaedrisch von sechs Wassermolekülen umgeben ist.

7.1.1.10 Dodekahydro-*closo*-Dodekaborate mit dreiwertigen Selten-Erd-Metallen

$[\text{M}(\text{H}_2\text{O})_9]_2[\text{B}_{12}\text{H}_{12}]_3 \cdot 15 \text{H}_2\text{O}$ (M = Pr und Ho) kristallisiert in der Raumgruppe $R\bar{3}c$ mit sechs Formeleinheiten pro Elementarzelle. Die Kristallstrukturen können als zwei voneinander unabhängige, ineinandergreifend-geschichtete Motive beschrieben werden mit dem $[\text{M}(\text{H}_2\text{O})_9]^{3+}$ -Kation und dem $[\text{B}_{12}\text{H}_{12}]^{2-}$ -Clusteranion als Strukturkomponenten. Die $[\text{B}_{12}\text{H}_{12}]^{2-}$ -Clusteranionen sind gemäß des α -Sm-Typs geordnet, wohingegen die Selten-Erd-Trikationen gemäß des Cu-Strukturtyps geordnet sind. $[\text{La}(\text{H}_2\text{O})_9]_2[\text{B}_{12}\text{H}_{12}]_3 \cdot 7 \text{H}_2\text{O}$ (triklin, $P\bar{1}$ (Nr. 2), $a = 1186,54(6)$, $b = 1277,09(7)$, $c = 1789,15(9)$ pm, $\alpha = 70,492(3)$, $\beta = 85,201(3)$, $\gamma = 87,633(3)^\circ$, $Z = 2$) mit 25 Kristallwassermolekülen wird bei der Reaktion von

Lanthannitrat $\text{La}(\text{NO}_3)_3 \cdot 6 \text{H}_2\text{O}$ mit der freien Säure $(\text{H}_3\text{O})_2[\text{B}_{12}\text{H}_{12}]$ erhalten. In der Kristallstruktur von $[\text{La}(\text{H}_2\text{O})_9]_2[\text{B}_{12}\text{H}_{12}]_3 \cdot 7 \text{H}_2\text{O}$ werden die La^{3+} -Kationen von den Sauerstoffatomen der Wassermoleküle koordiniert und formen ein verzerrtes, einfach überkapptes, quadratisches Antiprisma ($\text{CN} = 9$). Die Kristallstrukturen von $[\text{M}(\text{H}_2\text{O})_9]_2[\text{B}_{12}\text{H}_{12}]_3 \cdot 15 \text{H}_2\text{O}$ ($\text{M} = \text{Pr}$ und Ho) und $[\text{La}(\text{H}_2\text{O})_9]_2[\text{B}_{12}\text{H}_{12}]_3 \cdot 7 \text{H}_2\text{O}$ werden sowohl von starken $\text{O}-\text{H}^{\delta+} \cdots \delta^- \text{O}$ als auch schwachen $\text{B}-\text{H}^{\delta-} \cdots \delta^+ \text{H}-\text{O}$ -Wasserstoffbrückenbindungen stabilisiert. Die starken $\text{O}-\text{H}^{\delta+} \cdots \delta^- \text{O}$ Wasserstoffbindungen im $[\text{La}(\text{H}_2\text{O})_9]_2[\text{B}_{12}\text{H}_{12}]_3 \cdot 7 \text{H}_2\text{O}$ existieren einerseits von den Sauerstoffatomen des $[\text{La}(\text{H}_2\text{O})_9]^{3+}$ zu Kristallwassermolekülen und zu den koordinierenden Sauerstoffatome eines weiteren La^{3+} Kations, wohingegen die Sauerstoffatome von $[\text{M}(\text{H}_2\text{O})_9]^{3+}$ ($\text{M} = \text{Pr}$ und Ho) nur mit den Kristallwassermolekülen verbunden sind.

trigonal, $R\bar{3}c$ (Nr. 167), $Z = 6$	Gitterkonstanten	
	a / pm	c / pm
$[\text{Pr}(\text{H}_2\text{O})_9]_2[\text{B}_{12}\text{H}_{12}]_3 \cdot 15 \text{H}_2\text{O}$	1187,80(2)	7290,76(9)
$[\text{Ho}(\text{H}_2\text{O})_9]_2[\text{B}_{12}\text{H}_{12}]_3 \cdot 15 \text{H}_2\text{O}$	1172,65(2)	7204,12(9)

7.1.1.11 Gemischt-kationisches Holmium(III)-Oxonium Dodekahydro-*closo*-Dodekaborat-Hydrat

$[\text{Ho}(\text{H}_2\text{O})_9](\text{H}_3\text{O})_3[\text{B}_{12}\text{H}_{12}]_3 \cdot 9 \text{H}_2\text{O}$ wird durch die Reaktion von $[\text{Ho}(\text{H}_2\text{O})_9]_2[\text{B}_{12}\text{H}_{12}]_3 \cdot 15 \text{H}_2\text{O}$ und freier Säure $(\text{H}_3\text{O})_2[\text{B}_{12}\text{H}_{12}]$ in wässriger Lösung synthetisiert. Die Kristallstruktur von $[\text{Ho}(\text{H}_2\text{O})_9](\text{H}_3\text{O})_3[\text{B}_{12}\text{H}_{12}]_3 \cdot 9 \text{H}_2\text{O}$ (trigonal, $R3c$ (Nr. 161), $a = 2351,04(9)$, $c = 1472,73(6)$ pm, $Z = 6$) kann als drei voneinander unabhängige, ineinandergreifende-geschichtete Motive beschrieben werden mit $[\text{Ho}(\text{H}_2\text{O})_9]^{3+}$, $(\text{H}_3\text{O})^+$ und dem $[\text{B}_{12}\text{H}_{12}]^{2-}$ -Clusteranion als Strukturkomponenten. Alle Motive sind abwechselnd wie in der kubisch dichtesten Packung angeordnet mit der Stapelreihenfolge *abc*. Das Holmiumkation wird durch neun Sauerstoffatome der Wassermoleküle koordiniert und formt ein verzerrtes dreifach überkapptes trigonales Prisma.

7.1.2 Teilhydroxylierte Dodekahydro-*closo*-Dodekaborate

7.1.2.1 Undekahydro-Monohydroxo-*closo*-Dodekaborat-Monohydrate

In der Kristallstruktur von $(\text{H}_3\text{O})_2[\text{B}_{12}\text{H}_{11}(\text{OH})] \cdot \text{H}_2\text{O}$ besetzen die Oxoniumkationen H_3O^+ zwei kristallographisch unterschiedliche Positionen. Jedes Oxoniumkation $(\text{H}_3\text{O})^+$ ist

tetraedrisch von vier nächsten $[\text{B}_{12}\text{H}_{11}(\text{OH})]^{2-}$ -Clusteranionen durch zehn Wasserstoffatome und zwei Sauerstoffatome der Borkäfige koordiniert. Jedes Oxoniumkation $(\text{H}_3\text{O}_2)^+$ ist tetraedrisch von vier nächsten $[\text{B}_{12}\text{H}_{11}(\text{OH})]^{2-}$ -Clusteranionen durch vier Wasserstoffatome koordiniert, die ursprünglich von einer Dreiecksfläche stammen. Durch die Monohydroxilierung ist der Borkäfig von einem idealen Ikosaeder deutlich verzerrt. Die Kristallstruktur von $\text{Cs}_2[\text{B}_{12}\text{H}_{11}(\text{OH})] \cdot \text{H}_2\text{O}$ ist im Grunde isostrukturell mit der von $(\text{H}_3\text{O})_2[\text{B}_{12}\text{H}_{11}(\text{OH})] \cdot \text{H}_2\text{O}$. Die Cäsiumkationen besetzen drei kristallographisch unterschiedliche *Wyckoff* Positionen wohingegen die Sauerstoffatome der Oxoniumkationen $(\text{H}_3\text{O})^+$ und $(\text{H}_3\text{O}_2)^+$ in $(\text{H}_3\text{O})_2[\text{B}_{12}\text{H}_{11}(\text{OH})] \cdot \text{H}_2\text{O}$ nur zwei Positionen besetzen. Sowohl die Existenz der klassischen $\text{O}-\text{H}^{\delta+} \cdots \delta^- \text{O}$ -Wasserstoffbindungen als auch die *nicht*-klassische $\text{B}-\text{H}^{\delta-} \cdots \delta^+ \text{H}-\text{O}$ Wasserstoffbindungen sind in beiden Kristallstrukturen vorhanden.

orthorhombisch, Ama2 (Nr. 40), Z = 4	Gitterkonstanten		
	a / pm	b / pm	c / pm
$(\text{H}_3\text{O})_2[\text{B}_{12}\text{H}_{11}(\text{OH})] \cdot \text{H}_2\text{O}$	868,60(6)	1252,16(9)	1149,29(8)
$\text{Cs}_2[\text{B}_{12}\text{H}_{11}(\text{OH})] \cdot \text{H}_2\text{O}$	1039,54(7)	1365,67(9)	958,16(6)

7.1.2.2 Dicäsium-1,7-Dihydroxo-Dekahydro-*closo*-Dodekaborat

Die isomerische Bestimmung von $\text{Cs}_2[1,7-\text{B}_{12}\text{H}_{10}(\text{OH})_2]$ wird durch Kristallstrukturanalyse und eindimensionale NMR-Messungen durchgeführt. In der Kristallstruktur von $\text{Cs}_2[1,7-\text{B}_{12}\text{H}_{10}(\text{OH})_2]$ (orthorhombisch, Pnma (Nr. 62), $a = 1429,60(9)$, $b = 929,38(6)$, $c = 1030,70(7)$ pm, $Z = 4$) besetzen sowohl die Cäsiumkationen als auch die Sauerstoffatome der Hydroxylgruppen des Borkäfigs jeweils zwei unterschiedliche Positionen, wobei jeweils eine halbbesetzt ist. Das Cäsiumkation in der vollbesetzten Lage ist durch fünf Borkäfige umgeben, die als trigonale Bipyramide angeordnet sind, wobei zehn Wasserstoffatome und drei Sauerstoffatome der Hydroxylgruppen koordinieren (CN = 13). Das Cäsiumkation in der halbbesetzten Lage ist fast koplanar durch vier nächste Borkäfige umgeben und bindet zu zehn Wasserstoffatomen und den zwei Sauerstoffatomen der Hydroxylgruppen. Das *quasi*-ikosaedrische $[1,7-\text{B}_{12}\text{H}_{10}(\text{OH})_2]^{2-}$ -Clusteranion ist verzerrt im Vergleich zum Ausgangsclusterion $[\text{B}_{12}\text{H}_{12}]^{2-}$. Jeder der vier Borkäfige ist mit vier benachbarten Borkäfigen durch starke $\text{O}-\text{H}^{\delta+} \cdots \delta^- \text{O}$ -Brücken zwischen den Sauerstoffatomen der Hydroxylgruppen verbunden. Insgesamt bildet sich eine Pyramide. Die Thermoanalyse von $\text{Cs}_2[1,7-$

$B_{12}H_{10}(OH)_2]$ zeigte, dass die thermische Stabilität des Borkäfigs erheblich beeinflusst wird, wenn zwei Hydroxylgruppen eingeführt werden.

7.1.2.3 Dicäsium-1,2,3-Trihydroxo-Enneahydro-*closo*-Dodekaborat-Monohydrat

In der Kristallstruktur von $Cs_2[1,2,3-B_{12}H_9(OH)_3] \cdot H_2O$ (orthorhombisch, *Pbcm* (Nr. 57), $a = 916,35(6)$, $b = 1373,10(9)$, $c = 1039,41(7)$ pm, $Z = 4$) befinden sich drei Hydroxylgruppen auf einer Dreiecksfläche des Borkäfigs. Folglich wird dem $[B_{12}H_9(OH)_3]^{2-}$ -Clusteranion nach dem Ergebnis der Kristallstrukturanalyse das 1,2,3-Isomer zugeordnet. Die Cäsiumkationen besetzen drei kristallographisch unterschiedliche Lagen, wobei zwei Lagen halb besetzt sind. Jedes der zwei Cäsiumkationen in den halbbesetzten Lagen ist tetraedrisch von vier $[1,2,3-B_{12}H_9(OH)_3]^{2-}$ -Clusteranionen (CN = 12) umgeben, wohingegen die Kationen in der vollbesetzten Lage durch fünf Borkäfige, die als trigonale Bipyramide (CN = 13) angeordnet sind, koordiniert werden. Weitere Koordination findet durch Sauerstoffatome der freien Wassermoleküle statt. Die Dreifachhydroxilisierung des Borkäfigs verursacht eine deutliche Verzerrung der *quasi*-ikosaedrischen $[1,2,3-B_{12}H_9(OH)_3]^{2-}$ -Clusteranionen.

7.1.2.4 Dicäsium-1,2,3,5-Tetrahydroxo-Octahydro-*closo*-Dodekaborat-Dihydrat

Die Sauerstoffatome der Hydroxylgruppen in der Kristallstruktur von $Cs_2[1,2,3,5-B_{12}H_8(OH)_4] \cdot 2 H_2O$ (orthorhombisch, *Pbcm* (Nr. 57), $a = 972,16(6)$, $b = 1396,69(9)$, $c = 1074,71(7)$ pm, $Z = 4$) befinden sich in zwei vollbesetzten und einer halb besetzten *Wyckoff* position. Eines der beiden kristallographisch unterschiedlichen Cäsiumkationen ist tetraedrisch von vier *quasi*-ikosaedrischen $[1,2,3,5-B_{12}H_8(OH)_4]^{2-}$ -Clusteranionen umgeben, wobei acht Wasserstoffatome, zwei Sauerstoffatome der Hydroxylgruppen und drei Sauerstoffatome der freien Wassermoleküle (CN = 13) koordinativ benachbart sind. Das andere ist von fünf Borkäfigen umgeben (trigonal-pyramidal) und bindet somit an sieben Wasserstoffatome, fünf Sauerstoffatome der Hydroxylgruppen und ein Sauerstoffatom eines freien Wassermoleküls (CN = 13). Das *quasi*-ikosaedrische $[1,2,3,5-B_{12}H_8(OH)_4]^{2-}$ -Clusteranion ist etwas verzerrt gegenüber dem Ausgangs-Clusteranion $[B_{12}H_{12}]^{2-}$.

7.1.3 Dodekahydroxo-*closo*-Dodekaborate

7.1.3.1 Dirubidium-Dodekahydroxo-*closo*-Dodekaborat-Dihydrate

Durch die Reaktion von $Rb_2[B_{12}H_{12}]$ und Wasserstoffperoxid H_2O_2 bei 65° , 90° und $110^\circ C$ sind drei kristallographisch unterschiedliche Polymorphe (orthorhombisch primitiv und

basiszentriert, monoklin primitiv) des $\text{Rb}_2[\text{B}_{12}(\text{OH})_{12}] \cdot 2 \text{H}_2\text{O}$ erhalten worden. $^{11}\text{B}\{^1\text{H}\}$ -NMR- und Röntgenbeugungsmessungen erwiesen, dass eine vollständige Hydroxilierung stattgefunden hat und dass jeweils die polymorphe kristalline Phase angefallen ist, die bei der entsprechenden Reaktionstemperatur stabil ist. In allen drei Polytypen weisen die Rb^+ Kationen eine Koordinationszahl von 10 mit benachbarten Sauerstoffatomen von Wassermolekülen und Hydroxylgruppen der Borkäfige auf. Die Rubidiumkationen sind durch diese Sauerstoffatome verbunden und bilden ein eindimensionales (im monoklin primitivem Fall $\text{Rb}_2[\text{B}_{12}(\text{OH})_{12}] \cdot 2 \text{H}_2\text{O}$) oder ein dreidimensionales (im Fall der orthorhombisch $\text{Rb}_2[\text{B}_{12}(\text{OH})_{12}] \cdot 2 \text{H}_2\text{O}$) Polymernetzwerk. Jedes der *quasi*-ikosaedrischen $[\text{B}_{12}(\text{OH})_{12}]^{2-}$ -Clusteranionen in den orthorhombischen Strukturen von $\text{Rb}_2[\text{B}_{12}(\text{OH})_{12}] \cdot 2 \text{H}_2\text{O}$ ist genau oder annähernd koplanar von sechs Rb^+ Kationen umgeben. Im P-monoklinen $\text{Rb}_2[\text{B}_{12}(\text{OH})_{12}] \cdot 2 \text{H}_2\text{O}$ ist jedes $[\text{B}_{12}(\text{OH})_{12}]^{2-}$ -Clusteranionen umgeben von acht Rb^+ Kationen, die als ein Parallelepipid angeordnet sind. Alle drei Polytypen werden sowohl von starken $\text{O}-\text{H}^{\delta+} \cdots \delta^-\text{O}$ als auch schwachen $\text{B}-\text{H}^{\delta-} \cdots \delta^+\text{H}-\text{O}$ -Wasserstoffbrückenbindungen stabilisiert.

$\text{Rb}_2[\text{B}_{12}(\text{OH})_{12}] \cdot 2 \text{H}_2\text{O}$	Gitterkonstanten				
	a / pm	b / pm	c / pm	$\beta / ^\circ$	$V_m / \text{cm}^3 \text{mol}^{-1}$
orthorhombisch, Pnma (Nr. 62), Z = 4	1330,27(9)	1300,94(9)	918,59(6)	90	239,3
orthorhombisch, Cmce (Nr. 64), Z = 4	1577,73(9)	812,18(5)	1243,56(7)	90	239,9
monoklin, P2 ₁ /c (Nr. 14), Z = 2	812,30(6)	728,19(5)	1303,51(9)	97,096(3)	230,4

7.1.3.2 Cäsium-Dodekahydroxo-*hypocloso*-Dodekaborat

Paramagnetisches, luftbeständiges $\text{Cs}[\text{B}_{12}(\text{OH})_{12}]$ wird durch die Reaktion zwischen $\text{Cs}_2[\text{B}_{12}\text{H}_{12}]$ und Wasserstoffperoxid, H_2O_2 , bei relativ niedriger Temperatur hergestellt. Einkristallstrukturanalyse, ESR-, UV-VIS- und Cyclovoltametrie-Messungen erwiesen, dass bei der gewählten Synthesemethode nicht nur eine Hydroxilierung stattgefunden hat, sondern aber auch eine Einelektronenoxidation des Borkäfigs und dass ein stabiles Radikalanion *hypocloso*- $[\text{B}_{12}(\text{OH})_{12}]^{\cdot-}$ in Form eines Cäsiumsalzes als Hauptprodukt mit einem hohem Reinheitsgrad erhalten wurde. Das *hypocloso*-Dodekaborat-Radikalanion weist im Feststoff ein unaufgelöstes ESR-Signal bei $g = 2,0042$ auf, welches dem Freielektronenwert von

2,0023 sehr nahe kommt. $\text{Cs}[\text{B}_{12}(\text{OH})_{12}]$ ($a = 929,85(6)$ und $c = 1364,78(9)$ pm) kristallisiert trigonal in der Raumgruppe $R\bar{3}m$ (Nr. 166) mit drei Formeleinheiten pro Elementarzelle. Die Wechselwirkung zwischen den Cäsiumkationen über die Sauerstoffatome der Hydroxylgruppen im Kristall von $\text{Cs}[\text{B}_{12}(\text{OH})_{12}]$ ist abgeschwächt. Jedes Cäsiumkation ist von sechs radikal-monoanionischen Borkäfigen über zwölf Sauerstoffatome der Hydroxylgruppen ($\text{CN} = 12$) verzerrt oktaedrisch umgeben. Zwischen den Sauerstoffatomen der Hydroxylgruppen benachbarter Borkäfige sind starke Wasserstoffbrückenbindungen vorhanden. Das *hypocloso*- $[\text{B}_{12}(\text{OH})_{12}]^{-}$ -Clusteranion ist kaum verzerrt, auch wenn die Entfernung eines Elektrons vom Borkäfig durch externe Donorsubstituenten nur mit dem π -Rückbindungs-Effekt schwach kompensiert wird.

7.2 Ausblick

Synthese und Kristallstrukturbestimmung der Dodekahydro-*closo*-Dodekaborat-Salze von anorganischen Kationen wurden in dieser und einer anderen kürzlich angefertigten Arbeit systematisch durchgeführt jedoch verbleiben die Kristallstrukturen einiger Salze mit monovalenten (z. B. Ag^+ , Cu^+), divalenten (z. B. Be^{2+} , Cr^{2+} , Sn^{2+}), und trivalenten Kationen (z. B. Co^{3+} , Fe^{3+}) noch unbekannt und erfordern weitere Untersuchungen.

Mit Ausnahme des Cäsiumkations wurden die Synthesen und Strukturbestimmungen partiellhydroxylierter Dodekahydro-*closo*-Dodekaborat- $[\text{B}_{12}\text{H}_{12-n}(\text{OH})_n]^{2-}$ ($n = 1 - 4$) Salze anderer anorganischen Kationen nicht durchgeführt. Darüber hinaus sind kristallographische Daten partiell hydroxylierter Dodekahydro-*closo*-Dodekaborat- $[\text{B}_{12}\text{H}_{12-n}(\text{OH})_n]^{2-}$ Anionen mit $n > 4$ und eine schrittweise Synthesemethode für diese Verbindungen noch nicht zugänglich.

Perhydroxylierung des $[\text{B}_{12}\text{H}_{12}]^{2-}$ -Clusteranion ist der übliche Zwischenschritt der Funktionalisierung, aber nur die Synthese und Kristallstrukturbestimmung der Dodekahydroxo-*closo*-Dodekaborate der Alkalimetallkationen und von Cäsium-Dodekahydroxo-*hypocloso*-Dodekaborat waren bislang erfolgreich. Es ist allerdings schwierig, Einkristalle von Dodekahydroxo-*closo*-Dodekaborat- und Dodekahydroxo-*hypocloso*-Dodekaborat-Salzen anderer anorganischer Kationen durch konventionelle Methoden zu erhalten, da diese schwer löslich sind. Demzufolge sind neue Synthesemethoden wünschenswert. Des Weiteren sind ausführliche Untersuchungen erforderlich, um die Existenz des paramagnetischen, luftbeständigen $\text{Cs}[\text{B}_{12}(\text{OH})_{12}]$ zu beschreiben, bei dem der externe

Donorsubstituent OH^- des $[\text{B}_{12}(\text{OH})_{12}]^-$ -Anion die niedrige Elektrondichte in den Borkäfigen nur mit dem π -Rückbindungs-Effekt schwach kompensiert wird.

Die Funktionalisierung des dreidimensionalen aromatischen $[\text{B}_{12}\text{H}_{12-n}(\text{OH})_n]^{2-}$ -Clusteranions ($n = 1 - 4, 12$) ist eine neue Entwicklung in der Chemie der Borane. Obgleich die Synthese, Kristallisierung und Strukturbestimmung der funktionalisierten Dodekahydroxo-*closo*-Dodekaborat-Salze vieler organischer Kationen schon publiziert worden sind, sind die der anorganischen Kationen in Literatur noch nicht erhältlich. Diese Verbindungen sind ein interessantes und wichtiges Forschungsthema für die Zukunft.

8. References

- [1] A. Stock, *Hydrides of Boron and Silicon*, Cornell University Press, New York **1933**.
- [2] W. H. Eberhardt, B. Crawford, W. N. Lipscomb, *J. Chem. Phys.* **22** (1963) 989.
- [3] W. N. Lipscomb, *Boron Hydrides*, Benjamin, New York **1963**.
- [4] H. C. Longuet-Higgins, M. de V. Roberts, *Proc. Royal. Soc. (London) A* **230** (1955) 110.
- [5] J. Casanova (Ed.), *The Borane, Carborane, Carbocation Continuum*, Wiley, New York **1998**.
- [6] J. E. Huheey, *Inorganic Chemistry*, 4th ed., Harper Collins College, New York **1993**.
- [7] C. E. Housecroft, *Boranes and Metalloboranes*, Ellis Horwood, New York **1994**.
- [8] K. Wade, *Electron Deficient Compounds*, Nelson, London **1971**.
- [9] A. R. Pitochelli, M. F. Hawthorne, *J. Am. Chem. Soc.* **82** (1960) 3228.
- [10] K. Wade, *Adv. Inorg. Chem. Radiochem.* **18** (1976) 1.
- [11] O. Volkov, W. Dirk, U. Englert, P. Paetzold, *Z. Anorg. Allg. Chem.* **625** (1999) 1193.
- [12] R. D. Dobrott, W. N. Lipscomb, *J. Chem. Phys.* **37** (1962) 1779.
- [13] I. N. Polyakova, E. A. Malinia, N. T. Kuznetsov, *Crystallogr. Rep.* **48** (2003) 84.
- [14] K. Hofmann, B. Albert, *Z. Naturforsch.* **55 b** (2000) 499.
- [15] K. Hofmann, B. Albert, *Z. Kristallogr.* **220** (2005) 142.
- [16] E. L. Muetterties, J. H. Balthis, Y. T. Chia, W. H. Knoth, H. C. Miller, *Inorg. Chem.* **3** (1964) 444.
- [17] F. Klanberg, E. L. Muetterties, *Inorg. Chem.* **5** (1966) 1955.
- [18] L. J. Guggenberger, *Inorg. Chem.* **7** (1968) 2260.
- [19] L. J. Guggenberger, *Inorg. Chem.* **8** (1969) 2771.
- [20] F. Klanberg, D. R. Eaton, L. J. Guggenberger, E. L. Muetterties, *Inorg. Chem.* **6** (1967) 1271.
- [21] A. Franken, H. Thomson, W. Preetz, *Z. Naturforsch.* **51 b** (1996) 744.
- [22] I. Yu. Kuznetsov, D. M. Vinitskii, K. A. Solntsev, N. T. Kuznetsov, L. A. Butman, *Russ. J. Inorg. Chem.* **32** (1987) 1803.
- [23] W. Preetz, G. Peters, *Eur. J. Inorg. Chem.* **11** (1999) 1831.
- [24] R. K. Bohn, M. D. Bohn, *Inorg. Chem.* **10** (1971) 350.
- [25] G. Will, B. Kiefer, *Z. Anorg. Allg. Chem.* **627** (2001) 2100.
- [26] E. D. Jemmis, M. M. Balakrishnarajan, *J. Am. Chem. Soc.* **123** (2001) 4324.

- [27] J. I. Aihara, *J. Am. Chem. Soc.* **100** (1978) 3339.
- [28] A. S. Chulkov, L. A. Zharkova, E. G. Ippolitov, K. A. Solntsev, N. T. Kuznetsov, *Russ. J. Inorg. Chem.* **37** (1992) 1066.
- [29] W. H. Knoth, J. C. Sauer, D. C. England, W. R. Hertler, E. L. Muetterties, *J. Am. Chem. Soc.* **86** (1964) 3973.
- [30] U. Krause, W. Preetz, *Z. Anorg. Allg. Chem.* **621** (1995) 516.
- [31] O. Haeckel, W. Preetz, *Z. Anorg. Allg. Chem.* **624** (1998) 1089.
- [32] I. B. Sivaev, *Dissertation*, Uppsala University **2000**.
- [33] W. H. Knoth, H. C. Miller, J. C. Sauer, J. H. Balthis, Y. T. Chia, E. L. Muetterties, *Inorg. Chem.* **3** (1964) 159.
- [34] N. T. Kuznetsov, L. N. Kulikova, S. T. Zhukov, *Russ. J. Inorg. Chem.* **21** (1976) 51.
- [35] K. A. Solntsev, A. M. Mebel, N. A. Votnova, N. T. Kuznetsov, O. P. Charkin, *Koord. Khim.* **18** (1992) 340.
- [36] S. V. Ivanov, S. M. Miller, O. P. Anderson, K. A. Solntsev, S. H. Strauss, *J. Am. Chem. Soc.* **125** (2003) 4694.
- [37] I. Tiritiris, Th. Schleid, *Z. Anorg. Allg. Chem.* **630** (2004) 1555.
- [38] T. Peymann, C. B. Knobler, M. F. Hawthorne, *Inorg. Chem.* **37** (1998) 1544.
- [39] F. Haslinger, A. H. Soloway, D. N. Buttler, *J. Med. Chem.* **9** (1966) 581.
- [40] K. Yu. Zhizhin, L. V. Goeva, N. T. Kuznetsov, *Russ. J. Inorg. Chem.* **47** (2002) 341.
- [41] I. B. Sivaev, A. B. Bruskin, V. V. Nesterov, M. Yu. Antipin, V. I. Bregadze, S. Sjoeborg, *Inorg. Chem.* **38** (1999) 5887.
- [42] E. I. Tolpin, G. R. Wellum, S. A. Berley, *Inorg. Chem.* **17** (1978) 2867.
- [43] H. C. Miller, N. E. Miller, E. L. Muetterties, *J. Am. Chem. Soc.* **85** (1963) 3885.
- [44] H. C. Miller, N. E. Miller, E. L. Muetterties, *Inorg. Chem.* **3** (1964) 1456.
- [45] T. Peymann, E. Lork, D. Gabel, *Inorg. Chem.* **35** (1996) 1355.
- [46] I. B. Sivaev, S. Sjoeborg, V. I. Bregadze, D. Gabel, *Tetrahedron Lett.* **40** (1999) 3451.
- [47] I. B. Sivaev, V. I. Bregadze, S. Sjoeborg, *Collect. Czech. Chem. Commun.* **67** (2002) 679.
- [48] T. Peymann, C. B. Knobler, M. F. Hawthorne, *Inorg. Chem.* **39** (2000) 1163.
- [49] T. Peymann, A. Herzog, C. B. Knobler, M. F. Hawthorne, *Angew. Chem.* **113** (1999) 1130.
- [50] M. F. Hawthorne, *Pure Appl. Chem.* **75** (2003) 1157.
- [51] A. Maderna, C. B. Knobler, M. F. Hawthorne, *Angew. Chem. Int. Ed.* **40** (2001) 1661.

- [52] T. Li, S. S. Jalisatgi, M. J. Bayer, A. Maderna, S. I. Khan, M. F. Hawthorne, *J. Am. Chem. Soc.* **127** (2005) 17832.
- [53] J. Plešek, *Chem. Rev.* **92** (1992) 269.
- [54] H. S. Nalwa, *Handbook of Nanostructured Materials and Nanotechnology*, Academic Press, San Diego **1999**.
- [55] L. Ma, J. Hamdi, F. Wong, M. F. Hawthorne, *Inorg. Chem.* **45** (2006) 279.
- [56] I. B. Sivaev, V. I. Bregadze, N. T. Kuznetsov, *Russ. Chem. Bull.* **51** (2002) 1362.
- [57] T. P. Fehlner, *Molecular Clusters*, Cambridge University Press, Cambridge (U.K.) **2007**.
- [58] W. Mier, D. Gabel, U. Haberkorn, M. Eisenhut, *Z. Anorg. Allg. Chem.* **630** (2004) 1258.
- [59] J. H. Her, M. Yousufuddin, W. Zhou, S. S. Jalisatgi, J. G. Kulleck, J. A. Zan, S. J. Hwang, R. C. Bowman, T. J. Udovic, *Inorg. Chem.* **47** (2008) 9757.
- [60] S. L. Johnston, M. W. Lee, M. F. Hawthorne, *Appl. Radiology Suppl.* **32** (2003) 77.
- [61] M. F. Hawthorne, B. M. Ramachandran, R. D. Kennedy, C. B. Knobler, *Pure Appl. Chem.* **78** (2006) 1299.
- [62] M. W. Lee, O. M. Farha, M. F. Hawthorne, *Angew. Chem.* **119** (2007) 3078.
- [63] P. Mueller, *Crystal Structure Refinement*, Oxford University Press, Oxford (U.K.) **2006**.
- [64] Fa. STOE & Cie: *Program X-SHAPE, Version 1.06*, Darmstadt **1999**.
- [65] Fa. Stoe & Cie GmbH: *Program X-RED, Version 1.19*, Darmstadt **1999**.
- [66] P. Main, *Crystal Structure Analysis*, Oxford University Press, New York **2001**.
- [67] G. M. Sheldrick, *Program SHELXS-86*, Göttingen **1986**.
- [68] G. M. Sheldrick, *Program package SHELX-97*, Göttingen **1997**.
- [69] W. Massa, *Crystal Structure Determination*, 2nd ed., Springer, Berlin, Stuttgart **2004**.
- [70] G. M. Sheldrick, *Program SHELXL-93*, Göttingen **1993**.
- [71] Fa. STOE & CIE GmbH: *Program STOE Win Xpow, Version 1.2*, Darmstadt **2001**.
- [72] Fa. STOE & Cie GmbH: *Program X-STEP 32, Version 1.05f*, Darmstadt **2000**.
- [73] R. Hübenthal, R. Hoppe, *Program MAPLE 4.0*, Gießen **1995**.
- [74] Fa. CRYSTAL IMPACT, *Program Diamond, Version 2.1d*, Bonn **2000**.
- [75] M. E. Brown, *Introduction to Thermal Analysis*, Kluwer Academic, New York **2001**.
- [76] W. F. Hemminger, H. C. Cammenga, *Methoden der thermischen Analyse*, Springer, Berlin **1989**.

- [77] F. A. Bovey, *Nuclear Magnetic Resonance Spectroscopy*, 2nd ed., San Diego **1988**.
- [78] H. Guenther, *NMR Spectroscopy* 2nd ed., Wiley, Chichester (U.K.) **1995**.
- [79] A. K. Brisdon, *Inorganic Spectroscopic Methods*, Oxford University Press, New York **1998**.
- [80] H. Friebolin, *Basic One- and Two-Dimensional NMR Spectroscopy*, 4th ed., Wiley, Weinheim **2005**.
- [81] V. I. Ponomarev, T. Yu. Lyubeznova, K. A. Solntsev, N. T. Kuznetsov, *Koord. Khim.* **17** (1991) 21.
- [82] H. Kunkely, A. Vogler, *Inorg. Chim. Acta* **360** (2007) 679.
- [83] I. Tiritiris, Th. Schleid, *Z. Anorg. Allg. Chem.* **629** (2003) 1390.
- [84] I. Tiritiris, Th. Schleid, K. Müller, W. Preetz, *Z. Anorg. Allg. Chem.* **626** (2000) 323.
- [85] I. Tiritiris, *Dissertation*, Stuttgart University **2003**.
- [86] I. Tiritiris, Th. Schleid, *Z. Anorg. Allg. Chem.* **628** (2002) 1411.
- [87] Th. Hahn, A.C.J. Wilson (Eds.), *International Tables for Crystallography*, 3rd ed., Kluwer Academic Publisher, Dordrecht, Boston, London **1992**.
- [88] O. Volkov, C. Hu, P. Paetzold, *Z. Anorg. Allg. Chem.* **631** (2005) 1107.
- [89] I. Tiritiris, Th. Schleid, *Z. Anorg. Allg. Chem.* **629** (2004) 541.
- [90] I. Tiritiris, Th. Schleid, *Z. Anorg. Allg. Chem.* **634** (2008) 317.
- [91] I. Tiritiris, Th. Schleid, *Z. Anorg. Allg. Chem.* **634** (2008) 1353.
- [92] H. D. Lutz, K. Beckenkamp, T. Kellersohn, H. Möller, S. Peter, *J. Solid State Chem.* **124** (1996) 155.
- [93] I. Tiritiris, Th. Schleid, *Z. Anorg. Allg. Chem.* **627** (2001) 1836.
- [94] Th. Schölkopf, *Dissertation*, Stuttgart University **2009** in preparation.
- [95] Ng.-D. Van, I. Tiritiris, Th. Schleid, *Z. Anorg. Allg. Chem.* **630** (2004) 1764.
- [96] I. Tiritiris, Ng.-D. Van, Th. Schleid, *Z. Anorg. Allg. Chem.* (2009) submitted.
- [97] D. Shriver, P. Atkins, *Inorganic Chemistry* 4th ed., Oxford University Press, Oxford (U.K.) **2006**.
- [98] C. A. Reed, *Chem. Commun.* **2005** (2005) 1669.
- [99] V. S. Sergienko, A. B. Ilyukhin, A. V. Luzikova, M. A. Porai-Koshits, *Koord. Khim.* **17** (1991) 1489.
- [100] N. G. Furmanova, M. Kh. Rabadanov, T. S. Chernaya, M. S. Fonari, Yu. A. Simonov, E. V. Ganin, V. O. Gelmboldt, R. Ya. Grigorash, S. A. Kotlyar, G. L. Kamalov, *Crystallogr. Rep.* **53** (2008) 346.

- [101] W. K. Li, G. D. Zhou, T. C. W. Max, *Advanced Structural Inorganic Chemistry*, Oxford University Press, New York **2008**.
- [102] F. M. Chang, M. Jansen, D. Schmitz, *Acta Crystallogr. C* **39** (1983) 1497.
- [103] D. J. Stasko, K. J. Perzynski, M. A. Wasil, J. K. Brodbeck, K. Kirschbaum, Y. W. Kim, C. Lind, *Inorg. Chem.* **43** (2008) 3786.
- [104] T. Peymann, C. B. Knobler, S. I. Khan, M. F. Hawthorne, *J. Am. Chem. Soc.* **123** (2001) 2182.
- [105] E. L. Muetterties, W. H. Knoth, *Polyhedral Boranes*, Dekker, New York **1968**.
- [106] E. D. Jemmis, D. L. V. K. Prasad, *J. Solid State Chem.* **179** (2006) 2768.
- [107] M. L. McKee, *Inorg. Chem.* **41** (2002) 1295.
- [108] T. Peymann, C. B. Knobler, S. I. Khan, M. F. Hawthorne, *Angew. Chem.* **113** (2001) 1713.
- [109] O. K. Farha, R. L. Julius, M. W. Kee, R. E. Huertas, C. B. Knobler, S. I. Khan, M. F. Hawthorne, *J. Am. Chem. Soc.* **127** (2005) 18243.
- [110] M. J. Bayer, M. F. Hawthorne, *Inorg. Chem.* **43** (2004) 2018.
- [111] T. Peymann, C. B. Knobler, M. F. Hawthorne, *Chem. Comm.* **1999** (1999) 2039.

Curriculum Vitae

Surname: Nguyen
Name: Duc Van
Date of birth: 15th May 1972
Place of birth: Ha tinh, Vietnam
Nationality: Vietnamese
Current address: Traubenstrasse 19, D-71106 Magstadt, Germany

Education:

1979-1986 Primary School Khuong Thuong, Hanoi, Vietnam
1986-1989 Secondary School Trung Vuong, Dong da, Hanoi, Vietnam
1989-1993 Hanoi National University (Vietnam), Bachelor Degree in Chemistry
Studying Field: Inorganic Chemistry
1999-2001 International Training Institute for Materials Science (Vietnam), Master Degree
2002 to date Ph. D. programme, Institute of Inorganic Chemistry, University of Stuttgart (Germany)
Research Field: Solid-State Inorganic Chemistry
Supervisor: Prof. Dr. Thomas Schleid
Research Topic: New Salt-Like Dodecahydro-*closo*-Dodecaborates and Efforts for the Partial Hydroxylation of $[B_{12}H_{12}]^{2-}$ Anions